The role of CD2 in recognition of weak antigens and its implications for Adoptive Cell Transfer



Jesús Antonio Siller Farfán

Exeter College

University of Oxford

A thesis submitted for the degree of

Doctor of Philosophy

Hilary 2021

This thesis is dedicated to:

Juan Antonio Siller Valdez
Delia Ymelda Farfán Castro
Angela Julieta Siller Farfán

Acknowledgements

This has been a long, and at times very difficult, journey. I am indebted to many people who have selflessly supported me through my DPhil. I am convinced that, without their help, things would have been much different.

I want to start by thanking my supervisor, Prof. Omer Dushek. I admire him not only as a scientist, but also as a person. His willingness to help, as well as his open mind when engaging in scientific discussions, were always remarkable during my time in his group. I am also grateful for the support I received from him when I became involved with teaching at the Sir William Dunn School of Pathology.

I would also like to thank the examiners who accepted to review my work during my DPhil transfer and confirmation. In particular, I want to acknowledge Prof. Simon Davis and Prof. Tudor Fulga, as well as Dr. Mariolina Salio and Prof. Audrey Gérard. Special thanks to Prof. Michael Dustin and Dr. David Cole for agreeing to examine my thesis.

My gratitude goes to all the members of the Dushek, Brown, and van der Merwe laboratories. I have always thought that the friendliness and collegiality of the Molecular Immunology Group are extraordinary. When the biggest problem in a large research group is simply that the autoclave waste boxes are always full, you can count yourself as a lucky DPhil student.

Many thanks to all my friends from Monterrey and Oxford for putting up with me through all these years! In particular, I would like to express my sincere appreciation to Gareth and Lilli for always being there.

Most importantly, I want to say thank you to all my family in México. Words cannot do justice to the love and support I have received from my parents, Juan Antonio and Delia Ymelda; and my sister, Angela Julieta. This thesis is yours, too.

Funding and Authorship Declaration

This work received support from multiple funding sources, which are shown here in alphabetical order:

- Amelia Jackson Senior Studentship, Exeter College
- CONACyT-I^{2}T^2 Consortium (Grant 440334)
- Edward Penley Abraham Research Fund, Sir William Dunn School of Pathology
- EPSRC & BBSRC Centre for Doctoral Training in Synthetic Biology and the University of Oxford (Grant EP/EP/L016494/1)
- Secretariat of Public Education, México

I declare that, in some instances, the work of others is presented in this thesis. In particular, I wish to acknowledge that:

- The data from Figure 3.1 corresponds to published experiments, which were conducted by Pettmann *et al.*[1].
- Genomic Engineering Oxford (GEO, Sir William Dunn School of Pathology) was subcontracted to generate a CD2$^-$ clone of the 1G4 NF-κB/eGFP Jurkat cell line. Both the contents shown in Figure A.1 and the electropherogram presented in Section A.2 (Appendix A) were generated by GEO.
- Appendix C contains a copy, downloaded from Europe PubMed Central, of a review titled **Molecular mechanisms of T cell sensitivity to antigen**. This work was published in *Immunological Reviews*[2], and it was co-authored by my supervisor (Prof. Omer Dushek) and me.

Abstract

Adoptive cell transfer (ACT) of genetically modified T cells expressing engineered T cell receptors (TCRs) holds potential in the treatment of cancer. However, concerns about off-tumour toxicities continue to hinder widespread adoption of TCR-T cells. Current mitigation strategies against off-tumour toxicity such as affinity tuning, kill switches, and logic gates, can sometimes compromise the efficacy of ACT. In this work, we postulate that the human CD2 co-receptor can mediate off-tumour toxicities in ACT, and we propose the targeted manipulation of the CD2/CD58 axis to ameliorate these toxicities. We engineered a Chinese hamster ovary line and used it as a surrogate antigen presenting cell (APC), generating a xenogeneic platform to quantitatively study the role of human CD2 in enabling T cell recognition of low density and/or low affinity ligands (weak antigens). Using Jurkat and primary human $CD8^+$ T cells, we found that, when disrupting the CD2/CD58 axis through *CD2* ablation, T cell antigen sensitivity was reduced by 4–15 fold. In co-cultures between Jurkats and the T2 archetypal APC line, transducing the Jurkat effectors with elongated CD2 chimeras generated modest reductions in sensitivity (2–8 fold), a phenomenon that might be attributable to disruption of the CD2/CD58 canonical binding. Moreover, we showed in $CD8^+$ T cells that *CD2* knockout appeared to ameliorate the previously reported low affinity, self-pMHC cross-reactivity of the affinity enhanced wt/c51 TCR. Taken together, our results suggest that CD2 might contribute to two types of off-tumour toxicity observed in ACT, namely on-target/off-tumour and off-target/off-tumour cross-reactivity. Therefore, routine manipulation of the CD2/CD58 axis could provide a way of enhancing ACT safety when using engineered TCRs. Our findings could be applicable to other synthetic receptors, provided they exploit the CD2 co-receptor as TCRs do.

Contents

List of Figures ix

List of Tables xi

List of Abbreviations xii

1 Introduction 1
- 1.1 An overview of cancer immunotherapy . . . 1
- 1.2 The role of T cells . . . 5
  - 1.2.1 The cornerstones of adaptive immunity . . . 6
  - 1.2.2 T cell selection, central and peripheral tolerance . . . 8
  - 1.2.3 The inherent cross-reactivity of the TCR . . . 12
  - 1.2.4 Of TCRs and CARs . . . 14
- 1.3 The evolution and challenges of ACT . . . 16
  - 1.3.1 The clinical landscape of CAR-T cells . . . 18
  - 1.3.2 Current challenges in ACT . . . 20
- 1.4 Studying CD2 in the context of ACT . . . 27
  - 1.4.1 CD2 biology: an overview . . . 27
  - 1.4.2 A rationale for studying CD2 in ACT . . . 29
- 1.5 Scope and structure of this work . . . 31

2 Materials and methods 33
- 2.1 List of reagents . . . 34
- 2.2 Consumables and equipment . . . 39
- 2.3 Molecular biology . . . 40
  - 2.3.1 General subcloning routines . . . 40
  - 2.3.2 Plasmid constructs . . . 42
  - 2.3.3 Generation of messenger RNA . . . 45
- 2.4 APLs of the NY-ESO-1 epitope . . . 47
- 2.5 Flow cytometry . . . 47
  - 2.5.1 Preparation of pMHC tetramers . . . 47
  - 2.5.2 Cytometry and general data acquisition . . . 48
  - 2.5.3 Absolute cytometric quantitation of CD2 and CD58 . . . 49

2.6 Quantitation of cytokine production and cytotoxicity 50
2.6.1 Enzyme-linked immunoassays 50
2.6.2 T cell cytotoxicity 51
2.7 Tissue culture routines 51
2.7.1 Production of lentiviral supernatants 51
2.7.2 Cell lines: procurement, generation, and maintenance . . . 52
2.7.3 Primary cells 55
2.8 Stimulation and conjugation assays 57
2.8.1 Stimulation with adherent cells 57
2.8.2 Stimulation with suspension cells 58
2.8.3 Conjugation assays 59
2.9 Data analysis 60

3 Generation of a cellular platform to study the CD2/CD58 axis 62
3.1 Introduction 62
3.1.1 A look at the CD2/CD58 axis in a reductionist system . . 64
3.1.2 Platforms for assessing T cell activation 65
3.1.3 Chapter aim 70
3.2 Results 71
3.2.1 The effector NF-κB/eGFP Jurkat line 71
3.2.2 The target CHO-K1 cell line 71
3.2.3 CD2 engagement reduces the EC_{50} of activation 76
3.2.4 The CHO platform quantitatively recapitulates the phenotype of CD2 knockout cells 77
3.2.5 CD2 overexpression increases antigen sensitivity at the expense of specificity 78
3.3 Discussion 81
3.3.1 Revisiting the role of CD2 82
3.3.2 Improving the experimental platform 84

4 CD2 disruption as a strategy to ameliorate on-target/off-tumour toxicity 86
4.1 Introduction 87
4.1.1 On-target/off-tumour toxicity in ACT 87
4.1.2 Manipulating the CD2/CD58 axis 91
4.1.3 Chapter aim 91
4.2 Results 92
4.2.1 Elongated CD2 chimeras fail to antagonise endogenous CD2 in the CHO system 92

4.2.2 Tail-less CD2 chimeras do not antagonise endogenous CD2 in the CHO system . . . 94
4.2.3 Elongated CD2 chimeras reduce antigen sensitivity in a T2 APC system . . . 94
4.2.4 CD2 disruption in primary human CD8$^+$ T cells reduces antigen sensitivity, mitigating on-target/off-tumour toxicity 97
4.3 Discussion . . . 102
4.3.1 Disruption of the CD2/CD58 axis by transduction of elongated CD2 chimeras . . . 104
4.3.2 CD2 knockout in ACT . . . 107

5 CD2 influences off-target/off-tumour cross-reactivity in affinity enhanced receptors 110
5.1 Introduction . . . 110
5.1.1 Off-target/off-tumour toxicity in ACT . . . 111
5.1.2 Chapter aim . . . 114
5.2 Results . . . 114
5.2.1 CD2 knockout ameliorates cross-reactivity of the affinity enhanced wt/c51 TCR . . . 114
5.2.2 Impact of CD2 on the discrimination power of T cells . . . 117
5.3 Discussion . . . 121
5.3.1 CD2 and discrimination power . . . 122
5.3.2 Affinity enhanced receptors in ACT . . . 125

6 General conclusions 128
6.1 Summary . . . 128
6.2 Future directions . . . 131

References 133

Appendices

A Generation of the 1G4 CD2$^-$ NF-κB/eGFP Jurkat line 152
A.1 CRISPR/Cas9 *CD2* targeting strategy . . . 152
A.2 Sanger sequencing confirms successful disruption of the *CD2* gene 153
A.3 Validation of TCR levels in the CD2 knockout line . . . 157

B Characterisation of the 1G4 NF-κB/eGFP Jurkats expressing elongated CD2 chimeras 158
B.1 Expression of the CD2^{HA} chimeras . . . 159
B.2 The CD2^{HA} chimeras are functional and bind CD58 . . . 159

C Molecular mechanisms of T cell sensitivity to antigen 162

List of Figures

1.1 Schematic of a conventional α:β TCR 7
1.2 TCR gene rearrangement: V(D)J recombination 9
1.3 Selected examples of receptors that can be used in ACT 19
1.4 Current challenges in ACT 21

2.1 Summary of the CD2 chimeras used for cell transduction 46

3.1 In a reductionist system, engagement of the CD2 co-receptor improves T cell antigen sensitivity by almost 3 orders of magnitude 66
3.2 Generation of the 1G4 NF-κB/eGFP Jurkat cell line 72
3.3 Single clones of the CHO-A*02 cell line 73
3.4 Transduction of human CD58 in the CHO-A*02 cell line 74
3.5 Matching of HLA-A*02 levels in the CHO lines 75
3.6 Engagement of CD2 reduces EC_{50} of activation by a 15–fold factor 77
3.7 CD2 knockout reduces the EC_{50} of activation and recapitulates the results obtained with the CHO platform 78
3.8 The CHO APC platform recapitulates the effects of CD2 knockout in Jurkat cells 79
3.9 Overexpression of the CD2 receptor in the 1G4 NF-κB/eGFP Jurkat line 80
3.10 CD2 expression levels correlate with antigen sensitivity 81

4.1 On-target/off-tumour toxicity in ACT 89
4.2 Schematic of the elongated CD2 chimeras 93
4.3 In the HLA-A*02 CHO system, elongated CD2 chimeras fail to antagonise endogenous CD2 in the presence of CD58 95
4.4 In the presence of CD58, tail-less CD2 chimeras do not antagonise endogenous CD2 96
4.5 Elongated CD2 chimeras impair antigen sensitivity in a T2 APC system 97
4.6 Generation of primary 1G4 $CD2^-$ $CD8^+$ T cells 98
4.7 CD2 loss impairs antigen sensitivity in primary human $CD8^+$ T cells 100

4.8 CD2 loss reduces killing of T2 target cells bearing low levels of the NY-ESO-1 antigen . . . 102
4.9 CD2 loss reduces the amount of cytokine secretion but not the production thresholds . . . 103

5.1 Generation of primary wt/c51 CD2$^-$ CD8$^+$ T cells . . . 115
5.2 CD2 loss ameliorates MIP-1β-associated off-target cross-reactivity of the affinity enhanced wt/c51 TCR . . . 116
5.3 The cross-reactivity exhibited by the wt/c51 affinity enhanced TCR leads to production of the MIP-1β chemokine, but not to generation of IFN-γ, IL-2, or TNF-α . . . 117
5.4 CD2 loss improves discrimination power in the 1G4 NF-κB/eGFP reporter Jurkat line . . . 119
5.5 CD2 loss does not impair discrimination power in 1G4 CD8$^+$ T cells 120
5.6 CD2 and discrimination power in Jurkat and primary CD8$^+$ T cells 121

A.1 Strategy for *CD2* gene knockout in the Jurkat cell line . . . 153
A.2 Comparison between the 1G4 TCR levels of the parental and the CD2 knockout 1G4 Jurkat line . . . 157

B.1 Expression of the CD2^{HA} chimeras in the sub-lines of the 1G4 NF-κB/eGFP Jurkat line . . . 160
B.2 CD2^{HA} chimeras display binding to CD58 . . . 161

List of Tables

2.1 General and molecular biology reagents 34
2.2 Cell culture reagents 36
2.3 Flow cytometry antibodies 37
2.4 Buffers and their composition 38
2.5 Main consumables 39
2.6 Main equipment used 39
2.7 Affinity measurements for the 1G4 TCR 47

3.1 Quantitation of CD58 expression in selected cellular samples . . . 76

4.1 Summary of the activation metrics for 1G4 $CD8^+$ T cells co-cultured with $CD58^+$ HLA-A*02^+ CHO cells 99

List of Abbreviations

β2M . . . . . β_2 microglobulin

4PL . . . . . 4-parameter logistic (regression)

5PL . . . . . 5-parameter logistic (regression)

ACT . . . . . Adoptive cell transfer or adoptive cell therapy

AIRE . . . . . Autoimmune regulator

ALL . . . . . Acute lymphoblastic leukaemia

AP-1 . . . . . Activator protein 1

APC . . . . . Antigen presenting cell or allophycocyanin

APECED . . . Autoimmune polyendocrine syndrome type 1

APL . . . . . Altered peptide ligand

ATCC . . . . . American Type Culture Collection

BCG . . . . . Bacillus Calmette–Guérin

BCR . . . . . B cell receptor

BiTE . . . . . Bispecific T-cell engager

BSA . . . . . Bovine Serum Albumin

BTLA . . . . . B- and T-lymphocyte attenuator

BV . . . . . Brilliant Violet

CAIX . . . . . Carbonic anhydrase IX

CAR . . . . . Chimeric antigen receptor

CD . . . . . Cluster of differentiation

CDR . . . . . Complementarity-determining region

CEA . . . . . Carcinoembryonic antigen

CFSE . . . . . Carboxyfluorescein succinimidyl ester

CHO . . . . . Chinese hamster ovary

CRS . . . . . Cytokine release syndrome

cTEC . . . . . Cortical thymic epithelial cell

CTL . . . . . Cytotoxic T lymphocytes

CTLA4 . . . . Cytotoxic lymphocyte antigen 4

DC . . . . . Dendritic cell

DLBCL . . . . Diffuse large B-cell lymphoma

DMEM . . . . Dulbecco's modified Eagle medium

DMSO . . . . . Dimethyl sulfoxide

DN . . . . . Double-negative (thymocytes)

DP . . . . . Double-positive (thymocytes)

DPBS . . . . . Dulbecco's phosphate-buffered saline

E:T . . . . . Effector:Target (ratio)

EC_{50} . . . . . Half-maximal effective concentration

ECACC . . . . European Collection of Authenticated Cell Cultures

EDTA . . . . . Ethylenediaminetetraacetic acid

EF . . . . . Elongation factor

eGFP . . . . . Enhanced green fluorescent protein

EGFR . . . . . Epidermal growth factor receptor

ELISA . . . . . Enzyme-linked immunosorbent assay

EM . . . . . Effector memory

EMA . . . . . European Medicines Agency

E_{max} . . . . . Maximum effect

E_{min} . . . . . Baseline response

F:P . . . . . Fluorochome:Protein (ratio)

FACS . . . . . Fluorescence-activated cell sorting

FBS . . . . . Foetal bovine serum

Fyn . . . . . Proto-oncogene tyrosine-protein kinase

GEO . . . . . Genomic Engineering Oxford

GM-CSF . . . Granulocyte-macrophage colony-stimulating factor

gMFI . . . . . Geometric mean fluorescence intensity

GUV . . . . . Giant unilamellar vesicles

GvHD . . . . . Graft-versus-host-disease

HCMV . . . . Human cytomegalovirus

HER2/neu . . Human epidermal growth factor receptor 2

HIV . . . . . Human immunodeficiency virus

HLA . . . . . Human leukocyte antigen

HPV . . . . . Human papillomavirus

HVEM . . . . Herpesvirus entry mediator

ICAM . . . . . Intercellular adhesion molecule

IFN-γ . . . . . Interferon-γ

Ig . . . . . Immunoglobulin

IgSF . . . . . Immunoglobulin superfamily

IL . . . . . Interleukin

ILP . . . . . Invadosome-like protrusion

IS . . . . . Immunological synapse

ITAM . . . . . Immunoreceptor tyrosine-based activation motif

KS . . . . . Kinetic segregation

LAT . . . . . Linker for activation of T cells

Lck . . . . . Lymphocyte-specific protein tyrosine kinase

LCMV . . . . Lymphocytic choriomeningitis virus

LDH . . . . . Lactate dehydrogenase

LFA . . . . . Lymphocyte function-associated antigen

mAb . . . . . Monoclonal antibody

MAGE . . . . Melanoma-associated antigen

MART-1 . . . Melanoma antigen recognised by T cells 1

MDSC . . . . . Myeloid-derived suppressor cell

MHC . . . . . Major histocompatibility complex

MIP-1β . . . . Macrophage inflammatory protein 1β

mRNA . . . . Messenger RNA

mTEC . . . . . Medullary thymic epithelial cell

MUC1 . . . . . Mucin 1

NF-κB . . . . . Nuclear factor κ-light-chain-enhancer of activated B cells

NFAT . . . . . Nuclear factor of activated T cells

NHS . . . . . National Health Service

NK cell . . . . Natural killer cell

NY-ESO-1 . . New York esophageal squamous cell carcinoma-1

PBS . . . . . Phosphate-buffered saline

PCR . . . . . Polymerase chain reaction

PD1 . . . . . Programmed cell death 1

PD-L1 . . . . . Programmed death-ligand 1

PE . . . . . Phycoerythrin

PerCp-Cy5.5 . Peridin-chlorophyll a-protein cyanine-5.5

PLC-γ1 . . . . Phospholipase C gamma 1

pTα . . . . . Pre-TCR α chain

r/r . . . . . Relapsed or refractory

RAG . . . . . Recombination-activating gene

rpm . . . . . Revolutions per minute

RPMI . . . . . Roswell Park Memorial Institute

RSS . . . . . Recombination signal sequence

RT . . . . . Room temperature

SCD . . . . . Single chain dimer

SD . . . . . Standard deviation

SFK . . . . . Src family kinase

sgRNA . . . . Single guide RNA

SH3 . . . . . SRC homology 3

SHP2 . . . . . Src homology region 2 domain-containing phosphatase-2

SLAM . . . . . Signalling lymphocytic activation molecule

SLB . . . . . (Glass)-supported lipid bilayers

SMAC . . . . . Supramolecular activation cluster

SP . . . . . Single-positive (thymocytes)]

SPR . . . . . Surface plasmon resonance

STAT . . . . . Signal transducer and activator of transcription

SWDSP . . . . Sir William Dunn School of Pathology

T_{reg} . . . . . Regulatory T cell

TAA . . . . . Tumour associated antigen

TAE . . . . . Tris-acetate-EDTA

TanCAR . . . Bispecific tandem CAR

TAP . . . . . Transporter associated with antigen processing

TCR . . . . . T cell receptor

T_h . . . . . T helper cell

TIL . . . . . Tumour-infiltrating lymphocyte

TLS . . . . . Tumour lysis syndrome

TNF-α . . . . . Tumour necrosis factor α

T_{reg} . . . . . Regulatory T cell

TSA . . . . . Tumour specific antigen

TSS . . . . . Transcriptional start site

VEGF . . . . . Vascular endothelial growth factor

WPRE . . . . Woodchuck Hepatitis virus post-transcriptional regulatory element

WT1 . . . . . Wilms' tumour protein

ZAP-70 . . . . Zeta-chain-associated protein kinase 70

Me pongo el sol al hombro y el mundo es amarillo

I carry the sun on my shoulder — and the world is yellow

— Facundo Cabral

1 Introduction

Contents

1.1 An overview of cancer immunotherapy 1
1.2 The role of T cells 5
1.2.1 The cornerstones of adaptive immunity 6
1.2.2 T cell selection, central and peripheral tolerance . . . 8
1.2.3 The inherent cross-reactivity of the TCR 12
1.2.4 Of TCRs and CARs 14
1.3 The evolution and challenges of ACT 16
1.3.1 The clinical landscape of CAR-T cells 18
1.3.2 Current challenges in ACT 20
1.4 Studying CD2 in the context of ACT 27
1.4.1 CD2 biology: an overview 27
1.4.2 A rationale for studying CD2 in ACT 29
1.5 Scope and structure of this work 31

1.1 An overview of cancer immunotherapy

Some of the first studies observing the association between the immune system and cancer were conducted in the late 19th century. W. Busch and F. Fehleisen recorded, independently, spontaneous tumour regression in patients who contracted erysipelas, a skin infection caused by *Streptococcus pyogenes*[3,4]. A few years later, in 1891, W. Coley reported a number of cancer regressions

after injecting patients with extracts obtained from heat-inactivated bacteria such as *S. pyogenes* and *Serratia marcescens*[5,6]. Analyses conducted between 1969 and 1975, which looked at the efficacy of these extracts (known as Coley's toxins) in patients treated before 1940, suggested that up to 35% of patients with soft-tissue sarcoma achieved relapse-free survival for at least 10 years[7]. However, Coley's toxins failed to achieve widespread adoption for multiple reasons. First, W. Coley described more than 12 formulations for these toxins and employed diverse methods of administration. This, in turn, meant that other contemporary physicians failed to reproduce his findings[6,8]. Second, the advent of radiotherapy and chemotherapy during the first half of the 20$^{\text{th}}$ century provided physicians with new tools to tackle a broad range of malignancies[9]. In contrast, Coley's toxins appeared to work preferentially against soft-tissue sarcomas, exhibiting reduced response rates when used against other types of cancer such as melanoma or carcinoma[7,9]. In addition, the United States Federal Drug Administration (FDA) reclassified Coley's toxins as an investigational (or *new*) drug in the context of the 1962 Kefauver–Harris Amendments. This meant that the use of these toxins was strictly limited to clinical trials, which further hindered its adoption[6,9,10].

By the middle of the 20$^{\text{th}}$ century, L. Thomas and F. Macfarlane had independently postulated the cancer immunosurveillance hypothesis, arguing that the immune system was capable of recognising and destroying malignant cells presenting tumour specific neoantigens[11]. This hypothesis was further supported when interferon (IFN)-γ was shown to provide protection against tumour development[12,13], with subsequent studies[14] confirming that T cells were capable of directly attacking malignant tissue. Cancer immunotherapy proposes harnessing the immune system to combat cancer; the recent success of this approach has led some authors to consider immunotherapy as the fourth pillar against cancer, complementing the triad of surgery, chemotherapy, and radiotherapy[15]. Cancer immunotherapy can be divided into three broad categories: immune checkpoint blockade, cancer vaccines, and adoptive cell transfer (or adoptive cell therapy, ACT).

Immune checkpoint blockade

Immune checkpoint therapies have been helped by the improved understanding of the multiple co-stimulatory and co-inhibitory cell surface receptors[16] that regulate T cells. Under normal circumstances, co-inhibitory receptors such as cytotoxic lymphocyte antigen (CTLA)-4 and programmed cell death (PD)-1 prevent T cell overreaction and help maintain peripheral tolerance (see Section 1.2). Checkpoint therapy relies on the antibody blockade of inhibitory receptors or ligands, disengaging the regulatory axes of molecules such as CTLA4 and PD1 and enhancing antitumour immunity[17]. Multiple monoclonal antibodies (mAbs) against CTLA4, PD1, and programmed death-ligand 1 (PD-L1) are currently being used in the clinic after receiving regulatory approval from the United States Federal Drug Administration (FDA). We present a summary here:

- **Anti-CTLA4 mAbs:** Ipilimumab, a human immunoglobulin (Ig)-G1 anti-CTLA4 mAb, has been shown to improve the survival of patients with melanoma[18]. Ipilimumab was the first checkpoint mAb approved by the FDA, back in 2011.

- **Anti-PD1 mAbs:** Both pembrolizumab and nivolumab can improve the prognosis in multiple classes of cancer, including melanoma, renal and hepatocellular carcinoma, and Hodgkin lymphoma[3]. Uniquely, pembrolizumab was recently approved for use in solid tumours with microsatellite instability, making it the first tissue-agnostic, biomarker-defined therapy[19].

- **Anti-PD-L1 mAbs:** Atezolizumab, avelumab, and durvalumab, are all licensed for use against urothelial carcinoma. Additionally, avelumab is used for treatment of Merkel and renal cell carcinomas; durvalumab is also used against non-small-cell lung cancer[3].

Cancer vaccines

Cancer vaccines can be broadly classified depending on whether they act as prophylactic or therapeutic agents. In terms of prophylaxis, the protection offered by vaccines against hepatitis B and human papillomavirus (HPV) directly reduces the risk of liver and cervical cancer[20]. The majority of cancer vaccines are therapeutic, and in this category we can further divide them depending on the delivery chassis in cellular, peptide, DNA/RNA, and viral vector vaccines[20].

Cellular vaccines rely on either cancer cells or autologous dendritic cells (DCs) pulsed with cancer antigens. For example, GVAX vaccines rely on administering whole tumour cells that are genetically engineered to express granulocyte-macrophage colony-stimulating factor (GM-CSF). The tumour cells, which can be autologous or allogeneic, are irradiated to avoid further cellular division after infusion[21]. In DC vaccines, patient-derived DCs are exogenously loaded with peptide antigens or transfected with specific antigen genes. Sipuleucel-T is an FDA-approved vaccine for the treatment of metastatic castration-resistant prostate cancer: it is generated by *ex vivo* activation of autologous DCs using a chimeric protein obtained by fusing GM-CSF to prostatic acid phosphatase[22].

Viral vector vaccines employ viruses encoding cancer antigens, with the idea of eliciting antigen presenting cell (APC) activation and subsequent T cell priming against malignant cells. PROSTVAC-VF/Tricom is a regime that utilises one injection of vaccinia virus followed by six boosters with fowlpox virus. These viruses have been modified to encode prostate-specific antigen plus three co-stimulatory molecules, namely CD58, CD80, and the intercellular adhesion molecule (ICAM)-1[23]. PROSTVAC-VF/Tricom is currently being tested in combination with nivolumab (NCT02933255) and ipilimumab (NCT02506114) for prostate cancer.

Peptide and DNA/RNA cancer vaccines directly administer these molecules to the patient. Short synthetic peptides can bind directly to class I major histocompatibility complexes (MHCs) and activate $CD8^+$ T cells. Synthetic long peptides containing both MHC class I and II epitopes can be taken up by

professional APCs such as DCs, and induce priming of $CD4^+$ and $CD8^+$ T cells[20]. Both DNA and RNA vaccines follow a similar rationale, except that, after cellular delivery, the antigens need to undergo the process of transcription (for DNA only), translation, and MHC processing and presentation. As an example, VGX-3100 is a DNA vaccine expressing the HPV E6 and E7 antigens; it is currently undergoing phase III trials (NCT03185013 and NCT03721978) to assess efficacy against cervical high grade squamous lesions.

Adoptive cell transfer

The principle of ACT is the infusion of autologous or allogeneic T cells into patients with cancer. Some of the first ACT studies were conducted in the context of leukaemia, with allogeneic haematopoietic stem cell transplants mediating regression as a result of a T cell graft-versus-leukaemia response[24]. In 1988, Rosenberg *et al.*[25] showed the feasibility of isolating, expanding, and administering autologous tumour-infiltrating lymphocytes (TILs) to patients with metastatic melanoma. To overcome some of the difficulties associated with TILs, such as their absence in some cancer types, peripheral blood lymphocytes can be isolated from patients and genetically engineered. This enables the expression of transgenic T cell receptors (TCRs) against defined MHC-restricted antigens, as well as the possibility of bypassing MHC-restriction and targeting whole cell surface antigens through chimeric antigen receptors (CARs). In 2017, the FDA approved two CARs targeting the B-lymphocyte antigen CD19 for use against diffuse lymphoma and acute lymphoblastic leukaemia (ALL)[26,27].

1.2 The role of T cells

At its core, adoptive cell transfer consists on the infusion of T cells to a patient with cancer. These T cells are previously expanded *ex vivo* and, in some cases, genetically engineered. As we will see in further sections of this work (Section 1.3), there are a number of challenges that need to be addressed in order to ensure widespread applicability of ACT. Given that some of these challenges can be

better understood in light of the T cell biology, we will first present the reader with some key background material about these cells.

1.2.1 The cornerstones of adaptive immunity

The adaptive immune system, whose function is orchestrated by B and T cells, constitutes a specialised defence against a wide variety of pathogens that a host might encounter during its life. This system, found in jawed vertebrates (Gnathostomata infraphylum)[28], complements the functions of the innate immune system — which depends on defined molecular patterns and nonspecific defences. In the case of B cells, antigen recognition is mediated through Igs with a defined specificity, a process that relies on antigen recognition by their membrane bound B cell receptor (BCR), priming through interactions with T helper cells (T_h), and, ultimately, secretion of antibodies by plasma cells and establishment of memory B cells.

In contrast, antigen recognition by T cells relies on their membrane bound TCRs, which belong to the immunoglobulin superfamily (IgSF). The TCR of conventional α:β T cells* is a heterodimer composed by two (α and β) chains, which are linked by a disulfide bridge. Each chain features two extracellular domains, termed variable (V) and constant (C) regions (Figure 1.1). The TCR heterodimer is solely responsible for antigen recognition: in order to transduce signals, it associates with accessory chains to form an octameric complex. These chains include the CD3 complex (γ, δ, and ε chains) as well as the ζ chain (CD247) (Figure 1.1). Unlike antibodies, TCRs do not bind antigen in their native, three-dimensional conformation. Instead, the TCR recognises peptide strings presented on the surface of polymorphic MHC complexes, which requires a previous process of protein degradation, and peptide processing and loading[29].

*Unless otherwise stated, the term T cell will be used in this work to refer to conventional, MHC-restricted α:β T cells (as opposed to γ:δ, natural killer, or mucosal associated invariant T cells).

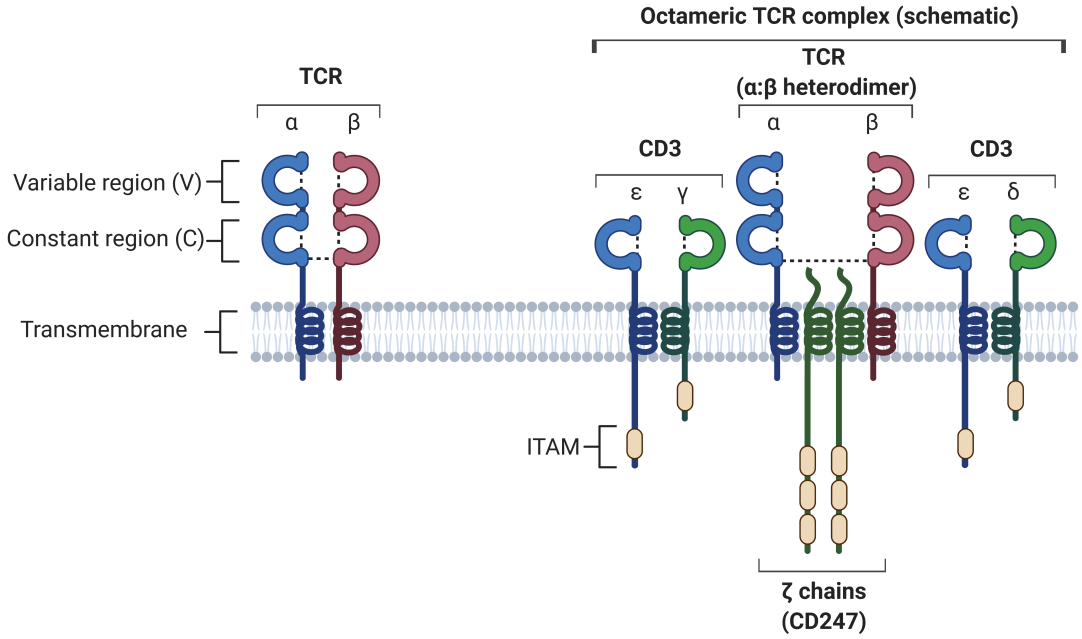


Figure 1.1: Schematic of a conventional α:β TCR. The α:β TCR heterodimer (left) mediates MHC-restricted antigen recognition. Each individual chain has two extracellular regions, termed variable (V) and constant (C). To achieve surface expression and signal transduction, this heterodimer forms an octameric complex (right), characterised by the presence of a ζ:ζ homodimer, as well as the ε:γ and ε:δ heterodimers from the CD3 complex. These accessory chains are responsible for signal transduction, a process mediated in first instance by phosphorylation of their immunoreceptor tyrosine-based activation motifs (ITAMs). This picture is not to scale and it is only used to illustrate the different components of the TCR complex. For a detailed structural view, see the work from De Dong *et al.*[30].

TCR gene rearrangement

The generation of TCRs occurs through several events sharing similarities with B cell immunoglobulin gene rearrangement, a process that was first explored by S. Tonegawa[31,32], who was then awarded the 1987 Nobel Prize in Physiology or Medicine. In a similar manner to the *IGK* and *IGL* loci, the *TRA* locus contains variable (V_α) and junction (J_α) gene segments. Conversely, the *TRB* locus shares some characteristics with the *IGH* locus, as it contains V_β, J_β, and diversity (D_β) segments (Figure 1.2). These gene segments are surrounded by 12- and 23-bp recombination signal sequences (RSSs), which are recognised by two proteins known as recombinating activating gene (RAG)-1 and RAG-2, whose protein products are essential in the V(D)J rearrangement process[33–35]

and eventual lymphocyte maturation[36].

The α chain of the TCR is generated through somatic VJ recombination, which brings together a V_α and a J_α segment, creating a $V_\alpha-$region exon. Once this rearrangement has taken place, mRNA splicing plays a role in forming a functional α chain by joining the VJ_α product to the unique C_α gene segment. Formation of a functional TCR β chain occurs through a similar VDJ recombination process. Here, the $V_\beta-$region exon is generated after a V_β, a D_β, and a J_β gene segment are brought together. This procedure takes place in two steps. First, DJ recombination brings together either: (i) the $D_{\beta 1}$ gene segment with any of the $J_{\beta 1}$ segments, or (ii) the $D_{\beta 2}$ gene segment with any of the $J_{\beta 2}$ segments. The subsequent V-DJ step brings joins a V_β segment with the recently rearranged DJ_β segment. The VDJ_β product is finally assembled with the C_β gene segment during splicing. T cell receptor diversity can be predominantly mapped to six (three per chain) variable loops known as complementarity determining regions (CDRs). For both the α and β chains, the CDR1 and CDR2 loops interact primarily with the MHC at the interface between the TCR and a peptide MHC (pMHC). They are encoded within the V gene segments. The CDR3 regions are located right at the centre of the TCR/peptide interface. The CDR3 loops are located right at the junction between the V, (D), and J gene segments, and they derive some of their variability from the random addition of P- and N-nucleotides (or, indeed, nucleotide deletion) at these junctions.[33–35]

1.2.2 T cell selection, central and peripheral tolerance

Positive and negative selection

T cells are tasked with the difficult job of scanning MHC complexes for foreign peptides that can be derived from a vast array of pathogens. They need to efficiently detect non-self (which is *a priori* unknown) pMHC while ignoring all the self-antigens presented by healthy tissues. Evidence suggests that they can do this with exquisite sensitivity, with single ligands being enough to elicit T cell activation[37,38]. Given that the theoretical number of possible TCRs that can be

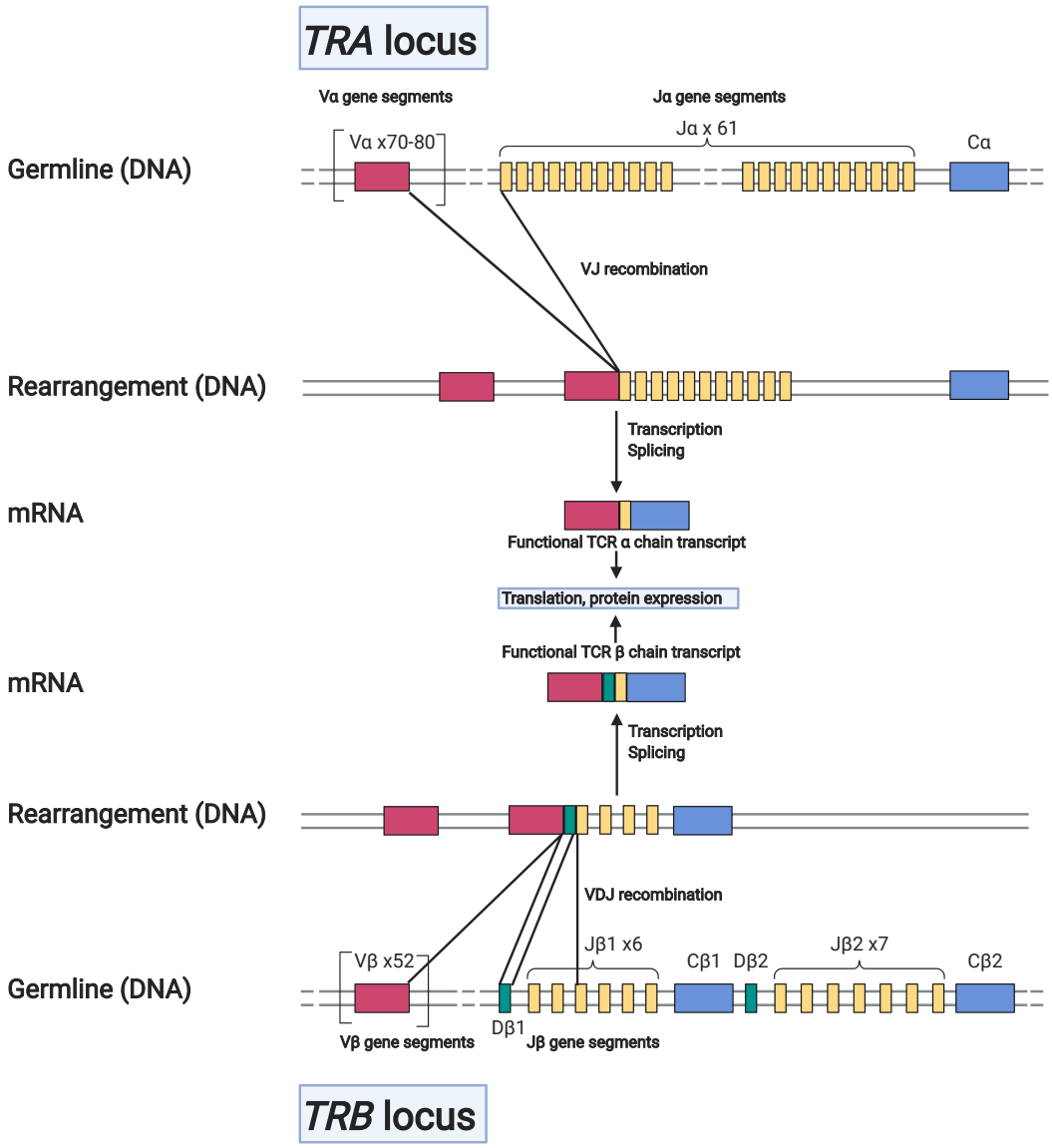


Figure 1.2: TCR gene rearrangement: V(D)J recombination. The generation of diverse α:β TCR chains relies on somatic recombination. The *TRA* locus undergoes VJ recombination, which brings together a V_α and a J_α segment. Once this process has taken place, RNA splicing ensures the generation of a complete α chain by bringing together the exons coding for the VJ_α product and the C_α region. Similarly, rearrangement in the *TRB* locus generates a VDJ_β V-region exon. Splicing ensures that this exon, and the one coding for C_β, are brought together before mRNA cytoplasmic export and translation. See main text for further details. For simplicity purposes, the picture does not depict the *TRD* locus, which is embedded in the *TRA* locus.

generated during the V(D)J recombination process is exceedingly large ($\sim 10^{15}$ for mice and $\sim 10^{18}$ for humans[39,40]), the immune system orchestrates a selection process to ensure the generation of useful and non self-reactive TCRs.

After pluripotent haematopoietic stem cells enter the thymus, cellular interactions with the thymic stroma enable them to start an initial differentiation phase[41], with expression of molecules such as CD2[42]. At this stage, these thymocytes have not undergone gene rearrangement and they do not express CD4 nor CD8 — they are termed double-negative (DN) thymocytes. The DN stage is characterised by the rearrangement and expression of the TCR β chain, which is initially paired with a surrogate pre-TCR α chain (pTα). The pTα:β heterodimer associates with the accessory CD3 and ζ chains, forming a pre-TCR complex. From here, cell proliferation and co-expression of CD4 and CD8 co-receptors ensues, which generates double-positive (DP) thymocytes. Double-positive thymocytes undergo rearrangement of the TCR α chain, which enables formation of an α:β TCR[41].

However, the random nature of the V(D)J recombination implies that a large number of these TCRs will not be functional as a result of not recognising MHC complexes. Positive selection occurs in the thymic cortex, where DP thymocytes interact with pMHCs presented by cortex thymic epithelial cells (cTECs). Only thymocytes capable of recognising MHC class I or class II complexes (with the help of the CD8 or CD4 co-receptor, respectively) will continue their maturation process, which will include the CD4 or CD8 lineage commitment — thus generating single-positive (SP) thymocytes. This process is the basis of MHC restriction; DP thymocytes unable to bind MHC do not receive any stimulation, and therefore undergo apoptosis (*death by neglect*)[41,43].

Negative selection of the SP thymocytes is a necessary process to ensure that T cells will not cross-react with self-antigens; it shapes central tolerance. Experimental systems have suggested that this process can occur in the thymic cortex or the medulla. During negative selection, DCs and medullary thymic epithelial cells (mTECs) present self-antigens[41,43]. Interestingly, mTECs express a protein known as autoimmune regulator (AIRE), which enables them to

express an array tissue-restricted proteins. *AIRE* mutations severely disrupt the negative selection process, leading to a syndrome known as autoimmune polyendocrinopathy-candidiasis-ectodermal dystrophy (APECED)[44]. During negative selection, thymocytes that bind to self-pMHC with strong affinities (and could potentially cross-react with healthy tissues in the periphery) are deleted from the existing pool. Besides TCR/pMHC signals, negative selection can be influenced by the action of both co-stimulatory (*e.g.*, CD5, CD28)[45] and co-inhibitory (*e.g.*, CTLA4)[46] receptors.

Peripheral tolerance

Central tolerance mechanisms are complemented by peripheral tolerance, which acts as an additional checkpoint to restrain peripheral lymphocytes recognising other self-antigens (which were not presented during the negative selection process), or developmental antigens[†]. First, we can consider T cell anergy[47]: naïve T cells that encounter a cognate antigen in the periphery and receive stimulation solely through their TCR (*i.e.*, without CD28/B7 co-stimulation in the context of an activated DC) will become hyporesponsive, repressing TCR signalling, IL-2 production, and proliferation.

Control of autoimmunity is also governed through co-inhibitory receptors, namely PD1 and CTLA4. The PD1 receptor, which expresses after T cell activation, binds to PD-L1 and PD-L2, counter-receptors that are constitutively expressed on APCs, and whose expression can be induced by pro-inflammatory cytokines on other tissues[3]. *Pdcd1*$^{-/-}$ mice display a range of autoimmune affectations, including splenomegaly[49] and lupus-like glomerulonephritis and arthritis[50]. The PD1 axis can aid the process of peripheral tolerance by restraining self-reactive T cells during initial activation, expansion, or at later effector stages in the periphery[43].

[†]Tolerance is also important for food or commensal antigens. In addition, T cell exhaustion[48] can be observed in the context of persistent exposure to *bona fide* antigens, such as chronic infection.

The inhibitory effects of CTLA4 are produced through different mechanisms. The CTLA4 receptor can compete directly with CD28 for available B7 ligands; besides direct competition for CD80 and CD86, it can also mediate their trans-endocytosis[51]. Moreover, the CTLA4 axis is known to recruit the SRC homology (SH)-2 domain-containing tyrosine phosphatase 2 (SHP2), which, in turn, inhibits phosphorylation of the TCR accessory components (such as the ζ chain) and the linker for activation of T cells (LAT)[3]. In agreement with its role as an inhibitory receptor, *Ctla4*$^{-/-}$ mice are affected by a severe lymphoproliferative disorder[52]. This inhibitory receptor is particularly relevant in lymphoid organs, namely: (i) during the initial priming process, where it is constitutively expressed by CD4$^+$ CD25$^+$ regulatory T cells (T_{regs}); and (ii) after T cell activation, when primed T cells express CTLA4, which modulates their state[3]. The characteristics of the PD1 and CTLA4 co-inhibitory receptors can help understand the premise behind immune checkpoint blockade, which we discussed in Section 1.1.

The regulatory tolerance coordinated by T_{regs} is not only enabled by their inhibitory membrane-bound receptors (such as CTLA4, LAG3, and TIGIT), but also through the production of inhibitory cytokines, including IL-10 and transforming growth factor (TGF)-β (reviewed by Schmidt *et al.*[53]). Tolerogenic DCs can supress T cell activation: although they provide TCR stimulation through self-pMHC, they do not offer *bona fide* co-stimulation (which can induce anergy) and can express PD-L1 and PD-L2. Other types of cells, such as lymph node stromal cells, appear to be capable of presenting MHC-I restricted antigens for the purposes of mediating peripheral tolerance[54].

1.2.3 The inherent cross-reactivity of the TCR

In 1998, D. Mason argued[55] against the *one clonotype — one specificity* paradigm, which postulated that a given lymphocyte would be highly specific for a single antigen only and would not recognise alternative ligands. Using a series of theoretical calculations, he reasoned that the universe of peptides that could bind to MHC class I and II would be in the order of $\sim 10^{10}$ for nonamers and

$\sim 6 \times 10^{12}$ for dodecamers[55]. For mice, the existence of a single clonotype for each combination would be dimensionally impossible[55]. More recent theoretical calculations suggest that mice and humans only maintain a total of $\sim 10^7$ and $\sim 10^{10}$ TCR clonotypes, respectively[56].

D. Mason posited that, given these restrictions, efficient detection of pathogens by the adaptive immune system required an elevated degree of TCR cross-reactivity. He presented conservative estimations that suggested a single TCR would recognise at least 3×10^5 peptides[55]. Later on, experimental work would support his view, with some TCRs such as the 1E6 receptor being shown to recognise more than 10^6 peptides[57]. For particular TCRs, studies have shown that binding orientation can play a role in their cross-reactivity: examples include the DMF4 and the 2C TCRs (see the review from Sewell[40]). In this particular context, we note that the 1E6 TCR can sustain cross-reactivity despite its rigid binding mode[40]. Moreover, Zareie *et al.* have recently shown[58] that the docking polarity of the TCR plays a crucial role in colocalising CD8 and Lck with the CD3 and ζ chains, and that TCRs that bind in a reverse orientation exhibit poor signalling — a mechanism that, in their view, could be used by the immune system to reduce the instances of cross-reactivity.

The inherent TCR cross-reactivity underlies the phenomenon of heterologous immunity, where a given TCR is capable of recognising different peptides derived from more than one pathogen. For example, the bacillus Calmette-Guérin (BCG) tuberculosis vaccine has been reported to induce protection against leprosy[59], and it could potentially provide protection against SARS-CoV-2[60]. Cross-reactivity can also mediate deleterious effects of autoimmune nature: although the central and peripheral tolerance mechanisms are meant to control self-reactive T cells[43], they are not infallible. If a weakly self-reactive cell enters the periphery and becomes activated after recognising an epitope derived from a pathogen, the highly sensitive memory T cells could ultimately mount a response against healthy tissues. This unintended cross-reactivity is known as molecular mimicry; the

appearance of autoimmune disease following the course of an infection supports this notion (reviewed by Cusick *et al.*[61]).

1.2.4 Of TCRs and CARs

In this work, we perform our experiments using a TCR. A proportion of the ACT clinical studies in malignancies are conducted using TCRs[62], with engineering strategies being actively developed[63]. As of today, however, CAR-T cells (more specifically, anti-CD19 CARs) dominate the landscape of ongoing trials[62] and clinically approved products (Section 1.3.1). In principle, we consider that our findings could have applicability in the field of CARs (Chapter 6). We should note, however, that the molecular architecture of TCRs and CARs is fundamentally different — something that, more likely than not, dictates the functional traits exhibited by these receptors.

As we previously indicated, the canonic α:β TCR heterodimer (Figures 1.1 and 1.3A) integrates into an octameric complex. Within this complex, signalling is provided by CD3 (formed by ε:δ and γ:ε heterodimers) and a ζ:ζ homodimer. These signalling chains feature immunoreceptor tyrosine-based activation motifs (ITAMs). The tyrosine residues of the ITAMs can undergo phosphorylation by Src family kinases (SFKs) such as Lck, which enables docking of the ZAP-70 tyrosine kinase[64]. There is not a consensus regarding the nature of the specific TCR triggering mechanism upon *bona fide* antigen recognition. Diverse models postulate this process occurs through receptor aggregation, conformational change (mechanotransduction), or segregation (reviewed by van der Merwe and Dushek[65]).

After ZAP-70 recruitment, this protein can undergo activation, a process mediated by Lck phosphorylation and trans-auto-phosphorylation. From here, ZAP-70 can phosphorylate the scaffold protein linker for activation of T cells (LAT) and the SLP-76 adaptor. After phosphorylation, LAT orchestrates the recruitment of multiple proteins, including Grb2, SOS, Gads, Vav1, and PLC-γ1. The LAT signalosome constitutes a pivotal point for the activation of TCR signalling through the major biochemical pathways of mitogen-activated protein

kinase (MAPK) and phosphatidylinositol lipids[66]. The cascades conclude with the activation of key transcription factors, including: (i) the nuclear factor κ-light-chain-enhancer of activated B cells (NF-κB), (ii) the nuclear factor of activated T cells (NFAT), and (iii) the activator protein (AP)-1[67].

In contrast, CARs are single chain molecules generated through the fusion of antibody-derived single-chain variable fragments (scFvs, which dictate CAR specificity) with intracellular signalling motifs. These motifs ordinarily incorporate the ζ chain plus a co-stimulatory motif derived from a TCR co-receptor such as 4-1BB (CD137) or CD28 (see Section 1.3 and Figures 1.3D to 1.3G). In the same way as the TCR, the specific triggering mechanism of CAR-T cells has not been elucidated; plausible processes include kinetic segregation (KS)[68] or mechanotransduction[69]. CAR triggering leads to phosphorylation of its ζ component and other proteins such as ZAP-70, SLP-76, and PLC-γ1[70]. Although this suggests similarities between the activation cascades mediated by CARs and TCRs, the former have been reported to signal even in the absence of LAT[71]. In addition, the distinct CAR designs that include additional domains from other receptors provide a co-stimulatory stimulus (signal 2) to T cells — something that does not happen with the canonical TCR[70].

One of the key differences between TCRs and CARs relates to antigen specificity and sensitivity. Since CARs derive their antigen specificity from scFvs, they are not MHC-restricted and can target membrane bound proteins (including specific glycoforms) and gangliosides[72]. However, CARs are known to exhibit reduced antigen sensitivity compared to TCRs, which can mediate activation with as little as one pMHC ligand[37,38]. The sensitivity defect of CARs is estimated to be of 2–3 orders of magnitude compared to TCRs[73,74], and it could be related to inefficient ZAP-70 recruitment and activation[68]. Appending further ITAMs does not rescue this defect[68], although co-opting the full TCR machinery through the expression of scFvs in the N-terminal region of the α, β, or CD3 chains[75] appears to improve the function of engineered T cells.

As we will discuss in the next section and throughout this work, these biological characteristics could explain some of the toxicities observed in ACT. Indeed, on account of their remarkable sensitivity, therapeutic TCRs can sometimes detect low levels of healthy tissues bearing tumour associated antigens (TAAs) and destroy them. Moreover, affinity enhanced TCRs —which did not undergo thymic selection— can cross-react with self-pMHC, severely compromising their safety[‡].

1.3 The evolution and challenges of ACT

Although the first clinical trials using autologous TILs and interleukin (IL)-2 showed promising response rates between 40 and 60%, the median duration of these responses was only 4 months[25,76]. Additional studies suggested that these infused TILs only persisted for 3–8 weeks[77]. In 2002, a study by Dudley *et al.*[78] illustrated how conditioning with cyclophosphamide and fludarabine improved the expansion profiles of TILs. Subsequent work indicated that lymphodepletion regimes were useful as they eliminated cellular *sinks* for cytokines such as IL-2, IL-7, and IL-15; eradicated immunosuppressive cells such as myeloid-derived suppressor cells (MDSCs) and $CD4^+$ $FOXP3^+$ T_{regs}; and upregulated co-stimulatory molecules expressed by tumours (see commentary from Neelapu[79]). These conditioning regimes are commonly used in ACT, as they have been proven to improve patients' outcomes[80].

The use of transgenic TCRs in ACT opened the possibility of treating cancer patients without having to first obtain reactive TILs from the patient. This process was first demonstrated by Morgan *et al.*[81]. They used the DMF4 TCR, a MART-1/HLA-A*02-reactive receptor that was transduced into *ex vivo* expanded peripheral blood lymphocytes and mediated some regression of metastatic melanoma. The development of affinity enhanced TCRs opened new opportunities for improving the responses mediated by wild type (usually low affinity) TCRs, although most of the promising results using these receptors have been limited to

[‡]This particular cross-reactivity, termed off-target/off-tumour toxicity, has not been clinically reported for conventional (*i.e.*, non-MHC restricted) CARs that derive their specificity from antibody-derived scFvs. Refer to Section 1.3.2.

those targeting the New York esophageal squamous cell carcinoma (NY-ESO)-1 antigen (reviewed by Rath and Arber[63]).

One of the developments that would play an important part in modern ACT stems from the work of Kuwana *et al.*[82], who —in 1987— demonstrated that T cells could be rewired and endowed with recognition against non-MHC restricted antigens. By transfecting a fusion receptor composed of antibody, Ig-derived variable regions and murine TCR constant regions[§], the authors generated a chimera that assembled with the accessory chains of the native TCR (Figure 1.3) and conferred T cells with anti-phosphorylcholine activity. Although the findings of Kuwana *et al.* would be replicated by others[83], this type of chimera (sometimes referred to as a T-Body) would fail to gain widespread adoption in the field. Considering the historical context, this could be attributed to the difficulties associated with co-transfecting T cells with two chimeric chains. Interestingly, the concept of T-Bodies has recently resurfaced[84] in the literature as a receptor candidate for further assessment in ACT.

Some of the first instances of rewiring T cells through the use of single chain fusion proteins can be found in the 1991 work of Irving and Weiss[85], and Romeo and Seed[86]. Irving and Weiss constructed a chimeric protein by fusing the extracellular and transmembrane region of the CD8 co-receptor with the cytoplasmic tail of the ζ chain (CD247) from the TCR complex. Expression of this CD8/ζ chimera was not dependent on the components of the CD3 complex and, upon anti-CD8 antibody stimulation, CD8/ζ Jurkat cells were capable of fluxing calcium, upregulating CD69, and producing IL-2[85]. Concurrently, Romeo and Seed reported the generation of CD4/ζ and CD4/FcRγ[¶] fusion proteins. When $CD8^+$ cytotoxic lymphocytes (CTLs) were transduced with either CD4/ζ or CD4/FcRγ, they acquired the capability of recognising and killing target cells expressing the gp120 human immunodeficiency virus (HIV) envelope protein[86].

[§]The fusion receptor was assembled by co-transfecting either V_H-C_α plus V_L-C_β or V_H-C_β plus V_L-C_α chains[82].

[¶]These chimeras had the extracellular region of the CD4 co-receptor fused to the transmembrane and cytosolic components of the ζ chain or the Fc receptor common γ chain (FcRγ)[86].

Shortly afterwards, Eshhar *et al.*[87] illustrated the feasibility of redirecting T cells against a wide variety of antigens through the expression of a single chain receptor. In their first iteration, these CARs (Figure 1.3) consisted of fusion proteins generated by joining an antigen-reactive scFv with a hinge, a transmembrane region, and a signalling tail derived from either the ζ or FCRγ chains. These CARs effectively endowed T cells with the specificity of antibodies, enabling recognition of non-MHC restricted antigens[87]. However, the *in vivo* efficacy of first generation CARs targeting cancer antigens was limited since the engineered T cells failed to exhibit robust proliferation and cytokine production[88]. Further progress in the field was made with the development of second and third generation CARs, characterised by possessing one or two extra co-stimulatory motifs derived from T cell co-receptors such as CD28, 4-1BB, OX40 (CD134) or CD27, among others. These additional domains can be helpful in enhancing T cell survival, proliferation, and cytotoxicity[89–91]. Further iterations, termed armoured constructs, enable constitutive expression of cytokines or soluble versions of certain ligands (*e.g.*, herpesvirus entry mediator — HVEM) to improve the activation profiles (see the reviews written by Royal and Lim[92] or Rafiq *et al.*[93]).

1.3.1 The clinical landscape of CAR-T cells

CAR-T cells have seen success in the context of haematological malignancies: as of 2021, there are three different products that have received regulatory approval from both the FDA and the European Medicines Agency (EMA)[94]. They are all second generation CARs targeting CD19:

- **Tisagenlecleucel (Kymriah):** Developed by Novartis, this anti-CD19 4-1BB/ζ CAR is indicated for the treatment of young adults with acute lymphoblastic B-cell leukaemia, as well as adults with diffuse large B-cell lymphoma (DLBCL).
- **Axicabtagene ciloleucel (Yescarta):** This anti-CD19 CD28/ζ CAR is currently indicated for treatment of relapsed or refractory (r/r) DLBCL. This product belongs to Kite Pharma and Gilead.

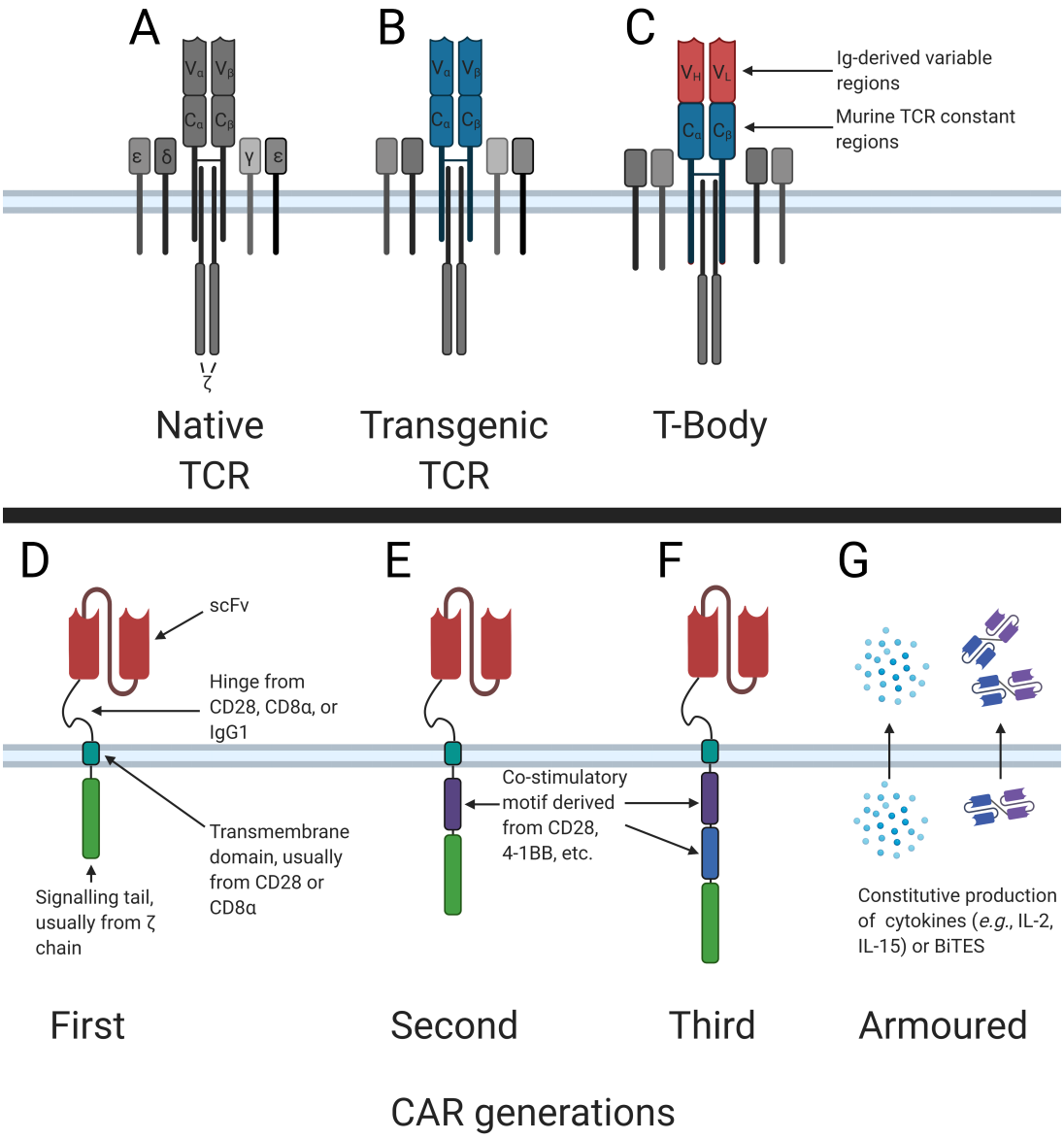


Figure 1.3: Selected examples of receptors that can be used in ACT. Infused T cells can express a variety of receptors, including: **A.** Their native TCR (when using autologous TILs), **B.** A transgenic TCR, **C.** A T-Body[84], or **D-F.** A first, second, or third generation CAR (depending on the number of co-stimulatory domains). **G.** When a CAR-T cell is engineered to express cytokines or other soluble molecules such as BiTEs, it is said to be *armoured.*

- **Brexucabtagene autoleucel (Tecartus):** Tecartus has the same architecture as Yescarta, but the manufacturing process includes a separate step for T cell enrichment. It has been licensed for use against r/r mantle cell lymphoma.

Despite the success of ACT against haematological malignancies, CARs have failed to exhibit similar results when targeting solid tumours (see next section). In fact, the vast majority of current CAR constructs undergoing testing are against markers associated with liquid tumours. In 2020, it was estimated[62] that more than 75% of the CAR-T cells in clinical trials targeted haematological markers (*e.g.*, CD19, CD20, CD22, or CD123), with the rest covering possible targets in solid tumours such as human epidermal growth factor receptor 2 (HER2/neu, also known as ERBB2), Mucin 1 (MUC1), or Glypican-3. In fact, no CAR-T cell trial targeting solid tumours has progressed to phases III–IV (compare this with the three FDA- and EMA-approved anti-CD19 CARs plus multiple additional therapies against r/r myeloma and r/r non-Hodgkin lymphoma in phases III–IV)[62,94].

1.3.2 Current challenges in ACT

Although the three CAR-T cell products that have been approved for clinical use against leukaemia and lymphoma are a testament of the success achieved by ACT, there are a large number of challenges that still need to be addressed (Figure 1.4). We can classify these challenges into three broad categories: streamlining manufacturing, preventing relapse, and reducing toxicity. In this section, we present a concise account of these opportunity areas, which have been reviewed extensively elsewhere[93,95]. Afterwards, we detail in Section 1.4 our rationale for studying the CD2 co-receptor in the context of ACT with a view towards ameliorating two types of *off-target* toxicity currently encountered in ACT — the main purpose of this work.

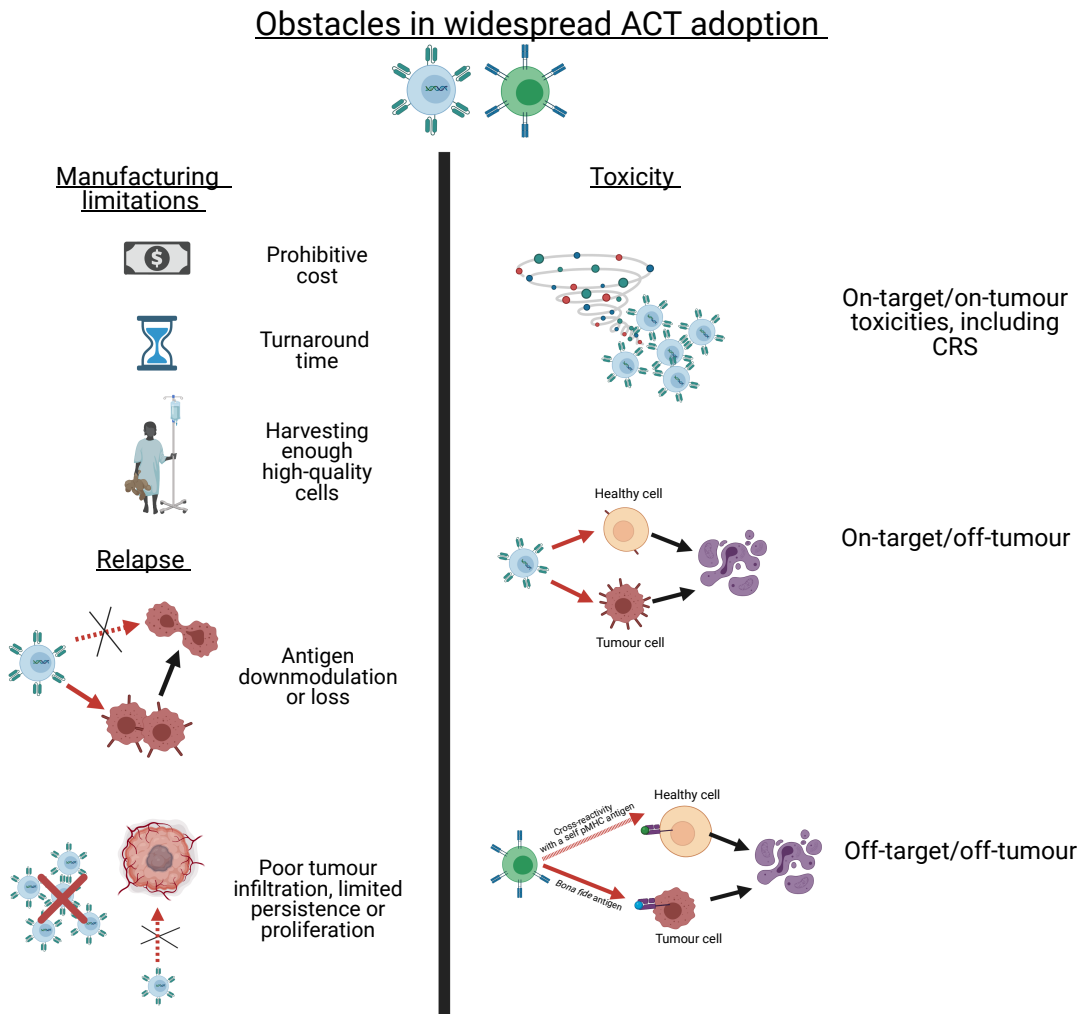


Figure 1.4: Current challenges in ACT. Despite the success of CAR-T cells against leukaemia and lymphoma, multiple problems prevent ACT from achieving wider adoption. These problems are mainly related to manufacturing, overall efficacy (particularly against solid tumours), and toxicities.

Manufacturing limitations

Widespread adoption of ACT is currently limited by the complex manufacturing process of autologous therapy products. First, we can consider the cost: it is estimated that treatment with axicabtagene ciloleucel (Yescarta) can cost more than 370 000 USD[96], something that has limited universal access to ACT in public health systems such as the National Health Service (NHS)[97]. In addition, obtaining enough T cells to start the process of *ex vivo* expansion and transduction can be problematic in paediatric patients or those suffering from lymphopaenia as a result of chemotherapy. Finally, the time required to complete the manufacturing

process and infuse the engineered T cells (2–4 weeks) can be too long for patients with very advanced malignancies[93].

In general, these limitations could be overcome by using allogeneic donor T cells for ACT, as the pipeline would be simplified and become independent of the health status of patients. Some studies have illustrated the feasibility of allogeneic ACT[98,99], although the main problem with this strategy stems from the unintended immune recognition between the T cells derived from the donor and the patient's tissue. In particular, graft-versus-host-disease (GvHD) has been linked to toxicity[98] and even patient fatalities[100]. Mitigation of GvHD can be achieved by selecting donor cells with specificity to non-self (*e.g.*, viral epitopes)[101], or by targeted genetic modifications such as disruption of the endogenous α or β TCR chains[93,102].

In addition to GvHD, there are also concerns about host-versus-graft reactions limiting the efficacy of allogeneic ACT. For this problem, potential solutions include the genetic disruption of human leukocyte antigen (HLA)-A[103] or β_2 microglobulin (β2M)[104]. Since these approaches would not solve the graft rejection mediated by natural killer (NK) cells, Mo *et al.*[105] have proposed armouring the donor T cells with alloimmune defence receptors, which can detect 4-1BB upregulation and mediate a targeted elimination of activated T or NK cells from the host.

Relapse prevention in solid and liquid tumours

Consistently achieving durable remission and long term survival of patients is an area where ACT has room for improvement. As we previously indicated, the needs are particularly pressing for solid malignancies as no ACT trial has progressed to phases III–IV[62,94]. However, cancer relapse has also been documented in trials against leukaemia where the CAR-T cells targeted CD19 (relapse rate of 30%)[106] or CD22 (relapse rate of 50%)[107].

Antigen modulation (including downmodulation or loss) can induce relapse in both solid[108] and liquid[106,107] malignancies. Gudipati *et al.*[68] have previously

shown that CARs are much less sensitive to antigen than TCRs by 2–3 orders of magnitude; therefore, the adoption of TCR-T cells could mitigate the instances of tumour escape as a result of antigen downmodulation[‖]. For antigen-negative relapses, a possible solution is the use of combinatorial approaches, which employ either bispecific tandem CARs (TanCARs) or the transduction of two individual CARs against different antigens[95,109]. Moreover, CAR-T cells targeting one antigen can be armoured to secrete bispecific T-cell engagers (BiTEs) against a second antigen, recruiting bystander T cells and minimising the risk of tumour escape[110].

Antigen-positive relapse can occur when the adoptively transferred T cells exhibit poor proliferation, short-term persistence and/or exhaustion. This problem can be intrinsic to the T cells or —particularly in the case of solid malignancies— caused by an immunosuppressive tumour microenvironment (TME). Studies with anti-CD19 CAR-T cells, have shown that second generation 4-1BB/ζ CARs ameliorate exhaustion compared to CD28/ζ and ζ receptors[111]. In addition to this, the number of ITAMs[112] in the ζ region of CARs affects the fate of engineered T cells, with fewer ITAMs favouring a naïve- or memory-like status over an effector-like one — potentially reducing exhaustion. Interestingly, it appears that the insertion site of CARs can steer T cell fate. In particular, insertion of the CAR construct in the *TRAC* locus appears to improve T cell activity and reduce tonic signalling[113]. Other studies have shown that T cell clones with *TET2* disruption as a result of CAR transduction display improved potency and a central memory phenotype[114].

The TME can prevent efficient T cell infiltration, survival, and proliferation; it represents a formidable challenge for therapies targeting solid malignancies. The TME is characterised by a series of aberrations as a result of uncontrolled cell proliferation, including: changes in the extracellular matrix, production of reactive oxygen species, low pH, limited nutrient availability, and hypoxic

[‖]For those cases where the target antigen is not-MHC restricted, such as EGFR or CD19, using T-Bodies could arguably bridge the CAR/TCR frontier, as seen in pre-clinical studies[84].

conditions [115]. The infiltrate can contain cells such as: (i) T_{regs} (which produce the IL-10 and TGF-β regulatory cytokines), (ii) MDSCs (which can suppress CTL response through the production of arginase-1 and prostaglandin E2), (iii) tumour-associated (M2) macrophages, which enable angiogenesis through secretion of vascular endothelial growth factor (VEGF), and (iv) neutrophils, which can also produce VEGF. Since these cells can downmodulate the action of adoptively transferred T cells and facilitate tumour growth, their presence represents a barrier to tumour clearance (see the reviews from D'Aloia *et al.*[109] and Rad *et al.*[115]). Although management of solid tumours is still an unmet need in ACT, possible avenues include the use of CAR-T cells that produce IL-2, IL-7, or IL-15[93,116], or that express an scFv recognising TGF-β[117] — potentially converting an inhibitory signal into a stimulatory one. In addition, the use of TCR-T cells and/or the CRISPR/Cas9-mediated disruption of inhibitory co-receptors such as PD1[118,119] could improve the efficacy of ACT.

Reducing toxicity

Adoptive cell transfer can result in diverse unintended toxicities, which we can broadly divide in **on-tumour** and **off-tumour**. One can start by considering **on-target/on-tumour** toxicities, which include cytokine release syndrome (CRS) as well as tumour lysis syndrome (TLS). In the case of CRS, an overactivation of the adoptively transferred cells can lead to a systemic and disordered production of pro-inflammatory cytokines by the infused cells, which in turn results in the activation of other immune cells (*e.g.*, monocytes, macrophages). This generates a feedback loop, with consequences that range from fever or hypotension to multiple organ failure[120]. In the case of TLS, the rapid destruction of malignant cells —with the subsequent release of their contents into the bloodstream— can compromise renal function as a result of a metabolic imbalance (hyperuricemia, hypocalcemia, and hyperphosphatemia)[121]. Cytokine release syndrome is usually treated with antibodies directed against the IL-6 receptor (tocilizumab) and corticosteroids[95,120]. Tumour lysis syndrome is usually treated with intravenous

hydration and rasburicase to mitigate hyperuricemia[121]. Moreover, acute toxicity episodes can be mitigated if the cells are engineered to express specific ligands such as CD20, in which case antibody-mediated depletion (with rituximab in the case of CD20) is used to kill the infused cells[93]. In addition, cells can be programmed to express kill switches, such as a modified caspase 9 protein that dimerises upon the administration of a small molecule, leading to apoptosis of the infused cells[93].

The use of anti-CD19 CARs has also been reported to cause neurotoxicity, oftentimes in association with CRS. Symptoms can range from confusion and agitation to seizures and cerebral oedema. Like CRS, treatment can include tocilizumab and corticosteroids such as dexamethasone (reviewed by Neelapu *et al.*[122]). The mechanisms responsible for neurotoxicity are yet to be fully elucidated, although suggestions include: (i) trafficking of CAR-T cells into the central nervous system, (ii) cytokine-mediated activation of brain vascular pericytes (which then produce IL-6 and start a feedback loop that increases permeability of blood brain barrier), and (iii) destruction of healthy brain mural cells expressing CD19[123,124].

In ACT, TCR- or CAR-T cells are rewired to target a particular antigen expressed by malignant cells. **On-target/off-tumour** toxicities occur when the engineered cells recognise this antigen in healthy tissues and destroy them. Theoretically, this problem could be avoided if lymphocytes were engineered to only target tumour specific antigens (TSAs) such as MHC-restricted neoantigens or virally-derived oncoproteins[63,125]. However, the majority of the current targets in ACT can be characterised as TAAs. We can place TAAs in different classes: (i) overexpressed self-antigens such as HER2/neu or Wilms' tumour protein (WT1), (ii) differentiation antigens such as melanoma antigen recognised by T cells (MART)-1 or oncofoetal antigens, and (iii) cancer/testis antigens, which include NY-ESO-1 and the melanoma-associated antigen (MAGE)[95,126].

On-target/off-tumour recognition of healthy cells has been observed in multiple instances of ACT. Parkhurst *et al.*[127] reported induced transient colitis when treating colorectal cancer with an engineered TCR recognising carcinoembryonic antigen (CEA), which is commonly overexpressed in epithelial cancers. The

adverse events were linked to destruction of intestinal crypt epithelial cells, which have weak CEA expression. Other instances of on-target/off-tumour toxicity have been reported for CARs targeting epidermal growth factor receptor (EGFR), carbonic anhydrase IX (CAIX), and NKG2DL[128–130]. In a CAR clinical study targeting HER2/neu[131], a patient fatality was registered; it is possible that this death was caused by recognition of low levels of the target antigen in lung epithelial cells. Some of the approaches suggested to prevent this type of toxicity include reducing the affinity of the engineered receptors[132–134], as well as programming cells so that they only become activated upon simultaneously recognising two TAAs[93] (detailed in Section 4.1.1).

Off-target/off-tumour toxicity occurs when T cells expressing a therapeutic receptor cross-react with an unintended antigen. This phenomenon has been documented in affinity enhanced TCRs, which have not undergone the process of thymic selection (Section 1.2.2) meant to prevent self-pMHC recognition. In a clinical trial with the affinity enhanced a3a MAGE-A3/HLA-A*01-reactive TCR (K_D = 2.3 μM), two patients died as a result of cardiovascular toxicity. This off-target/off-tumour toxicity was linked to the unintended recognition of a low affinity ($K_D \approx 100$ μM) peptide from titin protein presented on the HLA-A*01 of cardiomyocytes[135,136]. Further structural analyses[137] of the MAGE-A3$_{168-176}$ (EVDPIGHLY) and the titin$_{394-403}$ (ESDPIVAQY) epitopes** revealed that, in the TCR/MAGE-A3 and TCR/titin complexes, the TCR adopted very similar docking conformations. Hence, the off-target/off-tumour cross-reactivity of the a3a TCR could traced to the the titin/HLA-A*01 complex acting as a structural mimic of MAGE-A3/HLA-A*01.

We note that this type of toxicity has not been reported in clinical trials using CAR-T cells[138], although *in vitro* studies have shown that high affinity MHC-restricted CARs[139], as well as TCRs[140], can display a generalised cross-reactivity against self-peptides presented on the HLA. The prevalence of these

**These analyses used a TCR (termed MAG-IC3) derived from the original, wild type TCR (clone 103/EB81[136]) that recognised the MAGE-A3/HLA-A*01 complex. The MAG-IC3 K_D values for MAGE-A3 and titin are 7.1 and 76.7 nM, respectively[137].

problems could be mitigated by affinity tuning of the receptors and by robust pre-clinical screening procedures using different types of primary tissues and cell lines[141] (see Section 5.1.1).

1.4 Studying CD2 in the context of ACT

1.4.1 CD2 biology: an overview

Structure and binding kinetics

Human CD2 is a transmembrane protein that belongs to the IgSF: including its signal peptide, it has a length of 351 amino acids[††]. It is composed of two extracellular Ig-like domains (positions 25–128 and 129–209), a helical transmembrane region (positions 210–235) and a disordered, proline-rich cytoplasmic tail (positions 236–351) (UniProt P06729). In humans, it is expressed by T cells, NK cells, and thymocytes[42]. The main ligand of human CD2 is the ubiquitously expressed CD58, also known as lymphocyte function-associated antigen (LFA)-3. The CD58 ligand also possesses two Ig-like extracellular domains (UniProt P19256). Experimental reports have indicated that human CD2 can bind, albeit weakly, to CD48[142], a ligand that belongs to the signalling lymphocytic activation molecule family (SLAM) and is expressed mainly in haematopoietic cell lineages[143]. However, subsequent SPR analyses failed to detect binding between human CD2 and CD48[144], so it is not clear whether this interaction has functional significance in humans.

The CD2/CD58 complex is primarily stabilised by polar interactions between the membrane-distal domains of both molecules, and it spans an intercellular distance of 13–15 nm, similar to that of the TCR/pMHC complex[42,145]. The affinity (K_D) of this interaction is $\sim$5 μM[146], which is similar to that of other co-stimulatory axes such as CD28/CD80 (K_D = 4 μM[147]). In solution, the CD2/CD58 interaction has a fast off-rate ($k_{off} > 3.9$–$5.3\ s^{-1}$)[144,146].

[††]Throughout this work, references to specific amino acids will consider the signal peptide unless otherwise specified.

The 1982 work by Sánchez-Madrid *et al.*[148] found that blocking antibodies against human CD2 hindered killing by CTLs. Using *Cd2*$^{-/-}$ mice, Bachmann *et al.*[149] quantitated the changes in T cell antigen sensitivity linked to CD2 expression. He found that *in vitro* sensitivity was reduced by a factor of 3–10 fold, although *Cd2*$^{-/-}$ mice were still able to clear induced infections caused by lymphocytic choriomeningitis virus (LCMV). Evans *et al.*[150] also found that *Cd2*$^{-/-}$ mice were capable of initiating, mounting, and maintaining a normal immune response against LCMV.

It is difficult, however, to establish a direct parallelism between human and mouse CD2. First, rodents do not have a direct homologue to human CD58. The main counter-receptor of mouse CD2 is CD48, a molecule with a haematopoietic-restricted expression in both mouse and humans[143]. The affinity of rodent CD2/CD48 interactions has not been thoroughly documented, but it appears to be weak: Davis *et al.*[151] report a K_D of $\sim$90 μM for mouse, with a $k_{off} > 11$ s^{-1}. Work on rat CD2/CD48 interactions from van der Merwe *et al.*[152] found a $K_D \approx$ 60–90 μM, with a $k_{off} > 6$ s^{-1}. Despite its low affinity and fast off-rates, the CD2/CD48 interaction is biologically relevant, as it has been shown to improve the antigen sensitivity of mouse T cells[149,153]. The same can not be said of human CD2/CD48, where SPR analyses were not able to detect binding[144] and a definite biological relevance has yet to be established.

Of note, the CD48 counter-receptor can also bind to CD244 (also known as 2B4), another member of the SLAM family which is expressed on monocytes, NK cells, γ:δ T cells, and some CD8$^+$ T cells[143]. The CD48/CD244 human and mouse affinities are $\sim$8 and $\sim$16 μM, respectively[154]. In murine NK cell models, CD244 was shown to either promote or inhibit killing, an ambivalence that was explained by the existence of two isoforms with either a short or long cytoplasmic tail[155]. Expression of CD244 in CD8$^+$ T cells appears to mediate different effects. Reports indicate a role of CD244 in limiting cytotoxicity, reducing persistence of memory CD8$^+$ T cells during chronic infection, or even

increasing cytolysis through CD48/CD244 interactions between neighbouring T cells (reviewed by McArdel *et al.*[143]).

Signalling considerations

Not only does the CD2 co-receptor contribute to T cell activation as an adhesion molecule (promoting binding to cognate antigen)[2], but also its tail (which is conserved across species[156]) is involved in signalling. The disordered, proline-rich tail of CD2 contains five putative SH3 domains, which enable interactions with multiple proteins. Studies using either rat or human cells have suggested interactions with multiple proteins, including kinases (Fyn, Lck), CD2-binding proteins 1 and 2, CD2-associated protein, and Cbl-interacting protein of 85 kDa (reviewed by Binder *et al.*[42]). The CD2 receptor is also relevant in the context of the immunological synapse (IS), the interface formed between a T lymphocyte and a target cell[157] establishing a *bona fide* contact. Within the supramolecular activation clusters (SMACs) that characterise the IS, one can distinguish concentric regions — namely a central, peripheral, and distal SMAC (cSMAC, pSMAC, and dSMAC, respectively)[158]. The CD2/CD58 complexes can be found within the cSMAC, along other TCR/pMHC and co-stimulatory interactions such as CD28/CD80[159]. Recent evidence[160] suggests that CD2/CD58 can also be found within the frontier of the pSMAC and the dSMAC, forming a corolla capable of amplifying signalling from Src family kinases, PLC-γ1, and LAT.

1.4.2 A rationale for studying CD2 in ACT

In addition to the primary signal provided by an antigen, T cells receive further information through the integration of cues from co-stimulatory (or co-inhibitory) receptors, and cytokines. Co-signalling (see Chen and Flies[16]) has been extensively studied in the context of naïve T cell priming, and it is also a factor to consider in ACT. In the first instance, the improved survival and proliferation of CAR-T cells that express motifs derived from CD28 or 4-1BB is a testament to the importance of co-stimulation in ACT[89,90]. In addition, the absence of co-stimulation through

CD28 plus the engagement of inhibitory receptors such as PD1 has been recognised as a hindrance in tumour clearance (particularly in solid malignancies[161]). Finally, ACT can include the use of certain cytokines such as IL-2, IL-7, or IL-15 — either in the form of armoured CARs[92,93] or systemic administration[162].

We have previously written a review where we argued[2] that T cells employ a number of co-receptors and other molecular mechanisms in order to achieve high antigen sensitivity. We broadly classified them in mechanisms that: (i) promote binding to the cognate antigen, (ii) induce quick signalling, and (iii) amplify signalling. In the case of mechanisms that promote receptor/antigen binding, we recognised the role of the CD2 co-receptor in promoting and stabilising close contacts between a T cell and an APC or target antigen. This notion is supported by early studies using murine models, which found that *Cd2*$^{-/-}$ mice exhibited reduced antigen sensitivity compared to their wild type counterparts[149]. Although there are some differences between CD2 in mice and humans it is reasonable to consider that human CD2 plays a similar role in antigen sensitivity, a notion that has been previously entertained[163] but not thoroughly explored.

On the basis that human CD2 increases antigen sensitivity by promoting binding between a T cell and a target cell, we hypothesised that this co-receptor mediates the following unintended off-tumour toxicities in ACT:

- **On-target/off-tumour** toxicities that occur when engineered T cells targeting overexpressed TAAs destroy healthy tissues bearing low levels of the target antigen[131] (Figure 1.4).
- **Off-target/off-tumour** toxicities observed when engineered T cells expressing affinity enhanced receptors cross-react with self-peptides. Note that, usually, these unintended interactions possess a low affinity[136] (Figure 1.4).

Our starting rationale is that the CD2 co-receptor enables some of these toxicities in the context of ACT by virtue of enabling signalling when a T cell encounters a **weak antigen**. We define a weak antigen as one that either: (i) is expressed at low densities or (ii) has a low affinity to its receptor — and thus

might mediate unintended toxicities within our framework. **Here, we hypothesise that manipulation of the human CD2/CD58 axis can ameliorate the instances of either on-target/off-tumour or off-target/off-tumour toxicity in ACT**.

1.5 Scope and structure of this work

We consider this work as a starting point in assessing whether routine manipulations of the CD2/CD58 axis would be useful in reducing two different classes of off-target toxicity in ACT. Although we rely only on *in vitro* procedures, we make use of primary human $CD8^+$ T cells that are engineered using a similar pipeline as that followed in the clinic (Section 2.7.3). Wherever possible, we look at effector readouts such as killing and cytokine production, which are the terminal functions in ACT.

Including the introduction, we have divided this work into six chapters. Chapter 2 covers materials and methods and Chapter 6 presents the general conclusions. The rest of the material is divided as follows:

- **Chapter 3**, which establishes a cellular platform to assess the quantitative contribution of the human CD2/CD58 axis in antigen recognition. To minimise the risk of additional co-receptors providing compensatory mechanisms —and obscuring the specific effects mediated by CD2/CD58— the platform relies on cross-species interactions, using rodent cells as surrogate APCs.

- **Chapter 4** deals with on-target/off-tumour toxicity. Using the platform we developed, we assess two techniques to manipulate the CD2/CD58 axis. In particular, we trial direct genetic disruption of *CD2* and transduction of elongated CD2 chimeras (under the assumption that they might act as dominant negatives over endogenous CD2[145]).

- **Chapter 5** replicates the off-target/off-tumour cross-reactivity previously observed in an affinity enhanced TCR[140]. Afterwards, we quantify the effects of *CD2* disruption in the mitigation of this particular toxicity and, more generally, in T cell recognition of altered peptide ligands (APLs) with varying affinities.

2

Materials and methods

Contents

2.1 List of reagents 34
2.2 Consumables and equipment 39
2.3 Molecular biology 40
2.3.1 General subcloning routines 40
2.3.2 Plasmid constructs 42
2.3.3 Generation of messenger RNA 45
2.4 APLs of the NY-ESO-1 epitope 47
2.5 Flow cytometry 47
2.5.1 Preparation of pMHC tetramers 47
2.5.2 Cytometry and general data acquisition 48
2.5.3 Absolute cytometric quantitation of CD2 and CD58 . 49
2.6 Quantitation of cytokine production and cytotoxicity 50
2.6.1 Enzyme-linked immunoassays 50
2.6.2 T cell cytotoxicity 51
2.7 Tissue culture routines 51
2.7.1 Production of lentiviral supernatants 51
2.7.2 Cell lines: procurement, generation, and maintenance 52
2.7.3 Primary cells 55
2.8 Stimulation and conjugation assays 57
2.8.1 Stimulation with adherent cells 57
2.8.2 Stimulation with suspension cells 58
2.8.3 Conjugation assays 59
2.9 Data analysis 60

2.1 List of reagents

Table 2.1: General and molecular biology reagents. The abbreviations introduced in this table are: ethylenediaminetetraacetic acid (EDTA), bovine serum albumin (BSA), dimethyl sulfoxide (DMSO), enzyme-linked immunosorbent assay (ELISA), and phycoerythrin (PE).

Beginning of Table		
Reagent	**Manufacturer**	**Catalogue number**
0.5 M EDTA, pH 8.0	Thermo Fisher Scientific	15-575-020
2xYT medium	In-house provision	
Acetic acid	Merck	695092
Agar-agar	In-house provision	
Agarose	Bio-Rad	1613101
Ampicillin agar plates (100 μg/mL)	In-house provision	
BSA	Merck	A7906
Carbenicillin disodium salt	Merck	C1389
Chloramphenicol	Merck	C3175
CyQUANT LDH Cytotoxicity Assay	Thermo Fisher Scientific	C20301
DNA oligos	Merck (custom made)	
DMSO	Merck	D8418
DpnI	New England Biolabs	R0176S
Ethanol	Merck	32221
Ethidium bromide (10 mg/mL)	Merck	E1510
Gateway LR Clonase II Enzyme Mix	Thermo Fisher Scientific	11791-020
Gel Loading Dye, Purple (6X)	New England Biolabs	B7024S
GeneRuler 1 kb DNA ladder	Thermo Fisher Scientific	SM0313
HiSpeed Plasmid Maxi Kit	Qiagen	12662
Human IFN-γ Uncoated ELISA Kit	Thermo Fisher Scientific	88-7316-77
Human IL-2 Uncoated ELISA Kit	Thermo Fisher Scientific	88-7025-77
Human MIP-1β Uncoated ELISA Kit	Thermo Fisher Scientific	88-7034-77
Human TNF-α Uncoated ELISA Kit	Thermo Fisher Scientific	88-7346-77

Continuation of Table 2.1		
Reagent	**Manufacturer**	**Catalogue number**
Isopropanol	Merck	278475
Kanamycin agar plates (30 μg/mL)	In-house provision	
Kanamycin B sulfate salt	Merck	B5264
KLD Enzyme Mix	New England Biolabs	M0554S
MEGAclear Transcription Clean-up Kit	Thermo Fisher Scientific	AM1908
Methanol-free 16% formaldehyde (w/v)	Thermo Fisher Scientific	28906
mMESSAGE mMACHINE T7 ULTRA Transcription Kit	Thermo Fisher Scientific	AM1345
NEBuilder HiFi DNA Assembly Master Mix	New England Biolabs	E2621S
NEB 5-alpha competent *Escherichia coli*	New England Biolabs	C2987H
NEB Stable competent *E. coli*	New England Biolabs	C3040H
NucleoSpin Gel and PCR Clean-up Kit	Macherey-Nagel	123033668
Oligopeptides	GenScript (custom made)	
One Shot ccdB survival competent *E. coli*	Thermo Fisher Scientific	A10460
PE-streptavidin	Biolegend	405245
Q5 High Fidelity 2X Master Mix	New England Biolabs	M0492S
QIAPrep Spin Miniprep Kit	Qiagen	27106
Quantum MESF Alexa Fluor 647	Bangs Laboratories	BLI647A
Quantum MESF R-PE	Bangs Laboratories	827-5
Sulfuric acid	Merck	339741
Trizma base	Merck	T1503
TWEEN 20	Merck	P1379
End of Table		

Table 2.2: Cell culture reagents. The abbreviations introduced in this table are: carboxyfluorescein succinimidyl ester (CFSE), Dulbecco's modified Eagle medium (DMEM), Dulbecco's phosphate-buffered saline (DPBS), foetal bovine serum (FBS), and Roswell Park Memorial Institute (RPMI).

Beginning of Table		
Reagent	**Manufacturer**	**Catalogue number**
CFSE	Biolegend	423801
CTS OpTmizer T Cell Expansion SFM	Thermo Fisher Scientific	11132D
DMEM	Merck	D6429
DPBS	Merck	D8537
Dynabeads Human T-Activator CD3/CD28	Thermo Fisher Scientific	11132D
FBS	Merck	F9665
Ficoll Paque Plus	Amersham Biosciences	17-1440-02
G418 sulfate (50 mg/mL)	Thermo Fisher Scientific	10131027
ImmunoCult Human CD3/CD28 T Cell Activator	Stemcell Technologies	10991
L-Glutamine (200 mM)	Thermo Fisher Scientific	25030024
Lenti-X Concentrator	Takara Bio	631231
MojoSort Human anti-PE Nanobeads	Biolegend	480090
Opti-MEM with GlutaMAX	Thermo Fisher Scientific	51985034
Penicillin-streptomycin (10 000 U/mL and 10 000 μg/mL)	Thermo Fisher Scientific	15140122
Puromycin dihydrochloride	Merck	P8833
Recombinant human IL-2	PeproTech	200-02
RosetteSep Human $CD8^+$ T Cell Enrichment Cocktail	Stemcell Technologies	15063
RPMI 1640 Medium	Merck	R8758
Solution 13	Chemometec	910-3013
Tag-it Violet Dye	Biolegend	425101
TrypLE Express	Thermo Fisher Scientific	12604013
X-tremeGENE HP Transfection Reagent	Merck	06366546001

Continuation of Table 2.2		
Reagent	**Manufacturer**	**Catalogue number**
Zombie NIR Fixable Viability Kit	Biolegend	423106
End of Table		

Table 2.3: Flow cytometry antibodies. The abbreviations introduced in this table are: allophycocyanin (APC), brilliant violet (BV), and peridin-chlorophyll a-protein cyanine-5.5 (PerCp-Cy5.5).

Beginning of Table				
Antibody target (clone)	**Species**	**Conjugate**	**Manufacturer**	**Catalogue number**
FLAG tag (L5)	Mouse	PE	Biolegend	637310
HA tag (GG8-1F3.3.1)	Mouse	PE	Miltenyi Biotec	130-120-717
Human CD2 (TS1/8)	Mouse	APC	Biolegend	300214
Human CD2 (TS1/8)	Mouse	BV421	Biolegend	309128
Human CD2 (TS1/8)	Mouse	PE	Biolegend	309208
Human CD19 (HIB19)	Mouse	BV421	Biolegend	302234
Human CD45 (HI30)	Mouse	BV421	Biolegend	304032
Human CD58 (TS2/9)	Mouse	PE	Biolegend	330905
Human CD69 (FN50)	Mouse	Alexa Fluor 488	Biolegend	310916
Human CD69 (FN50)	Mouse	PerCp-Cy5.5	Biolegend	310926

Continuation of Table 2.3				
Antibody target (clone)	**Species**	**Conjugate**	**Manufacturer**	**Catalogue number**
Human CD137 (4B4-1)	Mouse	Alexa Fluor 647	Biolegend	309824
Human HLA-A2 (BB7.2)	Mouse	PE	Biolegend	343306
IgG1, κ isotype control (MOPC-21)	Mouse	APC	Biolegend	400120
IgG1, κ isotype control (MOPC-21)	Mouse	BV421	Biolegend	400158
IgG1, κ isotype control (MOPC-21)	Mouse	PE	Biolegend	400114
End of Table				

Table 2.4: Buffers and their composition. The abbreviations introduced in this table are: tris-acetate-EDTA (TAE) and phosphate-buffered saline (PBS).

Buffer	**Composition**
ELISA washing buffer	PBS 0.05% TWEEN 20
Flow cytometry fixing buffer	PBS 1% BSA 4% formaldehyde
Flow cytometry staining buffer	PBS 2% FBS 2 mM EDTA
TAE buffer, pH 8.0	40 mM Trizma base, 20 mM acetic acid, 1 mM EDTA

2.2 Consumables and equipment

Table 2.5: Main consumables.

Item	Manufacturer	Catalogue number
6-well tissue culture plates	Corning	3516
12-well tissue culture plates	Greiner	665180
96-well Maxisorp plates	Thermo Fisher Scientific	442404
96-well tissue culture plates, flat bottom	Corning	3596
96-well tissue culture plates, round bottom	Corning	3799
96-well tissue culture plates, conical bottom	Corning	3898
Syringe end filters 0.22 μm	Sartorius	16534-K
Syringe end filters 0.45 μm	Sartorius	16555-K
T25 flasks	Corning	430639
T75 flasks	Corning	430641U
T175 flasks	Corning	431080

Table 2.6: Main equipment used.

Beginning of Table	
Equipment	**Manufacturer**
Allegra X-15R centrifuge	Beckman Coulter
BD FACSAria III cell sorter	BD Biosciences
BD X-20 flow cytometer	BD Biosciences
Gel Doc XR system	Bio-Rad
Cytek flow cytometer	Cytek Bio
Cytoflex flow cytometer	Beckman Coulter
ECM 830 Square Wave Electroporator	BTX
ELx405 microplate washer	BioTek
Galaxy 170R incubator	Eppendorf
Megafuge 8R centrifuge	Thermo Fisher Scientific
Mini horizontal gel unit for electrophoresis	Geneflow
Nanodrop 2000 spectrophotometer	Thermo Fisher Scientific

Continuation of Table 2.6	
Equipment	**Manufacturer**
Nucleocounter NC-3000 cell counter	Chemometec
Proflex PCR thermal cycler	Thermo Fisher Scientific
SpectraMax M5 Gemini plate reader	Molecular Devices
End of Table	

2.3 Molecular biology

2.3.1 General subcloning routines

Polymerase chain reaction, electrophoresis, and Gibson assembly

Polymerase chain reaction (PCR) runs were carried out in a final volume of 50 μL using the Q5 High Fidelity 2X Master Mix (New England Biolabs), with the forward and reverse primers at a final concentration of 10 μM. Routine PCRs were conducted in a Proflex PCR thermal cycler (Thermo Fisher Scientific) and consisted of: (i) an initial denaturation (98 °C for 30 s); (ii) 25–35 cycles of denaturation (98 °C for 30 s), primer annealing (50–72 °C for 10–30 s), and extension (72 °C for 30 s/kb); and (iii) a final extension step (72 °C for 10 min). Products were purified with a NucleoSpin Gel and PCR Clean-up Kit (Macherey-Nagel) according to manufacturer's instructions. The concentration and purity of the products were verified using a Nanodrop 2000 spectrophotometer (Thermo Fisher Scientific).

For mutagenic PCRs, the KLD Enzyme (New England Biolabs) protocol was followed. Appropriate primers were designed using the NEBaseChanger tool (http://nebasechanger.neb.com/) and a routine PCR conducted. One microlitre of PCR product was mixed with 5 μL of KLD Reaction Buffer, 1 μL of KLD Enzyme Mix, and 3 μL of dH_2O. The reaction was incubated at 37 °C for 30 min and then at 25 °C for an additional 30 min. Samples were placed on ice for subsequent transformation.

In some instances, analytical or preparative agarose gel electrophoresis of DNA products was conducted. For this, a solution of tris-acetate-EDTA (TAE; EDTA

stands for ethylenediaminetetraacetic acid) buffer with 1% agarose was heated up using a microwave until the agarose was completely dissolved. The solution was allowed to cool down and ethidium bromide added to a final concentration of 0.5 μg/mL. Afterwards, the solution was used to cast a gel in a horizontal electrophoresis unit (Geneflow). DNA samples were mixed with gel loading dye (New England Biolabs) and subjected to electrophoretic separation for 30–50 min at 60–75 V. Results were verified using a Gel Doc XR system (Bio-Rad). In the case of preparative electrophoresis, DNA was recovered using the NucleoSpin Gel and PCR Clean-up Kit according to manufacturer's instructions.

Gibson assembly reactions were conducted using the NEBuilder HiFi DNA Assembly Master Mix (New England Biolabs). To reduce levels of background colonies, PCR products (25–50 μL) derived from plasmids were digested by direct addition of 10 U of DpnI followed by incubation at 37 °C for 1 h. All DNA products were purified and quantitated as previously described. For the assembly process, the manufacturer's protocol was followed. Chiefly, 20 μL reactions were conducted using a vector:insert DNA molar ratio of of 1:2 (using approximately 50–100 ng of vector per reaction). Samples were incubated at 50 °C for 60 min and then immediately placed on ice for subsequent transformation.

Bacterial transformation and plasmid isolation

E. coli strains were chosen according to the nature of the plasmid that would undergo propagation. In general, propagations were conducted with NEB 5-alpha competent bacteria (New England Biolabs). For lentiviral transfer plasmids and for plasmids carrying the *ccdB* gene, transformations used the NEB Stable (New England Biolabs) and the One Shot ccdB survival (Thermo Fisher Scientific) strains, respectively. In all cases, one aliquot of the chemically competent bacteria was thawed on ice and then carefully mixed with the plasmid of interest (50–100 ng in the case of retransformations and 2–10 μL of the final reaction for Gibson or mutagenic reactions). The bacteria were incubated on ice for 30 min and then heat shocked at 42 °C for 45 s, followed by a rest period of 5 min on ice.

Afterwards, 1 mL of 2xYT media was added and bacterial recovery allowed for 1 h at 37 °C before plating on the appropriate selection agar. Antibiotics used included: 100 μg/mL of ampicillin, 30 μg/mL of kanamycin, or 100 μg/mL of carbenicillin plus 35 μg/mL of chloramphenicol.

After overnight incubation at 37 °C, single colonies were aseptically transferred into 5 mL of 2xYT media with selection antibiotic. For small-scale plasmid isolation, bacteria were incubated at 37 °C and 180 revolutions per minute (rpm) for 16–20 h and then subjected to plasmid extraction using the QIAPrep Spin Miniprep Kit (Qiagen). For isolation at larger scales, the starter culture was grown for 8 h at 37 °C and 180 rpm, and then used to inoculate a larger volume (200–500 mL) of 2xYT media with selection antibiotic. Bacteria were then incubated at 37 °C and 180 rpm for 16–20 h before plasmid isolation was conducted with Qiagen's HiSpeed Plasmid Maxi Kit. In both instances, manufacturer's instructions were followed and the resultant plasmid solutions stored at 4 °C.

2.3.2 Plasmid constructs

Multiple plasmid constructs were used in this project. When working with second generation lentiviral transfer plasmids, packaging was carried out using psPAX2 (Addgene #12260) and pMD2.G (Addgene #12259). For transfer plasmids compatible with a third generation lentiviral system, the packaging plasmids included pMD2.G, pRSV-Rev (Addgene #12253), and pMDLg/pRRE (Addgene #12251). All these plasmids were a gift from D. Trono.

The 1G4 TCR is a receptor that binds the NY-ESO-$1_{157-165}$/HLA-A*02 pMHC complex; it was initially isolated from a patient with melanoma[164]. This TCR was a gift from Adaptimmune Ltd. The wt/c51 TCR is an affinity mutant derived from the 1G4 TCR; whereas the 1G4 TCR has an affinity of 32 μM (K_D) to the canonical NY-ESO-$1_{157-165}$/HLA-A*02 pMHC complex (SLLMWITQC), the wt/c51 has a K_D of 25 nM (see the work of Tan *et al.*[140]). This construct was also a gift from Adaptimmune Ltd. Both receptors were received in a third generation

self-inactivating transfer vector with an Elongation Factor (EF)-1α promoter and the Woodchuck Hepatitis virus post-transcriptional regulatory element (WPRE).

To generate the cell lines described in this work, multiple lentiviral transfer vectors were used. Their construction was aided by commercial synthesis services provided from Thermo Fisher Scientific, as well Gibson assembly and mutagenic PCR procedures. In all cases, constructs synthesised by Thermo Fisher Scientific were delivered in the Gateway-compatible pDONR221 vector (Thermo Fisher Scientific). The constructs were then shuttled into lentiviral transfer vectors, including the pLEX_307 (Addgene #41392, a gift from D. Trono) and the pLEX307-NeoR (Addgene #134365, a gift from O. Dushek). Note that the pLEX_307 backbone confers puromycin resistance, while the pLEX307-NeoR vector confers G418 resistance. The entry clones —contained in pDONR221— were recombined into lentiviral transfer vectors using the Gateway LR Clonase II Enzyme Mix (Thermo Fisher Scientific) according to the protocol suggested by the manufacturer.

A summary of the key characteristics of the lentiviral transfer vectors used is shown below. The reader can also refer to Figure 2.1 for a schematic of the CD2 chimeras generated. All references to specific amino acids are made considering the full-length protein (*i.e.*, the signal peptide is taken into account).

- **CD58$^{\mathbf{FLAG}}$**: Created by intercalating a FLAG tag (DYKDDDDK) between the signal peptide (amino acids 1–28) and the rest of the human CD58 protein (UniProt P19256, canonical isoform). The fusion protein was synthesised by Thermo Fisher Scientific and shuttled into pLEX_307.

- **SCD−HLA−A*02**: A single chain dimer (SCD) encoding a fusion of full-length human β2M and human HLA-A*02 (amino acids 25–365) via a $(GGGGS)_3$ linker was kindly provided by E. Denham. This construct was recombined into pLEX307-NeoR using Gibson assembly.

- **CD2$^{\mathbf{HA}}$**: Generated by intercalating an HA tag (YPYDVPDYA) between the signal peptide (amino acids 1–24) and the rest of human CD2

(UniProt P06729). The fusion protein was synthesised by Thermo Fisher Scientific and shuttled into pLEX_307.

- **$CD2^{HA}$-2Ig**: To generate this, a KDPK linker and the sequence corresponding to amino acids 25–209 of human CD2 —including a K67E mutation to abrogate CD58 binding[165]— was inserted between the ectodomains of $CD2^{HA}$ and its transmembrane region. This generated a CD2 chimera elongated by the two Ig domains provided by the V-type and C2-type Ig-like domains of human CD2. The fusion protein was synthesised by Thermo Fisher Scientific and shuttled into pLEX_307.

- **$CD2^{HA}$−4Ig**: Gibson assembly was carried out on the construct coding for $CD2^{HA}$-2Ig. This assembly was used to duplicate the two additional Ig domains carrying the K67E mutation and to place them right before the transmembrane region of the chimeric protein. This generated a CD2 chimera elongated by a total of four Ig domains.

- **$CD2^{HA}$−7Ig**: Created by inserting the seven Ig domains of human CD22 (UniProt P20273, amino acids 20–676) between the extracellular and transmembrane regions of $CD2^{HA}$. This process was conducted with Gibson assembly and using a human CD22 clone purchased from Invivogen.

- **$CD2^{HA}$−$CD43^{Ecto}$**: Created by inserting a GGGGS linker and the extracellular region (amino acids 20–253) of human CD43 (UniProt P16150) right before the transmembrane amino acids of $CD2^{HA}$. This process was conducted with Gibson assembly and using a human CD43 clone, a gift from Q. Sattentau.

- **$CD2^{HA}$ −ΔCyt, $CD2^{HA}$−2Ig−ΔCyt and $CD2^{HA}$−4Ig−ΔCyt**: Starting from $CD2^{HA}$, $CD2^{HA}$−2Ig and $CD2^{HA}$−4Ig, respectively, mutagenic PCR was conducted to delete amino acids 246-351 from the cytoplasmic tail of CD2, leaving only 10 amino acids in the intracellular region (amino acids

236-245). This deletion was carried out using the KLD Enzyme Protocol (New England Biolabs) described in Section 2.3.1.

- **lentiCRISPR−CD2$^{\mathbf{KO}}$**: This corresponds to a second generation lentiviral transfer plasmid containing: (i) a single guide RNA (sgRNA) targeting *CD2* (target sequence: 5'−CGATGATCAGGATATCTACA−3') under the control of a U6 promoter and (ii) human-optimised Cas9 nuclease from *S. pyogenes*. This plasmid was commercially acquired from Horizon Discovery (catalogue number GSGH11935). Note the lentiCRISPR-CD2$^{\mathrm{KO}}$ plasmid also confers puromycin resistance.

2.3.3 Generation of messenger RNA

In some instances, generation of messenger RNA (mRNA) coding for the 1G4 and the wt/c51 TCRs was conducted. To this end, T7-polymerase compatible PCR templates were generated. The forward primers had the following structure: 5'−(N_{6-10})<u>TAATACGACTCACTATAGGG</u>(N_{3-6})CCACC**ATG**G(N_{17-22})−3'. In the previous sequence, the T7 promoter sequence is <u>underlined</u> and the translation starting site is presented **in bold**. The reverse primers had the structure 5'−T_{70}**TTA**(N_{17-22})−3', with the stop anticodon **in bold**. PCR products were generated as described previously, and purified using the NucleoSpin Gel and PCR Clean-up Kit. In accordance to manufacturer's instructions, mRNA was synthesised using the mMESSAGE mMACHINE T7 ULTRA Transcription Kit, and purified using the MEGAclear Transcription Clean-up Kit (both from Thermo Fisher Scientific). The resultant products were stored at -80 °C and thawed right before use.

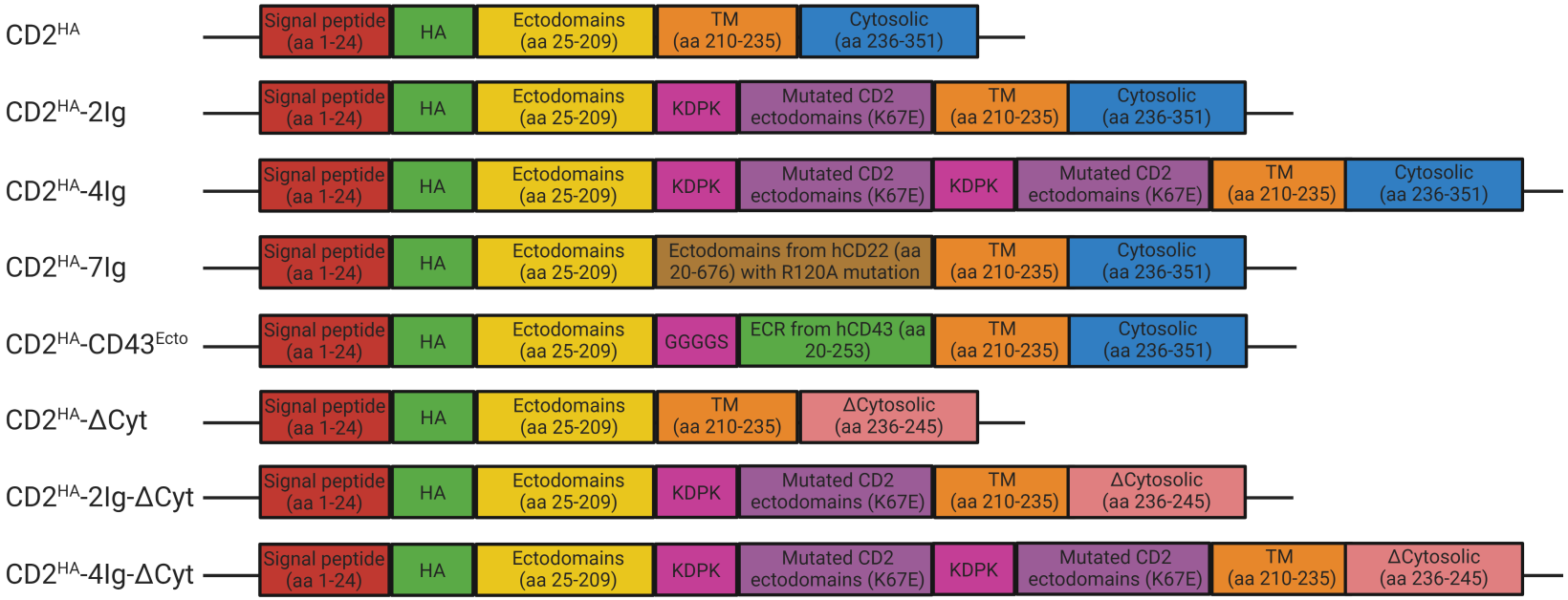


Figure 2.1: Summary of the CD2 chimeras used for cell transduction. Unless otherwise specified, the amino acid positions refer to those of full-length human CD2 (UniProt P06729). TM and ECR stand for transmembrane and extracellular region, respectively. HA refers to the protein tag derived from human influenza hemagglutinin (YPYDVPDYA).

2.4 APLs of the NY-ESO-1 epitope

The wild type NY-ESO-$1_{157-165}$ peptide (hereinafter NY-ESO-1 only), to which the 1G4 TCR binds, has the sequence SLLMWITQC. It appears that substitution of the cysteine in residue 9 by a valine (anchor position 165) can improve HLA-A*02 loading efficiency and, by extension, immunogenicity[164,166]. Therefore, this work incorporates the C9V mutation in all the APLs tested. This index peptide (SLLMWITQ**V**) is referred to as **9V**, and all the variants we employ are based on this index peptide. Table 2.7 summarises the identity of APLs tested, as well as their affinity (measured using surface plasmon resonance, SPR) to the 1G4 TCR as previously reported[1].

Table 2.7: Affinity measurements for the 1G4 TCR. The table summarises the K_D data obtained by Pettmann *et al.*[1] using surface plasmon resonance (SPR). The data corresponds to experiments conducted at 37 °C. SD stands for standard deviation. For the 4A, 5Y, and 5F low affinity peptides, the reported K_D values correspond to those obtained using the novel method by Pettmann *et al.*[1].

Name	Sequence	$K_D \pm$ SD (μM)
9V	SLLMWITQ**V**	7.97 ± 2.55
6V	SLLMW**V**TQ**V**	17.6 ± 5.28
3Y	SL**Y**MWITQ**V**	36.3 ± 10.4
6T	SLLMW**T**TQ**V**	84.6 ± 30.3
4D	SLL**D**WITQ**V**	90.8 ± 41.7
4A	SLL**A**WITQ**V**	299 ± 48.6
5Y	SLLM**Y**ITQ**V**	433 ± 103
5F	SLLM**F**ITQ**V**	1309 ± 505

2.5 Flow cytometry

2.5.1 Preparation of pMHC tetramers

Detection of the 1G4 or the wt/c51 TCR in T cells was conducted with fluorescent pMHC tetramers composed of refolded 9V pMHC complexes (a gift from M. Kutuzov) and PE streptavidin (Biolegend). Briefly, 66.6 μg of 9V pMHC were placed in a 1.5 mL microcentrifuge tube and continuously shaken (∼1000 rpm) at room temperature (RT). Afterwards, 10 μL of PE streptavidin were added

and the mixture incubated for 10 min. The aforementioned process was repeated a total of 10 times. The resultant solution was stored at 4 °C, and used at a working concentration of 1:250 to 1:1000.

2.5.2 Cytometry and general data acquisition

When a given experiment was carried out in a microtitre plate format, cells were transferred to a 96-well tissue culture plate with a conical bottom and pelleted at 520 × g for 5 min at 4 °C. The supernatant was reserved for enzyme-linked immunosorbent assays (ELISAs) and/or cytotoxicity assays (see Section 2.6). In experiments involving primary $CD8^+$ T lymphocytes, cells were first stained with a fixable viability dye (Zombie NIR Fixable Dye, Biolegend) according to manufacturer's instructions. Afterwards, all samples were stained with the desired flow cytometry antibodies in a volume of 40 μL. Staining was conducted with flow cytometry buffer, which had a composition of phosphate-buffered saline (PBS) with 1% foetal bovine serum (FBS) and 2 mM EDTA. Staining used working concentrations that ranged from 1:200 for most antibodies to 1:250 to 1:1000 for pMHC tetramers. Cells were incubated for 20 min at 4 °C, washed once, and resuspended in Dulbecco's PBS (DPBS) with 1% bovine serum albumin (BSA) and 4% formaldehyde. For some experiments, a Jurkat cell line with an enhanced green fluorescent protein (eGFP) was used. This reporter line contained a minimal promoter with an NF-κB responsive element, which was in turn tied to eGFP production. Samples that contained this reporter line were not fixed but only washed twice with flow cytometry staining buffer.

For experiments conducted in any other format, cells were transferred to a 1.5 mL microcentrifuge tube and pelleted at 520 × g for 5 min at 4 °C. They were then stained with flow cytometry buffer in a volume of 1 mL with the same antibody working concentrations described before. Cells in this format were incubated for 20 min at 4 °C and washed twice in flow cytometry buffer prior to analysis. All sample acquisition was conducted in either a BD X-20 (BD

Biosciences), a Cytek (Cytek Bio), or Cytoflex (Beckman Coulter) cytometer. Data was analysed in FlowJo V10.0 (TreeStar Inc).

When performing fluorescence-activated cell sorting (FACS), the aforementioned protocols were followed. However, the sorting process was conducted with a BD FACSAria III (BD Biosciences), which was solely operated by staff of the flow cytometry facility at the Sir William Dunn School of Pathology (SWDSP).

2.5.3 Absolute cytometric quantitation of CD2 and CD58

Absolute quantitation of the CD2 and CD58 molecules was conducted using the Quantum R-PE MESF Kit (Bangs Laboratories). This kit contains five different bead populations: a blank and four bead groups conjugated with known amounts of the phycoerythrin (PE) fluorophore. The beads were resuspended in flow cytometry buffer and ran through a cytometer, obtaining five discrete populations. The geometric mean fluorescence intensity (gMFI) of those populations was then calculated. The gMFI was correlated with the number of PE fluorophores to generate a standard curve; for this, the manufacturer provided specialised software (QuickCal, Bangs Laboratories).

Immediately afterwards, samples stained with anti-CD2 or anti-CD58 PE-conjugated antibodies were analysed using the same cytometer, their gMFI determined, and the number of PE fluorochromes calculated using the QuickCal software. According to Biolegend (personal communication), each anti-CD2 (catalogue number 309208) or anti-CD58 (catalogue number 330905) antibody is conjugated to one molecule of PE, indicating a fluorochrome:protein (F:P) ratio of 1:1. The manufacturer indicated that, after the antibody-PE conjugation reaction, the product is subjected to a size-exclusion chromatography plus an in-house (proprietary) method to remove free antibody, free PE, and unwanted fractions (*i.e.*, those conjugated at an F:P ratio different of 1:1). The manufacturer then collects the fraction with an F:P ratio of 1:1. Achievement of a conjugation ratio $\mathcal{L}$ close to 1 (with $\mathcal{L}$ representing $\frac{\mathrm{F}}{\mathrm{P}}$ or moles of fluorochrome per mole of antibody) can be verified through spectrophotometry using Equation 2.1:

$$\mathcal{L} = \frac{A_{566}}{\varepsilon_2 \times \frac{A_{280} - (A_{566} \times CF)}{\varepsilon_1}} \tag{2.1}$$

To calculate $\mathcal{L}$ in Equation 2.1, Biolegend uses batch-specific measurements, as well as several constants:

- **A_{280}:** The absorbance of the conjugate mixture at 280 nm (λ_{max} for protein).
- **A_{566}:** The absorbance of the conjugate mixture at 566 nm (λ_{max} for PE).
- **CF:** A correction factor, which compensates for the absorbance at 280 nm caused by the fluorescent dye. For PE, CF = 0.17.
- **ε_1 and ε_2:** molar extinction coefficients for the antibody and the fluorescent dye, respectively. For IgG, $\varepsilon_1 = 210\,000$ M^{-1} cm^{-1}; for PE, $\varepsilon_2 = 1\,863\,000$ M^{-1} cm^{-1}.

Therefore, considering that F:P = 1:1 for the antibodies used, the number of PE fluorophores per cell was assumed to be the number of CD2 or CD58 molecules per cell.

2.6 Quantitation of cytokine production and cytotoxicity

2.6.1 Enzyme-linked immunoassays

Supernatant recovered from $CD8^+$ T cell stimulation experiments was assayed for a number of human cytokines and chemokines, including IFN-γ, IL-2, macrophage inflammatory protein (MIP)-1β, and tumour necrosis factor (TNF)-α. For this, specialised kits supplied by Thermo Fisher Scientific were employed according to the recommendations of the manufacturer. Samples were processed using 96-well Maxisorp plates (Thermo Fisher Scientific) and the final readouts conducted using a SpectraMax M5 Gemini plate reader (Molecular Devices). Data was analysed using a web application provided by Elisakit (https://www.elisaanalysis.com/app) with 5-parameter logistic (5PL) regressions.

2.6.2 T cell cytotoxicity

Supernatant recovered from $CD8^+$ T cell cytotoxicity experiments was assayed using the CyQUANT LDH kit (Thermo Fisher Scientific), which is based on the release of lactate dehydrogenase (LDH) by target cells. The experiments included all the appropriate controls recommended by the manufacturer, and samples were processed as per the instructions included in the kit. Final cytotoxicity readouts were conducted using a SpectraMax M5 Gemini plate reader and the data analysed using Excel 365 (Microsoft).

2.7 Tissue culture routines

2.7.1 Production of lentiviral supernatants

Lentiviral supernatant for transduction of cell lines and primary cultures was produced following a modified version of the protocol reported by Lever *et al.*[167] in 2016. Almost all transfer vectors were amenable to third generation packaging plasmids: in those instances, 293T cells (ATCC CRL-3216, a gift from J. Nguyen) were plated at a 50% confluency in a volume of 3 mL and using a 6-well plate. Cells were allowed to attach overnight and, the following morning, transfected with a mixture of packaging plasmids (950 ng of pRSV-Rev, 370 ng of pMD2.G, and 950 ng of pMDLg/pRRE) and the desired lentiviral transfer plasmid (800 ng). For the lentiCRISPR-$CD2^{KO}$ plasmid, infectious particles were generated by transfecting 293T cells with 1433 ng of psPAX2, 433 ng of pMD2.G, and 1700 ng of lentiCRISPR-$CD2^{KO}$. In all cases, transfection was conducted using the X-tremeGENE HP Transfection Reagent (Merck), following the instructions of the manufacturer and transfecting with a ratio of 3 μL of transfection reagent to 1 μg of DNA.

Following transfection, the 293T cells were incubated at 37 °C 10% CO_2 (v/v) for 48 h and then the lentiviral supernatant filtered through a 0.45 μm syringe filter (Sartorius). This process generated roughly 2 mL of clarified supernatant per each well of a 6-well plate. The supernatant was then used without further

operations or pooled and concentrated into a smaller volume according to the protocol of the Lenti-X concentrator (Takara Bio) product. When lentiviral supernatant was not applied to cells immediately after production, it was frozen at −80 °C for future use.

2.7.2 Cell lines: procurement, generation, and maintenance

293T cells

Adherent 293T cells (ATCC CRL-3216) were a gift from J. Nguyen. They were cultured in DMEM 10% FBS with penicillin-streptomycin (100 U/mL and 100 μg/mL, respectively) at 37 °C and 10% CO_2 (v/v). Cells were maintained in T75 flasks, splitting them every 3 days by trypsinisation and dilution with a 1:30 subcultivation ratio. In all instances of this work, when counting cells was required, this was conducted using the NucleoCounter NC-3000 system (Chemometec) and the required consumables (Solution 13) from the manufacturer.

T2 cells

T2 cells (ATCC CRL-1992) were a gift from E. Abuh-Shah. They were cultured in RPMI 1640 10% FBS with penicillin-streptomycin (100 U/mL and 100 μg/mL, respectively) at 37 °C and 5% CO_2 (v/v). Cells were maintained in T75 flasks, splitting them every 3 days by dilution and ensuring the cultures were always maintained at densities between 5×10^4 and 1×10^6 cells/mL.

U-251 cells

The human glioblastoma cell line U-251 (ECACC 09063001) was a gift from V. Cerundolo. It was cultured in DMEM 10% FBS with penicillin-streptomycin (100 U/mL and 100 μg/mL, respectively) at 37 °C and 10% CO_2 (v/v). Cells were maintained in T175 flasks, splitting them every 3 days by trypsinisation and dilution with a 1:4 subcultivation ratio.

Jurkat cells

A reporter Jurkat line, derived from the E6-1 clone (ATCC TIB-152) by lentiviral transduction of the pSIRV-NF-κB plasmid (Addgene #118093) was a gift from P. Steinberger. Transduction of pSIRV-NF-κB generated a reporter cell line that contained an NF-κB responsive element, which was in turn tied to the production of eGFP. Throughout this thesis, this parental cell line is referred to as NF-κB/eGFP Jurkats.

All Jurkat cells were cultured in RPMI 1640 10% FBS with penicillin-streptomycin (100 U/mL and 100 μg/mL, respectively) at 37 °C and 5% CO_2 (v/v). Cells were maintained in T75 flasks, splitting them every 3 days by dilution with a 1:10 subcultivation ratio.

Approximately 1×10^6 NF-κB/eGFP Jurkat cells were transduced with 2 mL of lentiviral supernatant derived from the 1G4 TCR transfer plasmid and sorted for 1G4 TCR^+ cells. From the 1G4 NF-κB/eGFP Jurkat lineage, multiple additional cell lines were derived. Specifically, 1G4 NF-κB/eGFP Jurkats expressing the $CD2^{HA}$, $CD2^{HA}$−2Ig, $CD2^{HA}$−4Ig, $CD2^{HA}$−7Ig, $CD2^{HA}$−$CD43^{Ecto}$, $CD2^{HA}$ − ΔCyt, $CD2^{HA}$−2Ig−ΔCyt, and $CD2^{HA}$−4Ig−ΔCyt constructs were generated. In all cases, the transduction was conducted by addition of 2 mL of the corresponding lentiviral supernatant. After 24 h, cells underwent selection with puromycin, with a pulse of 500 ng/mL for 72 h and a further pulse of 1000 ng/mL for 72 h. Successful selection of the wild type chimeras was verified by flow cytometry by staining for the HA tag (Appendix B).

In addition, Genomic Engineering Oxford (GEO, SWDSP) was subcontracted to perform a CD2 knockout on the 1G4 NF-κB/eGFP Jurkat lineage. They conducted a CRISPR/Cas9-mediated disruption of the human *CD2* gene with a double targeted approach.

The approach used two guides: 5'−GGCACGTGGTTAAGCTCTCGGGG−3' and 5'−CTTGTAGATATCCTGATCATCGG−3', targeting the transcriptional start site (TSS) and exon 2 of *CD2*. After FACS enrichment and limiting dilution, GEO delivered a single clone termed 1G4 $CD2^-$ NF-κB/eGFP. This

Jurkat cell line was used along the other populations. For the avoidance of doubt, the transductions with the CD2 chimeras were conducted in the original 1G4 NF-κB/eGFP Jurkat line — so endogenous CD2 was not disrupted in the chimeras. More information, including the validation of this cell line, can be accessed in Appendix A.

CHO-K1 cells

Chinese hamster ovary (CHO)-K1 cells (ATCC CCL-61) were a gift from E. Denham. They were cultured in DMEM 10% FBS with penicillin-streptomycin (100 U/mL and 100 μg/mL, respectively) at 37 °C and 10% CO_2 (v/v). Cells were maintained in T175 flasks, splitting them every 3 days by trypsinisation and dilution using a 1:20 subcultivation ratio.

Approximately 1×10^6 CHO-K1 cells were transduced with 4 mL of lentiviral supernatant derived from the SCD-HLA-A*02 plasmid and subjected to selection (14 days) using 1 mg/mL of G418. A number of individual clones of the newly generated cell line (termed CHO-A*02) were obtained using limiting dilution. Successful transduction was verified by performing flow cytometry with an anti-human HLA-A*02 antibody. From those clones, an individual specimen (clone #1) was selected for further transduction with 2 mL of lentiviral supernatant derived from the $CD58^{FLAG}$ construct, obtaining a new population termed CHO-A*02-$CD58^{FLAG}$. Successful transduction was verified by performing flow cytometry with an anti-human CD58 antibody. Afterwards, cells from the CHO-A*02-$CD58^{FLAG}$ lineage were subjected to FACS to select for high levels of HLA-A*02 and CD58. After analysing the data acquired through flow cytometry and FACS, the sorted cell line was deemed to possess similar levels of HLA-A*02 to those of clone #3 of the CHO-A*02 lineage. Therefore, experiments in this work use these two lines to compare the effect of HLA-A*02 alone and HLA-A*02 plus CD58. Detailed information, including the rationale for this choice, can be seen in Section 3.2.2 of Chapter 3.

2.7.3 Primary cells

General considerations about culture

Primary $CD8^+$ T cells were cultured using the CTS OpTmizer T cell expansion media (Thermo Fisher Scientific), supplemented with 2 mM L-Glutamine (Thermo Fisher Scientific), penicillin-streptomycin (100 U/mL and 100 μg/mL, respectively), and recombinant human IL-2 at 100 U/mL (PeproTech). Cells were maintained at 37 °C and 5% CO_2 (v/v), splitting them every 2–3 days by dilution, achieving initial densities of 5×10^5 cells/mL. Ethical approval was obtained by the Inter-Divisional Research Ethics Committee of the University of Oxford (R51997/RE001).

Isolation of $CD8^+$ T cells

Human leukocyte cones were acquired from the NHS Blood and Transplant Service. Total $CD8^+$ T cells were isolated using the RosetteSep $CD8^+$ T Cell Enrichment Cocktail (Stemcell Technologies) according to manufacturer's instructions. Briefly, 2 mL of a leukocyte cone were mixed with 300 μL of antibody cocktail and incubated at RT for 20 min. The mixture was then diluted with an equal volume of DPBS and layered in a 15 mL conical tube over 5 mL of Ficoll Paque Plus (Amersham Biosciences) density gradient media. Afterwards, centrifugation was conducted at 1200 × g for 20 min at RT, with the brakes of the centrifuge disengaged. The enriched cell layer was harvested, mixed with 10 volumes of DPBS and centrifuged at 520 × g for 5 min. The resulting pellet was resuspended in full T cell media and adjusted at a concentration of 5×10^5 cells/mL. $CD8^+$ T cells were immediately activated by addition of human anti-CD3/CD28 Dynabeads (Thermo Fisher Scientific) at a ratio of 1:1 (beads:cell).

Some experiments in this work use the high affinity wt/c51 TCR (K_D = 25 nM). It is important to note that, in those experiments, only HLA-A*02$^-$ leukocyte cones were used for the isolation of $CD8^+$ T cells, as it has been shown[140] that this TCR displays an intrinsic cross-reactivity against self-peptides presented on HLA-A*02.

Transduction, enrichment, and electroporation of primary T cells

Twenty-four hours after isolation and activation with anti-CD3/CD28 beads, 2×10^6 $CD8^+$ T cells were transduced with concentrated lentiviral supernatant generated from the lentiCRISPR-$CD2^{KO}$ transfer vector (1 mL of concentrated supernatant, equivalent to 16 mL of raw supernatant). An equal number of cells was kept untransduced. Forty-eight hours post-transduction, the cells infected with the lentiCRISPR-$CD2^{KO}$ particles were subjected to puromycin selection, which included a pulse of 1.5 μg/mL for 72 h, and an additional pulse of 3 μg/mL for 72 h. Cells continued to be split by dilution every 2–3 days to an initial density of 5×10^5 cells/mL. The untransduced cells were not subjected to selection.

After puromycin selection, CD2 knockout efficiency was assessed by flow cytometry, with typical efficiencies in the range of 80–90%. The day before an experiment, T cells transduced with the lentiCRISPR-$CD2^{KO}$ construct were further enriched for $CD2^-$ cells using the MojoSort Human anti-PE Nanobeads (Biolegend). The nanobeads were coupled with an anti-CD2 PE antibody to facilitate depletion of $CD2^+$ T cells. After depletion, both the enriched $CD2^-$ $CD8^+$ T lymphocytes and the untransduced $CD8^+$ T lymphocytes were electroporated with mRNA constructs coding for either the 1G4 or the wt/c51 TCR. To do this, T cells were washed three times with Opti-MEM with GlutaMAX (Thermo Fisher Scientific) and resuspended at a concentration of 2.5×10^7 cells/mL. Two hundred microlitres (equivalent to 5×10^6 cells) of cell suspension were mixed with 20 μg of mRNA and the mixture placed into electroporation cuvettes with a 2 mm gap (Cuvette Plus, BTX). Electroporation was conducted using an ECM 830 Square Wave Electroporator (BTX) at 300 V for 2 ms. Cells were then gently transferred to 4 mL of prewarmed, complete CTS media and rested overnight. The efficiency of this procedure was verified the following morning by flow cytometry, staining for the TCR with fluorescent tetramers and for CD2 with a conjugated antibody. In general, CD2 depletion reached >95% for the $CD2^-$ population; TCR electroporation efficiencies ranged between 50–85% for

either the 1G4 or the wt/c51 constructs. Cells were immediately used for the experiments described in the following sections.

Regular T cell maintenance continued using fully supplemented CTS expansion media for 13–16 days post-isolation. In some instances, T cells showing signs of exhaustion —shrinkage and reduced proliferation— prior to the CD2 depletion procedure were subjected to an additional restimulation using the ImmunoCult Human CD3/CD28 T Cell Activator (Stemcell Technologies). When this operation was conducted, residual Dynabeads were removed using a Dynal MPC-1 magnet (Thermo Fisher Scientific) and resuspended at a density of 1×10^6 cells/mL. Cells were then restimulated according to manufacturer's instructions for 9–12 days. Prior to an experiment, these cells were subjected to CD2 depletion and TCR electroporation as described above.

Procurement of DCs

Monocyte-derived DCs (used in Table 3.1) were a gift from E. Abuh-Shah, who prepared them in accordance with a protocol previously described[160].

2.8 Stimulation and conjugation assays

2.8.1 Stimulation with adherent cells

Stimulation of both Jurkat and primary $CD8^+$ T cells was conducted with either derivatives of the CHO-K1 cell line or wild type U-251 cells (which are HLA-A*02^+). In the case of assays with CHO-K1 cells, the two lineages used as APCs were the CHO-A*02 and the CHO-A*02-$CD58^{FLAG}$ populations. Recall these cells were engineered to express human HLA-A*02 with or without human CD58 (Section 2.7.2).

When using adherent cells as APCs, 2–3 $\times$ 10^4 (depending on the specific experiment) cells were seeded in 96-well tissue culture flat bottom plates in a final volume of 100 μL. Cells were allowed to adhere overnight. The next day, serial dilutions of the desired APLs were generated using Opti-MEM 5% FBS with penicillin-streptomycin (100 U/mL and 100 μg/mL, respectively). These dilutions

were conducted using master stocks (10 mg/mL in DMSO) of the NY-ESO-1 peptide variants. Media was aspirated from the target cells and it was replaced with 200 μL of a defined concentration of the APL. The cells were pulsed for 90 min at 37 °C and 5% CO_2 (v/v), enabling exogenous loading of the peptide onto HLA-A*02. Afterwards, the media was aspirated again and T cells (either primary $CD8^+$ T lymphocytes or Jurkats) added to the wells in a volume of 200 μL. Effector cells were previously prepared by resuspending them in new media, which was full Opti-MEM for Jurkats and full CTS media for primary cells. In experiments with adherent cells, unless otherwise specified, effector cells were seeded at an effector:target (E:T) ratio of 2:1. In the case of primary cells, where TCR electroporation efficiency was not 100%, the corresponding adjustments where made so that the E:T ratio truly reflected two $1G4^+$ T cells per APC.

After adding the effector cells, the microtitre plate was gently centrifuged (15 × g for 3 min) and then incubated at 37 °C and 5% CO_2 (v/v). Unless otherwise specified, co-cultures with adherent cells lasted 24 h. Once the co-culture was conducted, cells were processed in accordance to the protocols described in Sections 2.5 and 2.6.

2.8.2 Stimulation with suspension cells

Standard stimulation assays

The transporter associated with antigen processing (TAP)-deficient, HLA-$A*02^+$ T2 suspension cell line was used as an APC in the same fashion as adherent cells. For experiments where exogenous APLs were loaded onto T2s, 3.3×10^4 T2 cells were seeded in a conical bottom microtitre plate in a volume of 110 μL. In parallel, serial dilutions of the NY-ESO-1 peptide of interest were generated using full RPMI 1640 as a diluent. A total of 110 μL of the diluted APL were added to the T2 cells, achieving a particular concentration in a final volume of 220 μL. The cells were pulsed for 90 min at 37 °C and 5% CO_2 (v/v), enabling exogenous loading of the peptide onto HLA-A*02. Following this, T2 cells were centrifuged (520 × g for 5 min). Once the supernatant was carefully removed, the target

cells were resuspended in 110 μL of full CTS (when stimulating primary cells) or RPMI 1640 (when stimulating Jurkat cells), of which 100 μL were transferred to a round bottom 96-well plate. Afterwards, 100 μL of effector cells were added to the plate, achieving a final volume of 200 μL. Unless otherwise specified, for experiments with Jurkat cells, an E:T ratio of 1:1 was used; for primaries, the E:T ratio was 3:1. In the case of primary cells, where TCR electroporation efficiency was not 100%, the corresponding adjustments where made so that the E:T ratio truly reflected three 1G4$^+$ T cells per APC.

After adding the effector cells, the microtitre plate was gently centrifuged (15 $\times$ g for 3 min) and then incubated at 37 °C and 5% CO_2 (v/v). Co-cultures using Jurkat cells lasted 24 h, while co-cultures with primary T lymphocytes lasted 6 h. Cells were processed in accordance to the protocols described in Sections 2.5 and 2.6.

Assessment of the wt/c51 TCR cross-reactivity

When assessing the effect of CD2 knockout in the self-antigen cross-reactivity reported[140] for the wt/c51 receptor, a modified protocol was employed. For these experiments, a total of 1 $\times$ 10^4 T2 cells (cultured in full CTS media) were seeded in 100 μL using round bottom 96-well plates. Afterwards, a defined number of primary CD8$^+$ T cells were added using a volume of 100 μL to achieve gross E:T ratios of 20:1, 10:1, 5:1, 2.5, and 1.25:1. The microtitre plate was gently centrifuged (15 $\times$ g for 3 min) and then incubated at 37 °C and 5% CO_2 (v/v) for 16 h. Cells were processed in accordance to the protocols described in Sections 2.5 and 2.6. For these assays, APCs were not exogenously loaded with any peptide.

2.8.3 Conjugation assays

Conjugation assays between different lineages of the Jurkat cells and the CHO-A*02 or CHO-A*02-CD58^{FLAG} APCs were conducted by staining 5 $\times$ 10^6 Jurkat cells with 5 μM carboxyfluorescein succinimidyl ester (CFSE, Biolegend). Simultaneously, 5 $\times$ 10^6 CHOs were stained with 5 μM Tag-it Violet (Biolegend). This

process was conducted according to manufacturer's protocol. After staining, cells were resuspended at a working concentration of 2×10^5 cells/mL with cold DPBS. Then, 200 μL of Jurkat cells were mixed with 100 μL of CHO cells inside of a standard FACS tube, which was promptly placed on ice for 1 h. After 1 h incubation —and without further processing— cells were subjected to flow cytometry analysis. The conjugation percentage was calculated as follows:

$$\% \text{ Conjugation} = \frac{\text{CFSE}^+ \text{ Violet}^+ \text{ cells}}{\text{CFSE}^+ \text{ cells}} \times 100 \tag{2.2}$$

Equation 2.2 effectively reflects the number of conjugated Jurkats (detected as CFSE$^+$ Violet$^+$, due to their physical association with CHO cells) over total Jurkats (all cells stained with CFSE). For conjugation assays, APCs were not exogenously loaded with any peptide.

2.9 Data analysis

In order to extract EC_{50} and E_{max} values from dose-response curves, a four-parameter logistic (4PL) regression was fitted, which had the following form:

$$y = E_{min} + \frac{E_{max} - E_{min}}{1 + \left(\frac{EC_{50}}{x}\right)^{\text{Hillslope}}} \tag{2.3}$$

In all the equations presented, y represents the cellular response and x the peptide concentration (usually in nM) used to pulse target cells. Fitting of Equation 2.3 was conducted using GraphPad v8.0 (Prism), a program also used to generate all graphs depicted in this work. Error bars in all graphs represent plus/minus one standard deviation (SD), unless otherwise indicated. In some select instances, where the 4PL regression algorithm was unable to fit a non-monotonic dose-response curve, a custom script developed by J. Nguyen and O. Dushek was used. This script uses the *lsqcurvefit* function in MATLAB

(Mathworks) to fit the data using the difference of two Hill equations, as per:

$$y = \mathrm{E_{min}} + \frac{a + \dfrac{b-a}{1+\left(\dfrac{c_1}{n}\right)^{n_1}} - \mathrm{E_{min}}}{1+\left(\dfrac{c_2}{n}\right)^{n_2}} \tag{2.4}$$

From Equation 2.4, it follows that $y_{max} = \mathrm{E_{max}}$, and the $\mathrm{EC_{50}}$ corresponds to the x value where $y = \frac{y_{max}}{2}$.

In some cases (particularly when working with low affinity APLs) where calculation of an $\mathrm{EC_{50}}$ value was not feasible due to the cell populations failing to saturate their response, we used a parameter termed $\mathrm{P_{15}}$ (for potency) instead. This parameter represents the concentration of antigen at which 15% of the total cell population becomes activated. To do this, we used a Python script developed by J. Pettmann[1] that fits a 4PL regression (Equation 2.3) using a Levenberg-Marquardt algorithm. From this fit, we interpolated the $\mathrm{P_{15}}$ value, which was then used to calculate the antigen discrimination power α (see the work of Pettmann *et al.*[1]) using the following expression:

$$\log_{10}(\mathrm{P_{15}}) = \mathrm{C} + \alpha \times \log_{10}(\mathrm{K_D}) \tag{2.5}$$

In Equation 2.5, $\mathrm{K_D}$ represents the reported affinity of the APL to the TCR. The C parameter (y-intercept) acts as a measure of sensitivity.

Statistical tests were conducted using GraphPad v8.0 or SPSS (IBM Software). The exact test used is indicated in each figure, with p-values being represented with the following symbols: n.s. (not significant) = $\mathrm{p} > 0.05$, * = $\mathrm{p} \leq 0.05$, ** = $\mathrm{p} \leq 0.01$, *** = $\mathrm{p} \leq 0.001$.

3

Generation of a cellular platform to study the CD2/CD58 axis

Contents

3.1 Introduction 62
3.1.1 A look at the CD2/CD58 axis in a reductionist system 64
3.1.2 Platforms for assessing T cell activation 65
3.1.3 Chapter aim 70
3.2 Results 71
3.2.1 The effector NF-κB/eGFP Jurkat line 71
3.2.2 The target CHO-K1 cell line 71
3.2.3 CD2 engagement reduces the EC_{50} of activation . . . 76
3.2.4 The CHO platform quantitatively recapitulates the phenotype of CD2 knockout cells 77
3.2.5 CD2 overexpression increases antigen sensitivity at the expense of specificity 78
3.3 Discussion 81
3.3.1 Revisiting the role of CD2 82
3.3.2 Improving the experimental platform 84

3.1 Introduction

T cell activation is influenced by the engagement of co-stimulatory and co-inhibitory receptors. Amongst the multiple axes that work in conjunction with the TCR/pMHC signal, the CD2/CD58 axis likely plays a role in achieving the

high antigen sensitivity that characterises T cells[163]. This notion is supported by instances of CD58 downregulation or loss linked to reduced immune activation in cancer[168–170] and human cytomegalovirus (HCMV)[171]. More recently, Pettmann *et al.*[1] showed in a reductionist system that engagement of the CD2 co-receptor can increase antigen sensitivity by almost 1000–fold.

If we consider that the CD2/CD58 axis acts preferentially under regimes characterised by low antigen density and/or low receptor/ligand affinity interactions, it might be possible to engineer this axis to ameliorate some cases of off-tumour toxicity in ACT (Section 1.4.2). In the first instance, we could prevent on-target/off-tumour toxicities that arise when targeting overexpressed TAAs; these toxicities are a result of the destruction of healthy tissue expressing low levels of the target antigen (Chapter 4). In addition, we could avoid off-target/off-tumour toxicities associated to self-pMHC cross-reactivity when using affinity enhanced receptors (Chapter 5).

To test this hypothesis, we considered it important to have a cellular platform to assess, in a precise manner, the sole effects of human CD2 engagement. Such a platform should: (i) enable titrations of antigens with varying affinities, and (ii) limit the amount of additional intercellular interactions that provide compensatory or inhibitory signals and act as confounding variables. As we argued in the introduction, previous studies of mouse CD2[149] might not provide a full picture of the human CD2 axis given the differences between human and mouse CD2 (Section 1.4.1). Moreover, those studies used macrophages as APCs. Therefore, in the absence of CD2 ligation, other interactions (*e.g.*, CD28/B7) could have provided compensatory signals.

In order to study the CD2/CD58 axis in isolation, we developed a platform using CHO-K1 cells as surrogate APCs. Given that CHO-K1 cells are epithelial ovary cells derived from hamster, they will have limited cognate ligands to human T cells (of note, they do not express hamster CD48, nor hamster CD86[172]). Here, we detail the strategy followed to generate two CHO-K1 sub-lines enabling assessment of the effects of human CD2 ligation. We characterise and validate

this system using a 1G4 NF-κB/eGFP Jurkat reporter cell line and conduct some foundational experiments to quantitatively probe the contribution of CD2/CD58 in antigen sensitivity.

3.1.1 A look at the CD2/CD58 axis in a reductionist system

The CD2 studies from Bachmann *et al.*[149], as well as those from Koyasu *et al.*[173] relied on cellular systems. Their work provided early evidence of CD2 playing a role in improving T cell sensitivity to antigen. Of note, Bachmann *et al.*[149] studied the murine CD2/CD48 axis using a p33/H-2D^{b}-reactive TCR, stimulating cells either through the p33 peptide (KAVYNFATM) or a low affinity variant (A4Y, KAV**A**NFATM). Although Bachmann *et al.* did not look at a full panel of SPR-characterised APLs, they recognised that the reduction in sensitivity as a result of CD2 loss was more prominent in the context of the A4Y low affinity peptide.

More recently, colleagues from our research group (Pettmann *et al.*[1]) developed a method to measure low TCR/pMHC affinity interactions ($K_D > 100$ μM), which was used to characterise a panel of APLs for the 1G4 TCR, an NY-ESO-1/HLA-A*02-reactive receptor (Table 2.7). Pettmann *et al.* then used a reductionist system to look at the activation of 1G4 T cell blasts recognising different concentrations of NY-ESO-1 affinity variants. This reductionist system relies on glass plates containing a BSA/streptavidin matrix, which is then functionalised through the addition of biotinylated pMHC and accessory molecules such as CD58 or ICAM-1. We consider this study to be of particular relevance for our work, as it looked systematically at the effect of peptide affinity and CD2/CD58 engagement in T cell activation.

Using CD69 as their main readout, Pettmann *et al.* measured the activation of 1G4 T cell blasts placed on glass plates functionalised with a wide range of NY-ESO-1 APLs. The affinities of these APLs (Table 2.7) ranged from ~8 μM (9V APL) to ~1.3 mM (5F APL). The findings in this reductionist system (Figure 3.1) illustrate the profound effect of human CD2/CD58 engagement. In the APLs

assayed, addition of the CD58 counter-receptor improved antigen sensitivity by approximately three orders of magnitude (Figure 3.1). This observation fits in a framework where CD2 mediates on-target/off-tumour toxicity in ACT, as it enables efficient T cell activation upon recognition of low levels of a TAA — which would be found in healthy tissues. Thus, it constitutes an important motivation for the work we conduct in Chapter 4 (see Figure 4.1).

In addition, the CD2/CD58 interaction was shown to have an outsize role in the maximum activation achieved when T cells interacted with low affinity APLs ($K_D \geq 400\ \mu M$). At high enough antigen doses, high and medium affinity peptides were capable of achieving a saturated response regardless of CD58 addition (Figure 3.1). Within the dose regimes assayed, however, CD2 engagement was necessary for rescuing cellular responses in the context of the 5Y ($K_D \approx 400\ \mu M$) and 5F ($K_D \approx 1.3$ mM) APLs (Figure 3.1). In our view, this finding supports the notion of CD2 mediating unintended, low affinity off-target/off-tumour toxicities that occur when affinity enhanced receptors cross-react with a low affinity self-antigen found on healthy tissues. As such, this finding was considered a motivation for Chapter 5 of the present work.

3.1.2 Platforms for assessing T cell activation

The results of the Pettmann *et al.*[1] systematic analysis of the CD2/CD58 interaction motivated our work. Given our interest in ensuring the applicability of our findings in ACT, we reasoned that the use of a cellular platform would enable us to look at terminal effector functions such as cytokine production and cytotoxicity. In this section, we discuss multiple platforms that have been used for assessing T cell activation; we also present our rationale for choosing CHO-K1 cells as surrogate APCs.

Acellular systems: general considerations

Fully synthetic platforms enable precise control of the amount of antigens and accessory ligands presented to T cells. Their relative simplicity is valuable

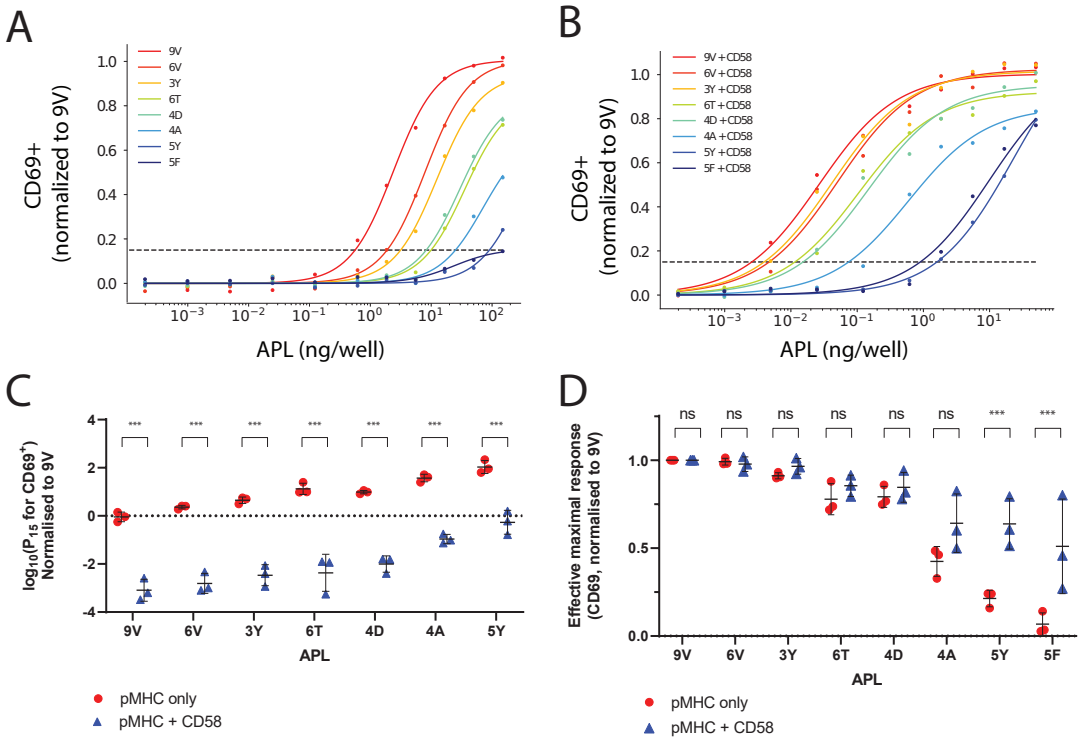


Figure 3.1: In a reductionist system, engagement of the CD2 co-receptor improves T cell antigen sensitivity by almost 3 orders of magnitude. $CD8^+$ T cell blasts expressing the 1G4 TCR were cultured, during 4 h, in streptavidin-coated plates functionalised with biotinylated pMHC molecules loaded with various APLs of the NY-ESO-1 epitope. Afterwards, flow cytometry was performed and T cell activation measured through the CD69 marker. The affinity of the APLs ranged between ∼8 μM (9V APL) and ∼1.3 mM (5F APL) (Table 2.7). **A.** Dose-response curves for plates functionalised with pMHC (antigen) only. **B.** Dose-response curves for plates functionalised with pMHC plus 125 ng/well of CD58. **C.** Improvement in antigen sensitivity after CD2 ligation was determined by comparing the amount of antigen required to activate 15% of the 1G4 T cell blasts (P_{15}). Note that no comparison for the 5F APL was conducted as these cells failed to achieve 15% activation for the pMHC only condition. **D.** Comparison between the effective maximum responses (fraction of CD69-expressing T cells) achieved for all the APLs assayed using the dose regimes shown in A and B. The A and B panels correspond to a representative donor out of three. For the activation metrics of each individual donor, data was normalised between 0 and 1 using 9V as an index peptide. Instead of EC_{50} and E_{max}, this analysis introduces the terms P_{15} and effective maximal response as the curves fitted did not achieve a saturation regime for some of the APLs tested (see Section 2.9). Statistical tests, which used log-transformed data, were conducted using a two-way ANOVA with a Šidák correction for multiple comparisons (n.s. = not significant, *** = $p \leq 0.001$). All these experiments were conducted by Pettmann *et al.*[1].

in signalling and reconstitution studies[174] to dissect key aspects of the T cell machinery. A simple approach consists in functionalising streptavidin-coated plates with biotinylated ligands[167,175]; T cells are then placed on these plates, enabling interaction with the ligand-rich streptavidin matrix. This approach has the drawback of restricting ligand diffusion, and it is not clear whether it would be fully amenable to microscopy. Glass-supported lipid bilayers (SLBs) can also be employed to mimic APCs: by using Ni^{2+}-chelating lipids, proteins with 6-histidine tags can be attached to these bilayers[176]. Under this setup, the ligands retain lateral mobility and microscopy can be conducted. For these reasons, SLBs have been broadly used in T cell activation studies, especially in those related to the T cell immunological synapse[68,176–178].

Ligands presented on SLBs are, however, restricted in their diffusion compared to a cellular system. Additionally, the stiffness of SLBs is approximately 10^3–10^4 fold higher than that of immune cells (0.1–1 kPa vs. 1 MPa)[179]. Of note, Lippert *et al.* recently reported the use of soft polydimethylsiloxane-supported lipid bilayers to achieve more physiological levels of stiffness[180]. Since these factors can influence T cell signalling, the use of free-standing systems such as giant unilamellar vesicles (GUVs) has been explored as an alternative to SLBs[174,179]. Giant unilamellar vesicles are also amenable to microscopy and, in contrast to SLBs, they emulate the typical dimensions and topological restrictions of APCs.

While the relative simplicity and high tunability of acellular systems made them potential candidates for assessing the CD2/CD58 axis, we reasoned that given the scope of our work, cell-based systems would be a better alternative. Until recently[181], most of the SLB or GUV platforms did not account for the glycocalyx, a vast interface of glycolipids and glycoproteins with important roles in the immune response and, more generally, in cell-cell communication. Under normal circumstances, the negatively charged glycoproteins of this matrix (including proteins expressed in immune cells such as CD43, CD45, and CD148) prevent membrane apposition. To overcome the repulsion of the glycocalyx proteins, T cells actively produce close contacts with actin-rich invadosome-like protrusions

(ILPs)[182], which enable close membrane apposition compatible with TCR/pMHC engagement. We have previously argued[2] that, in the context of ILPs, it was likely that the LFA-1/ICAM-1 ligation (with extracellular dimensions of ∼40 nm) paved the way for the smaller CD2/CD58 complex, which would be in turn responsible for stabilising the close contacts at a distance compatible to that of the TCR/pMHC complex (∼13–15 nm).

Taking into account that the glycocalyx interactions can affect antigen recognition, and that the CD2/CD58 axis plays a role in overcoming the hindrance of some large molecules of this matrix, we concluded that it would be difficult to emulate these interactions in a fully synthetic system. Finally, as we are interested in linking the implications of our work with ACT, we recognised the importance of measuring T cell killing — perhaps the main functional outcome in ACT. *In vitro* cytotoxic activity is a key measure of T cell activation which could not be assessed through SLBs or GUVs. Therefore, we decided that a cellular system would be better suited for the overarching goals of our research.

Cellular systems

Multiple approaches can be used to obtain APCs capable of stimulating T cells. In the particular context of ACT, autologous monocyte-derived DCs have been successfully used for clonal expansion of tumour-specific CTLs[183]. However, the generation of autologous monocyte-derived DCs can be time consuming in terms of the required isolation, induction, and maintenance. Stimulation of $CD8^+$ T cells with human cell lines such as K562 (ATCC CCL-243), which lack endogenous HLA-A, -B and -DR molecules, can also be achieved by transduction of the desired HLA allele and subsequent pulsing with specific antigens[136]. Since we are interested in studying the CD2/CD58 axis, the use of human cells would be sub-optimal. The CD58 counter-receptor is known to be expressed ubiquitously in human cells, and CD48 —another CD2 ligand— is predominantly expressed in cells from the haematopoietic lineage, which would include both DCs and

the erythroleukaemic K562 line. Moreover, both of these systems also express additional T cell co-stimulatory ligands such as CD86 or 4-1BBL[136,184].

In light of the previous information, the use of human APCs (whether autologous or allogeneic) would require knocking out CD58 and possibly CD48. We also considered the presence of B7 molecules undesirable, as these can increase antigen sensitivity[2,185] and act as confounding variables. These are only some examples of the large number of co-signalling axes that can become engaged upon a T cell encounter with an APC and play a role in antigen sensitivity (see Appendix C and the work of Chen and Flies[16]).

Given that we wanted to reduce the number of additional interactions to focus on the CD2/CD58 axis, and that knocking out a large number of molecules would not be practical, we turned our attention to xenogeneic APCs. The use of *Drosophila* cells, transfected with murine HLA plus the ICAM-1 and B7 co-stimulatory molecules was shown[186] to successfully stimulate mouse $CD8^+$ T cells. However, *Drosophila* cells have the drawback of requiring culture at temperatures between 22 and 25 °C, which presents a hurdle when simultaneously working with mammalian cells. Alternatively, rodent cells can be used as surrogate APCs: for example, Latouche and Sadelain[187] reported the use of NIH/3T3 (ATCC CRL-1658) mouse fibroblasts transduced with human HLA-A2, CD80, ICAM-1, and CD58 leading to successful T cell stimulation.

Ultimately, we decided to set up our experimental platform using the CHO-K1 cell line (ATCC CCL-61), which is a subclone of the CHO line (first isolated in 1957 by T. Puck). The CHO cells are of epithelial origin; they were obtained from an ovary biopsy of an adult chinese hamster (*Cricetulus griseus*). The CHO-K1 subclone is widely used for production of therapeutic proteins[188], as it is easy to culture. This subclone can be readily transfected and it also expresses high levels of heterologous proteins. Chinese hamster ovary cells have already been used in the past as surrogate APCs in a reductionist system. Specifically, Wild *et al.*[189] transfected variants of CD48 in a CHO N1.A4 cell line (which

expresses I-E^k) to determine how dimensions of the murine CD2/CD48 axis influenced TCR antigen recognition.

For our purposes, the use of a hamster APC also kept the number of potentially cross-reactive intercellular interactions to a minimum. When Xu *et al.*[172] performed a genomic screen of the CHO-K1 cell line, they found no evidence of CD58 homologues (expected, as rodents do not express this protein), nor of hamster CD48, CD86, or CD2. This is important because a hypothetical human/cricetine cross-reactivity of the CD48/CD244 or CD28/B7 molecules could influence activation, as shown by previous studies[185,190]. However, we note that the use of a cricetine, xenogeneic system has some potential downsides. Just as this system should not activate the CD28 co-stimulatory pathway, it would also not recapitulate co-inhibitory interactions such as the PD1/PD-L1 or BTLA/HVEM axes, which in certain instances are known to mediate tumour resistance to ACT[95,109,191]. In addition, CHO cells are known to express hamster ICAM-1[172], which displays a high degree of cross-reactivity with murine LFA-1 and has been reported to co-stimulate[192] and enhance antigen recognition[153] of mouse T cells. Considering: (i) the elevated structural homology between hamster and mouse ICAM-1 (>70%, see the Uniprot Q9ERF7 and P13597 entries) and (ii) the reported cross-reactivity between mouse ICAM-1 and human LFA-1[193,194], hamster ICAM-1 would be expected to interact with human LFA-1. Hence, our results should be assessed in light of both the experimental limitations and advantages of the CHO-K1 surrogate APC system.

3.1.3 Chapter aim

Here, we aim to generate, characterise, and validate two sub-clones of the CHO-K1 cell line that express human HLA-A*02 alone or in combination with human CD58. Using these lines, we endeavour to quantify the increase in antigen sensitivity that is mediated by human CD2. These cells are also used in Chapter 4.

3.2 Results

3.2.1 The effector NF-κB/eGFP Jurkat line

For the first stage of this project, we used the Jurkat leukaemic T cell line as an effector population. A Jurkat reporter cell line, derived from the E6-1 clone (ATCC TIB-152) by transduction of the pSIRV-NF-κB plasmid (Addgene #118093) was a gift from P. Steinberger. The NF-κB Jurkat lineage expresses an eGFP reporter gene under the control of a minimal promoter with an NF-κB responsive element and its use has been previously documented[195].

The NF-κB Jurkat line was transduced (Section 2.3.2) with the 1G4 TCR. This TCR, originally isolated from a melanoma patient[164] has previously been characterised[196], and used[1,167,175,197,198] in diverse studies. Moreover, a panel of APLs has been developed and characterised[1,166,167], which enables the functional study of TCR/pMHC interactions with varying affinities (Chapter 5).

Following transduction of the parental NF-κB/eGFP population, a sample was stained with fluorescent (PE) 9V pMHC tetramers, and sorted for tetramer-positive cells. This procedure generated a 1G4$^+$ Jurkat population with a TCR expression over 99% (Figure 3.2), which is subsequently referred to as the **1G4 NF-κB/eGFP** Jurkat cell line.

3.2.2 The target CHO-K1 cell line

Generation of HLA-A*02$^+$ CHO cells

As the 1G4 TCR binds to the NY-ESO-1$_{157-165}$ HLA-A*02 pMHC complex, we started our platform design by creating a CHO-K1 derivative line expressing HLA-A*02. An SCD encoding a fusion of human β2M (full length) and human HLA-A*02 (amino acids 25-365) via a $(GGGGS)_3$ linker was cloned into the pLEX307-NeoR transfer vector, which confers G418 resistance (Addgene #134365). Lentiviral supernatant generated with the SCD-HLA-A*02/pLEX307-NeoR backbone was used to transduce the parental CHO-K1 line. The bulk population was subjected to selection for 14 days with 1 mg/mL of G418 and then a limiting

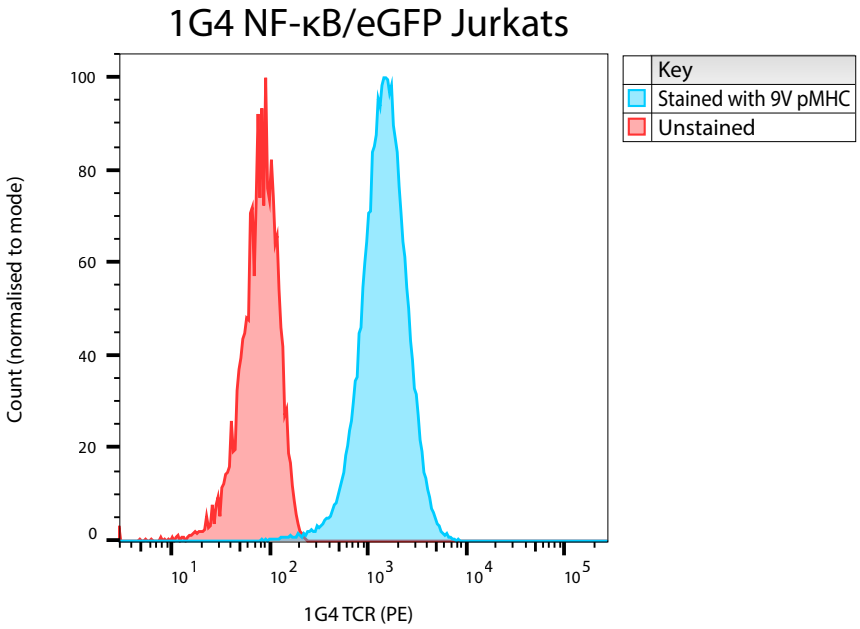


Figure 3.2: Generation of the 1G4 NF-κB/eGFP Jurkat cell line. Following transduction with the 1G4 TCR and FACS, a highly enriched population (>99%) of 1G4$^+$ NF-κB/eGFP Jurkats was obtained.

dilution was performed to obtain single clones expressing the SCD-HLA-A*02 construct. Three single clones of the newly generated CHO-A*02 line were recovered (Figure 3.3), which expressed the SCD coding for β2M and HLA-A*02 in a stable manner.

Transduction of human CD58 on the CHO-A*02 line

Single clone #1 of the CHO-A*02 line was initially selected for further manipulations as it expressed the highest levels of HLA-A*02 (Figure 3.3). It was transduced with the human CD58$^{\text{FLAG}}$ construct, which was contained in the pLEX_307 lentiviral transfer vector (Addgene #41392). Forty-eight hours post-transduction, the levels of CD58 were assessed by flow cytometry and compared to those of CHO-A*02 (clone #1), suggesting a high (>95%) efficiency in the lentiviral integration of this construct (Figure 3.4A). However, this process disrupted the expression levels of HLA-A*02, with the CHO-A*02-CD58$^{\text{FLAG}}$ sub-line displaying a reduced expression of HLA-A*02 compared to that of the

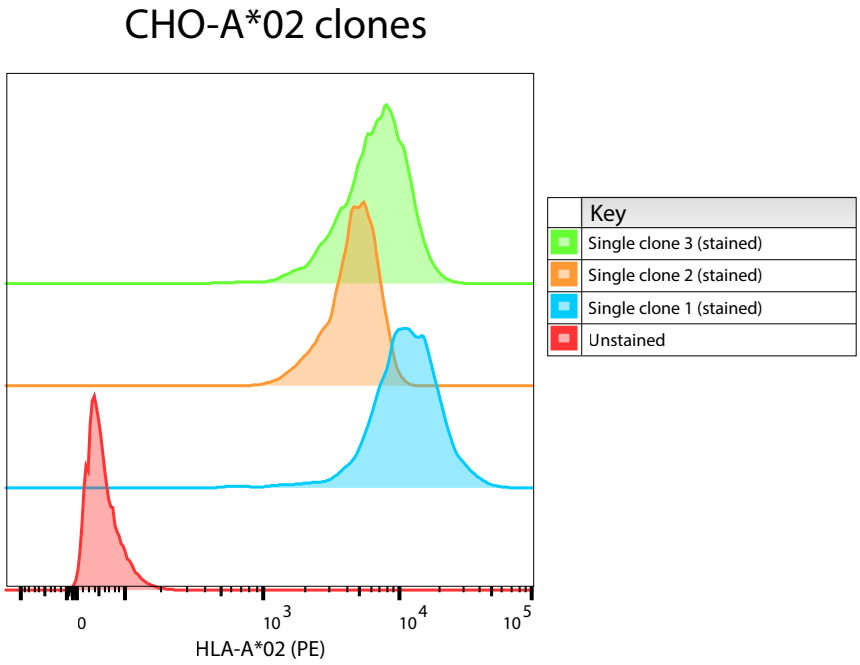


Figure 3.3: Single clones of the CHO-A*02 cell line. CHO-K1 cells were lentivirally transduced with an SCD coding for human β2M and HLA-A*02. Following G418 selection and limiting dilution, three clones with varying expression levels of HLA-A*02 were recovered.

CHO-A*02 (clone #1) parental line (Figure 3.4B). As having matched HLA-A*02 levels was deemed important to ensure the differences observed between the CHO-A*02 and the CHO-A*02-CD58$^{\mathrm{FLAG}}$ lines could be mainly attributed to the expression of human CD58, we sorted the CHO-A*02-CD58$^{\mathrm{FLAG}}$ population and selected for cells with high expression of HLA-A*02 and CD58. Although the sorting was not able to rescue the HLA expression to that of CHO-A*02 (clone #1), it achieved a very close match to the levels of HLA-A*02 displayed by the CHO-A*02 (clone #3) line (Figure 3.5). In light of this information, it was decided that the two cell lineages that would be used to assess the effects of CD58 expression would be the CHO-A*02 (clone #3) population and the sorted CHO-A*02-CD58$^{\mathrm{FLAG}}$ population (originally derived from clone #1 of the CHO-A*02 population). Henceforth, these two cell populations are referred to as **CHO-A*02** and **CHO-A*02-CD58$^{\mathrm{FLAG}}$** lines only.

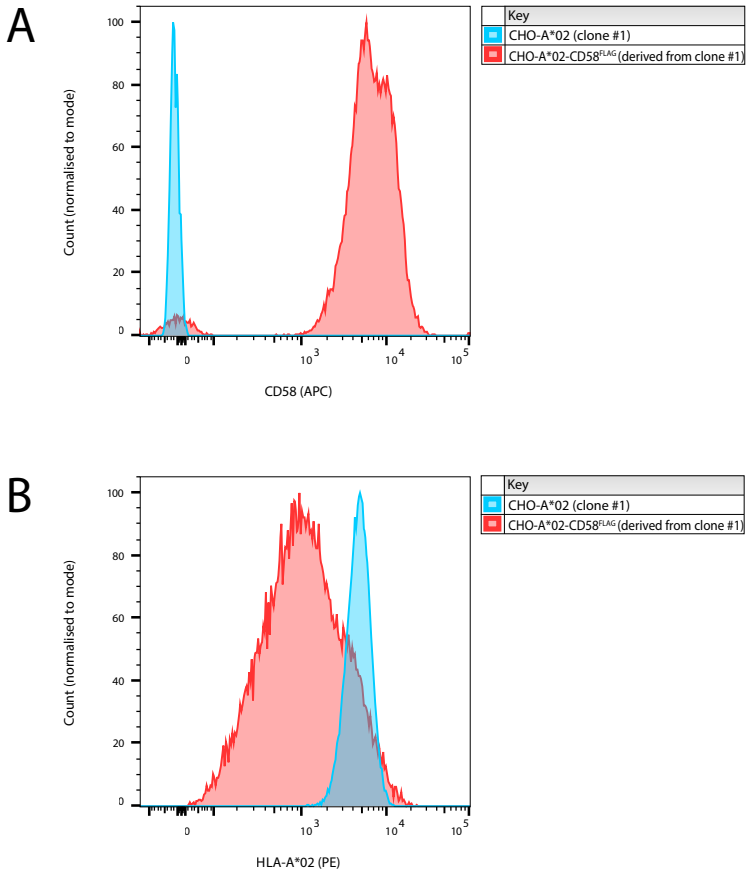


Figure 3.4: Transduction of human CD58 in the CHO-A*02 line. Clone #1 of the CHO-A*02 line was transduced with human CD58, generating the CHO-A*02-CD58$^{\mathrm{FLAG}}$ sub-line. **A.** CD58 is efficiently expressed in a large proportion of the derivative cell line. **B.** Compared to its parental line (CHO-A*02, clone #1), the CHO-A*02-CD58$^{\mathrm{FLAG}}$ sub-line exhibits reduced levels of HLA-A*02. These histograms reflect the expression levels of CD58 and HLA-A*02 prior to the sorting of the CHO-A*02-CD58$^{\mathrm{FLAG}}$ population

Characterisation of the CD58 levels in the CHO-A*02-CD58$^{\mathrm{FLAG}}$ cell line

To quantitate the levels of CD58 in the newly generated CHO-A*02-CD58$^{\mathrm{FLAG}}$ population, we used the R-PE Bangs Laboratories Quantitation Beads Kit. This kit contains several groups of beads, each group conjugated to a defined number of PE fluorophores. This enables the generation of a standard curve correlating the gmFI detected by the cytometer with the number of fluorophores conjugated to the different beads. By staining several samples with an anti-CD58 antibody

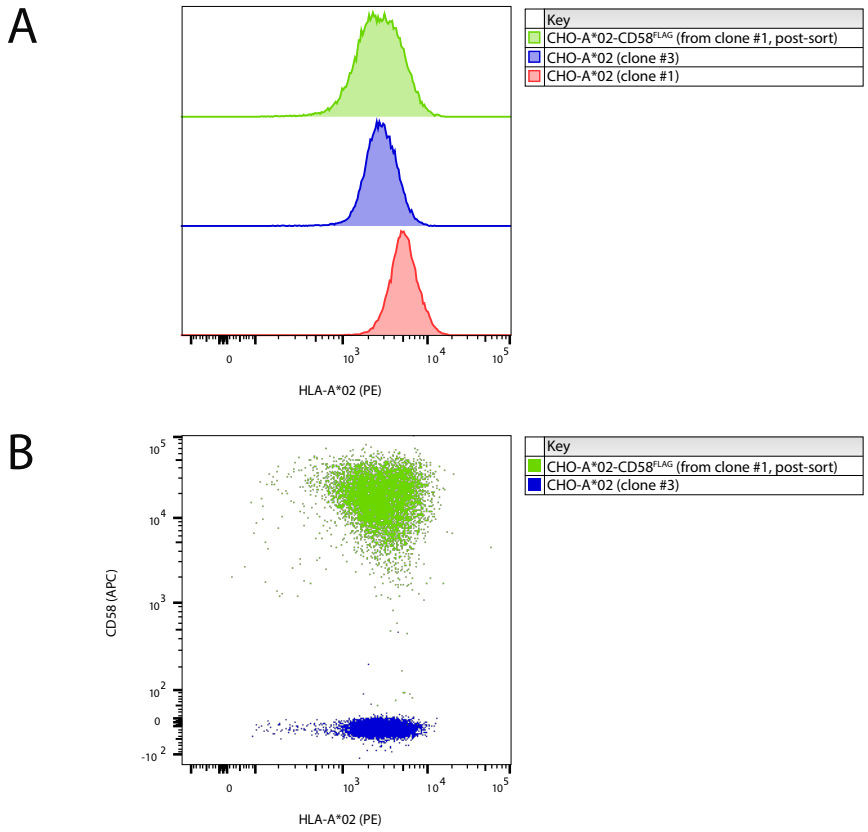


Figure 3.5: Matching of HLA-A*02 levels in the CHO lines. The sub-line CHO-A*02-CD58^{FLAG}, derived from the CHO-A*02 (clone #1) population, was sorted for high expression of HLA-A*02 and CD58. **A.** Whilst it was not possible to equate HLA-A*02 levels to that of the parental line, we noticed HLA-A*02 expression was matched to that of CHO-A*02 (clone #3). **B.** Post-sorting, the CHO-A*02-CD58^{FLAG} line displayed >99% of CD58^{+} cells and matched expression of HLA-A*02 to the CHO-A*02 (clone #3) lineage.

conjugated to PE*, one can determine the gMFI of these samples and use the standard curve to estimate the number of CD58 molecules. Our estimation of the average number of CD58 molecules per each CHO-A*02-CD58^{FLAG} cell, as well as CD58 levels in other selected samples can be found in Table 3.1.

*The ratio of PE molecules per one anti-CD58 antibody, known as the F:P ratio is 1:1. This information was obtained from a personal communication with Biolegend, the manufacturer of the anti-human CD58 (PE) antibody. The F:P ratio for PE anti-human CD2 is also 1:1. See Section 2.5.3 for further technical details.

Table 3.1: Quantitation of CD58 expression in selected cellular samples. The R-PE Quantitation Beads Kit (Bangs Laboratories) was used to estimate CD58 expression in several primary human samples and cell lines (n.a. = not available for cell lines).

Sample	Molecules per cell ± SD
CHO-A*02-CD58^{FLAG} cell line	7.6×10^6 ± n.a.
1G4 NF-κB/eGFP Jurkat cell line	9.4×10^4 ± n.a.
Immature monocyte-derived DCs	$2.5 \times 10^5 \pm 3.0 \times 10^4$
Mature monocyte-derived DCs	$5.5 \times 10^5 \pm 3.1 \times 10^4$
U-251 cell line	1.2×10^6 ± n.a.
T2 cell line	6.2×10^5 ± n.a

We note that the CHO-A*02-CD58^{FLAG} population expresses very high levels of CD58 (7.6×10^6 molecules/cell). These levels are approximately one order of magnitude higher than those of the U-251 glioblastoma cell line. The CHO-A*02-CD58^{FLAG} line also expresses higher CD58 levels than those found in professional APCs such as mature, monocyte-derived DCs. This is likely a consequence of the EF-1α promoter used to drive expression of CD58 in the CHO cells, which is generally regarded as a strong promoter across mammalian cells[199].

3.2.3 CD2 engagement reduces the EC_{50} of activation

We started using our system with the CHO-A*02 and the CHO-A*02-CD58^{FLAG} as APCs and the 1G4 NF-κB/eGFP Jurkats as effector cells. Our initial aim was to quantitatively determine the effect of CD2 engagement in antigen sensitivity in a human cell line. After a 24 h co-culture with exogenously pulsed target cells, we analysed eGFP expression on the Jurkats as a proxy for NF-κB activation (Figure 3.6A). We found that CD2 engagement led to a 15–fold reduction in the EC_{50} of activation. The EC_{50} without CD2 engagement was 4.36×10^{-1} nM; when the 1G4 NF-κB/eGFP Jurkats were co-cultured with CD58-expressing CHOs, the EC_{50} of activation was reduced to 2.89×10^{-2} nM (Figure 3.6B). These results indicate that, despite an increased affinity between human CD2/CD58 compared to that of rodent CD2/CD48, the CD2-mediated increase in antigen sensitivity is only marginally larger to that previously reported in murine T cells[149].

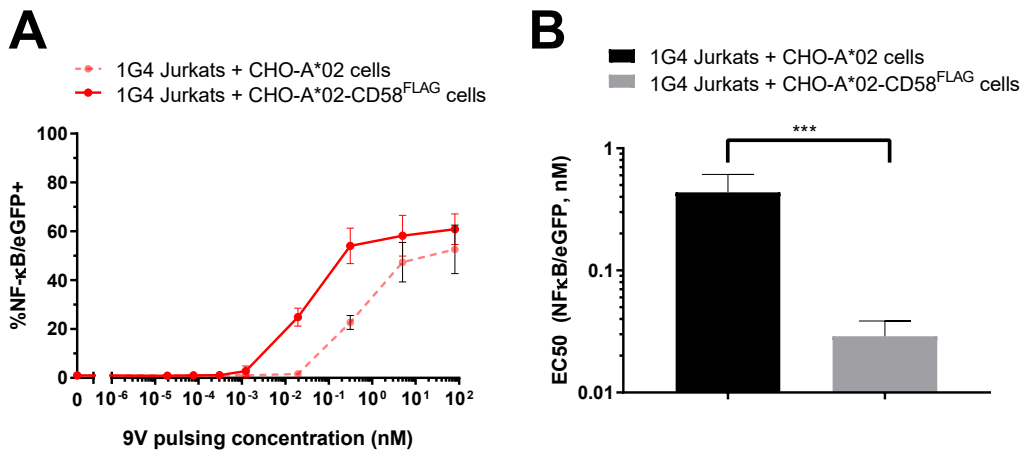


Figure 3.6: Engagement of CD2 reduces EC_{50} of activation by a 15–fold factor. A. The 1G4 NF-κB/eGFP line was co-cultured for 24 h with pulsed HLA-A*02$^+$ CHO cells with or without CD58 expression. Afterwards, eGFP expression was measured by flow cytometry as a proxy for NF-κB activation. **B.** The differences in EC_{50} of activation for the two conditions were deemed statistically significant (*** = $p \leq 0.001$) after fitting 4PL regressions and using an extra sum of squares F-test to compare models with either shared or different EC_{50} values. The data in this figure corresponds to the results of three independent experiments.

3.2.4 The CHO platform quantitatively recapitulates the phenotype of CD2 knockout cells

We next determined whether the phenotype observed when using HLA-A*02$^+$ CHO cells with and without CD58 expression could be reproduced by using a CD2 knockout Jurkat population. For this, we commissioned GEO (SWDSP) to generate a 1G4 CD2$^-$ NF-κB/eGFP Jurkat clone (Appendix A). We co-cultured both the 1G4 NF-κB/eGFP and the 1G4 CD2$^-$ NF-κB/eGFP lines with the CHO-A*02-CD58^{FLAG} population and measured the EC_{50} shift in antigen sensitivity as a result of CD2 ligation (Figure 3.7A). When comparing the CD2 knockout line with its wild type counterpart, we found that CD2 engagement mediated, on average, an 8–fold reduction in the EC_{50} of activation. Whereas the EC_{50} of the 1G4 CD2$^-$ NF-κB/eGFP population was 8.87×10^{-1} nM, the one of the 1G4 NF-κB/eGFP line was reduced to 1.13×10^{-1} nM (Figure 3.7B).

Finally, we compared the EC_{50} shifts registered in this setup with the ones we had previously obtained in Section 3.2.3, where we controlled CD2 ligation by

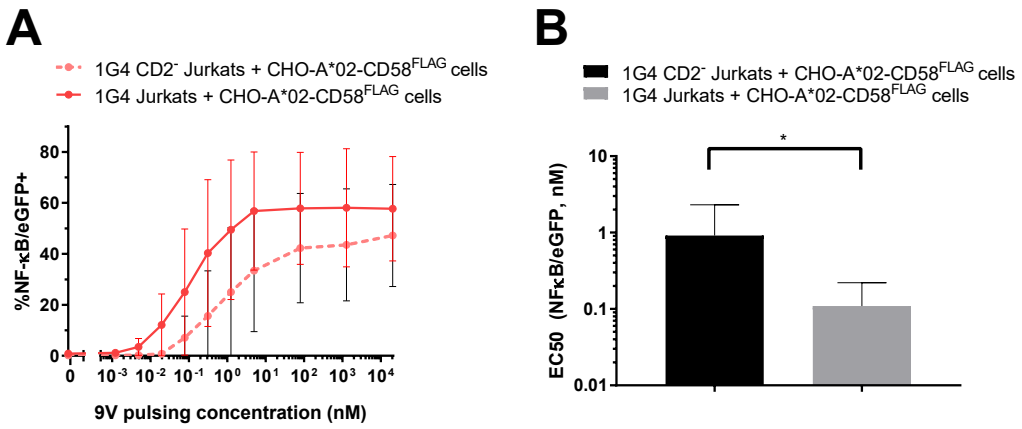


Figure 3.7: CD2 knockout reduces the EC_{50} of activation and recapitulates the quantitative results obtained with the CHO platform. **A.** The 1G4 NF-κB/eGFP and the 1G4 CD2$^-$ NF-κB/eGFP cell lines were co-cultured for 24 h with pulsed HLA-A*02$^+$ CD58$^+$ CHO cells. Afterwards, eGFP expression was measured by flow cytometry as a proxy for NF-κB activation. **B.** The differences in EC_{50} of activation for the two conditions were deemed statistically significant (* = $p \leq 0.05$) after fitting 4PL regressions and using an extra sum of squares F-test to compare models with either shared or different EC_{50} values. The data in this figure corresponds to the results of four independent experiments.

the addition of CD58 in APCs. Our results (Figure 3.8) indicate that the changes in antigen sensitivity as a result of CD2 engagement are the same regardless of whether the CD2/CD58 axis is disrupted by: (i) modifying expression of the CD58 ligand (CHO-A*02 vs. CHO-A*02-CD58^{FLAG}), or (ii) modifying expression of the CD2 receptor (1G4 Jurkats vs. 1G4 CD2$^-$ Jurkats).

3.2.5 CD2 overexpression increases antigen sensitivity at the expense of specificity

Human T cell leukaemia lines, such as the Jurkat or the HuT 78 lines, are routinely used to study TCR-proximal signalling events. Compared to primary T cells, they are easier to procure, culture, and transduce. Nonetheless, we acknowledge that caution should be exercised when interpreting the data obtained from immortalised cells: in the case of the E6.1 Jurkat lineage, reports have suggested these cells exhibit constitutive activation of phosphoinositide 3-kinase-mediated pathways, increased Ca^{2+} fluxes, and augmented phosphorylation of molecules

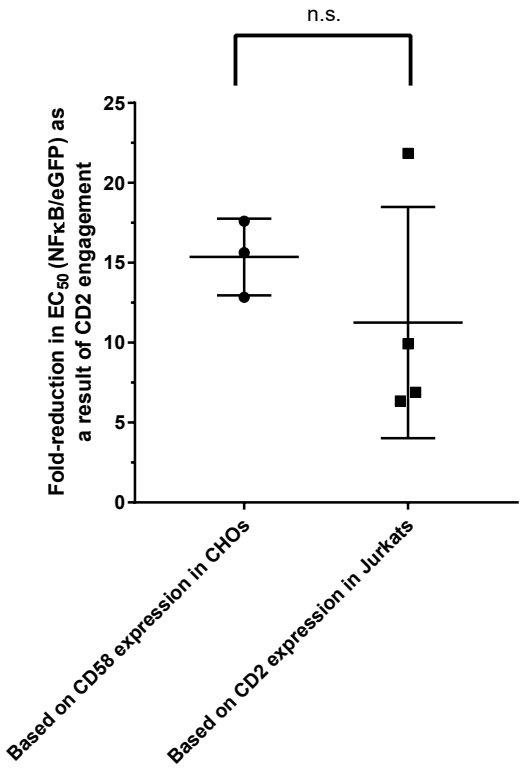


Figure 3.8: The CHO APC platform recapitulates the effects of CD2 knockout in Jurkat cells. We calculated the fold-reduction in EC_{50} of activation (as a function of NF-κB/eGFP$^+$ Jurkat cells) that could be attributed to the action of the CD2/CD58 axis. The data points to the left correspond to the experiments detailed in Section 3.2.3, where the 1G4 NF-κB/eGFP Jurkat line was co-cultured with HLA-A*02$^+$ CHO cells with or without CD58 expression. The data on the right reflects the metrics of the experiments from this section, where we co-cultured either the 1G4 NF-κB/eGFP or the 1G4 CD2$^-$ NF-κB/eGFP line with CHOs expressing both HLA-A*02 and CD58. All data points correspond to individual experiments, with the comparison between groups being conducted with a Mann-Whitney test (n.s. = not significant).

such as PLCγ1, Vav1, and Erk1/Erk2[200,201]. Expression of surface receptors such as CD44 or 4-1BB is also absent in the Jurkat E6.1 clone.

We hypothesised that reduced CD2 levels (compared to those exhibited by primary T cells) could also influence the phenotype described in the previous section. To test this, the R-PE Quantitation Beads Kit was used to quantitate CD2 levels in the 1G4 NF-κB/eGFP Jurkat line, and we found that these Jurkats expressed approximately 2.9×10^4 CD2 molecules/cell, an average density of $\sim$41 CD2 molecules/μm^2. This was only a fraction ($\sim$20%) of the reported[160]

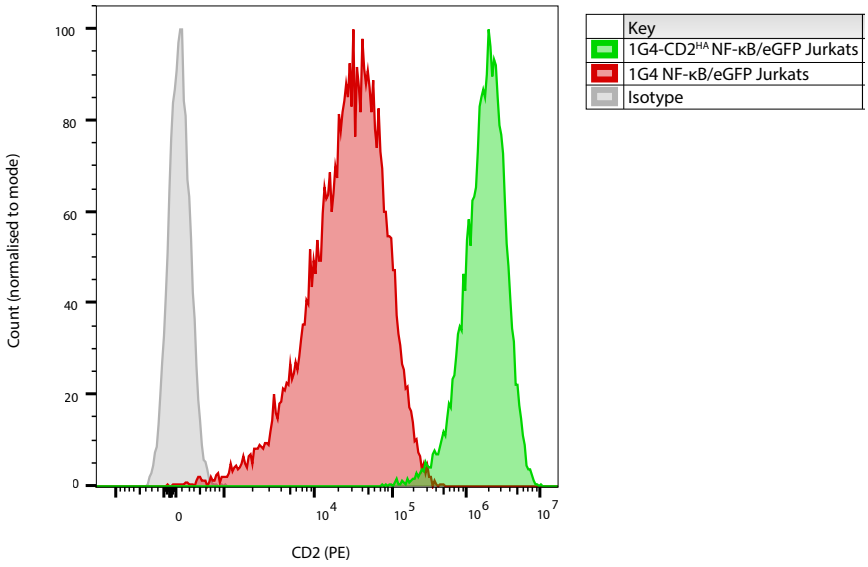


Figure 3.9: Overexpression of the CD2 receptor in the 1G4 NF-κB/eGFP Jurkat line. The 1G4 NF-κB/eGFP Jurkat population was lentivirally transduced with CD2 to account for the relative deficiency of this molecule compared to primary T cells[160]. After quantitating CD2 levels in the newly created 1G4-CD2^{HA} NF-κB/eGFP sub-line, it was found that it expressed supra-physiological CD2 levels: $\sim 3.3 \times 10^3$ molecules/μm^2 compared to $\sim$210 CD2 molecules/μm^2 in primary CD4$^+$ and CD8$^+$ EM cells[160].

CD2 densities in primary effector memory (EM) CD4$^+$ and CD8$^+$ T cells, which average $\sim$200 and $\sim$225 CD2 molecules/μm^2, respectively[†]. In light of this finding, we transduced the 1G4 NF-κB/eGFP Jurkats with additional human CD2 using the lentiviral supernatant produced from the CD2^{HA}/pLEX_307 vector. The 1G4-CD2^{HA} NF-κB/eGFP sub-line displayed an 80–fold increase in CD2 levels compared to the parental lineage (Figure 3.9). This also meant that, compared to primary T cells, this sub-line expressed supra-physiological CD2 levels ($\sim 3.3 \times 10^3$ molecules/μm^2) by a 15–fold factor.

When the 1G4-CD2^{HA} NF-κB/eGFP Jurkat population was co-cultured with CHO cells, we found that, upon CD2 engagement, a fraction (10%) of cells displayed antigen-independent activation. Surprisingly, engagement of the CD2/CD58 axis was capable of reducing the EC$_{50}$ of activation by 85–fold, going from 6.74×10^{-1} nM to 7.87×10^{-3} nM (Figure 3.10). Therefore, increased

[†]We assumed a spherical conformation for all cells plus an average diameter of 15 μm for Jurkats and of 10.5 μm for primary T cells.

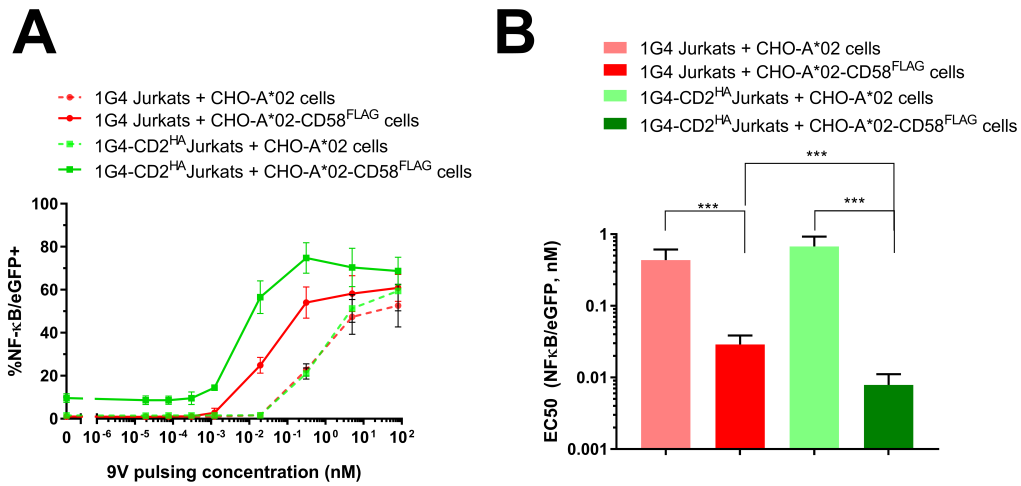


Figure 3.10: CD2 expression levels correlate with antigen sensitivity. A. The CD2-overexpressed 1G4-CD2^{HA} NF-κB/eGFP Jurkat population was co-cultured for 24 h with pulsed HLA-A*02^{+} CHO cells with or without CD58. Activation was then assessed via flow cytometry. Engagement of overexpressed CD2 leads to antigen-independent activation of a proportion of Jurkat cells. In addition, the CD2/CD58 axis mediates a 15–fold EC_{50} reduction in the 1G4 NF-κB/eGFP parental line, and an 85–fold EC_{50} reduction in the 1G4-CD2^{HA} NF-κB/eGFP sub-line. The data from the parental line, in red, has been repeated from Figure 3.6 to aid visualisation of the shift. Note the E_{min} ($\sim$8%) of the 1G4-CD2^{HA} NF-κB/eGFP population co-cultured with CHO-A*02-CD58^{FLAG} cells was deemed to be different (*** = $p \leq 0.001$) to that of the other conditions. This calculation was performed by fitting 4PL regressions and using an extra sum of squares F-test to compare models with either shared or different E_{min} values. **B.** The differences in EC_{50} of activation for the conditions assayed were deemed statistically significant (*** = $p \leq 0.001$) after fitting 4PL regressions and using pairwise extra sum of squares F-tests with a Bonferroni correction to compare models with either shared or different EC_{50} values. Data corresponds to the results of three independent experiments.

CD2 expression levels can improve antigen sensitivity, but might also lead to antigen-independent T cell activation.

3.3 Discussion

Here, we established a cellular platform to interrogate the CD2/CD58 axis in the context of antigen recognition. The use of rodent APCs minimised the number of extraneous stimuli that T cells could receive along with the TCR/pMHC signal. However, as we first mentioned in the introduction, our xenogeneic system is likely providing a co-stimulatory input through hamster ICAM-1 and human

LFA-1 (see Section 3.3.2 of this discussion). We characterised the CHO-A*02 and CHO-A*02-CD58^{FLAG} cell lines, ensuring that they had matched expression of HLA-A*02 and quantitating the number of CD58 molecules they expressed. We validated the usefulness of these lines by showing that not having CD58 in the CHOs produced a similar phenotype to that of removing CD2 from the 1G4 NF-κB/eGFP Jurkat effector population. Finally, we showed that engagement of the CD2/CD58 axis increased antigen sensitivity in the Jurkat line by a factor of 8–15 fold, and that CD2 overexpression further increased sensitivity (up to 85–fold) at the expense of specificity.

3.3.1 Revisiting the role of CD2

Although early work in mouse CD2 revealed the role of this receptor in improving antigen sensitivity, the small change (3–10 fold) mediated by this protein[149], and the fact that *Cd2*$^{-/-}$ mice mounted normal immune responses[150], meant that little attention was devoted to human CD2. Anton van der Merwe[163] reasoned that the roles of human and murine CD2 could be similar — namely enhancing antigen recognition at low antigen doses and/or low affinities. However, given the differences in affinity between the human CD2/CD58 and the murine CD2/CD48 complex (plus the restricted expression of CD48), he argued the role of CD2 could be more prominent in humans. Recent studies have suggested this could be the case: there is evidence of CD2 acting as a key co-stimulatory receptor for human CD28^{-} CD8^{+} T cells[202], as well as mediating granule polarisation and killing in CTLs[203]. In addition, downregulation or loss of CD58 can reduce immune activation in the context of cancer or infection[169–171].

Our efforts in quantitating the role of the human CD2/C58 axis in a cellular system were motivated by the remarkable effect of CD2 engagement reported by Pettmann *et al.*[1] in a reductionist system (Figure 3.1). Such a platform suggested that the availability of CD58 was capable of: (i) improving antigen sensitivity by almost three orders of magnitude, and (ii) enabling T cell activation

by very low affinity antigens. As these phenotypes could be associated with on-target/off-tumour and off-target/off-tumour cross-reactivity, they also constitute a motivation for the work we conduct in Chapters 4 and 5. Our CHO-A*02 cellular system enabled us to determine improvement in antigen sensitivity (EC_{50}), as a result of CD2/CD58 engagement. According to our results, it appears the human CD2/CD58 axis mediates an increase of one order of magnitude in sensitivity even in the absence of compensatory mechanisms such as CD28/B7 co-stimulation. Nonetheless, we cannot rule out a compensation mechanism mediated by LFA-1 (see next section). In any case, however, the discrete increases in antigen sensitivity as a result of human CD2 engagement are in the same order of magnitude as those reported for murine CD2[149].

We also found that increased CD2 levels correlate with an improvement in sensitivity. Indeed, overexpression of this receptor could increase antigen sensitivity by up to 85–fold when the 1G4-$CD2^{HA}$ NF-κB/eGFP Jurkat line was cultured with CD58-expressing CHOs. Surprisingly, CD2 overexpression was linked to antigen-independent activation of a fraction ($\sim$10%) of cells. We think there are distinct possibilities that account for this observation. First, this phenomenon could be mediated by the forced CD45-kinase segregation as a result of the sheer number of CD2/CD58 close contacts. As the kinetic segregation (KS) model posits[204], exclusion of the CD45 phosphatase from the TCR/pMHC engagement zones occurs due to its large extracellular domain ($\sim$22 nm), which in turn enables continued TCR phosphorylation by Lck and downstream signalling to occur. In this respect, Chang *et al.*[205] have previously reported —in SLBs— T cell signalling mediated solely by forced CD45 exclusion at close contacts, which was achieved by an engineered, high affinity rat CD2/CD48 interaction that mimics that of human CD2/CD58.

The non-physiological levels of CD2/CD58 complexes that would be formed upon co-culturing 1G4-$CD2^{HA}$ NF-κB/eGFP Jurkats with CHO-A*02-$CD58^{FLAG}$ cells could be mediating other phenomena. For example, engagement of a large number of CD2 molecules could mimic the TCR-dependent, mitogenic

stimuli reported when cross-linking CD2 through the use of monoclonal antibody combinations[206,207]. Indeed, we can consider that some of the anti-CD2 pairs that induce stimulation target the T11.1 and T11.2 epitopes[207], which are part of the CD2 adhesion domain[42]. Moreover, we cannot rule out the possibility of the sheer number of CD2/CD58 interactions acting as *cellular amplifiers* of Jurkat/CHO xenorecognition events (see the concept of $k_{amp}{}^{2}$). Interestingly, xenogeneic responses appear to be dependent on interaction of accessory molecules[208], which we are artificially promoting in our assays.

3.3.2 Improving the experimental platform

The CHO-A*02 and CHO-A*02-CD58^{FLAG} cell lines allow us to interrogate the CD2/CD58 axis in a cellular setting whilst minimising the number of T cell extraneous interactions. Genomic studies of the CHO-K1 cell line[172] have shown there is no expression of CD48 or CD86. Since this line was not derived from a haematopoietic lineage, it is unlikely it would express other ligands typically associated to professional APCs, such as CD80, 4-1BBL, or CD70 (and it is unclear whether those would even cross-react with the corresponding human receptors). Nonetheless, the CHO cell lines could be validated by staining them with monoclonal hamster antibodies against those molecules to further cement this notion.

We acknowledge, however, that CHO cells *do* express a large number of cell adhesion molecules[209], including ICAM-1[172]. For several reasons, we would be inclined to suggest the existence of cellular interactions between hamster ICAM-1 and human LFA-1 in our system. We can first start by considering the degrees of sequence homology between hamster (UniProt Q9ERF7), murine (UniProt P13597), and human (UniProt P05362) ICAM-1. Hamster and murine ICAM-1 share a sequence homology greater than 70%; this is likely to explain the characterised cross-reactivity between hamster ICAM-1 and murine LFA-1[153,192]. These experimental reports have confirmed: (i) the contribution of hamster ICAM-1 to antigen sensitivity in mouse T cells[153], and (ii) that hamster ICAM-1

can act as a *bona fide* co-stimulatory molecule for murine cells[192]. Human ICAM-1 shares a sequence homology of ∼50% to mouse and hamster ICAM-1, although this identitity percentage goes up to 70% when comparing domains one and two of human and mouse ICAM-1[194]. Consequently, this can explain the cross-species recognition between human LFA-1 and mouse ICAM-1[193,194].

Therefore, a hamster ICAM-1 synergy with human LFA-1 would presumably mirror the antigen sensitivity enhancement observed by Milstein *et al.*[153] in the context of hamster ICAM-1 and murine LFA-1. This, in turn, would partially mask the EC_{50} shifts we report in our CHO-A*02 platform. To account for this possibility, further experiments are required. If we focus on the CHO-A*02 system, we could use blocking antibodies against hamster ICAM-1 (such as the clone J5-3F9[153]) or perform CRISPR/Cas9-mediated disruption of this protein in our CHO cells[209]. If these knockout lines are recreated from the CHO-K1 line, they could also be generated using polyclonal populations at each step, avoiding the variability that can result between any two given single clones. Alternatively, our research group has developed a series of mutants derived from the U87 and U251 glioblastoma cell lines, which have a either a wild type, $CD58^-$, ICAM-1^-, or $CD58^-$ ICAM-1^- phenotype. Using this platform, we could isolate the contributions of CD58 and ICAM-1. Moreover, we would also recapitulate the presence of inhibitory ligands that are known to be expressed by gliomas and present in the U87 and U251 lines — namely PD-L1[210].

4

CD2 disruption as a strategy to ameliorate on-target/off-tumour toxicity

Contents

4.1 Introduction 87
4.1.1 On-target/off-tumour toxicity in ACT 87
4.1.2 Manipulating the CD2/CD58 axis 91
4.1.3 Chapter aim 91
4.2 Results 92
4.2.1 Elongated CD2 chimeras fail to antagonise endogenous CD2 in the CHO system 92
4.2.2 Tail-less CD2 chimeras do not antagonise endogenous CD2 in the CHO system 94
4.2.3 Elongated CD2 chimeras reduce antigen sensitivity in a T2 APC system 94
4.2.4 CD2 disruption in primary human $CD8^+$ T cells reduces antigen sensitivity, mitigating on-target/off-tumour toxicity 97
4.3 Discussion 102
4.3.1 Disruption of the CD2/CD58 axis by transduction of elongated CD2 chimeras 104
4.3.2 CD2 knockout in ACT 107

4.1 Introduction

Therapies using CAR-T cells have seen success against haematological malignancies: both the FDA and the EMA have approved three different anti-CD19 CARs (Kymriah, Yescarta, and Tecartus) for treatment of certain types of leukaemia and lymphoma (Section 1.3.1). Widespread adoption of ACT using CAR-T or TCR-T cells still faces multiple challenges, which we outlined in Chapter 1. The dissimilar nature of these unmet needs (poor proliferation and/or persistence, solid malignancies, antigen modulation, and over-activation concerns) means that multiple strategies will be needed to improve ACT. Here, we will focus on tackling the problem of on-target/off-tumour toxicity, which occurs when engineered T cells attack healthy tissues expressing a target TAA (usually at a lower level compared to that of cancer cells).

Having previously shown that the CD2/CD58 axis improves T cell antigen sensitivity, in this chapter we show that CD2 disruption can be a viable strategy for ameliorating instances of on-target/off-tumour toxicity in ACT. In order to disrupt CD2, we explore two experimental approaches: transduction of elongated CD2 chimeras in Jurkat cells and *CD2* knockout in primary cultures. Using those approaches, we establish that T cell activation can be selectively reduced at low antigen doses without abolishing efficacy at high antigen densities.

4.1.1 On-target/off-tumour toxicity in ACT

T cell sensitivity

T lymphocytes are remarkably sensitive: when detecting antigens through their TCR, there is evidence[37,211,212] suggesting activation can be elicited with as few as 1–10 cognate pMHCs. From an evolutionary point of view, this adaptation likely derives from the fact that, during infection, T cells are presented with a reduced number of pMHC ligands. Using a recombinant TCR, Yang *et al.*[213] found that *in vitro* human immunodeficiency virus (HIV)-infected $CD4^+$ T cells only expressed between 8–46 HIV epitopes. In the case of influenza A viruses, particular epitopes have been reported at densities as low as 0.5 copies/cell[214]. Other viruses, such

as CMV, are known to downregulate specific pMHC complexes from ∼10 000 to less than 100 copies per infected cell[215]. T cells must overcome these challenges with high antigen sensitivity in order to ensure detection of an infection.

Several molecular mechanisms[2] are responsible for the antigen detection capabilities of the TCR. Given the architectural differences between CARs and TCRs, it is plausible to consider CARs do not capitalise on all the endogenous machinery of the T cell. A reflection of this can be seen in the reduced antigen sensitivity (2–3 orders of magnitude) CARs exhibit when directly benchmarked against TCRs[68,74]. This defect, which is relative to the TCR, still implies that CAR-T cells can lyse targets expressing as little as 100–200 ligands[73,216,217].

Sensitivity trade-offs in ACT

Whilst high sensitivity is useful in the context of infection, it carries some risks when using engineered T cells in cancer immunotherapy. The problem we explore here stems from the fact that the majority of the CARs target TAAs that are overexpressed in malignancies, as the number of reported TSAs amenable to CAR therapy is limited*. Considering that TAAs are also expressed in healthy tissues, TCR- and CAR-T cells can display on-target/off-tumour toxicity, attacking cells bearing physiological levels of the target antigen (Figure 4.1)[138].

As we indicated in Chapter 1, on-target/off-tumour recognition of healthy cells has been observed in multiple instances of ACT. Commonly cited examples include the reports of Parkhurst *et al.*[127], who observed transient colitis when treating colorectal cancer with an engineered TCR recognising CEA. This side effect was caused by detection (and subsequent destruction) of healthy intestinal crypt epithelial cells, which have weak CEA expression. On-target/off-tumour toxicities have been observed in CARs targeting EGFR, CAIX, HER2/neu, and NKG2DL[128–131]. It is likely that the fatality reported by Morgan *et al.*[131] was caused by recognition of low levels of HER2/neu in lung epithelial cells.

*The literature reports few potential TSAs for CAR-T cell therapy. They usually include EGFRvIII and aberrant glycoforms of MUC1 and CD43[218–220]. For TCR-T cells, MHC-restricted neoantigens represent a large pool of TSAs[221].

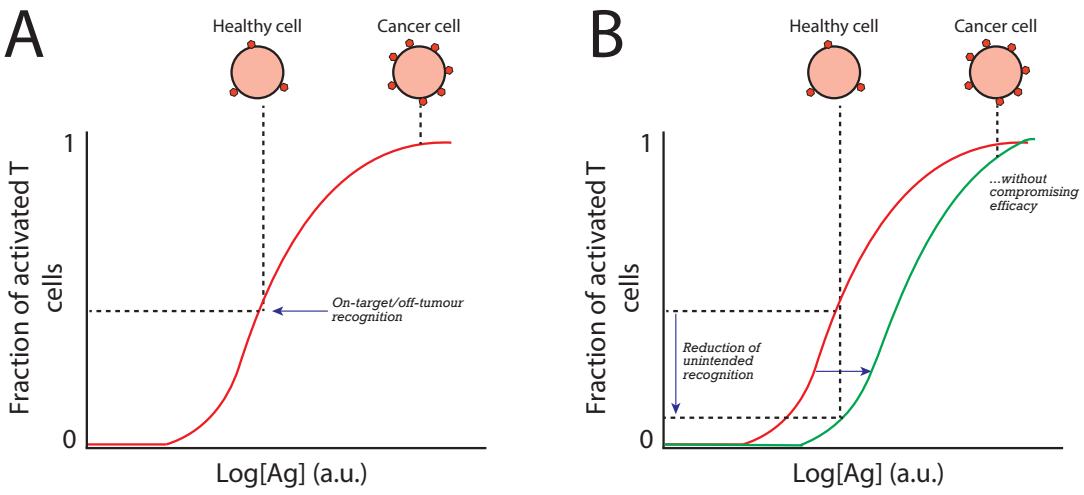


Figure 4.1: On-target/off-tumour toxicity in ACT. A. On-target/off-tumour toxicity arises when targeting TAAs that are overexpressed in malignant cells. As a result of their high sensitivity, a proportion of T cells can become activated and attack healthy tissues expressing low levels of the TAA. **B.** A possible strategy to ameliorate this problem is to reduce T cell activation at low antigen doses. To avoid compromising the outcome of ACT, this reduction in antigen sensitivity should not impair efficacy (E_{max}) at high antigen doses.

Multiple ideas have been explored to reduce the risk of on-target/off-tumour toxicity. They can be placed into different categories:

- **Refining the administration protocols:** Additional studies using anti-HER2/neu CARs have reduced the severity of adverse events by infusing smaller amounts of CAR-T cells (three infusions of 10^8 cells[222], compared to a single dose of 10^{10} cells reported in the Morgan *et al.*[131] study). Other authors have trialled infusions without lymphodepletion or IL-2 support[223]. These measures can also help with instances of T cell overactivation when targeting malignant tissue (on-target/on-tumour toxicity, recall Chapter 1).

- **Affinity tuning:** Evidence suggests that reductions in the affinity of CAR-T cells to their antigen improves their capability in discriminating between healthy tissues and tumours. This enables them to lyse targets overexpressing a TAA while sparing healthy tissues bearing low TAA levels[132–134].

- **Dual targeting:** Some authors have proposed the use of combinatorial signalling approaches, where only simultaneous engagement of two ligands can trigger the engineered T cells[224–226]. This assumes that only malignant cells would co-express the two TAA, with healthy cells expressing a single TAA being spared.

- **Synthetic circuits:** More recently, Hernández-López *et al.*[227] explored the use of a synNotch platform to generate a positive feedback circuit endowing HER2/neu CAR-T cells with an ultrasensitive threshold. The design relies on a low affinity (K_D = 210 nM) synNotch that recognises HER2/neu, and, upon engagement, releases a transcription factor driving the expression of a high affinity (K_D = 17.6 nM) anti-HER2/neu CAR. The signalling cascade is only completed when HER2/neu is present at high densities ($\sim 10^6$ molecules/cell), so T cell activation is restrained at low antigen densities.

These clinical and experimental approaches do provide useful ways to limit toxicities associated to on-target/off-tumour recognition events. However, we note that in order to warrant widespread adoption, most of these strategies will require engineering on a case-by-case basis. Depending on the specific CAR/ligand interaction, it will be necessary to perform affinity tuning for the scFv involved (including those used in hypothetical synNotch circuits). In the case of logic gates, unique antigen combinations will need to be found and trialled for different malignancies. Moreover, if one of the two antigens targeted is downregulated by the tumour, the efficacy of the treatment would be compromised. Finally, the literature reports all these improvements in the context of CARs; it is unclear whether the TCR would be amenable to these approaches given its high sensitivity and the complex interactions between TCR/pMHC affinity and activation[1,228].

4.1.2 Manipulating the CD2/CD58 axis

The dimensions of the TCR/pMHC and the CD2/CD58 complexes are roughly the same, spanning an intermembrane distance of ∼13–15 nm[204,229]. Evidence suggests that TCR triggering is dependent on the dimensions of the pMHC ligand and the CD48 counter-receptor[145,189]. Consistent with the KS model, elongation of either pMHC or CD48 reduces sensitivity to antigen and impairs overall T cell response. These elongations are thought to prevent the formation of close TCR/pMHC contacts, which under normal circumstances lead to the exclusion of phosphatases such as CD45 and allow sustained Lck-mediated phosphorylation of the TCR.

We reasoned that, by generating elongated variants of the CD2 receptor and transducing them into the 1G4 NF-κB/eGFP Jurkat line, we could recapitulate the inhibitory effect observed by Wild *et al.*[189] when elongating CD48 on target cells. Our reasoning considered that, when presented with CD58 on CHO cells, these chimeras would outcompete endogenous CD2 and hinder TCR/pMHC binding at low antigen densities. This, in turn, would result in a reduction in antigen sensitivity compatible with our objective of mitigating on-target/off-tumour cross-reactivity.

Here, we tested a number of CD2 chimeras, which we elongated by inserting spacers between their extracellular and transmembrane domains. To generate these chimeras, we have inserted either: (i) two, four, or seven Ig domains, or (ii) the extracellular region of CD43 (Figure 4.2). As an additional way of manipulating the CD2/CD58 axis, we also explored direct CRISPR/Cas9-mediated *CD2* disruption in primary human CD8$^+$ T cells.

4.1.3 Chapter aim

In light of the information obtained in Chapter 3, the overarching aim of this chapter is to show that disruption of the CD2/CD58 axis leads to a reduction in T cell sensitivity (EC_{50}) without compromising efficacy (E_{max}) at high antigen densities. This has the potential of reducing instances of on-target/off-tumour toxicity (Figure 4.1) in ACT. We aim to achieve this phenotype by disrupting

CD2 through two different strategies. For the first one, we transduce elongated CD2 chimeras that outcompete endogenous CD2 and impair recognition of T2 target cells by the 1G4 NF-κB/eGFP Jurkat cell line. In the second approach, we generate primary 1G4 CD2^{-} CD8^{+} T cells, which display reduced sensitivity compared to their CD2 wild type counterparts when recognising either CHO-A*02-CD58$^{\mathrm{FLAG}}$ or T2 cells.

4.2 Results

4.2.1 Elongated CD2 chimeras fail to antagonise endogenous CD2 in the CHO system

To antagonise endogenous CD2 with exogenous, elongated CD2 chimeras, we designed a collection of elongated CD2 constructs using the CD2$^{\mathrm{HA}}$ protein as a starting point (see Figure 4.2 and Section 2.3.2). Our chimeras elongated the extracellular region of CD2 by either two, four, or seven Ig domains (CD2$^{\mathrm{HA}}$-2Ig, CD2$^{\mathrm{HA}}$-4Ig, and CD2$^{\mathrm{HA}}$-7Ig, respectively). We also generated an additional CD2$^{\mathrm{HA}}$ chimera by appending the extracellular region of human CD43 right after the two CD2 ectodomains (CD2$^{\mathrm{HA}}$-CD43$^{\mathrm{Ecto}}$). Based on the literature[229–231], the extended conformations of our constructs spanned extracellular distances between ∼15 and ∼50 nm, compared to the ∼7.5 nm of the native CD2 receptor (Figure 4.2).

After transduction and puromycin selection of the parental 1G4 NF-κB/eGFP Jurkat line, four additional sub-lines expressing the elongated constructs were obtained. We then corroborated similar expression levels for these chimeras (transduction efficiencies >95%) and binding of these constructs to CD58 (Appendix B). We conducted a series of co-cultures with pulsed CHO-A*02 and CHO-A*02-CD58$^{\mathrm{FLAG}}$ cells to check whether these constructs outcompeted endogenous CD2 and reduced T cell antigen sensitivity. The experiments were conducted in two parts; the first one assessed the 1G4-CD2$^{\mathrm{HA}}$-2Ig and the 1G4-CD2$^{\mathrm{HA}}$-4Ig NF-κB/eGFP Jurkat lines, the second part assessed the 1G4-CD2$^{\mathrm{HA}}$-7Ig and the 1G4-CD2$^{\mathrm{HA}}$-CD43$^{\mathrm{Ecto}}$ NF-κB/eGFP Jurkat populations. In

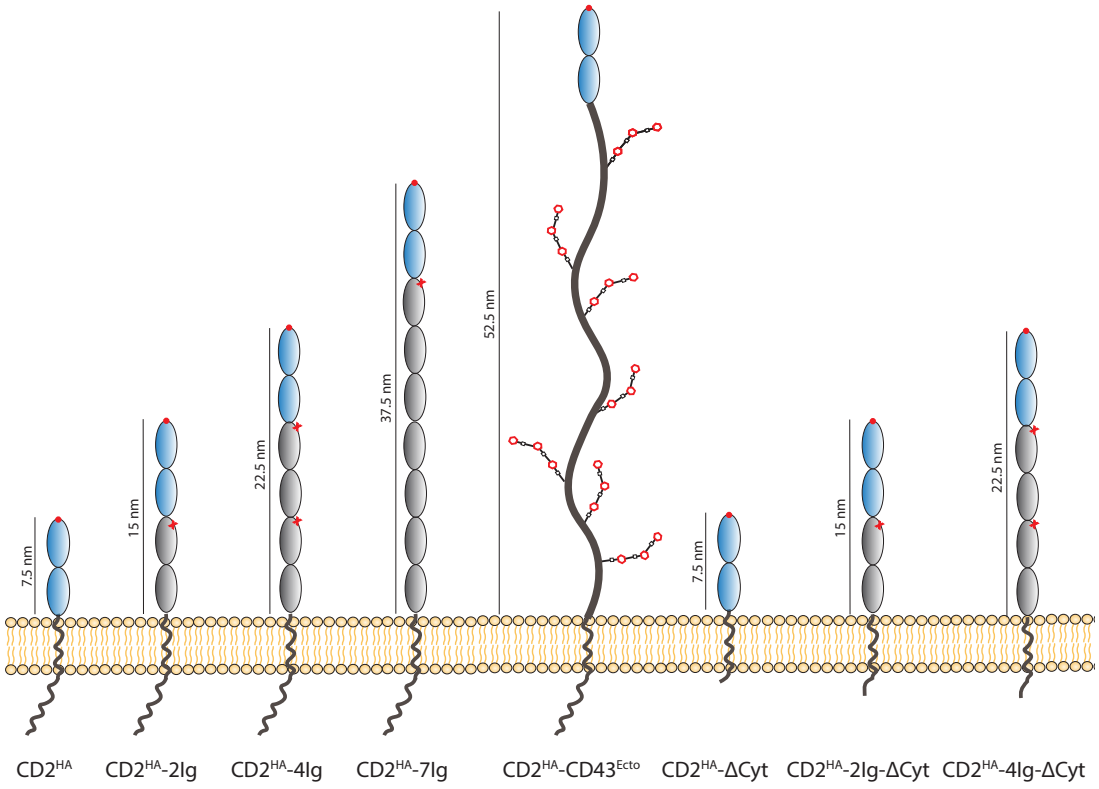


Figure 4.2: Schematic of the elongated CD2 chimeras. Using the $CD2^{HA}$ construct as a starting point, a series of elongated chimeras were generated by introducing either two, four, or seven Ig domains in the extracellular region of this receptor. An additional construct was generated by appending the extracellular amino acids from the CD43 glycoprotein. Moreover, select tail-less CD2 elongated variants (ΔCyt series), which only had 10 amino acids in their cytosolic region, were generated by deleting amino acids 246-351 of their full tail counterparts. The theoretical, approximate dimensions are indicated for each construct. The red circle corresponds to the HA tag. For all the $CD2^{HA}$-2Ig and $CD2^{HA}$-4Ig constructs, where the additional Ig domains were obtained by duplicating the ectodomains of CD2, the red cross represents the K67E mutation, which abolishes CD58 binding[165]. In the case of the $CD2^{HA}$-7Ig chimera, where the elongation was made with CD22, the cross represents the R120A mutation to abolish sialic acid binding[232]. The specific references to amino acids are made considering the full-length original protein (see Section 2.3.2 for further details on the cassettes). The figures are not to scale and the measurements indicated assume a fully extended conformation of the constructs. We note others[153] have suggested that appending additional Ig domains increases intermembrane separation by only $\sim$1 nm/Ig-like domain.

all experiments, we always used the parental 1G4 reporter line as a reference. Our data indicated (Figure 4.3) that none of these chimeras lead to a reduction in sensitivity upon CD2/CD58 engagement, with all the sub-lines showing activation phenotypes mirroring those of the parental line.

4.2.2 Tail-less CD2 chimeras do not antagonise endogenous CD2 in the CHO system

In addition to the elongated CD2 chimeras with functional cytosolic tails, we also generated tail-less variants of the CD2 receptor, which only had 10 amino acids in their cytosolic region. These variants, termed $CD2^{HA}-\Delta Cyt$, $CD2^{HA}-2Ig-\Delta Cyt$, and $CD2^{HA}-4Ig-\Delta Cyt$, were generated from their full-tail counterparts by deleting amino acids 246-351 (Figures 2.1 and 4.2). After transducing these receptors into the 1G4 NF-κB/eGFP Jurkat line, we conducted a set of experiments using the same configuration described in the previous section. We then compared the activation profiles obtained when co-culturing the Jurkat variants with either CHO-A*02 or CHO-A*02-$CD58^{FLAG}$ cells (Figure 4.4). Our results suggested that these tail-less chimeras also failed to outcompete endogenous CD2 and reduce T cell antigen sensitivity. In fact, upon CD58 engagement, the EC_{50} of activation was comparable to that of the parental 1G4 NF-κB/eGFP Jurkat population.

4.2.3 Elongated CD2 chimeras reduce antigen sensitivity in a T2 APC system

After observing that the elongated CD2 constructs did not act as dominant negatives in the CHO-A*02 platform, we asked whether a different phenotype would be observed when using a standard APC. In the first instance, we considered that the very high levels of CD58 expressed in the CHO lines, in the order of 7.6×10^6 molecules/cell (Table 3.1) meant that the elongated chimeras were not expressed in sufficiently high quantities to preferentially bind all CD58 in the target cells and outcompete endogenous CD2. To test this hypothesis, we repeated some of the previous co-cultures using the HLA-A*02^+ lymphoblast

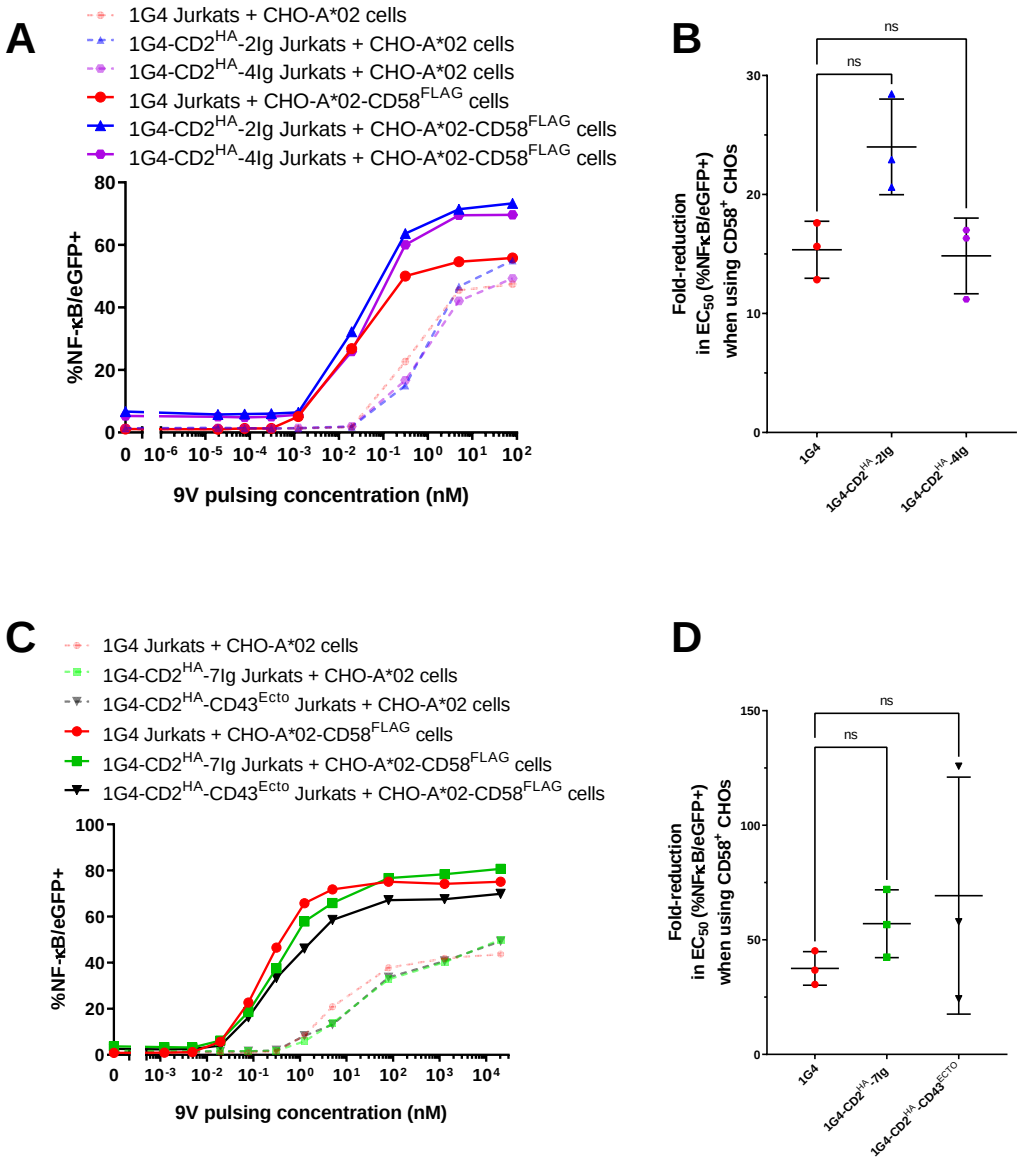


Figure 4.3: In the HLA-A*02 CHO system, elongated CD2 chimeras fail to antagonise endogenous CD2 in the presence of CD58. The parental 1G4 NF-κB/eGFP Jurkat line was transduced with a series of $CD2^{HA}$ chimeras whose ectodomains were elongated by appending either two, four, seven Ig domains, or the extracellular region of CD43. All these sub-lines were co-cultured in the presence of 9V-pulsed HLA-A*02 CHO cells with or without CD58 expression. The experiments were conducted in two parts (**A-B** and **C-D**), each one with three independent repeats. **A and B.** In the presence of CD58, the $CD2^{HA}$-2Ig and $CD2^{HA}$-4Ig chimeras do not act as dominant negatives for endogenous CD2, as they do not reduce EC_{50} of activation. **C and D.** Same as for A and B, except that the constructs tested were $CD2^{HA}$-7Ig and $CD2^{HA}$-$CD43^{Ecto}$. The changes in EC_{50} of activation were analysed using a Kruskal-Wallis *post hoc* Dunn's test; n.s. = not significant. The graphs shown in A and C correspond to a representative experiment. Note the data from the parental line in A and B has already been presented in Section 3.2.3.

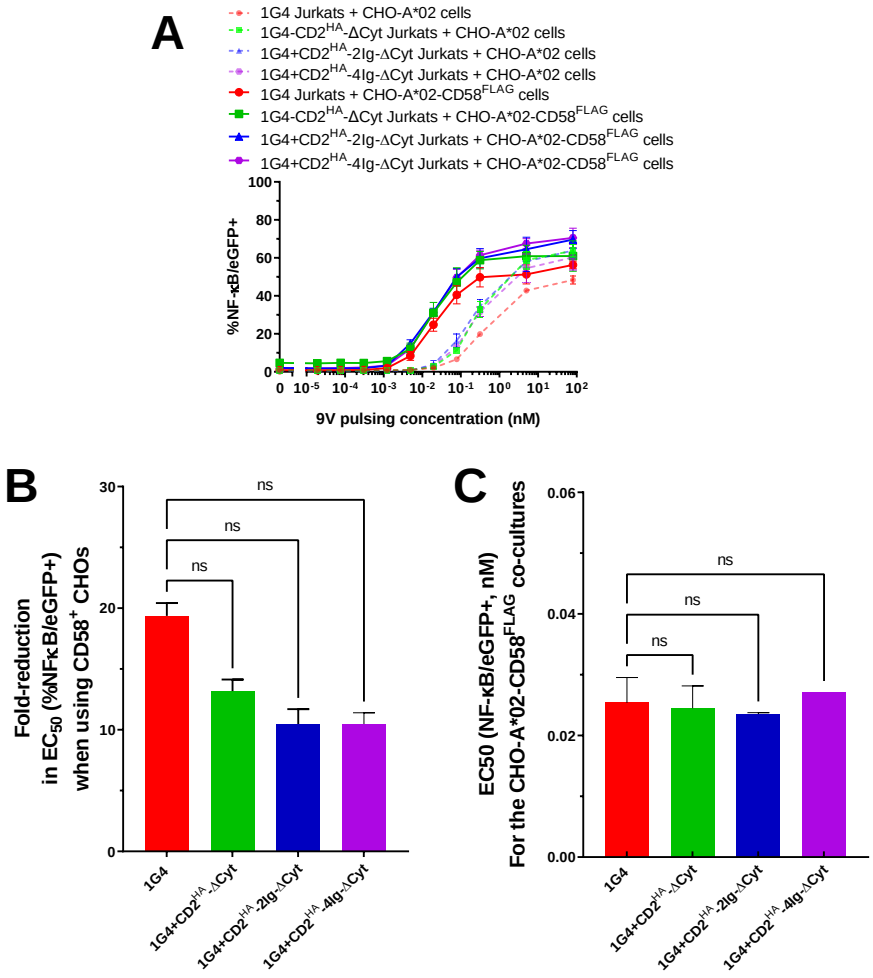


Figure 4.4: In the presence of CD58, tail-less CD2 chimeras do not antagonise endogenous CD2. The parental 1G4 NF-κB/eGFP Jurkat line was transduced with a series of tail-less, dead CD2 chimeras. These chimeras, termed $CD2^{HA}-\Delta Cyt$, $CD2^{HA}-2Ig-\Delta Cyt$, and $CD2^{HA}-4Ig-\Delta Cyt$, were identical to their full-tail counterparts except that they only contained 10 amino acids in their cytosolic region (Figure 2.1). The Jurkat sub-lines were co-cultured in the presence of HLA-A*02 CHO cells with or without CD58 expression, which had been exogenously pulsed with the 9V peptide. **A.** In the presence of CD58, the $CD2^{HA}-\Delta Cyt$, $CD2^{HA}-2Ig-\Delta Cyt$, and $CD2^{HA}-4Ig-\Delta Cyt$ chimeras do not act as dominant negatives over endogenous CD2, since they do not reduce the EC_{50} of activation. **B.** For each line, we compared the change in EC_{50} resulting from using the CHO-A*02-$CD58^{FLAG}$ cells (using the CHO-A*02 cells as a reference). No significant differences were observed between the parental line and those transduced with the tail-less CD2 variants. **C.** We also calculated the raw EC_{50} values for all the co-cultures between Jurkats and CHO-A*02-$CD58^{FLAG}$ cells. These values were comparable to those registered for the parental line, suggesting that these tail-less chimeras were not mediating a change in antigen sensitivity. For this experiment, we conducted two independent repeats. The statistical comparisons were carried out using a Kruskal-Wallis *post hoc* Dunn's test; n.s. = not significant.

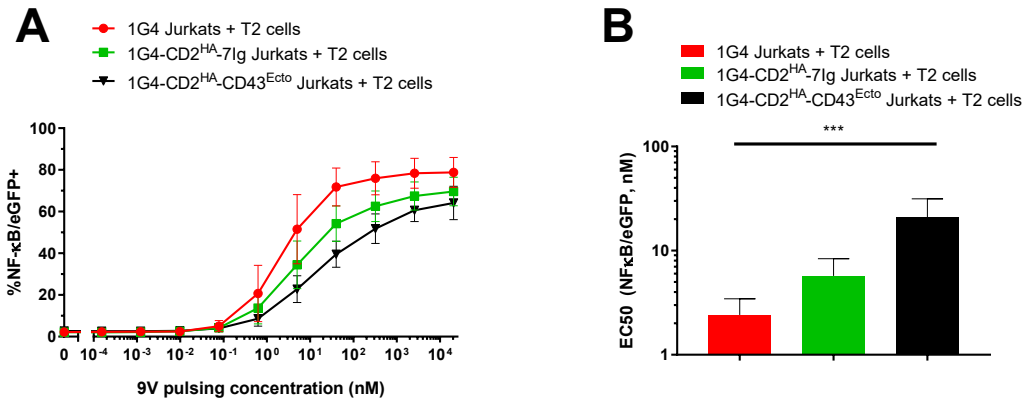


Figure 4.5: Elongated CD2 chimeras impair antigen sensitivity in a T2 APC system. A. Co-cultures between T2 cells and the reporter Jurkat lines carrying the 1G4 TCR only (parental line) or this TCR plus the elongated $CD2^{HA}$-7Ig or $CD2^{HA}$-$CD43^{Ecto}$ constructs were conducted. Transduction of either construct appears to impair antigen sensitivity relative to the parental 1G4 NF-κB/eGFP Jurkat reporter line. **B.** The differences in EC_{50} of activation were deemed statistically significant (*** = $p \leq 0.001$) by fitting 4PL regressions and using an extra sum of squares F-test to compare models with either shared or different EC_{50} values. The data corresponds to the results of three independent experiments.

T2 cell line, which we knew expressed fewer CD58 molecules (approximately 6.2×10^5 molecules/cell, recall Table 3.1).

When performing co-cultures between the Jurkat lines and T2 cells pulsed with the 9V peptide (Figure 4.5A), we found statistically significant reductions in the antigen sensitivity exhibited by the 1$CD2^{HA}$-7Ig and $CD2^{HA}$-$CD43^{Ecto}$ reporter Jurkat lines. Whereas for the 1G4 parental line the EC_{50} of activation was 2.41 nM, we calculated a modest 2–fold increase for the cells expressing the $CD2^{HA}$-7Ig construct (EC_{50} = 5.73 nM). The 1G4-$CD2^{HA}$-$CD43^{Ecto}$ sub-line displayed an impairment in sensitivity of approximately 8–fold (EC_{50} = 21.03 nM) (Figure 4.5B).

4.2.4 CD2 disruption in primary human $CD8^+$ T cells reduces antigen sensitivity, mitigating on-target/off-tumour toxicity

Through the use of the CHO-A*02 APC system and the generation of a CD2 knock-out Jurkat clone (Sections 3.2.3 and 3.2.4), we showed in the 1G4 NF-κB/eGFP

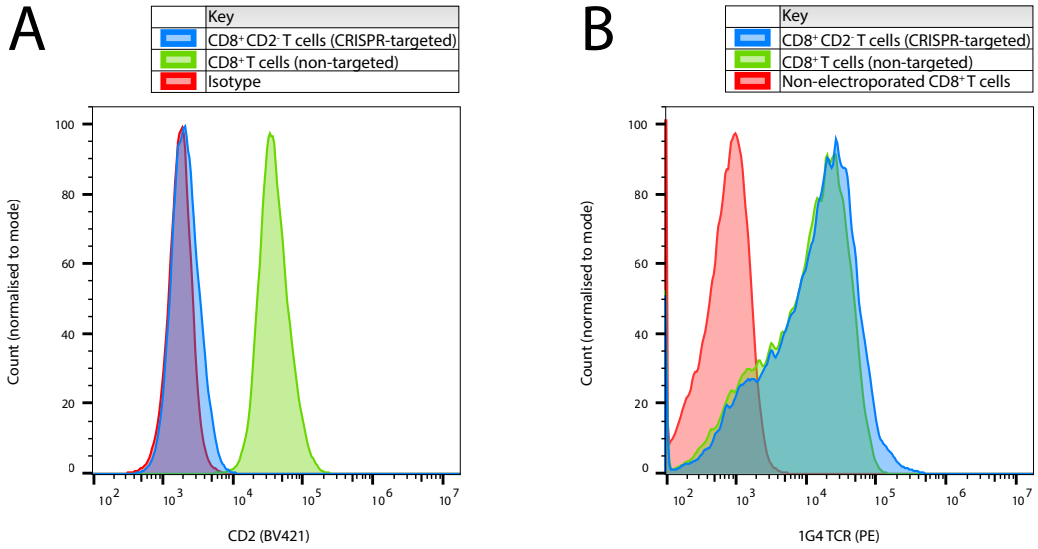


Figure 4.6: Generation of primary 1G4 CD2$^-$ CD8$^+$ T cells. Through the combination of a lentiCRISPR commercial system targeting *CD2*, a depletion step of CD2$^+$ T cells, and electroporation of the 1G4 TCR, we obtained highly enriched populations of 1G4$^+$ CD2$^-$ CD8$^+$ T cells. **A.** CD2 depletion efficiencies routinely reached levels >95%. **B.** After electroporation, the CD2$^-$ CD8$^+$ T cells expressed 1G4 TCR levels similar to those of their CD2 wild type counterparts. Electroporation efficiencies ranged between 50–85%.

Jurkat line that CD2 mediated an increase in antigen sensitivity. In the previous section, we demonstrated that, under certain circumstances, expression of elongated CD2 chimeras can impair T cell antigen sensitivity. In principle, we consider that these CD2 disruptions —either in the form of a knockout or by expression of a competing chimera— produce a phenotype that would mitigate on-target/off-tumour recognition events in ACT.

To further support our hypothesis, we recognised the need of showing similar phenotypes using primary T cells and functional readouts such as cytotoxicity. We devised an experimental strategy to generate primary 1G4 CD2$^-$ CD8$^+$ human T cells. The strategy relied on a lentiCRISPR commercial system targeting *CD2*, a CD2 depletion step, and mRNA electroporation of the 1G4 TCR (Section 2.7.3). This enabled us to routinely obtain CD8$^+$ T cell populations with CD2 depletion efficiencies over 95% and TCR electroporation efficiencies ranging between 50–85%. Levels of the 1G4 TCR were not affected by the CD2 status of the cell (Figure 4.6).

First, we queried the effect of CD2 loss in primary CD8$^+$ T cells recognising

the 9V peptide loaded onto CHO-A*02-CD58^{FLAG} cells. We performed the CD8$^+$/CHO co-cultures for 6 h at an E:T ratio of 2:1, which we adjusted for electroporation efficiency (two 1G4$^+$ CD8$^+$ T cells per CHO cell). As functional readouts, we measured the gMFI of the 4-1BB and CD25 activation markers. To account for biological and technical variability, the maximum gMFI value of each independent donor was normalised to one before calculating the averages. Table 4.1 and Figure 4.7 summarise the results obtained, which suggest a 5–6 fold decrease in antigen sensitivity linked to CD2 knockout.

Table 4.1: Summary of the activation metrics for 1G4 CD8$^+$ T cells co-cultured with CD58$^+$ HLA-A*02$^+$ CHO cells. 1G4 CD8$^+$ T cells with or without CD2 expression were co-cultured with CD58-expressing CHOs as surrogate APCs. Co-cultures were performed at an adjusted E:T ratio of 2:1 and lasted 6 h. Upregulation of the 4-1BB and CD25 activation markers was assessed via flow cytometry, and the EC_{50} of activation calculated for each experimental condition by fitting a 4PL regression to the data shown in Figure 4.7. The table also shows the n–fold reduction in antigen sensitivity displayed by CD2 knockout cells compared to their wild type counterparts.

Readout	**EC_{50} (nM) for 1G4 CD8$^+$ T cells**	**EC_{50} (nM) for 1G4 CD2$^-$ CD8$^+$ T cells**	**n–fold reduction in antigen sensitivity**
4-1BB gmFI	4.84×10^{-2} nM	2.81×10^{-1} nM	5.81
CD25 gMFI	1.61×10^{-2} nM	7.91×10^{-2} nM	4.93

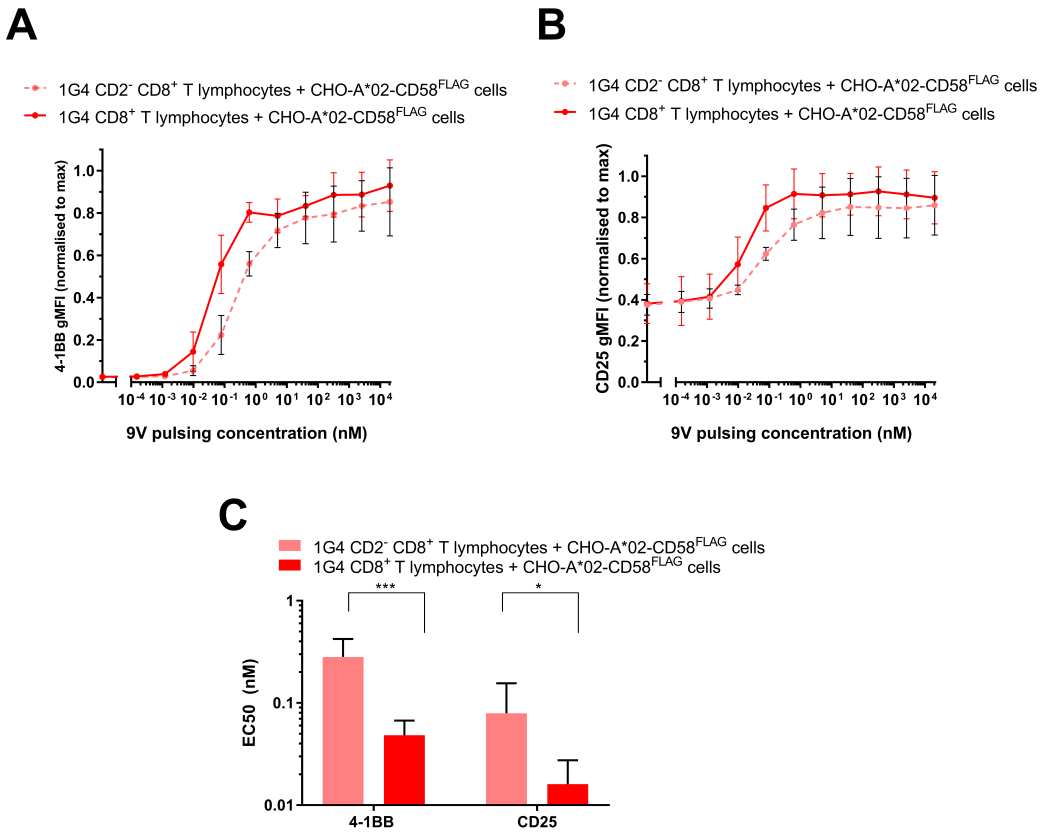


Figure 4.7: CD2 loss impairs antigen sensitivity in primary human CD8$^+$ T cells. CD8$^+$ T cells expressing the 1G4 TCR and with either a CD2 knockout or CD2 wild type status were co-cultured with CD58$^+$ HLA-A*02$^+$ CHO cells. Co-cultures were performed at an adjusted E:T ratio of 2:1 and lasted 6 h. Upregulation of the 4-1BB (**A**) or CD25 (**B**) cell surface markers was assessed as an indicator for antigen sensitivity, suggesting a loss of potency —but not efficacy— as a result of CD2 knockout. **C.** The differences in EC_{50} of activation were deemed statistically significant (* = $p \leq 0.05$, *** = $p \leq 0.001$) by fitting 4PL regressions and using an extra sum of squares F-test for this parameter. The data corresponds to the results of three independent experiments; the maximum gMFI value of each independent donor was normalised to one before calculating the averages. Data corresponds to the results of three independent experiments.

We next investigated the impact of CD2 disruption in cytotoxicity and cytokine production. To this end, we conducted a series of 6 h co-cultures (3:1 adjusted E:T ratio) between T2 cells and 1G4 $CD8^+$ or 1G4 $CD2^-$ $CD8^+$ T cells. In this context, we measured acute cytotoxicity and production of the IL-2, TNF-α, IFN-γ cytokines; we also measured production of the MIP-1β chemokine. The cytotoxicity readout was consistent with the results we showed previously. Concretely, the CD2 wild type CTLs displayed an EC_{50} for killing of 2.82×10^{-2} nM. A statistically significant 4–fold reduction in antigen sensitivity (EC_{50}) was observed in the $CD2^-$ $CD8^+$ T cells ($EC_{50} = 1.11 \times 10^{-1}$ nM) (Figure 4.8A). We also calculated the excess killing, here defined as the absolute difference in cytotoxicity between the CD2 wild type and the CD2 knockout 1G4 $CD8^+$ T cells. This measure (Figure 4.8B) showed that CD2-mediated killing occurred mainly at antigen concentrations between $\sim 10^{-2}$ and $\sim 10^{0}$ nM. This suggested that, for killing, this receptor acted preferentially at lower antigen densities, which often represent on-target/off-tumour responses.

In parallel, we quantitated the amount of IFN-γ, IL-2, MIP-1β, and TNF-α produced during the $CD8^+$/T2 co-cultures (Figure 4.9). To account for biological and technical variability, the amount of maximum amount of cytokine produced by each independent donor (*i.e.*, regardless of CD2 status) was normalised to one before calculating the averages of the three independent repeats. Our results suggested that the loss of CD2 did not impair the potency (EC_{50}, Figure 4.9E) of cytokine production. However, with the exception of the MIP-1β chemokine, CD2 knockout reduced the maximum amount of cytokine (E_{max}, Figure 4.9F) that is produced. This reduction in E_{max} of cytokine production, which amounted to approximately 50%, resulted interesting as it did not correlate with a proportional affectation in the E_{max} for cytotoxicity (Figure 4.8). This suggested that, at high antigen densities, CD2 knockout still enabled efficient killing with low cytokine release.

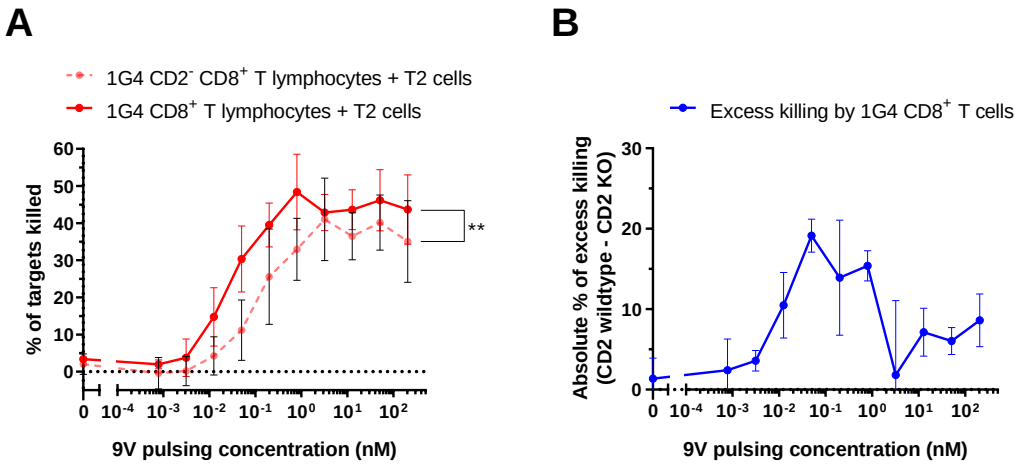


Figure 4.8: CD2 loss reduces killing of T2 target cells bearing low levels of the NY-ESO-1 antigen. $CD8^+$ T cells expressing the 1G4 TCR and with either a $CD2^-$ or CD2 wild type status were co-cultured with 9V-pulsed HLA-A*02^+ T2 cells. Co-cultures lasted 6 h and were conducted at an adjusted 3:1 E:T ratio (*i.e.*, three $1G4^+$ $CD8^+$ T cells per one T2 cell). **A.** Killing of T2 cells bearing different amounts of the 9V NY-ESO-1 peptide was assessed by LDH release after the co-culture. A calculation of the EC_{50} of killing suggests a sensitivity impairment linked to CD2 loss. **B.** Determination of excess killing by the CD2 wild type CTLs, which indicates that the CD2 receptor acts preferentially at low antigen densities. The differences in EC_{50} of activation were deemed statistically significant (** = $p \leq 0.01$) by fitting 4PL regressions and using an extra sum of squares F-test for this parameter. The data corresponds to the results of three independent experiments.

4.3 Discussion

In this chapter, we used Jurkat and primary $CD8^+$ T cells to explore how disrupting the function of CD2 impacts antigen sensitivity and activation efficacy. Our results show the feasibility of knocking out *CD2* in primary human $CD8^+$ T cells. They also indicate that disrupting CD2 can selectively reduce T cell killing at lower antigen concentrations (5–6 fold consistent increase in EC_{50}) without severely compromising efficacy at higher concentrations. In our view, these *in vitro* findings warrant further exploration in the context of documented receptors displaying on-target/off-tumour toxicity[127].

In the future, it would be important to determine whether the findings we have made using a TCR translate to CAR-T cells. The use of the 1G4 TCR enabled us to precisely titrate the amount of antigen presented to cells, which

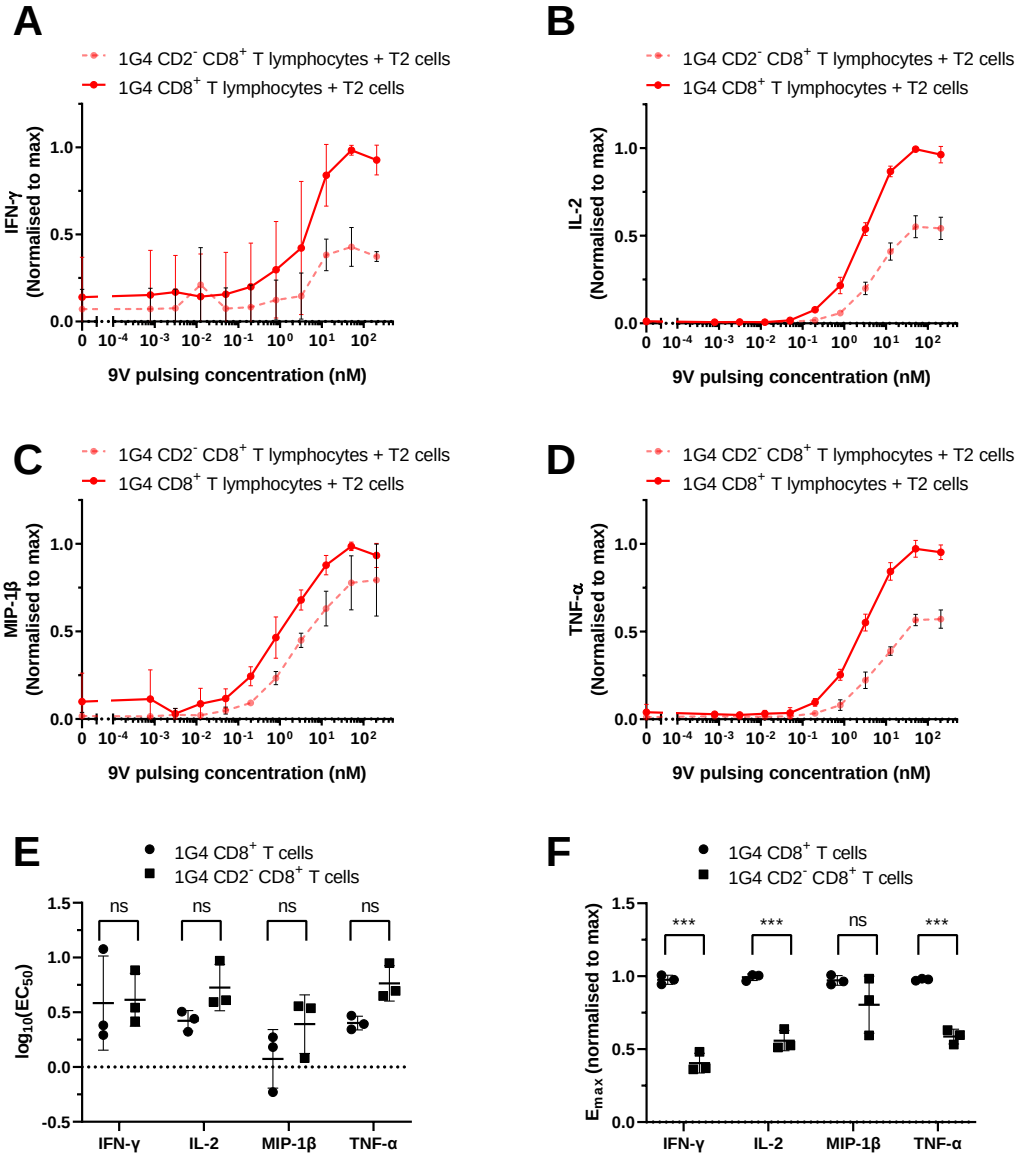


Figure 4.9: CD2 loss reduces the amount of cytokine secretion but not the production thresholds. $CD8^+$ T cells expressing the 1G4 TCR and with either a $CD2^-$ or CD2 wild type status were co-cultured with HLA-A*02^+ T2 cells. Co-cultures lasted 6 h and were conducted at an adjusted 3:1 E:T ratio. The figure shows normalised production of IFN-γ (**A**), IL-2 (**B**), MIP-1β (**C**), and TNF-α (**D**). The EC_{50} (**E**) and relative E_{max} (**F**) values were extracted from fitted 4PL regressions for each cytokine or chemokine (A-D), and t-tests (corrected for multiple comparisons with the Holm-Šidák method) conducted to assess the statistical significance of changes mediated by CD2 status. All the EC_{50} metrics were log-normalised to account for the log-normal distribution of this parameter. The data corresponds to the results of three independent experiments; to generate the plots, the maximum cytokine production of each independent donor was normalised to one before calculating the averages. n.s. = not significant, *** = $p \leq 0.001$.

was necessary to assess the quantitative effects of CD2 disruption. Validating these results in the context of CAR-T cells is a logical next step. For this, we could use a series of MHC-restricted CARs that also recognise the NY-ESO-1 peptide[139]. Alternatively, canonical CARs could be presented with varying amounts of their target antigen by electroporating different amounts of mRNA in target cells or by engineering stable cell lines with distinct expression profiles. In all instances, further validation should be conducted by establishing co-cultures with primary tissues bearing physiological (low) amounts of a given TAA. Ideally, CD2 disruption should reduce on-target/off-tumour toxicity in contexts where this phenomenon[132,134] has been observed with CARs. In our opinion, the applicability of this approach in CAR ACT will be contingent on CARs relying on CD2 for cellular adhesion to a similar extent as the TCR does. Evidence suggests that CARs can capitalise on CD2-mediated signalling[170,233], although no direct comparisons between CD2 adhesion and signalling capitalisation by CARs and TCRs have been reported in the literature.

4.3.1 Disruption of the CD2/CD58 axis by transduction of elongated CD2 chimeras

The apparent inability of the elongated CD2 chimeras to reduce antigen sensitivity appears to be at odds with the work showing reduced activation when elongating the CD48 or CD80 counter-receptors[189,234]. We would first note this unexpected result only occurred with the CHO-A*02-CD58^{FLAG} line and not with T2 cells, where the CD2^{HA}-7Ig and CD2^{HA}-CD43^{Ecto} constructs did reduce sensitivity. There are, nonetheless, several possibilities that might explain the lack of a dominant negative phenotype in the CHO system (Figures 4.3 and 4.4). One prospective explanation is that the number of CD58 molecules in the CHO cells was greater than *all* the CD2 molecules expressed by the 1G4 NF-κB Jurkat sub-lines. We previously showed (Section 3.2.2) that CHO-A*02-CD58^{FLAG} cells expressed an average of $\sim 7.6 \times 10^6$ CD58 molecules/cell. In contrast, we estimated that the Jurkat sub-lines expressed an average of $\sim 3 \times 10^4$ molecules/cell of endogenous

CD2 and $\sim 2.3 \times 10^6$ molecules/cell of the $CD2^{HA}$ construct. Since this construct expressed at slightly higher levels than all the elongated chimeras (Appendix B), we would expect all the Jurkat sub-lines to express fewer than $\sim 2.3 \times 10^6$ CD2 chimeras/cell. This implies the chimeras could not bind and sequester all the accessible CD58 molecules (which would effectively outcompete endogenous CD2).

Milstein *et al.*[153] performed a series of experiments where they placed murine T cells in SLBs functionalised with both CD48 and a CD48-CD22 chimera (elongated with three Ig domains derived from CD22). Some of their findings suggest —perhaps counterintuitively— that the very high levels of CD58 expressed by our CHO cells could generate a biochemical regime where endogenous CD2 binding is facilitated. In the Milstein *et al.* study, wild type CD48 was shown to be 10–fold more efficient than CD48-CD22 in promoting cell adhesion. This was theorised to be caused by the greater molecular reach of CD48-CD22 and/or increased entropy loss upon CD2/CD48-CD22 binding. This, in turn, meant that when the two adhesion molecules coexisted, CD2/CD48 binding and interference against the CD2/CD48-CD22 interaction was favoured under multiple concentration regimes[153].

Unlike Milstein *et al.*, we trialled an elongation of the CD2 receptor. Nonetheless, it is plausible to assume that, compared to endogenous CD2, our CD2 chimeras would: (i) be less efficient at mediating adhesion, and (ii) be affected by similar entropy-loss binding penalties as the CD48-CD22 construct[†]. Thus, we could picture a regime where canonical CD2/CD58 binding takes preference over the interactions we engineered. Interestingly, this could explain why Wild *et al.*[189] and Lim *et al.*[234] observed clear phenotypes when elongating, respectively, the CD48 and CD80 counter-receptors. Indeed, these systems did not have to deal with binding equilibriums between competing receptors or counter-receptors.

[†]The decreased efficiency in all of our chimeras would be, arguably, mediated in the first instance by their elongation. The $CD2^{HA}$-ΔCyt series also failed to act as a dominant negative (Figure 4.4). In this respect, we note that the tail of rat CD2 was shown to not play a key role in mediating CD2/CD48 adhesion[235]. In the context of the IS, more recent reports[160] have indicated that the tail of human CD2 can influence the efficiency of formation of a CD2 corolla between the pSMAC and the dSMAC, which is capable of enhancing T cell signalling.

We did, however, observe a modest phenotype when Jurkats expressing the elongated CD2 chimeras were presented with T2 cells (Figure 4.5). Compared to CHO-A*02-CD58^{FLAG} cells, T2 cells express fewer CD58 ligands ($\sim$6.2 $\times$ 10^5 molecules/cell). As Jurkat cells expressing the CD2 variants appear to have $\sim$2 $\times$ 10^6 molecules/cell (Section 3.2.5), a simple explanation is that, in this regime, they can sequester all the available CD58 and impair endogenous CD2 binding. Alternatively, these differences in CD58 expression could imply that Jurkat/T2 co-cultures establish a different binding equilibrium to that of Jurkat/CHO co-cultures — one that enables interference against CD2/CD58 canonical binding[153]. These possibilities can be further explored by assessing the phenotype of these chimeras in cells that express even fewer CD58 molecules, such as immature monocyte-derived DCs (Table 3.1) or, potentially, primary tissues expressing a TAA.

Although our initial rationale when designing these chimeras was influenced by the KS model[189,204,234], we acknowledge that the phenotype observed in the Jurkat/T2 co-cultures could be a reflection of the elongated CD2 chimeras physically impairing the binding of other co-stimulatory axes, namely CD28/B7 or LFA-1/ICAM-1 (T2 cells express CD80, CD86, and ICAM-1). These interactions are also known to enhance T cell antigen sensitivity; their contribution has been observed both in reductionist systems[1,198], as well as in human and murine cellular settings[149,153,185,236]. If this explains the results observed, then the KS model would not necessarily mediate this phenotype since this interference is compatible with other proposed triggering mechanisms, such as those predicated on TCR conformational changes or aggregation[65].

The experiments with these CD2^{HA} elongated chimeras were only conducted in the 1G4 NF-κB/eGFP Jurkat reporter line. If promising results are obtained with some of the approaches suggested above, this would warrant exploring the strategy in the context of primary T cells expressing transgenic TCRs or CARs.

4.3.2 CD2 knockout in ACT

The reduced antigen sensitivity exhibited by the 1G4 $CD2^-$ $CD8^+$ T cells is consistent with published reports in rodents[149] and with the findings of the Jurkat/CHO co-cultures we conducted in Chapter 3. The overall phenotype, particularly in terms of killing (Figure 4.8), could mitigate the risks associated with on-target/off-tumour toxicity without compromising the efficacy of TCR-T cells. This can be readily tested in an engineered TCR that recognises CEA[127], which was shown to induce colitis in patients after attacking healthy crypt epithelial cells with weak CEA expression.

Determining the overall viability of CD2 knockout in TCR ACT to increase the safety of engineered cells requires assessment of additional factors. First, there are challenges associated with routinely performing CRISPR/Cas9-mediated *CD2* disruption followed by depletion of $CD2^+$ T cells. If we consider the process of preparing autologous cells for ACT, additional steps will impact time, costs, and yields. We note, however, that novel CRISPR-compatible clinical pipelines have been recently described[118]; these improved procedures illustrate the feasibility of simultaneously targeting up to three genes for disruption in ACT. The process could be further simplified should allogeneic ACT become the norm[237], with the T cell master stocks having a $CD2^-$ status. In Chapter 5, we present evidence suggesting that CD2 mediates some allorecognition, which —if fully confirmed— would increase the attractiveness of CD2 as a target for this kind of technology.

We also appreciate that the idea of knocking out a co-stimulatory receptor such as CD2 is not an ordinary one. As expected, most of the work in ACT improvement looks at disruption (via CRISPR/Cas9 or checkpoint blockade) of inhibitory receptors such as PD1 or the B- and T-lymphocyte attenuator (BTLA)[93,118,238]. Given that recent works have illustrated the importance of CD2 expression in the context of granule polarisation in CTLs[203], as well as signal integration in TILs[160], it is reasonable to take heed of these findings. We would argue that the CD2-associated dysfunctional phenotypes reported in those works might not be encountered in *ex vivo* expanded T cells. For example,

Zurli *et al.*[203] indicate that the biological signatures associated to CD2 are only observed in freshly isolated CD57$^+$ CD8$^+$ T cells. This observation was made by the group in light of previous work[239] suggesting a fundamental difference in the polarisation of lytic granules of freshly isolated CTLs compared to that of *in vitro* expanded blasts. It is possible that a similar phenomenon is occurring in the impaired CD2^{lo} TILs characterised by Demetriou *et al.*[160]. Should this be the case, disrupting CD2 in blasted cells (for immunotherapy purposes) would not impair overall efficacy (E_{max}). In our opinion, the results of the acute cytotoxicity assays we performed (Figure 4.8) support this possibility, although further tests are required to ensure that CD2$^-$ T cells exhibit appropriate engraftment and long-term proliferation capabilities.

In the particular case of anti-CD19 CARs, Majzner *et al.*[170] have shown that CD58 aberrations in target cells compromise the long term success of ACT. Accordingly, CD2 disruption could also affect CAR activity. Should this prove to be a persistent problem with the approach we have presented, we would analyse the possibility of restoring CD2 signalling (but not adhesion) by co-transduction of a CD19 CAR with a CD2 signalling motif, which was the strategy followed by Majzner *et al.* to combat CD58 loss in large B cell lymphoma.

We acknowledge the different E_{max} phenotypes observed when CD2 was removed from primary CD8$^+$ T cells. Indeed, whilst killing was marginally affected (Figure 4.8) and no changes in MIP-1β were observed, we found significant reductions in the production of IFN-γ, IL-2, and TNF-α as a result of CD2 loss (Figure 4.9). Several studies have postulated the existence of a hierarchy for T cell effector functions upon antigen stimulation, with killing[240] (perforin cytolysis[241]) or MIP-1β production[242] being more sensitive than proliferation or the production of IFN-γ, IL-2, and/or TNF-α. However, we note there is not complete consensus in this area, with other studies suggesting the existence of a shared threshold for all these effector functions[198]. Nonetheless, it is known that the cytotoxicity (which, in the case of perforin-mediated killing relies on preformed granules) is a quick process —in the order of minutes— that does not require the formation

of a stable immunological synapse[212]. This is in contrast to proliferation or IL-2 production, where sustained signalling, in the order of hours, is necessary[243]. Thus, it is reasonable to assume that even if CD2 loss shifted the antigen sensitivity threshold, the polarisation and release of preformed cytotoxic granules would not necessarily be compromised (see also the work of Kabanova *et al.*[239]).

In the case of the MIP-1β chemokine, we point out that the existence of preformed chemokine vesicles has been confirmed for other proteins of the β-chemokine family, such as CCL5[244] (also known as RANTES, which stands for regulated on activation, normal T cell expressed and secreted). Secretion of β-chemokines can be quicker than that of cytokines such as IFN-γ[244], so regardless of the existence of preformed MIP-1β, this chemokine could be under the control of different cellular switches than those regulating IFN-γ, IL-2, and TNF-α. Moreover, the CD2 receptor has been associated with signal transducer and activator of transcription (STAT)-mediated activation of intronic IFN-γ elements in mucosal T cells[245] and —more generally— with stabilisation of mRNA coding for IL-2 and IFN-γ[246]. In any case, we consider that the reduction in overall production of cytokines such as IFN-γ, IL-2, and TNF-α (Figure 4.9) might not be a major concern. In ACT, the generation of synthetic constructs or strategies that preserve cytotoxic capabilities while reducing cytokine production is commonly sought[75,247]. Reduced cytokine release can be helpful, as it reduces the risk of CRS, which is part of the on-target/on-tumour toxicity sometimes observed in ACT[138].

5

CD2 influences off-target/off-tumour cross-reactivity in affinity enhanced receptors

Contents

5.1 Introduction 110
5.1.1 Off-target/off-tumour toxicity in ACT 111
5.1.2 Chapter aim 114
5.2 Results 114
5.2.1 CD2 knockout ameliorates cross-reactivity of the affinity enhanced wt/c51 TCR 114
5.2.2 Impact of CD2 on the discrimination power of T cells 117
5.3 Discussion 121
5.3.1 CD2 and discrimination power 122
5.3.2 Affinity enhanced receptors in ACT 125

5.1 Introduction

Early studies in TCR-T ACT relied on receptors that were directly cloned from TILs recovered from patients. For example, some of the first TCRs trialled were the DMF4[81] and DMF5[248]. Both are MART-1/HLA-A*02-reactive receptors (with K_D values of 29 and 5.6 μM, respectively[249]) originally obtained from a

patient that underwent TIL therapy for metastatic melanoma[78]. These studies suggested that higher receptor affinities correlated with improved prognoses, as the response rates of the DMF5 TCR were superior to those of the DMF4 TCR (30 vs. 13%, respectively)[81,248]. The correlation between affinity and functional response has, since then, been supported by further *in vitro* work with affinity enhanced variants of the 1G4 receptor[140].

Affinity enhanced TCRs have been used in multiple clinical trials to target TAAs such as NY-ESO-1[250] and MAGE-A3[135,137,251]. Although high affinity receptors have the potential[140] of improved efficacy compared to their wild type counterparts, trials have revealed instances[135,137] of off-target/off-tumour toxicity. This type of toxicity occurs when a TCR cross-reacts with a self-antigen (which usually has a low affinity) presented on healthy tissues. This type of toxicity has limited the use of TCR ACT. In fact, it appears that out of multiple affinity enhanced TCRs targeting NY-ESO-1, CEA, and MAGE-A3, only the 1G4-α95:LY TCR (against NY-ESO-1) has been deemed safe after clinical trials. See the review from Rath and Arber[63].

Considering the evidence of mouse CD2 studies[149] and the information we obtained in Chapter 4, it is reasonable to consider that human CD2, an adhesion co-receptor, enhances sensitivity of T cells to low affinity pMHCs. Hence, we hypothesised that in the context of affinity enhanced TCRs, CD2 could be: (i) dispensable for on-target, high affinity *bona fide* interactions, and (ii) mediating the off-target/off-tumour toxicities that occur when affinity enhanced TCRs cross-react with low affinity self-pMHCs. On this basis, we propose ablation of CD2 to mitigate the cross-reactivity reported in some affinity enhanced TCRs.

5.1.1 Off-target/off-tumour toxicity in ACT

The rationale for generating affinity enhanced TCRs

Ever since the work of Rosenberg *et al.*[25], the use of TCR-based ACT has continued to garner interest for cancer immunotherapy, especially in light of the difficulties found when targeting solid tumours with CARs[252]. Although HLA

restriction poses a limitation for TCR ACT, the umbrella of possible targets is broad, including both TAAs (*e.g.*, WT1, MART-1, NY-ESO-1, MAGE) and TSAs (*e.g.*, neoantigens and virally-derived oncoproteins)[63,125].

Early studies targeting TAAs relied on naturally-occurring TCRs found in reactive TILs of patients. This was the case with the DMF4 TCR[78], used for treatment of metastatic melanoma. The subpar outcomes of naturally-occurring TCRs against TAAs (13% response rate for the DMF4 TCR[81]) are likely to stem from the thymic selection process. Positive and negative thymic selection are conductive to the generation of T cells capable of recognising non-self pMHC while ablating highly reactive TCRs against self-antigens. Ultimately, this results in wild type TCR/pMHC affinities usually ranging between 1–100 μM[253], which might not be enough to ensure efficient tumour clearance. This limitation can be partially understood in light of the correlation between T cell avidity and target cytolysis[254]. Moreover, $CD4^+$ T cells transduced with low affinity class I restricted TCRs can fail to recognise the target antigen[254], which will in turn impair CTL survival and proliferation within tumours. Lack of a $CD4^+$ response in ACT would also negate other effects such as angiogenesis inhibition and direct CD4-mediated killing (reviewed by Stone and Kranz[255]).

Some of these challenges can be addressed by generating TCRs with supraphysiological affinities, a possibility that was first explored by Holler *et al.*[256] using yeast display. Concurrent with an improved understanding of the TCR/pMHC binding structure –particularly the CDR2/MHC and CDR3/peptide interactions[257]— subsequent studies replicated these findings and achieved affinity mutants of the 1G4 TCR with a K_D in the pM range[258]. Certain affinity enhanced receptors appear to overperform their wild type counterparts both *in vitro*[140,259] and *in vivo*[260], exhibiting increased sensitivity and functionality. Some of the *in vivo* effects appear to be mediated by $CD4^+$ T cells, as the increased affinity means that the receptor is functional even in the absence of CD8/MHC binding[260].

Disadvantages of affinity enhanced receptors

Despite the usefulness of engineering TCRs to increase their affinity, there are multiple reports regarding loss of specificity in these receptors. In the particular case of 1G4 TCR variants, affinities above 450 nM correlate with cross-reactivity against self-pMHC, illustrating the problem of off-target/off-tumour toxicities[140,254]. For example, the wt/c51 receptor is an affinity mutant (K_D = 25 nM) derived from the 1G4 TCR. Although it displays improved sensitivity and functionality compared to the clinically trialled 1G4-α95:LY TCR (also known as c259/wt, K_D = 730 nM), its cross-reactivity against self-pMHC[140] would make it unsuitable for clinical use.

In a trial with the affinity enhanced a3a MAGE-A3/HLA-A*01-reactive TCR ($K_D \approx 2$ μM), two fatalities were registered and traced to off-target/off-tumour toxicity. The a3a TCR induced cardiovascular toxicity as a result of recognising a titin peptide presented on cardiomyocytes (with a K_D of $\sim$100 μM)[135,137]. Moreover, high affinity TCRs can contribute to T cell exhaustion as a result of tonic signalling mediated by self-peptides[261]. Sometimes, they can exhibit reduced sensitivity, a phenomenon that occurs after a particular affinity ceiling[262].

In the case of CAR-T cells, no off-target recognition events have been documented in human clinical trials, although we note that some scFvs recognising the EGFRvIII TSA can cross-react with wild type EGFR[263,264]. In addition, a high affinity (K_D = 2–4 nM) MHC-restricted CAR recognising NY-ESO-1 exhibited cross-reactivity against HLA-A*02$^+$ cells; its specificity was restored by reducing the affinity to approximately 700 nM[139].

To minimise the risks of unintended TCR/pMHC recognition, affinity enhancement should consider the balance between improving functionality and the risks of losing specificity[255]. *In vitro* systems can detect broad cross-reactivity against HLA, but in order to find specific epitopes expressed in highly differentiated cells (such as the one from titin), they need to be robust*. Concretely, screening procedures using multiple primary tissues and cell lines[141] should be in place

*For example, titin would be expressed in beating cardiomyocytes derived from induced pluripotent stem cells but not in CM9 cardiomyocytes[136].

when characterising novel TCRs. Other practical considerations include the use of suicide genes and cellular elimination tags, which could aid in quickly depleting cross-reactive T cells if needed[63].

5.1.2 Chapter aim

Here, we work with the wt/c51 TCR (K_D = 25 nM), an HLA-A*02 cross-reactive variant of the 1G4 receptor. Having hypothesised that CD2 mediates some of the off-target/off-tumour toxicities observed in affinity enhanced receptors, our main aim is to show that CD2 disruption reduces the self-pMHC cross-reactivity of wt/c51 $CD8^+$ T cells.

5.2 Results

5.2.1 CD2 knockout ameliorates cross-reactivity of the affinity enhanced wt/c51 TCR

Dunn *et al.*[265] derived the wt/c51 variant from the 1G4 TCR using directed evolution of the CDR2. The wt/c51 TCR features the VGAGI > V**AIQT** mutation in the CDR2β, which increases its affinity to NY-ESO-1/HLA-A*02 from ~32 μM to 25 nM[265]. This receptor exhibits loss of specificity: it was shown that it produced MIP-1β when wt/c51 $CD8^+$ T cells were co-cultured with HLA-A*02^+ NY-ESO-1^- lines[140].

We asked whether CD2 disruption via CRISPR/Cas9 could ameliorate the cross-reactivity previously reported for the wt/c51 TCR. As previously described in Section 4.2.4, we carried out a process of lentiviral transduction with the lentiCRISPR-$CD2^{KO}$ vector, which was followed by puromycin selection, $CD2^-$ enrichment, and electroporation of the wt/c51 TCR, ultimately generating wt/c51 $CD2^-$ $CD8^+$ T cells (Figure 5.1). We note that, given the reported cross-reactivity of this receptor, we isolated our $CD8^+$ T cells from HLA-A*02^- donors. After generating wt/c51 $CD8^+$ T cells with and without CD2, we conducted a series of 16 h co-cultures with HLA-A*02^+ T2 cells at different E:T ratios. We then quantitated the amount of MIP-1β, IFN-γ, IL-2, and TNF-α produced by the

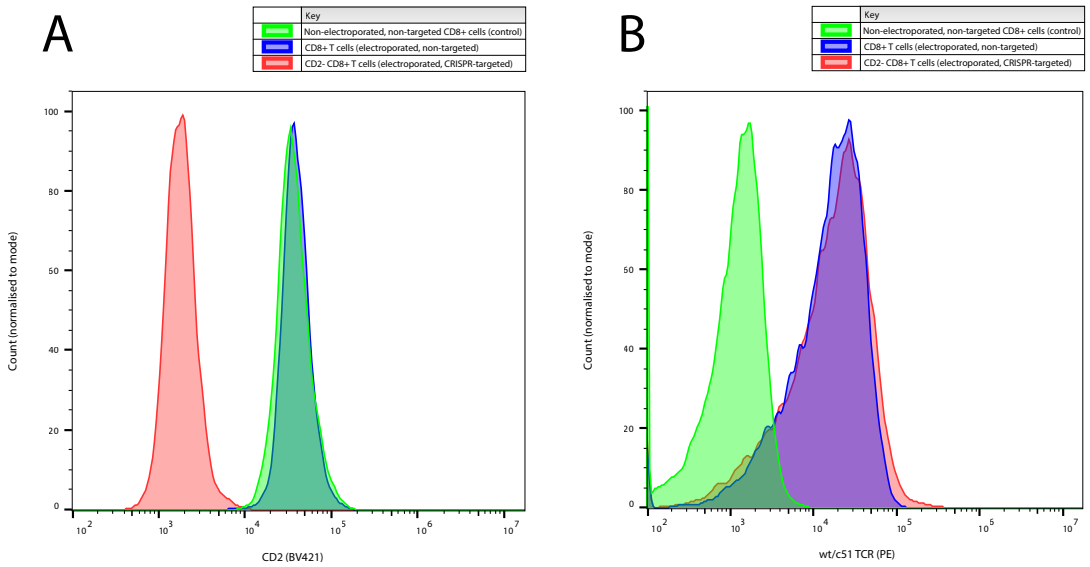


Figure 5.1: Generation of primary wt/c51 CD2$^-$ CD8$^+$ T cells. Through the combination of a lentiCRISPR commercial system targeting *CD2*, a depletion step of CD2$^+$ T cells, and electroporation of the wt/c51 TCR, we obtained highly enriched populations of wt/c51$^+$ CD2$^-$ CD8$^+$ T cells. **A.** CD2 depletion efficiencies routinely reached levels >95%. **B.** After electroporation, the CD2$^-$ CD8$^+$ T cells expressed wt/c51 TCR levels similar to those of their CD2 wild type counterparts. Electroporation efficiencies ranged between 50–85%.

CD8$^+$ T cells. Our results with the MIP-1β chemokine (Figure 5.2) show that, at high E:T ratios, CD2$^+$ CD8$^+$ T cells expressing the wt/c51 TCR do cross-react with T2 cells as evidenced by the production levels of MIP-1β.

As hypothesised, production of MIP-1β in the wt/c51 CD2$^-$ CD8$^+$ T cells is reduced compared to their CD2 wild type counterparts (Figure 5.2). We note, however, that only MIP-1β was produced by the wt/c51 TCR in an antigen-independent manner. Indeed, in line with the previous reports of Tan *et al.*[140] it was not possible to detect production of IFN-γ, IL-2, or TNF-α (Figure 5.3). In principle, this suggests that CD2 disruption merits further exploration as a mechanism to ameliorate the self-pMHC reactivity exhibited by affinity enhanced TCRs. Should these results be confirmed in the context of multiple engineered TCRs and other critical effector functions such as cytotoxicity, *CD2* knockout could be routinely integrated to TCR ACT pipelines, as avoiding cross-reactivity would broaden applicability and improve the therapeutic profile of these affinity enhanced receptors.

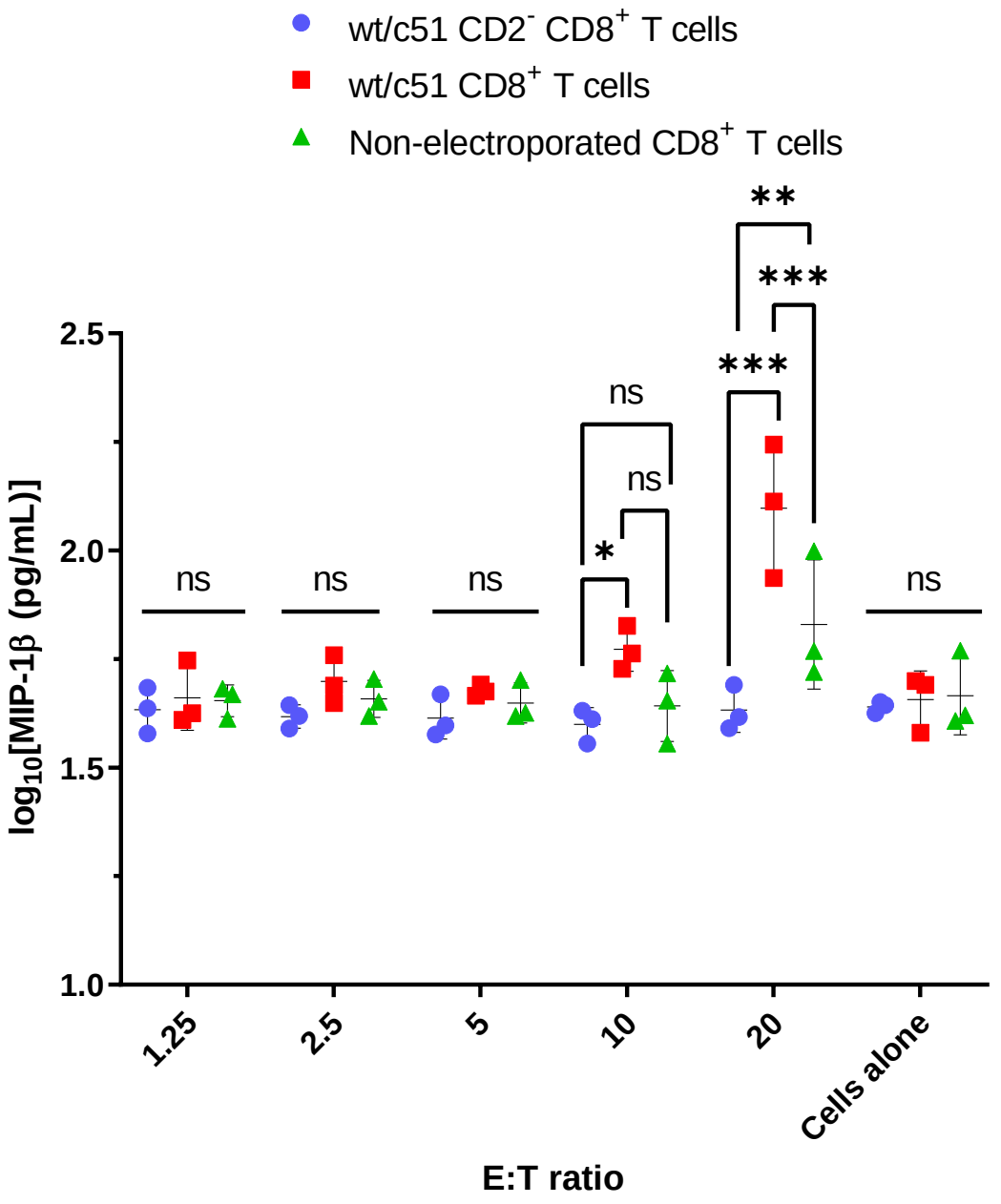


Figure 5.2: CD2 loss ameliorates MIP-1β-associated off-target cross-reactivity of the affinity enhanced wt/c51 TCR. HLA-A*02$^-$ CD8$^+$ T cells expressing the wt/c51 TCR and with either CD2$^-$ or CD2 wild type expression were co-cultured at different E:T ratios for 16 h with HLA-A*02$^+$ T2 cells. Afterwards, supernatants were assayed for production of the MIP-1β chemokine. We performed statistical analyses using a two-way ANOVA with a *post hoc* Tukey test for each E:T condition. n.s. = not significant, * = $p \leq 0.05$, ** = $p \leq 0.01$, *** = $p \leq 0.001$. Data has been log-transformed (raw values can be found in Figure 5.3). Figure corresponds to the results of three independent experiments.

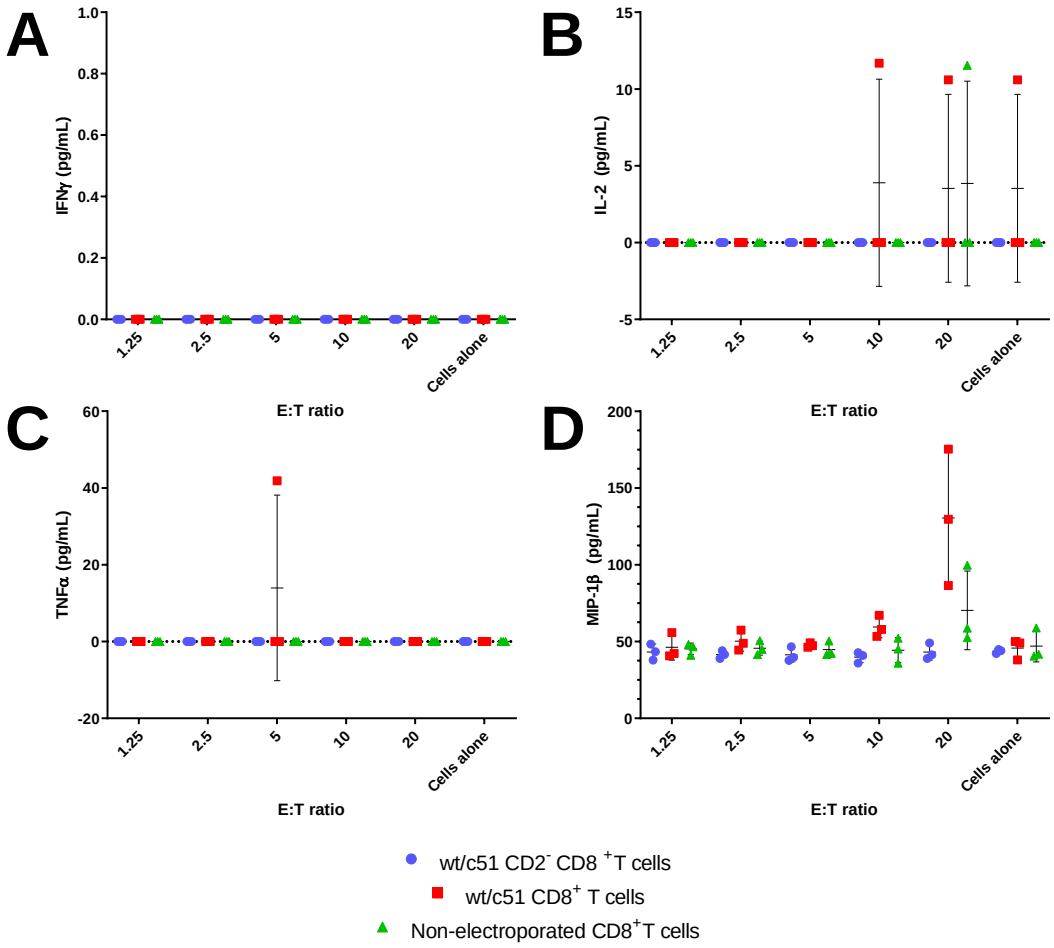


Figure 5.3: The cross-reactivity exhibited by the wt/c51 affinity enhanced TCR leads to production of the MIP-1β chemokine, but not to generation of IFN-γ, IL-2, or TNF-α. HLA-A*02$^-$ CD8$^+$ T cells expressing the wt/c51 TCR and with either CD2$^-$ or CD2 wild type expression were co-cultured at different E:T ratios for 16 h with HLA-A*02$^+$ T2 cells. Afterwards, supernatants were assayed for production of IFN-γ (**A**), IL-2 (**B**), TNF-α (**C**), or MIP-1β (**D**). Data corresponds to the results of three independent experiments. Note that it was only possible to conduct statistical analyses on log-transformed data for the MIP-1β chemokine (Figure 5.2).

5.2.2 Impact of CD2 on the discrimination power of T cells

One of the better documented instances of off-target/off-tumour toxicity as a result of affinity enhancement is that of the a3a TCR, which recognises the MAGE-A3/HLA-A*01 complex (EVDPIGHLY, $K_D \approx 2\ \mu M$). This receptor was shown to cross-react against a titin peptide presented on cardiomyocytes (ESDPIVAQY), leading to acute toxicity and two fatalities[135–137]. The affinity between the a3a

TCR and titin was estimated to be 100 μM[137], illustrating the risks of unintended recognition events against low affinity self-pMHCs.

Since a series of NY-ESO-1 APLs have been rationally engineered and characterised for the 1G4 TCR (Table 2.7)[1], we considered this receptor would be a suitable model to recreate low-affinity, off-target interactions of ~100 μM like those reported for a3a/titin. We hypothesised that, without engagement of the CD2/CD58 axis, the reactivity exhibited by 1G4 $CD8^+$ T cells recognising low affinity APLs would be substantially reduced. We first used a series of co-cultures between the parental and the CD2 knockout 1G4 NF-κB/eGFP Jurkat reporter lines and the HLA-A*02$^+$ U-251 glioblastoma cell line, which was pulsed with the 9V ($K_D \approx 8$ μM), 3Y ($K_D \approx 36$ μM), and 4D ($K_D \approx 91$ μM) APLs[†]. Co-cultures lasted 24 h and were performed using a 2:1 E:T ratio.

As low affinity peptides are unable to achieve saturation of cellular responses, EC_{50} calculations could generate imprecise results. Hence, we used a custom script developed by Pettmann *et al.*[1], which fits a 4PL regression and then interpolates the concentration of antigen required to induce activation of 15% of the cells for a chosen readout (Section 2.9). This parameter is referred to as a P_{15} value (for potency). To systematically analyse the relation between P_{15}, varying affinities, and CD2 status, we calculated the antigen discrimination power α of Jurkats with and without CD2. To this end, we fitted a log-transformed power law with the form $\log_{10}(P_{15}) = C + \alpha \times \log_{10}(K_D)$. In this expression, K_D represents the reported affinity of the APL to the TCR. The term C, which is the y-intercept, represents a measure of sensitivity.

When we analysed the results obtained with 1G4 NF-κB/eGFP Jurkats and U-251 co-cultures, our hypothesis held true (Figure 5.4). Indeed, the discrimination power α increased upon CD2 loss: the parental line registered discrimination values of $\alpha = 1.99$, whilst the CD2 knockout sub-line had $\alpha = 3.12$.

[†]The U-251 glioblastoma cell line was chosen instead of the CHO system because J. Pettmann reported (personal communication) abnormal interactions between the SCD and some NY-ESO-1 APLs. For example, variants such as 5F ($K_D \approx 1.3$ mM) exhibited enhanced activation when comparing the SCD with native HLA-A*02 molecules. This phenomenon did not affect the 9V peptide.

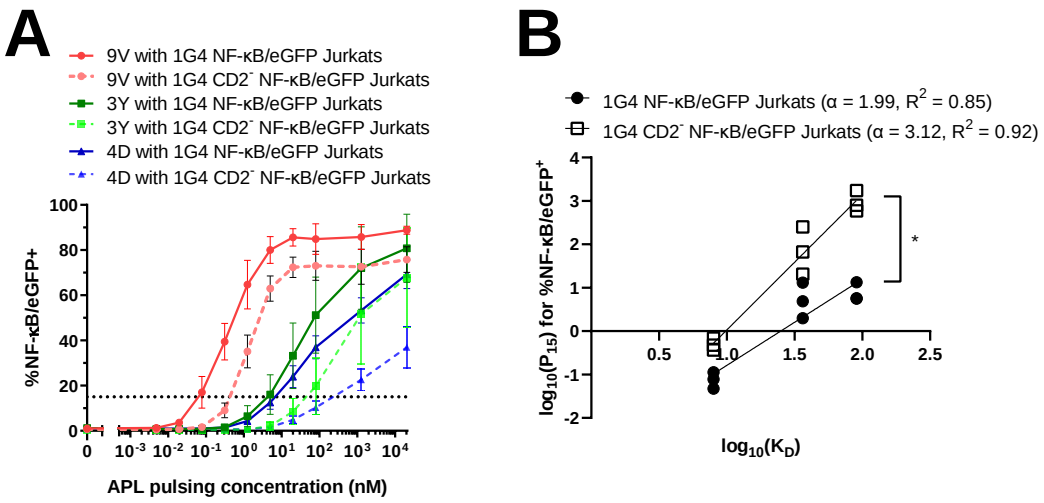


Figure 5.4: CD2 loss improves discrimination power in the 1G4 NF-κB/eGFP reporter Jurkat line. The 1G4 NF-κB/eGFP and 1G4 CD2$^-$ NF-κB/eGFP Jurkat reporter lines were co-cultured (24 h, E:T = 2:1) with HLA-A*02$^+$ U-251 cells exogenously pulsed with different APLs of the NY-ESO-1 epitope. **A.** After co-culture, flow cytometry was performed to determine cellular activation via the NF-κB/eGFP reporter. **B.** From the dose-response curves in A, a custom script (Section 2.9)[1] was used to interpolate the activation potency (P_{15}). The log-transformed P_{15} values were plotted against the log-transformed K_D values of the APLs assayed, and a linear regression performed. The slope α of this regression represents the antigen discrimination power[1]. Data corresponds to the results of three independent experiments. The differences in the discrimination power α were deemed statistically significant (* = $p \leq 0.05$) using an extra sum of squares F-test for this parameter.

Within the CD2 knockout population, saturation of cellular activation was not achieved even at concentrations over 20 μM of the 4D NY-ESO-1 APL. To further contextualise this, our α calculations mean that the ∼10–fold affinity decrease between the 9V and 4D peptides can be compensated by the parental line if presented with 97–fold more peptide ($10^{\alpha} = 10^{1.99} = 97$). The CD2 knockout sub-line would require a 1300–fold increase ($10^{\alpha} = 10^{3.12} = 1318$) in the amount of 4D recognised to compensate for this change in affinity.

Considering the importance of validating experimental results in Jurkats using primary human cells, we replicated the experiments using CD8$^+$ and CD2$^-$ CD8$^+$ T cells. A small adjustment was made in the APL panel, choosing to integrate 6T ($K_D \approx 85$ μM) instead of 3Y ($K_D \approx 36$ μM) to have another antigen in the low affinity region. As with previous runs, these cells were generated

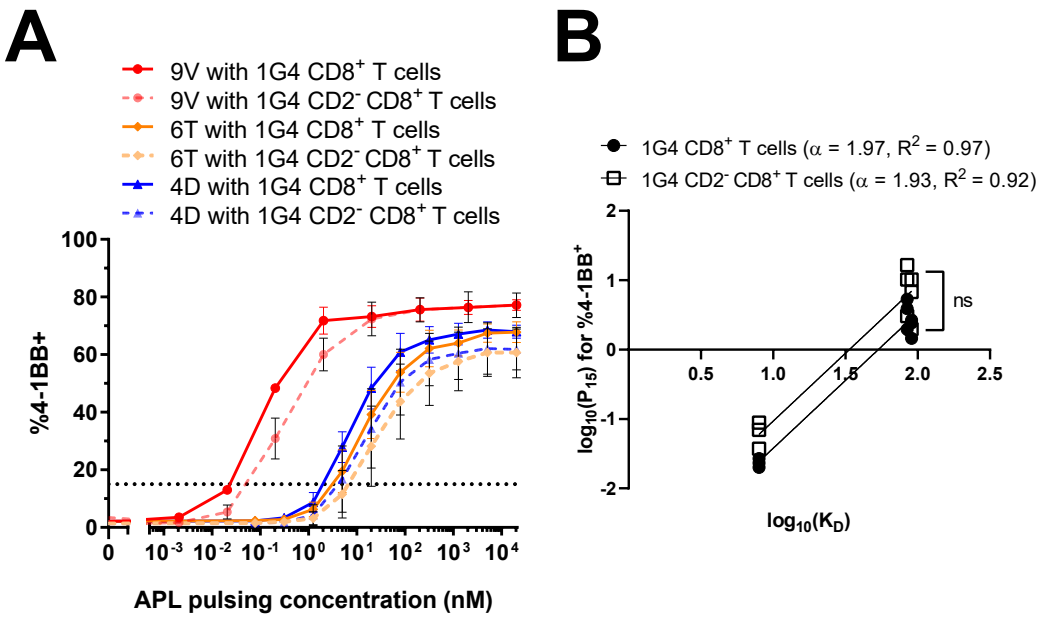


Figure 5.5: CD2 loss does not impair discrimination power in 1G4 CD8$^+$ T cells. Human CD8$^+$ T cells with either CD2$^-$ or CD2 wild type expression were electroporated with the 1G4 TCR and then co-cultured (6 h, adjusted E:T = 2:1) with HLA-A*02$^+$ U-251 cells exogenously pulsed with different APLs of the NY-ESO-1 peptide. **A.** After a 6 h co-culture, flow cytometry was performed to infer cellular activation via the 4-1BB activation marker. **B.** From the dose-response curves in A, a custom script (Section 2.9) was used to interpolate the P_{15} of activation. The log-transformed P_{15} values were plotted against the log-transformed K_D values of the APLs assayed, and a linear regression performed. The slope α of this regression represents the discrimination power[1]. Data corresponds to the results of three independent experiments. The differences in the discrimination power α were deemed non statistically significant (n.s. = $p > 0.05$) using an extra sum of squares F-test for this parameter.

through lentiviral transduction with a lenti-CRISPR system targeting *CD2*, and electroporated with mRNA encoding the 1G4 TCR prior to the experiments. Co-cultures between CD8$^+$ T cells and U-251 cells lasted 6 h and were performed at an adjusted E:T ratio of 2:1.

Unexpectedly, CD2 disruption in CD8$^+$ T cells did not affect the discrimination power, with robust responses registered for both the 6T and 4D peptides regardless of CD2 status (Figure 5.5). The discrimination power α of 1G4 CD8$^+$ T cells was 1.97; for 1G4 CD2$^-$ CD8$^+$ T cells, we calculated an α of 1.93. Hence, CD2 loss appears to impact the discrimination power in Jurkat cells, but not in primary human CD8$^+$ T cells (see Figure 5.6 for a side-by-side comparison).

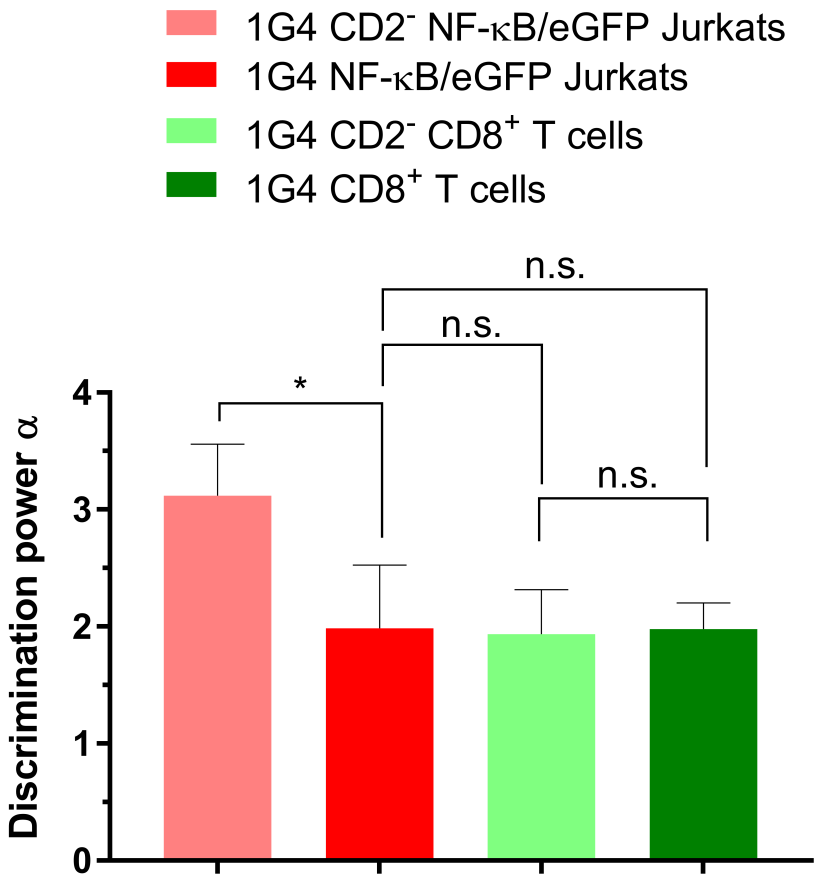


Figure 5.6: CD2 and discrimination power in Jurkat and primary CD8$^+$ T cells. A comparison of the discrimination power α exhibited by Jurkat and CD8$^+$ T cells suggests that only Jurkats present an increase in this metric upon CD2 loss. The discrimination power of primary CD8$^+$ T cells (regardless of CD2 status) is similar to that of the parental 1G4 NF-κB/eGFP Jurkat line. Multiple comparisons were conducted in log-transformed data using a one-way ANOVA with a *post hoc* Tukey test (n.s. = not significant, * = $p \leq 0.05$).

5.3 Discussion

In this chapter, we showed that CD2 loss ameliorates the previously reported cross-reactivity (correlated to non-specific MIP-1β production) of the affinity enhanced wt/c51 TCR. In addition, we looked at the role of CD2 in the antigen discrimination power of Jurkats and CD8$^+$ T cells expressing the 1G4 TCR. Our results indicated that, in Jurkats, CD2 loss improves the discrimination power α, which would be useful in the context of mitigating off-target/off-tumour toxicity. However, primary human CD2$^-$ CD8$^+$ displayed the same discrimination

power as their CD2 wild type counterparts, which prevents us from making a definite conclusion.

5.3.1 CD2 and discrimination power

The data shown in Section 5.2.2, includes discrepancies between the results obtained in Jurkat and $CD8^+$ T cells. Moreover, the fact that 1G4 $CD8^+$ T cells recognising the 6T and 4D APLs (K_D values of ~85 and ~91 μM, respectively) sustained similar responses regardless of their CD2 status (Figure 5.5) is at odds with the reduction in cross-reactivity mediated by CD2 knockout with the wt/c51 TCR. Here, we will try to explain the phenotypes observed and reconcile our findings.

Antigen discrimination power in Jurkat and $CD8^+$ T cells

Initially, we hypothesised that the loss of CD2 would abrogate cellular responses between the TCR and low affinity pMHCs. We proposed this in light of: (i) the role of CD2 as an adhesion molecule that increases the *effective* k_{on} of the TCR/pMHC interaction[2], and (ii) the reduction in the cross-reactivity between the wt/c51 receptor and self-pMHC upon CD2 disruption. Arguably, the cross-reactive interaction(s) would be low affinity ones, considering they are derived from self-pMHC[255] and only elicit MIP-1β production but not generation of IFN-γ, IL-2 or TNF-α[140] (see also Figure 5.3). Hence, we considered that the formation of complexes such as a3a/titin ($K_D \approx 100$ μM) or —in the case of our platform— 1G4/4D ($K_D \approx 91$ μM) would be impaired in the absence of CD2.

Our hypothesis held true in the experiments using the 1G4 NF-κB/eGFP Jurkat cell line (Figure 5.4); when CD2 was removed from effector cells, the activation mediated by the 4D low affinity peptide was curtailed to a greater extent compared to the results with 9V. This was parsed as an increase of the discrimination power α (3.12 for the CD2 knockout population versus 1.99 for the parental line). A larger α for the CD2 knockout Jurkats implies that, compared

to the parental counterpart, they reduce their potency more rapidly when the TCR/pMHC affinity decreases[1].

A similar experimental setup with primary $CD8^+$ T cells indicated that CD2 loss did not impair discrimination power (Figure 5.5). The cellular responses for the 6T and 4D peptides overlapped for the CD2 knockout and wild type populations. The discrimination power we calculated for both populations ($\alpha \approx 2$), was in agreement with previously reported values for cellular systems[1]. Using a reductionist system, Pettmann *et al.*[1] argued that CD2 enhances antigen discrimination: they did so by functionalising streptavidin plates with biotinylated ligands, and comparing activation mediated by pMHC alone or pMHC plus CD58. It is likely that we did not observe this phenotype because, in our system, other adhesion interactions such as LFA-1/ICAM-1, compensated for the lack of CD2. Moreover, we would require to screen more peptides before making conclusions in this regard, as Pettmann *et al.* screened eight peptides with affinities ranging from 8 μM to 1.3 mM (Figure 3.1), whereas we only screened three with a narrower affinity window. Our limited selection of APLs when assessing the activation metrics of 1G4 $CD8^+$ T cells is a reflection of difficulties in obtaining high numbers of $CD2^-$ $CD8^+$ T cell blasts. This, in turn, suggests that our CD2 knockout protocol could be improved by migrating from a lentiCRISPR approach to Cas9 delivery through mRNA[104] or ribonucleoprotein complexes[119]. Moreover, it would important to perform a detailed screening of the discrimination power of the wt/c51 TCR. This would require, in first instance, the measurement of affinities of this TCR to a variety of NY-ESO-1 APLs. To the best of our knowledge, systematic analyses of the discrimination power of affinity enhanced TCRs have not been reported in the literature.

In our view, the differences between Jurkat and primary $CD8^+$ T cells lacking CD2 stem from the absence of CD8 expression in the 1G4 NF-κB/eGFP Jurkat reporter line. The CD8 co-receptor is known to enhance T cell activation, especially in the context of low affinity interactions[266,267]. Therefore, the contribution of CD8 would be greater in the context of 1G4 recognising

4D ($K_D \approx 91$ μM) than 9V ($K_D \approx 8$ μM). For class I restricted TCRs, affinity enhancement enables activation of $CD4^+$ T cells, but it can sometimes come at the expense of CTLs cross-reacting against self-derived pMHC[254]. Zhao *et al.* have shown that this cross-reactivity can be mitigated when CD8 binding is not present[254] and, interestingly, CD8 engagement appears to reduce antigen discrimination power[1]. To test this, we could repeat our experiments and use either: (i) blocking antibodies to abrogate the CD8/MHC interaction[254], (ii) a direct comparison between $CD4^+$ and $CD8^+$ T cells expressing the 1G4 TCR, (iii) CD8-null (D227K/T228A) HLA-A2*01 complexes[268], or (iv) a combination of the above. Depending on the results, combined disruption of both CD2 and CD8 could be studied, but it would be necessary to show that long term viability of these adoptively transferred cells would not be compromised.

Reconciliating the off-target behaviours of the wt/c51 and 1G4 TCRs

Although CD2 disruption reduced off-target cross reactivity of the wt/c51 TCR against self-pMHC, this was not the case for the 1G4 TCR interacting with the 4D or 6T APLs ($K_D \approx 90$ μM). One simple explanation is that the affinity of the wt/c51 TCR towards self-pMHC presented on HLA-A*02 is substantially lower than 90 μM. This would imply that that CD2 exhibits increased biological activity at even lower affinities, mirroring the behaviour of CD8. A reductionist system testing APLs of the NY-ESO-1 peptide with very low affinities ($K_D > 430$ μM) suggests this might be the case, with 1G4 $CD8^+$ T cells being strongly dependent on CD2/CD58 engagement to activate under these affinities[1].

Alternatively, one should consider the possibility that the cross-reactivity of certain affinity enhanced receptors such as the wt/c51[140] or b2a[136] TCRs is mediated primarily and/or solely by binding to MHC. This would be in contrast to other affinity enhanced TCRs whose cross-reactivity derived from a defined pMHC complex (*e.g.*, a3a/titin). However, experimental reports[269] with affinity enhanced variants of the MEL5 and ILA1 TCRs have shown that the specificity of TCR/pMHC interactions can override TCR/MHC interactions, as those TCRs

were unable to bind *null* pMHC[‡]. This notion could be readily tested in a cellular platform with the wt/c51 or b2a TCRs, by co-culturing $CD8^+$ T cells with target cells pulsed with large concentrations of null peptides and verifying that cross-reactivity is abolished.

5.3.2 Affinity enhanced receptors in ACT

Positive and negative thymic selection guide the generation of endogenous TCRs that, for the most part, fall within a defined (1–100 μM) range of affinities[253]. Positive selection ensures a certain degree of self-pMHC recognition, a feature that has been considered useful in keeping the cells primed through partial phosphorylation of the TCR ζ chain and recruitment of signalling molecules[270]. In contrast, negative selection eliminates clones that bind too strongly to self-pMHC and would target the host's own cells. This process could explain why endogenous TCRs recognising TAAs register, on average, lower affinity to their cognate peptides (mean $K_D = 96.6$ μM) than those reactive against viral antigens (mean $K_D = 8.25$ μM)[271]. This, in turn, might explain low response rates in ACT trials using wild type TCRs, such as the DMF4 receptor ($K_D = 29$ μM)[249].

Increasing affinity by engineering TCRs can improve the functional profile of T cells in terms of antigen sensitivity, cytokine production, and —particularly for class I TCRs— reactivity of $CD4^+$ T cells[254,255,259]. However, affinity enhancement can eventually lead to cross-reactivity against self-derived peptides, a phenomenon documented for the wt/c51 ($K_D = 25$ nM) and other 1G4-derived receptors with affinities above 450 nM[140,254].

We showed that CD2 knockout in $CD8^+$ T cells expressing the wt/c51 TCR abolished the cross-reactivity against self-pMHC presented on HLA-A*02 (Figure 5.2). We conducted our assays using the MIP-1β chemokine as our main readout, in line with the experimental procedures of Tan *et al.*[140]. Just as Tan *et al.* did, we screened the supernatants for production if IFN-γ, TNF-α, and IL-2: in line with their findings, the wt/c51 cross-reactivity did not induce production

[‡]Peptides where all but the anchor residues were substituted with either glycine or alanine.

of any of these cytokines (Figure 5.3). Since previous reports have found that MIP-1β is the most sensitive readout for CD8$^+$ T cells[272], this could explain the results observed. Although we showed in the previous chapter (Figure 4.9) that CD2 loss can reduce the E_{max} for several cytokines produced upon cognate antigen recognition, MIP-1β was an exception. In our view, this reinforces the idea that for the wt/c51, CD2 knockout is impairing off-target TCR triggering — and not simply reducing the overall cytokine production capabilities of the T cells assayed. Furthermore, we would propose the addition of other controls such as non-electroporated CD2$^-$ CD8$^+$ T cells, which would provide insights about the nature of the non-specific recognition displayed by non-electroporated CD8$^+$ T cells (Figure 5.2). In our experimental setup, the wt/c51 TCR only displayed non-specific activation at very high E:T ratios (10:1). We consider this happened because T2 cells are TAP-deficient, which means that they are unable to load their MHC class I molecules through the formation of canonical peptide loading complexes[273]. Although TAP-independent loading of some endogenous peptides occurs, overall HLA-A*02 expression and stability is compromised[274]. To validate our results, it would be appropriate to replicate the phenotype observed using other HLA-A*02$^+$ immortalised lines (*e.g.*, MCF7, M9) and/or primary cells[140]. Moreover, since CTL killing is more sensitive than cytokine production[212], this effector function should also be assayed.

In addition, a cost/benefit analysis of removing CD2 should be conducted, especially in light of the existence of additional affinity enhanced variants of the 1G4 TCR that do not cross-react with self-pMHC. For example, a population of wt/c51 CD2$^-$ CD8$^+$ T cells could be benchmarked against CD2-expressing CD8$^+$ T cells bearing the 1G4-α95:LY TCR (K_D = 730 nM)[259], a receptor that has already been successfully used in clinical trials[250]. Finally, we would suggest replicating the phenotype observed with other engineered CARs or TCRs known to exhibit HLA cross-reactivity, such as the NY-ESO-1/HLA-A*02-reactive T1 CAR (K_D = 2 nM)[139], or the gp100/HLA-A*02-reactive wt/G4N (K_D = 35 nM) and MAGE-A3/HLA-A*01-reactive b2a TCRs[136]. Should these experiments

prove successful, routine ACT pipelines could integrate *CD2* disruption along the same lines we discussed in Chapter 4.

6
General conclusions

Contents

6.1 Summary 128
6.2 Future directions 131

6.1 Summary

The success of ACT in the treatment of leukaemia and lymphoma has been remarkable: axicabtagene ciloleucel (Yescarta) was approved by the FDA based on a trial that demonstrated an overall response rate of 82% and a complete remission rate of 58%[275]. It is also a testament to the potential of ACT, with multiple possibilities currently being explored. Indeed, as of 2020, it is estimated there are approximately 400 CAR-T and 50 TCR-T cell clinical trials ongoing[62]. However, there are many challenges that need to be addressed before widespread adoption of ACT can be achieved, including cost, efficacy, and diverse types of toxicity. In this work, we have proposed manipulations of the CD2/CD58 axis as a potential way of mitigating on-target/off-tumour (Chapter 4) and off-target/off-tumour (Chapter 5) toxicity in ACT. In our view,

these problems arise as a result of CD2 acting preferentially when the cognate antigen is expressed at low densities or has a low affinity (weak antigens).

Our work included the generation of a surrogate APC using an HLA-A*02^{+} CHO cell line, which was then transduced with human CD58. This cellular platform, amenable to high throughput screening procedures, enabled us to isolate and quantitate the contribution of human CD2 to antigen sensitivity. Our results with a 1G4 NF-κB/eGFP reporter Jurkat cell line suggested an improvement of 10–15 fold in sensitivity upon CD2 ligation (Figure 3.8). Interestingly, CD2 overexpression (15 times increase compared to primary CD8^{+} T cells) led to an 85–fold increase in antigen sensitivity, which came at the cost of antigen-independent activation for a proportion of the cell population assayed (Figure 3.10). This behaviour could be caused by the sheer number of CD2/CD58 close contacts causing: (i) forced CD45-kinase segregation, (ii) amplification of xenorecognition events, or (iii) CD2 aggregation followed by TCR-dependent activation, mimicking some anti-CD2 mitogenic antibodies. Further experiments are required to elucidate the exact mechanism promoting this unspecific activation.

The data generated suggests that the sensitivity shift was similar regardless of whether we modified the status of the CD58 ligand (on CHOs) or the CD2 co-receptor (on Jurkats). When we tested additional ways of manipulating the CD2/CD58 axis, such as the transduction of elongated CD2 chimeras, these failed to act as dominant negatives when tested in Jurkat/CHO co-cultures (Figures 4.3 and 4.4). However, an 8–fold impairment in antigen sensitivity was observed when co-culturing 1G4-CD2$^{\mathrm{HA}}$-CD43$^{\mathrm{Ecto}}$ NF-κB/eGFP Jurkats with T2 cells (Figure 4.5). In contrast to the CHO cell system, Jurkat/T2 co-cultures featured: (i) additional cellular interactions (*e.g.*, CD28/CD80, CD28/CD86), and (ii) a reduction in the number of possible CD2/CD58 total interactions (recall Table 3.1 and Section 4.3.1).

To further confirm our findings, we conducted co-culture assays between 1G4 CD8^{+} T cells (with a CD2^{+} or CD2^{-} status) and either CHO or T2 cells. We looked at cell surface activation markers such as 4-1BB and CD25 (Figure 4.7,

with CHOs), and killing plus cytokine production (Figure 4.8, with T2s). With the exception of some cytokines, the loss of CD2 had little effect in the E_{max} of activation. Antigen sensitivity was consistently reduced by factors between 4–6 fold, in line with previous reports using mouse cells[149]. When assaying cytokine production after a $CD8^+$/T2 co-culture, we found that for IFN-γ, IL-2, MIP-1β, and TNF-α, the EC_{50} of production did not change when CD2 was disrupted (Figure 4.9). However, the E_{max} was impaired in all cytokines with the exception of MIP-1β. This observation could be partially explained by the reports of CD2 stabilising IL-2 and IFN-γ mRNA[246], and by the fact that MIP-1β chemokine production appears more sensitive to antigen than other readouts[272]. The reduction in antigen sensitivity observed supports the notion of manipulating the CD2/CD58 axis in order to reduce the incidence of on-target/off-tumour cross-reactivity.

Additionally, we assessed the role of CD2 in the context of off-target/off-tumour recognition by the affinity enhanced wt/c51 TCR[140]. We found that CD2 loss abrogated the production of MIP-1β associated with cross-reactivity against self-pMHC (Figure 5.2). However, further experiments (such as cytotoxicity assessments) are required as the wt/c51 TCR only mediated unspecific MIP-1β production; we could not detect IFN-γ, IL-2, or TNF-α. When we assessed the role of CD2 in recognition of APLs of the NY-ESO-1 peptide, however, we encountered discrepancies between the phenotype exhibited by Jurkats and $CD8^+$ T cells expressing the 1G4 TCR. When using Jurkats, CD2 loss improved antigen discrimination, which would potentially prevent off-target/off-tumour recognition events as those observed with the a3a TCR[135,137] (Figure 5.4). In contrast, no apparent differences were observed when assaying primary $CD8^+$ T cells under a similar set up (Figure 5.5). We consider this discrepancy stems from the fact that the NF-κB/eGFP Jurkats do not express the CD8 co-receptor; experimental reports using a reductionist system suggest that when CD8 binding is abrogated, antigen discrimination is improved[1]. Therefore, although some evidence points

out that CD2 loss might mediate cross-reactivity in affinity enhanced TCRs, further research using other cross-reactive TCRs (*e.g.*, a3a, b2a) is still required.

6.2 Future directions

The surrogate APC system, using CHO cells, represents a potential way of assessing other co-stimulatory or co-inhibitory axes in isolation as it minimises the risk of compensatory mechanisms acting as confounding variables. However, we would suggest the additional disruption of certain molecules such as hamster CAMs[172,209] given the reports of: (i) interactions between human LFA-1 and murine ICAM-1[193], and (ii) the co-stimulatory effects of hamster ICAM-1[153,192] in mouse T cells. The transduction of an HLA-A*02 SCD enables detailed antigen titrations (useful for TCRs and MHC-restricted CARs); cell surface ligands could be titrated by generating a collection of stable cell lines[227] or by mRNA electroporation[132].

Having characterised the reduction in antigen sensitivity as a result of CD2 loss using the 1G4 TCR, a reasonable step in the same direction would be assessing this approach using a previously reported case of on-target/off-tumour toxicity. In particular, we could test the anti-CEA TCR that destroyed epithelial cells in the colonic crypts of patients being treated for colorectal adenocarcinoma[127]. Given our results were obtained using a TCR, we cannot make any conclusions about the validity of CD2 disruption when using CAR-T cells — although reports suggest that CD2 ligation influences CAR activation under some settings[170,233]. Using our platform, it would be relatively easy to test MHC-restricted CARs such as the D52N receptor (which also recognises the NY-ESO-1 epitope[139]). Should results suggest that this approach is valid, it could be benchmarked against other alternatives for on-target/off-tumour toxicity mitigation, including affinity tuning[132] and synNotch circuits[227].

Finally, we think our results warrant the screening of other affinity enhanced, cross-reactive TCRs such as the a3a[135,137] or b2a[136] receptors. Using our pipeline, we could ascertain if CD2 disruption also reduces the off-target/off-tumour

toxicities reported for them. Should that be the case, we would suggest comparing $CD2^-$ $CD8^+$ T cells expressing the wt/c51 TCR (K_D = 25 nM)[140] with CD2 wild type $CD8^+$ T cells transduced with the 1G4-α95:LY TCR (K_D = 730 nM)[250,259]. As the 1G4-α95:LY TCR is not known to be cross-reactive, the use of wt/c51 $CD2^-$ $CD8^+$ T cells would need to demonstrate advantages such as improved sensitivity or cytotoxicity in order to warrant routine manipulation of the CD2/CD58 axis. Genetic disruption of receptors presents another manufacturing challenge in autologous ACT, although genetic editing techniques continue to improve[118]. Should allogeneic ACT[98,99] become the norm, routine CD2 ablation would become much more accessible and it could be practised as a way of improving the safety of adoptively transferred cells.

Many patients with leukaemia and lymphoma have benefited from CAR-T cells, and there is no doubt that ACT has come a long way since the early work of S. Rosenberg in 1988. The multiple challenges faced by the field should continue to be addressed in order to help ACT reach its full potential.

References

1. Pettmann, J. *et al.* The discriminatory power of the T cell receptor. *eLife* **10,** 2020.11.16.384495 (2021).
2. Siller-Farfán, J. A. & Dushek, O. Molecular mechanisms of T cell sensitivity to antigen. *Immunological Reviews* **285,** 194–205 (2018).
3. Waldman, A. D., Fritz, J. M. & Lenardo, M. J. A guide to cancer immunotherapy: from T cell basic science to clinical practice. *Nature Reviews Immunology* **20,** 651–668 (2020).
4. Oelschlaeger, T. A. Bacteria as tumor therapeutics? *Bioengineered bugs* **1,** 146–147 (2010).
5. Coley, W. B. II. Contribution to the Knowledge of Sarcoma. *Annals of surgery* **14,** 199–220 (1891).
6. McCarthy, E. F. The toxins of William B. Coley and the treatment of bone and soft-tissue sarcomas. *The Iowa Orthopaedic Journal* **26,** 154–158 (2006).
7. Starnes, C. O. Coley's toxins in perspective. *Nature* **357,** 11–12 (1992).
8. The failure of the erysipelas toxins. *Journal of the American Medical Association* **XXIII,** 919 (1894).
9. Hobohm, U. Fever and cancer in perspective. *Cancer immunology, immunotherapy : CII* **50,** 391–396 (2001).
10. Carlson, R. D., Flickinger, J. C. J. & Snook, A. E. Talkin' Toxins: From Coley's to Modern Cancer Immunotherapy. *Toxins* **12** (2020).
11. Ribatti, D. The concept of immune surveillance against tumors. The first theories. *Oncotarget* **8,** 7175–7180 (2017).
12. Dighe, A. S., Richards, E., Old, L. J. & Schreiber, R. D. Enhanced in vivo growth and resistance to rejection of tumor cells expressing dominant negative IFN gamma receptors. *Immunity* **1,** 447–456 (1994).
13. Kaplan, D. H. *et al.* Demonstration of an interferon gamma-dependent tumor surveillance system in immunocompetent mice. *Proceedings of the National Academy of Sciences* **95,** 7556–7561 (1998).
14. Halliday, G. M., Patel, A., Hunt, M. J., Tefany, F. J. & Barnetson, R. S. Spontaneous regression of human melanoma/nonmelanoma skin cancer: association with infiltrating CD4+ T cells. *World Journal of Surgery* **19,** 352–358 (1995).
15. Hunter, P. The fourth pillar: Despite some setbacks in the clinic, immunotherapy has made notable progress toward becoming an additional therapeutic option against cancer. *EMBO Reports* **18,** 1889–1892 (2017).

16. Chen, L. & Flies, D. B. Molecular mechanisms of T cell co-stimulation and co-inhibition. *Nature Reviews Immunology* **13,** 227–242 (2013).

17. Pardoll, D. M. The blockade of immune checkpoints in cancer immunotherapy. *Nature Reviews Cancer* **12,** 252–264 (2012).

18. Schadendorf, D. *et al.* Pooled Analysis of Long-Term Survival Data From Phase II and Phase III Trials of Ipilimumab in Unresectable or Metastatic Melanoma. *Journal of Clinical Oncology* **33,** 1889–1894 (2015).

19. Boyiadzis, M. M. *et al.* Significance and implications of FDA approval of pembrolizumab for biomarker-defined disease. *Journal for ImmunoTherapy of Cancer* **6,** 35 (2018).

20. Hollingsworth, R. E. & Jansen, K. Turning the corner on therapeutic cancer vaccines. *npj Vaccines* **4,** 7 (2019).

21. Hege, K. M., Jooss, K. & Pardoll, D. GM-CSF Gene-Modifed Cancer Cell Immunotherapies: Of Mice and Men. *International Reviews of Immunology* **25,** 321–352 (2006).

22. Kantoff, P. W. *et al.* Sipuleucel-T Immunotherapy for Castration-Resistant Prostate Cancer. *The New England Journal of Medicine* **363,** 411–422 (2010).

23. Singh, P., Pal, S. K., Alex, A. & Agarwal, N. Development of PROSTVAC immunotherapy in prostate cancer. *Future Oncology* **11,** 2137–2148 (2015).

24. Weiden, P. L. *et al.* Antileukemic effect of graft-versus-host disease in human recipients of allogeneic-marrow grafts. *The New England Journal of Medicine* **300,** 1068–1073 (1979).

25. Rosenberg, S. A. *et al.* Use of Tumor-Infiltrating Lymphocytes and Interleukin-2 in the Immunotherapy of Patients with Metastatic Melanoma. *The New England Journal of Medicine* **319,** 1676–1680 (1988).

26. Federal Drug Administration. *Axicabtagene ciloleucel.* https://www.fda.gov/downloads/BiologicsBloodVaccines/CellularGeneTherapyProducts/ApprovedProducts/UCM581226.pdf, last accessed 29/04/2021.

27. Federal Drug Administration. *Tisagenlecleucel.* https://www.fda.gov/downloads/BiologicsBloodVaccines/CellularGeneTherapyProducts/ApprovedProducts/UCM573941.pdf, last accessed 29/04/2021.

28. Cooper, M. D. & Alder, M. N. The evolution of adaptive immune systems. *Cell* **124,** 815–822 (2006).

29. Germain, R. N. MHC-dependent antigen processing and peptide presentation: Providing ligands for T lymphocyte activation. *Cell* **76,** 287–299 (1994).

30. Dong, D. *et al.* Structural basis of assembly of the human T cell receptor–CD3 complex. *Nature* **573,** 546–552 (2019).

31. Hozumi, N. & Tonegawa, S. Evidence for somatic rearrangement of immunoglobulin genes coding for variable and constant regions. *Proceedings of the National Academy of Sciences of the United States of America* **73,** 3628–3632 (1976).

32. Tonegawa, S. Somatic generation of antibody diversity. *Nature* **302,** 575–581 (1983).

33. Thompson, C. B. New insights into V(D)J recombination and its role in the evolution of the immune system. *Immunity* **3,** 531–539 (1995).

34. Attaf, M., Legut, M., Cole, D. K. & Sewell, A. K. The T cell antigen receptor: the Swiss army knife of the immune system. *Clinical and experimental immunology* **181,** 1–18 (2015).

35. Murphy, K. & Weaver, C. *Janeway's immunobiology* (Garland science, 2016).

36. Shinkai, Y. *et al.* RAG-2-deficient mice lack mature lymphocytes owing to inability to initiate V(D)J rearrangement. *Cell* **68,** 855–867 (1992).

37. Huang, J. *et al.* A Single Peptide-Major Histocompatibility Complex Ligand Triggers Digital Cytokine Secretion in CD4+ T Cells. *Immunity* **39,** 846–857 (2013).

38. Sykulev, Y., Joo, M., Vturina, I., Tsomides, T. J. & Eisen, H. N. Evidence that a Single Peptide–MHC Complex on a Target Cell Can Elicit a Cytolytic T Cell Response. *Immunity* **4,** 565–571 (1996).

39. Zarnitsyna, V., Evavold, B., Schoettle, L., Blattman, J. & Antia, R. Estimating the Diversity, Completeness, and Cross-Reactivity of the T Cell Repertoire. *Frontiers in Immunology* **4,** 485 (2013).

40. Sewell, A. K. Why must T cells be cross-reactive? *Nature reviews. Immunology* **12,** 669–677 (2012).

41. Klein, L., Kyewski, B., Allen, P. M. & Hogquist, K. A. Positive and negative selection of the T cell repertoire: what thymocytes see (and don't see). *Nature Reviews Immunology* **14,** 377–391 (2014).

42. Binder, C. *et al.* CD2 Immunobiology. *Frontiers in Immunology* **11,** 1090 (2020).

43. Xing, Y. & Hogquist, K. A. T-cell tolerance: central and peripheral. *Cold Spring Harbor perspectives in biology* **4,** a006957 (2012).

44. Villaseñor, J., Benoist, C. & Mathis, D. AIRE and APECED: molecular insights into an autoimmune disease. *Immunological reviews* **204,** 156–164 (2005).

45. Kishimoto, H. & Sprent, J. Several different cell surface molecules control negative selection of medullary thymocytes. *The Journal of experimental medicine* **190,** 65–73 (1999).

46. Takahashi, S. *et al.* In vivo overexpression of CTLA-4 suppresses lymphoproliferative diseases and thymic negative selection. *European journal of immunology* **35,** 399–407 (2005).

47. Mueller, D. L., Jenkins, M. K. & Schwartz, R. H. An accessory cell-derived costimulatory signal acts independently of protein kinase C activation to allow T cell proliferation and prevent the induction of unresponsiveness. *Journal of immunology (Baltimore, Md. : 1950)* **142,** 2617–2628 (1989).

48. Wherry, E. J. T cell exhaustion. *Nature immunology* **12,** 492–499 (2011).

49. Nishimura, H., Minato, N., Nakano, T. & Honjo, T. Immunological studies on PD-1 deficient mice: implication of PD-1 as a negative regulator for B cell responses. *International immunology* **10,** 1563–1572 (1998).

50. Nishimura, H., Nose, M., Hiai, H., Minato, N. & Honjo, T. Development of lupus-like autoimmune diseases by disruption of the PD-1 gene encoding an ITIM motif-carrying immunoreceptor. *Immunity* **11,** 141–151 (1999).

51. Qureshi, O. S. *et al.* Trans-endocytosis of CD80 and CD86: a molecular basis for the cell-extrinsic function of CTLA-4. *Science (New York, N.Y.)* **332,** 600–603 (2011).

52. Waterhouse, P. *et al.* Lymphoproliferative Disorders with Early Lethality in Mice Deficient in Ctla-4. *Science* **270,** 985 LP –988 (1995).

53. Schmidt, A., Oberle, N. & Krammer, P. Molecular Mechanisms of Treg-Mediated T Cell Suppression. *Frontiers in Immunology* **3,** 51 (2012).

54. Krishnamurty, A. T. & Turley, S. J. Lymph node stromal cells: cartographers of the immune system. *Nature Immunology* **21,** 369–380 (2020).

55. Mason, D. A very high level of crossreactivity is an essential feature of the T-cell receptor. *Immunology Today* **19,** 395–404 (1998).

56. Lythe, G., Callard, R. E., Hoare, R. L. & Molina-París, C. How many TCR clonotypes does a body maintain? *Journal of theoretical biology* **389,** 214–224 (2016).

57. Wooldridge, L. *et al.* A single autoimmune T cell receptor recognizes more than a million different peptides. *The Journal of biological chemistry* **287,** 1168–1177 (2012).

58. Zareie, P. *et al.* Canonical T cell receptor docking on peptide–MHC is essential for T cell signaling. *Science* **372,** eabe9124 (2021).

59. Setia, M. S., Steinmaus, C., Ho, C. S. & Rutherford, G. W. The role of BCG in prevention of leprosy: a meta-analysis. *The Lancet. Infectious diseases* **6,** 162–170 (2006).

60. Gonzalez-Perez, M., Sanchez-Tarjuelo, R., Shor, B., Nistal-Villan, E. & Ochando, J. The BCG Vaccine for COVID-19: First Verdict and Future Directions. *Frontiers in Immunology* **12,** 579 (2021).

61. Cusick, M. F., Libbey, J. E. & Fujinami, R. S. Molecular mimicry as a mechanism of autoimmune disease. *Clinical reviews in allergy & immunology* **42,** 102–111 (2012).

62. Yu, J. X., Upadhaya, S., Tatake, R., Barkalow, F. & Hubbard-Lucey, V. M. Cancer cell therapies: the clinical trial landscape. *Nature Reviews Drug Discovery* **19,** 583–584 (2020).

63. Rath, J. A. & Arber, C. Engineering Strategies to Enhance TCR-Based Adoptive T Cell Therapy. *Cells* **9,** 1485 (2020).

64. Courtney, A. H., Lo, W.-L. & Weiss, A. TCR Signaling: Mechanisms of Initiation and Propagation. *Trends in Biochemical Sciences* **43,** 108–123 (2018).

65. Van der Merwe, P. A. & Dushek, O. Mechanisms for T cell receptor triggering. *Nature Reviews Immunology* **11,** 47–55 (2011).

66. Brownlie, R. & Zamoyska, R. LAT Polices T Cell Activation. *Immunity* **31,** 174–176 (2009).

67. Brownlie, R. J. & Zamoyska, R. T cell receptor signalling networks: branched, diversified and bounded. *Nature Reviews Immunology* **13,** 257–269 (2013).

68. Gudipati, V. *et al.* Inefficient CAR-proximal signaling blunts antigen sensitivity. *Nature Immunology* **21,** 848–856 (2020).

69. Li, R., Ma, C., Cai, H. & Chen, W. The CAR T-Cell Mechanoimmunology at a Glance. *Advanced science (Weinheim, Baden-Wurttemberg, Germany)* **7,** 2002628 (2020).

70. Lindner, S. E., Johnson, S. M., Brown, C. E. & Wang, L. D. Chimeric antigen receptor signaling: Functional consequences and design implications. *Science Advances* **6,** eaaz3223 (2020).

71. Dong, R. *et al.* Rewired signaling network in T cells expressing the chimeric antigen receptor (CAR). *The EMBO Journal* **39,** e104730 (2020).

72. Rossig, C., Kailayangiri, S., Jamitzky, S. & Altvater, B. *Carbohydrate targets for CAR T cells in solid childhood cancers* 2018.

73. Watanabe, K. *et al.* Target antigen density governs the efficacy of anti-CD20-CD28-CD3 ζ chimeric antigen receptor-modified effector CD8+ T cells. *The Journal of Immunology* **194,** 911–20 (2015).

74. Harris, D. T. *et al.* Comparison of T Cell Activities Mediated by Human TCRs and CARs That Use the Same Recognition Domains. *The Journal of Immunology* **200,** 1088–1100 (2018).

75. Baeuerle, P. A. *et al.* Synthetic TRuC receptors engaging the complete T cell receptor for potent anti-tumor response. *Nature Communications* **10,** 1–12 (2019).

76. Rosenberg, S. A. *et al.* Treatment of patients with metastatic melanoma with autologous tumor-infiltrating lymphocytes and interleukin 2. *Journal of the National Cancer Institute* **86,** 1159–1166 (1994).

77. Rosenberg, S. A. *et al.* Gene transfer into humans–immunotherapy of patients with advanced melanoma, using tumor-infiltrating lymphocytes modified by retroviral gene transduction. *The New England Journal of Medicine* **323,** 570–578 (1990).

78. Dudley, M. E. *et al.* Cancer regression and autoimmunity in patients after clonal repopulation with antitumor lymphocytes. *Science* **298,** 850–854 (2002).

79. Neelapu, S. S. CAR-T efficacy: is conditioning the key? *Blood* **133,** 1799–1800 (2019).

80. Rosenberg, S. A. *et al.* Durable complete responses in heavily pretreated patients with metastatic melanoma using T-cell transfer immunotherapy. *Clinical Cancer Research* **17,** 4550–4557 (2011).

81. Morgan, R. A. *et al.* Cancer regression in patients after transfer of genetically engineered lymphocytes. *Science* **314,** 126–129 (2006).

82. Kuwana, Y. *et al.* Expression of chimeric receptor composed of immunoglobulin-derived V resions and T-cell receptor-derived C regions. *Biochemical and Biophysical Research Communications* **149,** 960–968 (1987).

83. Gross, G., Waks, T. & Eshhar, Z. Expression of immunoglobulin-T-cell receptor chimeric molecules as functional receptors with antibody-type specificity. *Proceedings of the National Academy of Sciences* **86,** 10024 LP –10028 (1989).

84. Liu, Y. *et al.* Chimeric STAR receptors using TCR machinery mediate robust responses against solid tumors. *Science Translational Medicine* **13,** eabb5191 (2021).

85. Irving, B. A. & Weiss, A. The cytoplasmic domain of the T cell receptor ζ chain is sufficient to couple to receptor-associated signal transduction pathways. *Cell* **64,** 891–901 (1991).

86. Romeo, C. & Seed, B. Cellular immunity to HIV activated by CD4 fused to T cell or Fc receptor polypeptides. *Cell* **64,** 1037–1046 (1991).

87. Eshhar, Z., Waks, T., Gross, G. & Schindler, D. G. Specific activation and targeting of cytotoxic lymphocytes through chimeric single chains consisting of antibody-binding domains and the γ or ζ subunits of the immunoglobulin and T-cell receptors. *Proceedings of the National Academy of Sciences* **90,** 720–724 (1993).

88. Brocker, T. Chimeric Fv-zeta or Fv-epsilon receptors are not sufficient to induce activation or cytokine production in peripheral T cells. *Blood* **96,** 1999–2001 (2000).

89. Maher, J., Brentjens, R. J., Gunset, G., Rivière, I. & Sadelain, M. Human T-lymphocyte cytotoxicity and proliferation directed by a single chimeric TCRζ/CD28 receptor. *Nature Biotechnology* **20,** 70–75 (2002).

90. Imai, C. *et al.* Chimeric receptors with 4-1BB signaling capacity provoke potent cytotoxicity against acute lymphoblastic leukemia. *Leukemia* **18,** 676–684 (2004).

91. Khalil, D. N., Smith, E. L., Brentjens, R. J. & Wolchok, J. D. The future of cancer treatment: Immunomodulation, CARs and combination immunotherapy. *Nature Reviews Clinical Oncology* **13,** 273–290 (2016).

92. Roybal, K. T. & Lim, W. A. Synthetic Immunology: Hacking Immune Cells to Expand Their Therapeutic Capabilities. *Annual Review of Immunology* **35,** 229–253 (2017).

93. Rafiq, S., Hackett, C. S. & Brentjens, R. J. Engineering strategies to overcome the current roadblocks in CAR T cell therapy. *Nature Reviews Clinical Oncology* **17,** 147–167 (2020).

94. Exley, A. R. & McBlane, J. Regulating innovation in the early development of cell therapies. *Immunotherapy Advances* **1** (2021).

95. Shah, N. N. & Fry, T. J. Mechanisms of resistance to CAR T cell therapy. *Nature Reviews Clinical Oncology* **16,** 372–385 (2019).

96. Hay, A. E. & Cheung, M. C. CAR T-cells: costs, comparisons, and commentary. *Journal of Medical Economics* **22,** 613–615 (2019).

97. The National Institute for Health and Care Excellence. *Axicabtagene ciloleucel for treating diffuse large B-cell lymphoma and primary mediastinal B-cell lymphoma after 2 or more systemic therapies.* https://www.nice.org.uk/guidance/ta559/documents/appraisal-consultation-document, last accessed 29/04/2021.

98. Kebriaei, P. *et al.* Phase I trials using Sleeping Beauty to generate CD19-specific CAR T cells. *The Journal of Clinical Investigation* **126,** 3363–3376 (2016).

99. Ghosh, A. *et al.* Donor CD19 CAR T cells exert potent graft-versus-lymphoma activity with diminished graft-versus-host activity. *Nature Medicine* **23,** 242–249 (2017).

100. Pichereau, C. *et al.* Trajectories of acute graft-versus-host disease and mortality in critically ill allogeneic-hematopoietic stem cell recipients: the Allo-GRRR-OH score. *Bone marrow transplantation* **55,** 1966–1974 (2020).

101. Tzannou, I. *et al.* Off-the-Shelf Virus-Specific T Cells to Treat BK Virus, Human Herpesvirus 6, Cytomegalovirus, Epstein-Barr Virus, and Adenovirus Infections After Allogeneic Hematopoietic Stem-Cell Transplantation. *Journal of Clinical Oncology* **35,** 3547–3557 (2017).

102. Qasim, W. *et al.* Molecular remission of infant B-ALL after infusion of universal TALEN gene-edited CAR T cells. *Science Translational Medicine* **9** (2017).

103. Torikai, H. *et al.* Toward eliminating HLA class I expression to generate universal cells from allogeneic donors. *Blood* **122,** 1341–1349 (2013).

104. Ren, J. *et al.* Multiplex Genome Editing to Generate Universal CAR T Cells Resistant to PD1 Inhibition. *Clinical Cancer Research* **23,** 2255–2266 (2017).

105. Mo, F. *et al.* Engineered off-the-shelf therapeutic T cells resist host immune rejection. *Nature Biotechnology* **39,** 56–63 (2021).

106. Maude, S. L. *et al.* Chimeric Antigen Receptor T Cells for Sustained Remissions in Leukemia. *The New England Journal of Medicine* **371,** 1507–1517 (2014).

107. Fry, T. J. *et al.* CD22-targeted CAR T cells induce remission in B-ALL that is naive or resistant to CD19-targeted CAR immunotherapy. *Nature Medicine* **24,** 20–28 (2018).

108. Hegde, M. *et al.* Combinational targeting offsets antigen escape and enhances effector functions of adoptively transferred T cells in glioblastoma. *Molecular Therapy* **21,** 2087–2101 (2013).

109. D'Aloia, M. M. *et al.* CAR-T cells: The long and winding road to solid tumors review-article. *Cell Death and Disease* **9,** 282 (2018).

110. Choi, B. D. *et al.* CAR-T cells secreting BiTEs circumvent antigen escape without detectable toxicity. *Nature Biotechnology* **37,** 1049–1058 (2019).

111. Long, A. H. *et al.* 4-1BB costimulation ameliorates T cell exhaustion induced by tonic signaling of chimeric antigen receptors. *Nature Medicine* **21,** 581–590 (2015).

112. Feucht, J. *et al.* Calibration of CAR activation potential directs alternative T cell fates and therapeutic potency. *Nature Medicine* **25,** 82–88 (2019).

113. Eyquem, J. *et al.* Targeting a CAR to the TRAC locus with CRISPR/Cas9 enhances tumour rejection. *Nature* **543,** 113–117 (2017).

114. Fraietta, J. A. *et al.* Disruption of TET2 promotes the therapeutic efficacy of CD19-targeted T cells. *Nature* **558,** 307–312 (2018).

115. Sadeghi Rad, H. *et al.* Understanding the tumor microenvironment for effective immunotherapy. *Medicinal research reviews* **41,** 1474–1498 (2021).

116. Krenciute, G. *et al.* Transgenic Expression of IL15 Improves Antiglioma Activity of IL13Rα2-CAR T Cells but Results in Antigen Loss Variants. *Cancer immunology research* **5,** 571–581 (2017).

117. Chang, Z. L. *et al.* Rewiring T-cell responses to soluble factors with chimeric antigen receptors. *Nature Chemical Biology* **14,** 317–324 (2018).

118. Stadtmauer, E. A. *et al.* CRISPR-engineered T cells in patients with refractory cancer. *Science* **367** (2020).

119. Choi, B. D. *et al.* CRISPR-Cas9 disruption of PD-1 enhances activity of universal EGFRvIII CAR T cells in a preclinical model of human glioblastoma. *Journal for ImmunoTherapy of Cancer* **7,** 304 (2019).

120. Brudno, J. N. & Kochenderfer, J. N. Recent advances in CAR T-cell toxicity: Mechanisms, manifestations and management. *Blood Reviews* **34,** 45–55 (2019).

121. Lewis, O. & Pastores, S. M. *Tumor Lysis Syndrome in the Cancer Patient BT - Oncologic Critical Care* (eds Nates, J. L. & Price, K. J.) 1119–1133 (Springer International Publishing, Cham, 2020).

122. Neelapu, S. S. *et al.* Chimeric antigen receptor T-cell therapy — assessment and management of toxicities. *Nature Reviews Clinical Oncology* **15,** 47–62 (2018).

123. Parker, K. R. *et al.* Single-Cell Analyses Identify Brain Mural Cells Expressing CD19 as Potential Off-Tumor Targets for CAR-T Immunotherapies. *Cell* **183,** 126–142 (2020).

124. Gust, J. *et al.* Endothelial Activation and Blood-Brain Barrier Disruption in Neurotoxicity after Adoptive Immunotherapy with CD19 CAR-T Cells. *Cancer Discovery* **7,** 1404–1419 (2017).

125. Coulie, P. G., Van den Eynde, B. J., van der Bruggen, P. & Boon, T. Tumour antigens recognized by T lymphocytes: at the core of cancer immunotherapy. *Nature Reviews Cancer* **14,** 135–146 (2014).

126. Vigneron, N. Human Tumor Antigens and Cancer Immunotherapy. *BioMed Research International* **2015,** 948501 (2015).

127. Parkhurst, M. R. *et al.* T cells targeting carcinoembryonic antigen can mediate regression of metastatic colorectal cancer but induce severe transient colitis. *Molecular Therapy* **19,** 620–6 (2011).

128. VanSeggelen, H. *et al.* On-target off-tumor toxicity; when enhancing an NKG2D-based CAR in vitro led to severe toxicities in vivo. *Journal for ImmunoTherapy of Cancer* **2,** P15 (2014).

129. Guo, Y. *et al.* Phase I Study of Chimeric Antigen Receptor–Modified T Cells in Patients with EGFR-Positive Advanced Biliary Tract Cancers. *Clinical Cancer Research* **24,** 1277 LP –1286 (2018).

130. Lamers, C. H. *et al.* Treatment of Metastatic Renal Cell Carcinoma With Autologous T-Lymphocytes Genetically Retargeted Against Carbonic Anhydrase IX: First Clinical Experience. *Journal of Clinical Oncology* **24,** e20–e22 (2006).

131. Morgan, R. A. *et al.* Case report of a serious adverse event following the administration of T cells transduced with a chimeric antigen receptor recognizing ERBB2. *Molecular Therapy* **18,** 843–51 (2010).

132. Liu, X. *et al.* Affinity-Tuned ErbB2 or EGFR Chimeric Antigen Receptor T Cells Exhibit an Increased Therapeutic Index against Tumors in Mice. *Cancer Research* **75,** 3596–3607 (2015).

133. Caruso, H. G. *et al.* Tuning Sensitivity of CAR to EGFR Density Limits Recognition of Normal Tissue While Maintaining Potent Antitumor Activity. *Cancer Research* **75,** 3505–3518 (2015).

134. Drent, E. *et al.* A Rational Strategy for Reducing On-Target Off-Tumor Effects of CD38-Chimeric Antigen Receptors by Affinity Optimization. *Molecular Therapy* **25,** 1946–1958 (2017).

135. Linette, G. P. *et al.* Cardiovascular toxicity and titin cross-reactivity of affinity-enhanced T cells in myeloma and melanoma. *Blood* **122,** 863–871 (2013).

136. Cameron, B. J. *et al.* Identification of a Titin-Derived HLA-A1-Presented Peptide as a Cross-Reactive Target for Engineered MAGE A3-Directed T Cells. *Science Translational Medicine* **5,** 103–197 (2013).

137. Raman, M. C. C. *et al.* Direct molecular mimicry enables off-target cardiovascular toxicity by an enhanced affinity TCR designed for cancer immunotherapy. *Scientific Reports* **6,** 18851 (2016).

138. Sun, S., Hao, H., Yang, G., Zhang, Y. & Fu, Y. Immunotherapy with CAR-Modified T Cells: Toxicities and Overcoming Strategies. *Journal of Immunology Research* **2018,** 2386187 (2018).

139. Maus, M. V. *et al.* An MHC-restricted antibody-based chimeric antigen receptor requires TCR-like affinity to maintain antigen specificity. *Molecular Therapy - Oncolytics* **3** (2016).

140. Tan, M. P. *et al.* T cell receptor binding affinity governs the functional profile of cancer-specific CD8+ T cells. *Clinical and Experimental Immunology* **180,** 255–270 (2015).

141. Sanderson, J. P. *et al.* Preclinical evaluation of an affinity-enhanced MAGE-A4-specific T-cell receptor for adoptive T-cell therapy. *Oncoimmunology* **9,** 1682381 (2020).

142. Arulanandam, A. R. *et al.* A soluble multimeric recombinant CD2 protein identifies CD48 as a low affinity ligand for human CD2: divergence of CD2 ligands during the evolution of humans and mice. *Journal of Experimental Medicine* **177,** 1439–1450 (1993).

143. McArdel, S. L., Terhorst, C. & Sharpe, A. H. Roles of CD48 in regulating immunity and tolerance. *Clinical Immunology* **164,** 10–20 (2016).

144. Van der Merwe, P. A. *et al.* Human cell-adhesion molecule CD2 binds CD58 (LFA-3) with a very low affinity and an extremely fast dissociation rate but does not bind CD48 or CD59. *Biochemistry* **33,** 10149–10160 (1994).

145. Choudhuri, K., Wiseman, D., Brown, M. H., Gould, K. & van der Merwe, P. A. T-cell receptor triggering is critically dependent on the dimensions of its peptide-MHC ligand. *Nature* **436,** 578–582 (2005).

146. Dustin, M. L. Adhesive bond dynamics in contacts between T lymphocytes and glass-supported planar bilayers reconstituted with the immunoglobulin-related adhesion molecule CD58. *The Journal of Biological Chemistry* **272,** 15782–15788 (1997).

147. Van der Merwe, P. A., Bodian, D. L., Daenke, S., Linsley, P. & Davis, S. J. CD80 (B7-1) binds both CD28 and CTLA-4 with a low affinity and very fast kinetics. *Journal of Experimental Medicine* **185,** 393–403 (1997).

148. Sanchez-Madrid, F. *et al.* Three distinct antigens associated with human T-lymphocyte-mediated cytolysis: LFA-1, LFA-2, and LFA-3. *Proceedings of the National Academy of Sciences* **79,** 7489–7493 (1982).

149. Bachmann, M. F., Barner, M. & Kopf, M. CD2 sets quantitative thresholds in T cell activation. *Journal of Experimental Medicine* **190,** 1383–1391 (1999).

150. Evans, C. F., Rall, G. F., Killeen, N., Littman, D. & Oldstone, M. B. CD2-deficient mice generate virus-specific cytotoxic T lymphocytes upon infection with lymphocytic choriomeningitis virus. *Journal of Immunology* **151,** 6259–6264 (1993).

151. Davis, S. J., Ikemizu, S., Wild, M. K. & van der Merwe, P. A. CD2 and the nature of protein interactions mediating cell-cell recognition. *Immunological Reviews* **163,** 217–236 (1998).

152. Van der Merwe, P. A., Brown, M. H., Davis, S. J. & Barclay, A. N. Affinity and kinetic analysis of the interaction of the cell adhesion molecules rat CD2 and CD48. *The EMBO journal* **12,** 4945–4954 (1993).

153. Milstein, O. *et al.* Nanoscale increases in CD2-CD48-mediated intermembrane spacing decrease adhesion and reorganize the immunological synapse. *The Journal of biological chemistry* **283,** 34414–34422 (2008).

154. Brown, M. H. *et al.* 2B4, the natural killer and T cell immunoglobulin superfamily surface protein, is a ligand for CD48. *The Journal of experimental medicine* **188,** 2083–2090 (1998).

155. Schatzle, J. D. *et al.* Characterization of inhibitory and stimulatory forms of the murine natural killer cell receptor 2B4. *Proceedings of the National Academy of Sciences of the United States of America* **96,** 3870–3875 (1999).

156. Davis, S. J. & Van Der Merwe, P. A. The structure and ligand interactions of CD2: Implications for T-cell function. *Immunology Today* **17,** 177–187 (1996).

157. Dustin, M. L. Modular design of immunological synapses and kinapses. *Cold Spring Harbor Perspectives in Biology* **1,** a002873 (2009).

158. Freiberg, B. A. *et al.* Staging and resetting T cell activation in SMACs. *Nature Immunology* **3,** 911–917 (2002).

159. Siokis, A., Robert, P. A., Demetriou, P., Dustin, M. L. & Meyer-Hermann, M. F-Actin-Driven CD28-CD80 Localization in the Immune Synapse. *Cell Reports* **24,** 1151–1162 (2018).

160. Demetriou, P. *et al.* A dynamic CD2-rich compartment at the outer edge of the immunological synapse boosts and integrates signals. *Nature Immunology* **21,** 1232–1243 (2020).

161. Gajewski, T. F. *et al.* Immune resistance orchestrated by the tumor microenvironment. *Immunological Reviews* **213,** 131–145 (2006).

162. Redeker, A. & Arens, R. Improving Adoptive T Cell Therapy: The Particular Role of T Cell Costimulation, Cytokines, and Post-Transfer Vaccination. *Frontiers in Immunology* **7,** 345 (2016).

163. Van der Merwe, P. A. A subtle role for CD2 in T cell antigen recognition. *Journal of Experimental Medicine* **190,** 1371–1374 (1999).

164. Chen, J.-L. *et al.* Identification of NY-ESO-1 Peptide Analogues Capable of Improved Stimulation of Tumor-Reactive CTL. *The Journal of Immunology* **165,** 948–955 (2000).

165. Peterson, A. & Seed, B. Monoclonal antibody and ligand binding sites of the T cell erythrocyte receptor (CD2). *Nature* **329,** 842–846 (1987).

166. Aleksic, M. *et al.* Dependence of T Cell Antigen Recognition on T Cell Receptor-Peptide MHC Confinement Time. *Immunity* **32,** 163–174 (2010).

167. Lever, M. *et al.* Architecture of a minimal signaling pathway explains the T-cell response to a 1 million-fold variation in antigen affinity and dose. *Proceedings of the National Academy of Sciences* **113,** E6630–E6638 (2016).

168. Abdul Razak, F. R., Diepstra, A., Visser, L. & Van Den Berg, A. CD58 mutations are common in Hodgkin lymphoma cell lines and loss of CD58 expression in tumor cells occurs in Hodgkin lymphoma patients who relapse. *Genes and Immunity* **17,** 363–366 (2016).

169. Patel, S. J. *et al.* Identification of essential genes for cancer immunotherapy. *Nature* **548,** 537–542 (2017).

170. Majzner, R. G. *et al.* CD58 Aberrations Limit Durable Responses to CD19 CAR in Large B Cell Lymphoma Patients Treated with Axicabtagene Ciloleucel but Can be Overcome through Novel CAR Engineering. *62nd American Society of Hematology Meeting and Exposition* **1,** 11–12 (2020).

171. Wang, E. C. Y. *et al.* Suppression of costimulation by human cytomegalovirus promotes evasion of cellular immune defenses. *Proceedings of the National Academy of Sciences* **115,** 4998–5003 (2018).

172. Xu, X. *et al.* The genomic sequence of the Chinese hamster ovary (CHO)-K1 cell line. *Nature Biotechnology* **29,** 735–741 (2011).

173. Koyasu, S. *et al.* Role of interaction of CD2 molecules with lymphocyte function-associated antigen 3 in T-cell recognition of nominal antigen. *Proceedings of the National Academy of Sciences of the United States of America* **87,** 2603–2607 (1990).

174. Carbone, C. B. *et al.* In vitro reconstitution of T cell receptor-mediated segregation of the CD45 phosphatase. *Proceedings of the National Academy of Sciences* **114,** E9338–E9345 (2017).

175. Trendel, N. *et al.* Perfect adaptation of CD8 T cell responses to constant antigen input over a wide range of affinities is overcome by costimulation. *Science Signaling* **14,** eaay9363 (2021).

176. Dustin, M. L., Starr, T., Varma, R. & Thomas, V. K. Supported planar bilayers for study of the immunological synapse. *Current Protocols in Immunology* **18,** 2–35 (2007).

177. Valvo, S. *et al.* Comprehensive analysis of immunological synapse phenotypes using supported lipid bilayers. *Methods in Molecular Biology* **1584,** 423–441 (2017).

178. Vardhana, S. & Dustin, M. Supported planar bilayers for the formation of study of immunological synapses and Kinapse. *Journal of Visualized Experiments* **19,** 947 (2008).

179. Jenkins, E. *et al.* Reconstitution of immune cell interactions in free-standing membranes. *Journal of Cell Science* **132** (2019).

180. Lippert, A. H. *et al.* Soft Polydimethylsiloxane-Supported Lipid Bilayers for Studying T Cell Interactions. *Biophysical journal* **120,** 35–45 (2021).

181. Purcell, S. C. & Godula, K. Synthetic glycoscapes: addressing the structural and functional complexity of the glycocalyx. *Interface Focus* **9,** 20180080 (2019).

182. Sage, P. T. *et al.* Antigen Recognition Is Facilitated by Invadosome-like Protrusions Formed by Memory/Effector T Cells. *The Journal of Immunology* **188,** 3686–3699 (2012).

183. Kurokawa, T., Oelke, M. & Mackensen, A. Induction and clonal expansion of tumor-specific cytotoxic T lymphocytes from renal cell carcinoma patients after stimulation with autologous dendritic cells loaded with tumor cells. *International Journal of Cancer* **91,** 749–756 (2001).

184. Chang, Y. H. *et al.* Dichotomous Expression of TNF Superfamily Ligands on Antigen-Presenting Cells Controls Post-priming Anti-viral CD4+ T Cell Immunity. *Immunity* **47,** 943–958 (2017).

185. Viola, A. & Lanzavecchia, A. T cell activation determined by T cell receptor number and tunable thresholds. *Science* **273,** 104–106 (1996).

186. Sun, S. *et al.* Dual function of Drosophila cells as APCs for naive CD8+ T cells: implications for tumor immunotherapy. *Immunity* **4,** 555–564 (1996).

187. Latouche, J. B. & Sadelain, M. Induction of human cytotoxic T lymphocytes by artificial antigen-presenting cells. *Nature Biotechnology* **18,** 405–409 (2000).

188. Wurm, F. M. Production of recombinant protein therapeutics in cultivated mammalian cells. *Nature Biotechnology* **22,** 1393–1398 (2004).

189. Wild, M. K. *et al.* Dependence of T cell antigen recognition on the dimensions of an accessory receptor-ligand complex. *Journal of Experimental Medicine* **190,** 31–41 (1999).

190. Jutz, S. *et al.* A cellular platform for the evaluation of immune checkpoint molecules. *Oncotarget* **8,** 64892–64906 (2017).

191. Cheng, J. *et al.* Understanding the Mechanisms of Resistance to CAR T-Cell Therapy in Malignancies. *Frontiers in Oncology* **9,** 1237 (2019).

192. Gaglia, J. L., Mattoo, A., Greenfield, E. A., Freeman, G. J. & Kuchroo, V. K. Characterization of endogenous Chinese hamster ovary cell surface molecules that mediate T cell costimulation. *Cellular immunology* **213,** 83–93 (2001).

193. Johnston, S. C., Dustin, M. L., Hibbs, M. L. & Springer, T. A. On the species specificity of the interaction of LFA-1 with intercellular adhesion molecules. *The Journal of Immunology* **145,** 1181–1187 (1990).

194. Núñez, D. *et al.* A Functional Analysis on the Interspecies Interaction between Mouse LFA-1 and Human Intercellular Adhesion Molecule-1 at the Cell Level. *Frontiers in immunology* **8,** 1817 (2017).

195. Ratzinger, F. *et al.* Azithromycin suppresses CD4(+) T-cell activation by direct modulation of mTOR activity. *Scientific Reports* **4,** 7438 (2014).

196. Sami, M. *et al.* Crystal structures of high affinity human T-cell receptors bound to peptide major histocompatibility complex reveal native diagonal binding geometry. *Protein Engineering, Design & Selection* **20,** 397–403 (2007).

197. Abu-Shah, E. *et al.* A tissue-like platform for studying engineered quiescent human T-Cells' interactions with dendritic cells. *eLife* **8** (2019).

198. Abu-Shah, E. *et al.* Human CD8 + T Cells Exhibit a Shared Antigen Threshold for Different Effector Responses. *The Journal of Immunology* **205,** 1503–1512 (2020).

199. Qin, J. Y. *et al.* Systematic comparison of constitutive promoters and the doxycycline-inducible promoter. *PLoS ONE* **5,** e10611–e10611 (2010).

200. Astoul, E., Edmunds, C., Cantrell, D. A. & Ward, S. G. PI 3-K and T-cell activation: limitations of T-leukemic cell lines as signaling models. *Trends in Immunology* **22,** 490–496 (2001).

201. Bartelt, R. R., Cruz-Orcutt, N., Collins, M. & Houtman, J. C. D. Comparison of T cell receptor-induced proximal signaling and downstream functions in immortalized and primary T cells. *PLoS ONE* **4,** e5430–e5430 (2009).

202. Leitner, J., Herndler-Brandstetter, D., Zlabinger, G. J., Grubeck-Loebenstein, B. & Steinberger, P. CD58/CD2 Is the Primary Costimulatory Pathway in Human CD28-CD8+ T Cells. *The Journal of Immunology* **195,** 477–487 (2015).

203. Zurli, V. *et al.* Phosphoproteomics of CD2 signaling reveals AMPK-dependent regulation of lytic granule polarization in cytotoxic T cells. *Science Signaling* **13,** eaaz1965 (2020).

204. Davis, S. J. & van der Merwe, P. A. The kinetic-segregation model: TCR triggering and beyond. *Nature Immunology* **7,** 803–809 (2006).

205. Chang, V. T. *et al.* Initiation of T cell signaling by CD45 segregation at 'close contacts'. *Nature Immunology* **17,** 574–582 (2016).

206. Spruyt, L. L., Glennie, M. J., Beyers, A. D. & Williams, A. F. Signal transduction by the CD2 antigen in T cells and natural killer cells: requirement for expression of a functional T cell receptor or binding of antibody Fc to the Fc receptor, Fc gamma RIIIA (CD16). *The Journal of experimental medicine* **174,** 1407–1415 (1991).

207. Bagnasco, M. *et al.* Anti-T11.1 and -T11.2 monoclonal antibodies play a different role in CD2-mediated signal transduction. *Human Immunology* **38,** 172–178 (1993).

208. MOSES, R. D., WINN, H. J. & AUCHINCLOSS, H. J. R. Evidence that multiple defects in cell-surface molecule interactions across species differences are responsible for diminished xenogeneic T cell responses. *Transplantation* **53** (1992).

209. Louie, S. *et al.* Endothelial intercellular cell adhesion molecule 1 contributes to cell aggregate formation in CHO cells cultured in serum-free media. *Biotechnology Progress* **36** (2020).

210. Xue, S., Song, G. & Yu, J. The prognostic significance of PD-L1 expression in patients with glioma: A meta-analysis. *Scientific Reports* **7,** 4231 (2017).

211. Irvine, D. J., Purbhoo, M. A., Krogsgaard, M. & Davis, M. M. Direct observation of ligand recognition by T cells. *Nature* **419,** 845–849 (2002).

212. Purbhoo, M. A., Irvine, D. J., Huppa, J. B. & Davis, M. M. T cell killing does not require the formation of a stable mature immunological synapse. *Nature Immunology* **5,** 524–530 (2004).

213. Yang, H. *et al.* Elimination of Latently HIV-infected Cells from Antiretroviral Therapy-suppressed Subjects by Engineered Immune-mobilizing T-cell Receptors. *Molecular Therapy* **24,** 1913–1925 (2016).

214. Keskin, D. B. *et al.* Physical detection of influenza A epitopes identifies a stealth subset on human lung epithelium evading natural CD8 immunity. *Proceedings of the National Academy of Sciences* **112,** 2151 LP –2156 (2015).

215. Lemmermann, N. A. W. *et al.* Immune evasion proteins of murine cytomegalovirus preferentially affect cell surface display of recently generated peptide presentation complexes. *Journal of Virology* **84,** 1221–36 (2010).

216. Bluhm, J. *et al.* CAR T Cells with Enhanced Sensitivity to B Cell Maturation Antigen for the Targeting of B Cell Non-Hodgkin's Lymphoma and Multiple Myeloma. *Molecular Therapy* **26,** 1906–1920 (2018).

217. Stone, J. D., Aggen, D. H., Schietinger, A., Schreiber, H. & Kranz, D. M. A sensitivity scale for targeting T cells with chimeric antigen receptors (CARs) and bispecific T-cell Engagers (BiTEs). *Oncoimmunology* **1,** 863–873 (2012).

218. Posey, A. D. *et al.* Engineered CAR T Cells Targeting the Cancer-Associated Tn-Glycoform of the Membrane Mucin MUC1 Control Adenocarcinoma. *Immunity* **44,** 1444–1454 (2016).

219. Wang, Z. & Cao, Y. J. Adoptive Cell Therapy Targeting Neoantigens: A Frontier for Cancer Research. *Frontiers in Immunology* **11,** 176 (2020).

220. Tuccillo, F. M. *et al.* Aberrant glycosylation as biomarker for cancer: Focus on CD43. *BioMed Research International* **2014,** 1–13 (2014).

221. Tan, X. *et al.* dbPepNeo: a manually curated database for human tumor neoantigen peptides. *Database* **2020** (2020).

222. Hegde, M. *et al.* Expansion of HER2-CAR T cells after lymphodepletion and clinical responses in patients with advanced sarcoma. *Journal of Clinical Oncology* **35,** 10508 (2017).

223. Ahmed, N. *et al.* Human Epidermal Growth Factor Receptor 2 (HER2) -Specific Chimeric Antigen Receptor-Modified T Cells for the Immunotherapy of HER2-Positive Sarcoma. *Journal of Clinical Oncology* **33,** 1688–1696 (2015).

224. Kloss, C. C., Condomines, M., Cartellieri, M., Bachmann, M. & Sadelain, M. Combinatorial antigen recognition with balanced signaling promotes selective tumor eradication by engineered T cells. *Nature Biotechnology* **31,** 71–75 (2013).

225. Lanitis, E. *et al.* Chimeric antigen receptor T Cells with dissociated signaling domains exhibit focused antitumor activity with reduced potential for toxicity in vivo. *Cancer Immunology Research* **1,** 43–53 (2013).

226. Wilkie, S. *et al.* Dual targeting of ErbB2 and MUC1 in breast cancer using chimeric antigen receptors engineered to provide complementary signaling. *Journal of Clinical Immunology* **32,** 1059–1070 (2012).

227. Hernandez-Lopez, R. A. *et al.* T cell circuits that sense antigen density with an ultrasensitive threshold. *Science* **371,** 1166 LP –1171 (2021).

228. Gálvez, J., Gálvez, J. J. & García-Peñarrubia, P. Is TCR/pMHC Affinity a Good Estimate of the T-cell Response? An Answer Based on Predictions From 12 Phenotypic Models. *Frontiers in Immunology* **10,** 349 (2019).

229. Anton van der Merwe, P., McNamee, P. N., Davies, E. A., Barclay, A. & Davis, S. J. Topology of the CD2–CD48 cell-adhesion molecule complex: implications for antigen recognition by T cells. *Current Biology* **5,** 74–84 (1995).

230. Cyster, J. G., Shotton, D. M. & Williams, A. F. The dimensions of the T lymphocyte glycoprotein leukosialin and identification of linear protein epitopes that can be modified by glycosylation. *The EMBO Journal* **10,** 893–902 (1991).

231. Ereño-Orbea, J. *et al.* Molecular basis of human CD22 function and therapeutic targeting. *Nature Communications* **8,** 764 (2017).

232. Angata, T. & Varki, A. Cloning, characterization, and phylogenetic analysis of siglec-9, a new member of the CD33-related group of siglecs. Evidence for co-evolution with sialic acid synthesis pathways. *The Journal of Biological Chemistry* **275,** 22127–22135 (2000).

233. Cheadle, E. J. *et al.* Ligation of the CD2 co-stimulatory receptor enhances IL-2 production from first-generation chimeric antigen receptor T cells. *Gene Therapy* **19,** 1114–1120 (2012).

234. Lim, H.-S. *et al.* Costimulation of IL-2 Production through CD28 Is Dependent on the Size of Its Ligand. *The Journal of Immunology* **195,** 5432–5439 (2015).

235. Dustin, M. L. *et al.* Low Affinity Interaction of Human or Rat T Cell Adhesion Molecule CD2 with Its Ligand Aligns Adhering Membranes to Achieve High Physiological Affinity*. *Journal of Biological Chemistry* **272,** 30889–30898 (1997).

236. Bachmann, M. F. *et al.* Distinct roles for LFA-1 and CD28 during activation of naive T cells: adhesion versus costimulation. *Immunity* **7,** 549–57 (1997).

237. Depil, S., Duchateau, P., Grupp, S. A., Mufti, G. & Poirot, L. 'Off-the-shelf' allogeneic CAR T cells: development and challenges. *Nature Reviews Drug Discovery* **19,** 185–199 (2020).

238. McGowan, E. *et al.* PD-1 disrupted CAR-T cells in the treatment of solid tumors: Promises and challenges. *Biomedicine & Pharmacotherapy* **121,** 109625 (2020).

239. Kabanova, A. *et al.* Human Cytotoxic T Lymphocytes Form Dysfunctional Immune Synapses with B Cells Characterized by Non-Polarized Lytic Granule Release. *Cell Reports* **15,** 9–18 (2016).

240. Valitutti, S., Müller, S., Dessing, M. & Lanzavecchia, A. Different responses are elicited in cytotoxic T lymphocytes by different levels of T cell receptor occupancy. *The Journal of experimental medicine* **183,** 1917–1921 (1996).

241. Hemmer, B., Stefanova, I., Vergelli, M., Germain, R. N. & Martin, R. Relationships Among TCR Ligand Potency, Thresholds for Effector Function Elicitation, and the Quality of Early Signaling Events in Human T Cells. *The Journal of Immunology* **160,** 5807 LP –5814 (1998).

242. Van den Berg, H. A. *et al.* Cellular-level versus receptor-level response threshold hierarchies in T-cell activation. *Frontiers in immunology* **4,** 250 (2013).

243. Huppa, J. B., Gleimer, M., Sumen, C. & Davis, M. M. Continuous T cell receptor signaling required for synapse maintenance and full effector potential. *Nature Immunology* **4,** 749–755 (2003).

244. Catalfamo, M. *et al.* Human CD8+ T Cells Store RANTES in a Unique Secretory Compartment and Release It Rapidly after TcR Stimulation. *Immunity* **20,** 219–230 (2004).

245. Gonsky, R., Deem, R. L., Young, H. A. & Targan, S. R. CD2 mediates activation of the IFN-gamma intronic STAT binding region in mucosal T cells. *European Journal of Immunology* **33,** 1152–1162 (2003).

246. Musgrave, B. L., Watson, C. L., Haeryfar, S. M. M., Barnes, C. A. & Hoskin, D. W. CD2-CD48 interactions promote interleukin-2 and interferon-gamma synthesis by stabilizing cytokine mRNA. *Cellular Immunology* **229,** 1–12 (2004).

247. Xu, Y. *et al.* A novel antibody-TCR (AbTCR) platform combines Fab-based antigen recognition with gamma/delta-TCR signaling to facilitate T-cell cytotoxicity with low cytokine release. *Cell Discovery* **4,** 62 (2018).

248. Johnson, L. A. *et al.* Gene therapy with human and mouse T-cell receptors mediates cancer regression and targets normal tissues expressing cognate antigen. *Blood* **114,** 535–546 (2009).

249. Borbulevych, O. Y., Santhanagopolan, S. M., Hossain, M. & Baker, B. M. TCRs used in cancer gene therapy cross-react with MART-1/Melan-A tumor antigens via distinct mechanisms. *The Journal of Immunology* **187,** 2453–2463 (2011).

250. Robbins, P. F. *et al.* A pilot trial using lymphocytes genetically engineered with an NY-ESO-1-reactive T-cell receptor: long-term follow-up and correlates with response. *Clinical Cancer Research* **21,** 1019–1027 (2015).

251. Morgan, R. A. *et al.* Cancer regression and neurological toxicity following anti-MAGE-A3 TCR gene therapy. *Journal of Immunotherapy* **36,** 133–151 (2013).

252. Zhang, J. & Wang, L. The Emerging World of TCR-T Cell Trials Against Cancer: A Systematic Review. *Technology in Cancer Research & Treatment* **18,** 1533033819831068–1533033819831068 (2019).

253. Stone, J. D., Chervin, A. S. & Kranz, D. M. T-cell receptor binding affinities and kinetics: impact on T-cell activity and specificity. *Immunology* **126,** 165–176 (2009).

254. Zhao, Y. *et al.* High-affinity TCRs generated by phage display provide CD4+ T cells with the ability to recognize and kill tumor cell lines. *The Journal of Immunology* **179,** 5845–5854 (2007).

255. Stone, J. D. & Kranz, D. M. Role of T cell receptor affinity in the efficacy and specificity of adoptive T cell therapies. *Frontiers in Immunology* **4,** 244 (2013).

256. Holler, P. D. *et al.* In vitro evolution of a T cell receptor with high affinity for peptide/MHC. *Proceedings of the National Academy of Sciences* **97,** 5387–5392 (2000).

257. Rudolph, M. G. & Wilson, I. A. The specificity of TCR/pMHC interaction. *Current opinion in immunology* **14,** 52–65 (2002).

258. Li, Y. *et al.* Directed evolution of human T-cell receptors with picomolar affinities by phage display. *Nature Biotechnology* **23,** 349–354 (2005).

259. Robbins, P. F. *et al.* Single and dual amino acid substitutions in TCR CDRs can enhance antigen-specific T cell functions. *The Journal of Immunology* **180,** 6116–6131 (2008).

260. Soto, C. M. *et al.* MHC-class I-restricted CD4 T cells: a nanomolar affinity TCR has improved anti-tumor efficacy in vivo compared to the micromolar wild-type TCR. *Cancer Immunology, Immunotherapy* **62,** 359–369 (2013).

261. Duong, M. N., Erdes, E., Hebeisen, M. & Rufer, N. Chronic TCR-MHC (self)-interactions limit the functional potential of TCR affinity-increased CD8 T lymphocytes. *Journal for ImmunoTherapy of Cancer* **7,** 284 (2019).

262. Thomas, S. *et al.* Human T cells expressing affinity-matured TCR display accelerated responses but fail to recognize low density of MHC-peptide antigen. *Blood* **118,** 319–329 (2011).

263. Ellwanger, K. *et al.* Highly Specific and Effective Targeting of EGFRvIII-Positive Tumors with TandAb Antibodies. *Frontiers in Oncology* **7,** 100 (2017).

264. Jungbluth, A. A. *et al.* A monoclonal antibody recognizing human cancers with amplification/overexpression of the human epidermal growth factor receptor. *Proceedings of the National Academy of Sciences* **100,** 639–644 (2003).

265. Dunn, S. M. *et al.* Directed evolution of human T cell receptor CDR2 residues by phage display dramatically enhances affinity for cognate peptide-MHC without increasing apparent cross-reactivity. *Protein Science* **15,** 710–721 (2006).

266. Holler, P. D. & Kranz, D. M. Quantitative Analysis of the Contribution of TCR/pepMHC Affinity and CD8 to T Cell Activation. *Immunity* **18,** 255–264 (2003).

267. Laugel, B. *et al.* Different T cell receptor affinity thresholds and CD8 coreceptor dependence govern cytotoxic T lymphocyte activation and tetramer binding properties. *The Journal of Biological Chemistry* **282,** 23799–23810 (2007).

268. Purbhoo, M. A. *et al.* The Human CD8 Coreceptor Effects Cytotoxic T Cell Activation and Antigen Sensitivity Primarily by Mediating Complete Phosphorylation of the T Cell Receptor ζ Chain*. *Journal of Biological Chemistry* **276,** 32786–32792 (2001).

269. Cole, D. K. *et al.* T-cell receptor (TCR)-peptide specificity overrides affinity-enhancing TCR-major histocompatibility complex interactions. *The Journal of Biological Chemistry* **289,** 628–638 (2014).

270. Stefanová, I., Dorfman, J. R. & Germain, R. N. Self-recognition promotes the foreign antigen sensitivity of naive T lymphocytes. *Nature* **420,** 429–434 (2002).

271. Aleksic, M. *et al.* Different affinity windows for virus and cancer-specific T-cell receptors: implications for therapeutic strategies. *European Journal of Immunology* **42,** 3174–3179 (2012).

272. Tan, M. P. *et al.* Human leucocyte antigen class I-redirected anti-tumour CD4(+) T cells require a higher T cell receptor binding affinity for optimal activity than CD8(+) T cells. *Clinical and Experimental Immunology* **187,** 124–137 (2017).

273. Hosken, N. A. & Bevan, M. J. Defective presentation of endogenous antigen by a cell line expressing class I molecules. *Science* **248,** 367 LP –370 (1990).

274. Wei, M. L. & Cresswell, P. HLA-A2 molecules in an antigen-processing mutant cell contain signal sequence-derived peptides. *Nature* **356,** 443–446 (1992).

275. Yip, A. & Webster, R. M. The market for chimeric antigen receptor T cell therapies. *Nature Reviews Drug Discovery* **17,** 161–162 (2018).

Appendices

A

Generation of the 1G4 CD2$^-$ NF-κB/eGFP Jurkat line

In several experiments of this work we make use of a 1G4 CD2$^-$ NF-κB/eGFP Jurkat population, which is a clone derived from the 1G4 NF-κB/eGFP parental line. A detailed description of the parental line can be found in Section 2.7.2. The 1G4 CD2$^-$ NF-κB/eGFP Jurkat line is a single clone homozygous for the *CD2* null mutation. Its generation was sub-contracted to GEO, a core facility at the SWDSP.

A.1 CRISPR/Cas9 *CD2* targeting strategy

Genomic Engineering Oxford carried out a double-targeted approach, which disrupted simultaneously the TSS and exon 2 of *CD2* (Figure A.1). The guides chosen by GEO were:

- 5'−GGCACGTGGTTAAGCTCTCGGGG−3', targeting the TSS
- 5'−CTTGTAGATATCCTGATCATCGG−3', targeting exon 2

Following FACS enrichment and limiting dilution, a number of single clones were obtained. As shown in the next section, one single clone —originally termed

1C4— exhibited successful disruption of the *CD2* gene, and it is referred to as the 1G4 CD2⁻ NF-κB/eGFP Jurkat line throughout this work.

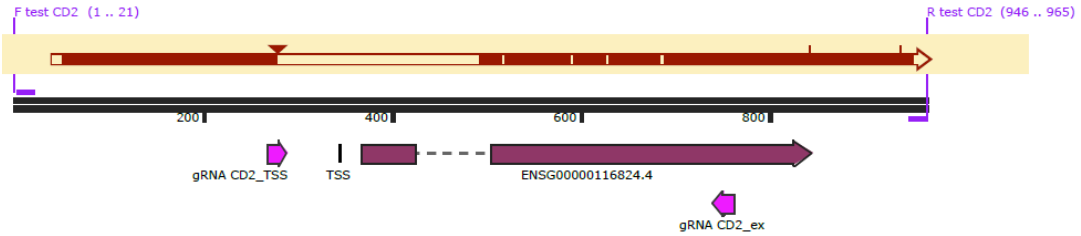


Figure A.1: Strategy for *CD2* gene knockout in the Jurkat cell line. Using the CRISPR/Cas9 gene-editing technique, GEO conducted a double-targeted approach to simultaneously disrupt the TSS and exon 2 of human *CD2* in the 1G4 NF-κB/eGFP Jurkat cell line. Flanking primers were designed to determine, by Sanger sequencing, successful *CD2* disruption.

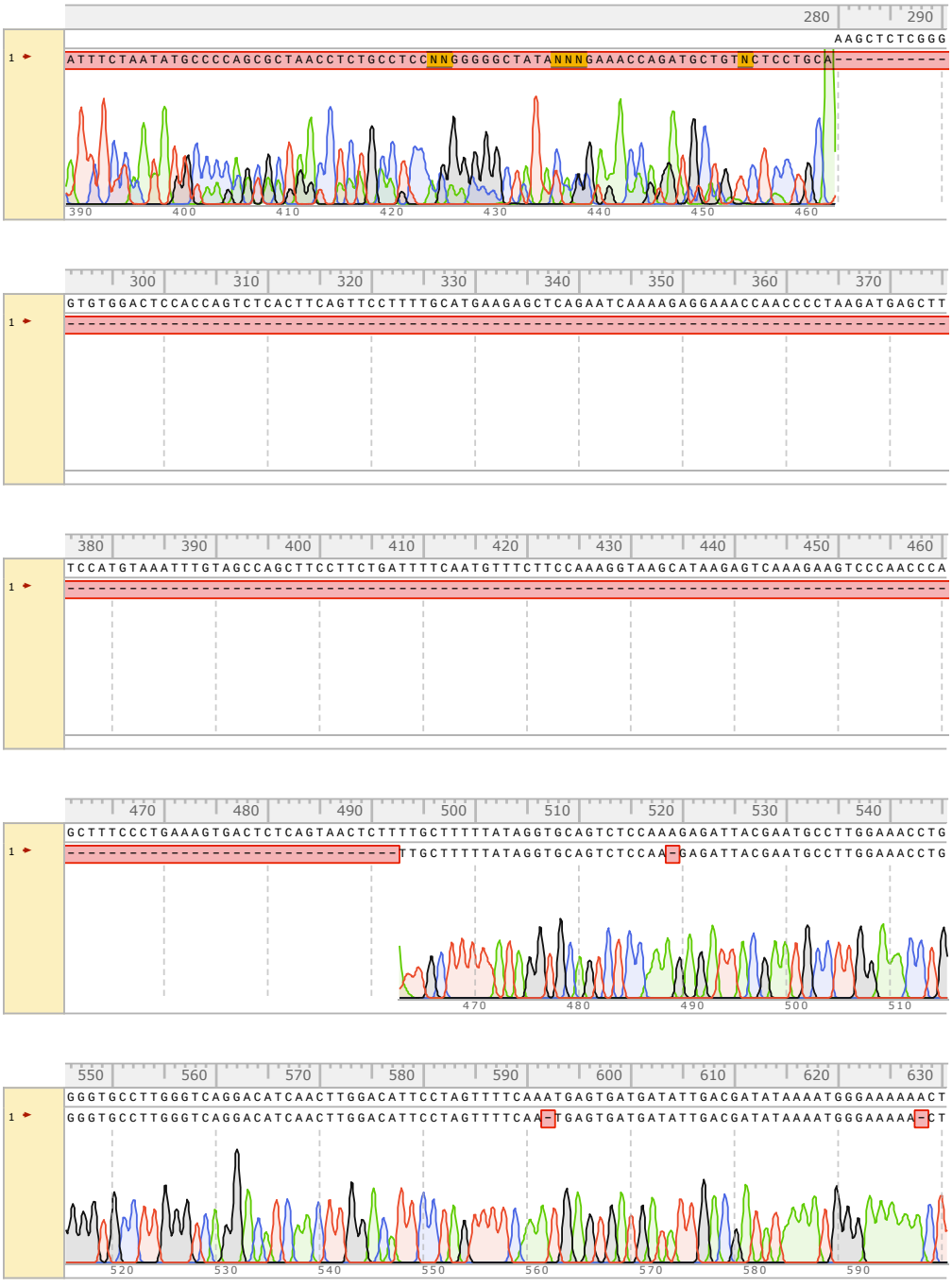
A.2 Sanger sequencing confirms successful disruption of the *CD2* gene

What follows are the results of the Sanger sequencing flanking the areas of *CD2* shown in Figure A.1. This was the confirmation presented by GEO to us when handing over the 1G4 CD2⁻ NF-κB/eGFP Jurkat line.

PCR WT CD2 Hsa.dna (Linear / 965 bp)



PCR WT CD2 Hsa.dna (Linear / 965 bp)



PCR WT CD2 Hsa.dna (Linear / 965 bp)



Original Sequence:
1 .. 965

452116901_1C4_CD2_F_G06
943 bases / Jul 3, 2019
16 .. 921 (7 gaps)

A.3 Validation of TCR levels in the CD2 knock-out line

Once we received the 1G4 CD2⁻ NF-κB/eGFP Jurkat sub-line from GEO, we conducted a staining of the 1G4 TCR with fluorescent PE 9V pMHC tetramers to ensure that CD2 loss had not substantially affected TCR levels. We used the 1G4 NF-κB/eGFP Jurkat line as a reference, finding similar TCR levels between these two populations (Figure A.2).

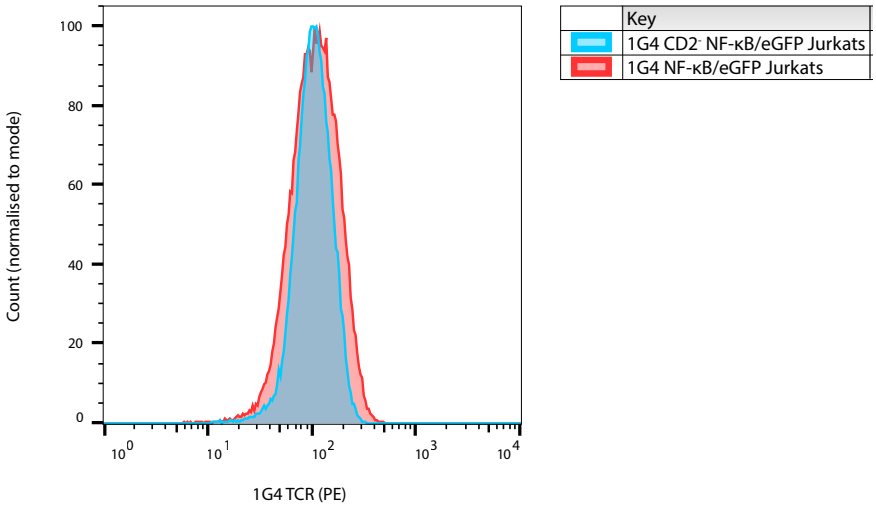


Figure A.2: Comparison between the 1G4 TCR levels of the parental and the CD2 knockout 1G4 Jurkat line. Fluorescent PE 9V pMHC tetramers were used to stain the 1G4 NF-κB/eGFP and the 1G4 CD2⁻ NF-κB/eGF cell lines for expression of the 1G4 TCR.

B

Characterisation of the 1G4 NF-κB/eGFP Jurkats expressing elongated CD2 chimeras

Contents

A.1 CRISPR/Cas9 *CD2* targeting strategy 152
A.2 Sanger sequencing confirms successful disruption of the *CD2* gene 153
A.3 Validation of TCR levels in the CD2 knockout line . 157

In Section 4.2, we introduced several sub-lines of the 1G4 NF-κB/eGFP parental Jurkat reporter line. They were characterised by expressing a series of CD2 chimeras with elongated ectodomains (see Figure 4.2), which we reasoned would outcompete endogenous CD2 and, by interfering with the KS equilibrium[189], reduce antigen sensitivity in a manner that would mitigate the risk of on-target/off-tumour toxicity. This appendix presents some quality control checks covering expression and binding of these chimeras. The reader can find information about the lentiviral transfer vectors in Section 2.3.2.

B.1 Expression of the CD2^{HA} chimeras

The parental 1G4 NF-κB/eGFP Jurkat line was lentivirally transduced with particles coding for the CD2^{HA}, CD2^{HA}−2Ig, CD2^{HA}−4Ig, CD2^{HA}−7Ig, and CD2^{HA}−CD43^{Ecto} chimeras. After 24 h, cells were subjected to puromycin selection (500 ng/mL for 72 h followed by 1000 ng/mL for another 72 h). Transduction efficiency is shown in Figure B.1; data was collected by staining for the HA tag and performing flow cytometry.

B.2 The CD2^{HA} chimeras are functional and bind CD58

In order to verify that the elongated CD2^{HA} chimeras were functional, we performed a series of conjugation assays between the different 1G4 NF-κB/eGFP Jurkat variants and CHO-A*02 APCs (with and without CD58 expression). Chiefly, we stained the Jurkat cells with 5 μM CFSE (Biolegend) and the CHOs with 5 μM Tag-it Violet (Biolegend) according to the manufacturer's protocol. Afterwards, 1 h co-cultures using a 2:1 E:T ratio were conducted in a final volume of 300 μL and with a grand total of 6×10^4 cells. Co-cultures were conducted in cold DPBS and maintained at 4 °C to minimise signalling-mediated adhesion. Conjugation between Jurkats and CHOs was calculated as described in Section 2.8.3. We present the results in Figure B.2, which indicate all the Jurkat sub-lines displayed enhanced levels of cellular adhesion when co-cultured with the CHO-A*02-CD58^{FLAG} population.

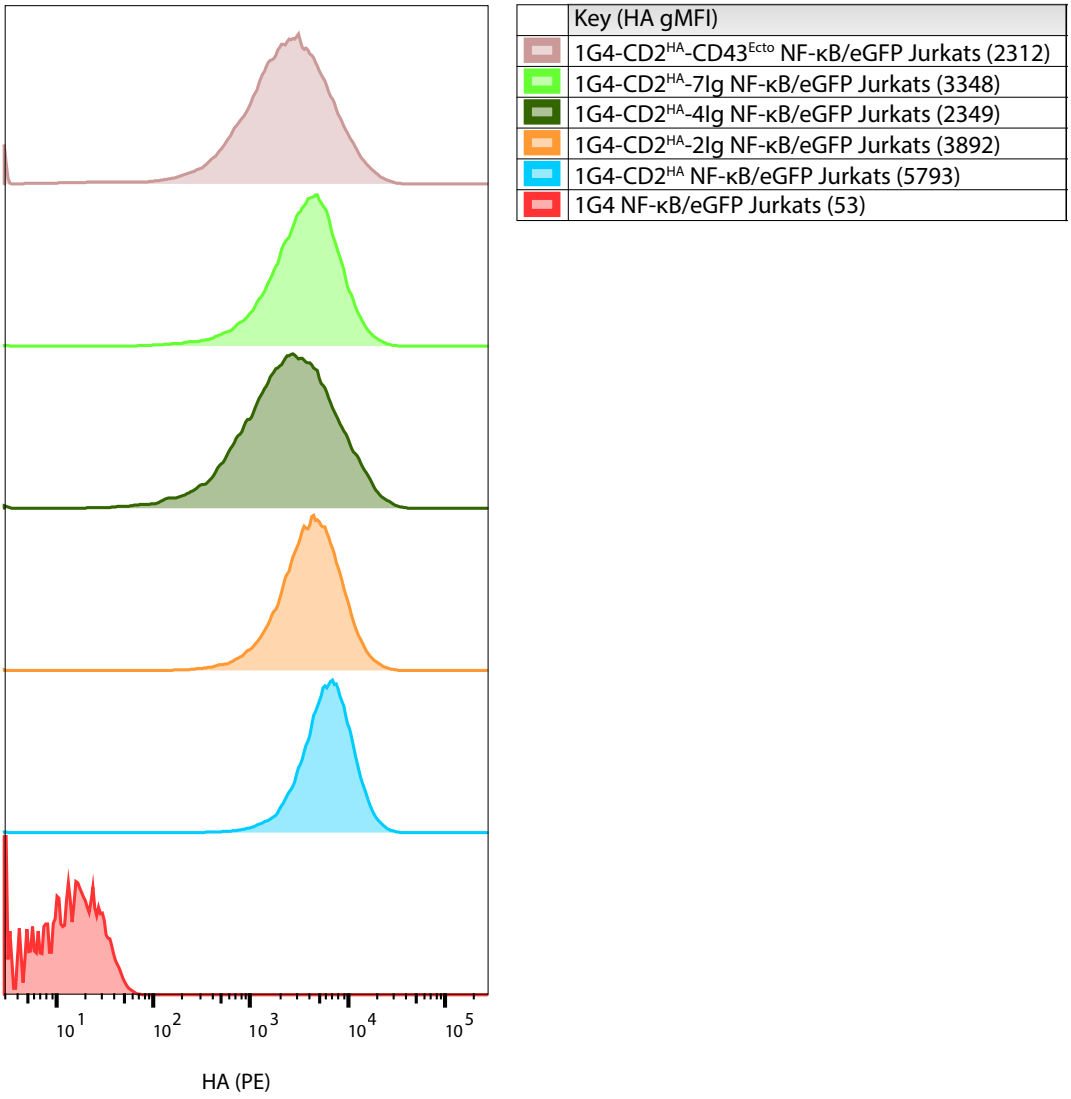


Figure B.1: Expression of the CD2^{HA} chimeras in the sub-lines of the 1G4 NF-κB/eGFP Jurkat line. Derivative sub-lines of the 1G4 NF-κB/eGFP reporter Jurkat population were generated by lentiviral transduction with a series of CD2 chimeras (CD2^{HA}, CD2^{HA}−2Ig, CD2^{HA}−4Ig, CD2^{HA}−7Ig, and CD2^{HA}−CD43^{Ecto}) followed by puromycin selection. Detection of the HA tag via flow cytometry reveals a high proportion of transduced cells (>95%). The gMFI of the HA tag is indicated for each sample, suggesting that all derivative lines do not vary in expression of these constructs by more than 2–3 fold.

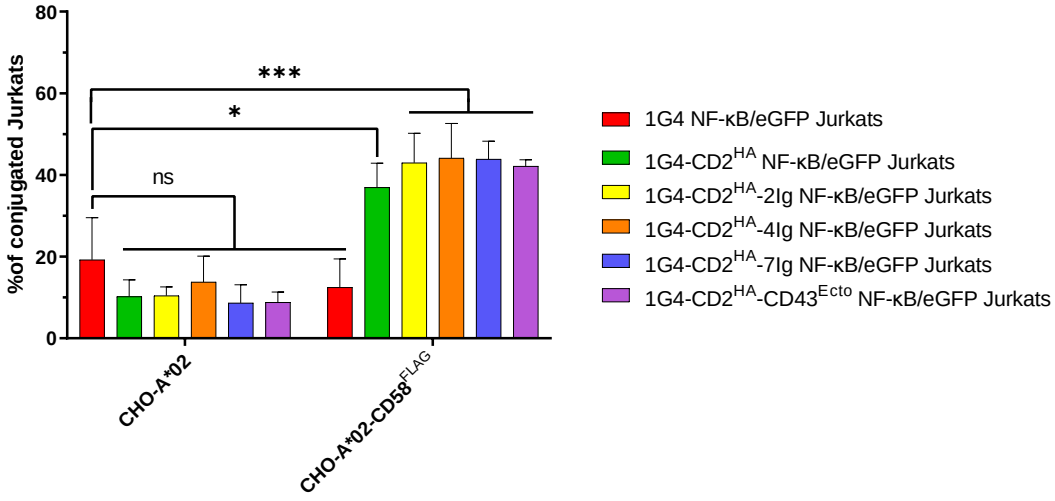


Figure B.2: $CD2^{HA}$ chimeras display binding to CD58. Derivative sub-lines of the 1G4 NF-κB/eGFP reporter Jurkat population were generated by lentiviral transduction with a series of CD2 chimeras ($CD2^{HA}$, $CD2^{HA}-2Ig$, $CD2^{HA}-4Ig$, $CD2^{HA}-7Ig$, and $CD2^{HA}-CD43^{Ecto}$) followed by puromycin selection. These lines were used in conjugation assays (1 h at 4 °C) to determine binding to the CHO-A*02 and CHO-A*02-$CD58^{FLAG}$ cell lines. The conjugations were conducted in a final volume of 300 μL of DPBS with a grand total of 6×10^4 cells at an E:T ratio of 2:1. To determine the percentage of conjugated Jurkats, a differential intracellular staining of effector (CFSE) and target (Tag-it Violet) cells was conducted prior to the co-culture (see Section 2.8.3 for details). Results indicate that all these chimeras are functional and mediate cellular adhesion via CD58. The data corresponds to the results of three independent experiments, with statistical significance determined with a *post hoc* Dunnett test using the 1G4 NF-κB/eGFP - CHO-A*02 conjugation pair as a control. ns = not significant, * = $p \leq 0.05$, *** = $p \leq 0.001$.

C

Molecular mechanisms of T cell sensitivity to antigen

During my doctoral studies, Prof. Omer Dushek and I wrote a review focused on the molecular mechanisms that enable the extraordinary sensitivity of T cells. This review was published in *Immunological Reviews*. A full copy, downloaded from Europe PubMed Central (https://europepmc.org/article/med/30129204), is attached to this thesis.

Molecular mechanisms of T cell sensitivity to antigen

Jesús A. Siller-Farfán[†], Omer Dushek[†¶]

[†]Sir William Dunn School of Pathology, University of Oxford, Oxford, UK
[¶]Corresponding author

June 27, 2018

Correspondence to:

Omer Dushek

Sir William Dunn School of Pathology

South Parks Road

University of Oxford

Oxford OX1 3RE

United Kingdom

Telephone: +44 (0) 1865 275576

e-mail: omer.dushek@path.ox.ac.uk

Abstract

T cells initiate and regulate adaptive immune responses that can clear infections. To do this, they use their T cell receptors (TCRs) to continually scan the surfaces of other cells for cognate peptide antigens presented on major histocompatibility complexes (pMHCs). Experimental work has established that as few as $\sim$1-10 pMHCs are sufficient to activate T cells. This sensitivity is remarkable in light of a number of factors, including the observation that the TCR and pMHC are short molecules relative to highly abundant long surface molecules, such as CD45, that can hinder initial binding and moreover, the TCR/pMHC interaction is of weak affinity with solution lifetimes of $\sim$1 seconds. Here, we review experimental and mathematical work that has contributed to uncovering molecular mechanisms of T cell sensitivity. We organise the mechanisms by where they act in the pathway to activate T cells, namely mechanisms that 1) promote TCR/pMHC binding, 2) induce rapid TCR signalling, and 3) amplify TCR signalling. We discuss work showing that high sensitivity reduces antigen specificity unless molecular feedbacks are invoked. We conclude by summarising a number of open questions.

Keywords: T cells, T cell receptor, antigen, MHC, sensitivity, lymphocyte signalling, mathematical modelling

1 The Challenge

T cells are important players in adaptive immunity. They are activated to respond when their T cell receptors (TCRs) recognise antigens in the form of short peptides bound to major histocompatibility complexes (pMHCs) on the surfaces of other cells, which are collectively known as antigen presenting cells (APCs). Upon activation, T cells are able to clear infections through multiple mechanisms. For example, $CD8^+$ T cells can directly kill virally infected cells and $CD4^+$ T cells provide help to B cells to produce viral-specific antibodies. Through these and other mechanisms, T cells are able to initiate and regulate immune responses that can clear infections.

Experimental work over the past two decades has clearly shown that T cells can become activated when recognising even a single pMHC ligand on the APC surface. This level of sensitivity was indirectly inferred in early studies (1); subsequent microscopy based studies have been able to directly observe this sensitivity at the single cell level. In the case of $CD4^+$ T cells, it has been observed that a single pMHC can not only produce an early calcium response (2) but can also lead to cytokine secretion after several hours (3). As for $CD8^+$ T cells, it has been observed that 3 pMHC ligands can induce target cell killing (4). The precise number of pMHC antigens required for T cell activation will likely depend on the affinity of the interaction and other variables such as the life history of the T cell, but it is clear that T cells can be activated in response to $\sim$1-10 pMHC antigens.

The sensitivity displayed by T cells is remarkable in light of a number of observations (*Fig. 1*). First, initial TCR/pMHC binding is unfavourable because the TCR and pMHC are short molecules spanning $\sim$ 7 nm (5). They reside within highly abundant large surface glycoproteins such as the phosphatase CD45, whose extracellular domain extends $\sim$ 22 nm (6). Second, once binding takes place, individual TCR/pMHC interactions are short lived (lifetimes as short as $\sim$0.1-10 s), yet continued TCR/pMHC interactions for minutes to hours can be required for full T cell activation (7, 8). This is made even more remarkable by noting that the TCR/pMHC interaction is subjected to tensile forces at the contact interface (9), which may further reduce the lifetime at interfaces (10, 11). Finally, T cells are able to ignore APCs that express a high abundance of self pMHCs while retaining sensitivity against a few foreign pMHC that may be chemically similar. This ability is known as antigen discrimination and, as we discuss below, it can place constraints on sensitivity (12, 13). Collectively, these observations suggest that mechanisms must be in place to convert a low number of highly improbable and transient pMHC interactions into a signal that can lead to the activation of T cells.

Why are T cells highly sensitive? The most likely explanation is that they have evolved high sensitivity because only a small number of pMHC ligands are presented to them during infections. During a viral infection, a fraction of viral proteins will be degraded into peptides, which will then be presented on the cell surface as a heterogeneous mixture of foreign pMHC ligands. The copy number of any single pMHC is unlikely to be large. This is consistent with a study that found that a recombinant TCR was only able to recognise 8-46 pMHCs after *in vitro* infection with HIV (14). In addition, viruses, such as HIV (15) and CMV (16), are known to downregulate pMHC as an escape mechanism (e.g. CMV can downregulate expression from 10,000 to less than 100 copies per cell (16)). It follows that for efficient detection of infection, T cells must exhibit high

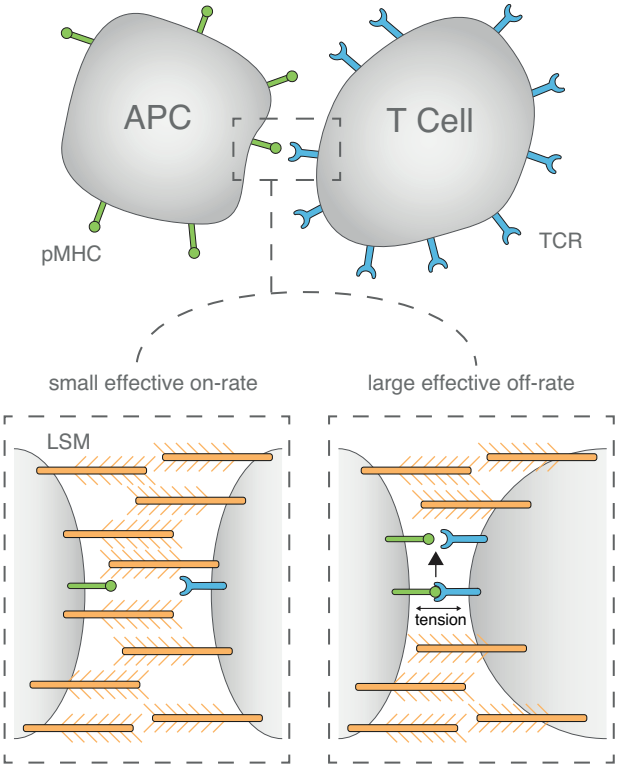


Figure 1: T cells are activated by sustained interactions with as few as ∼1-10 pMHC ligands on the surfaces of APCs. This sensitivity is difficult to understand because a number of factors seemingly reduce TCR/pMHC interactions. First, the TCR and pMHC are short molecules residing within highly abundant long surface molecules (LSMs). This reduces the probability that the membranes will come into proximity to allow for TCR/pMHC binding (bottom left). Second, the TCR/pMHC interaction off-rate is large, with lifetimes of ∼1 s when measured in solution using surface plasmon resonance (SPR). Moreover, it can be subjected to tensile forces at the cellular interface that further increase the effective off-rate. Therefore, T cells employ a number of mechanisms to ensure that TCR/pMHC interactions can be sustained and detected.

sensitivity to pMHC antigens.

In this review, we focus on molecular mechanisms that have contributed to our understanding of how T cells are able to recognise a small number of weakly binding pMHC ligands. We then highlight that the requirement of T cells to discriminate between foreign and self pMHC antigens places constraints on sensitivity that can be overcome with feedbacks. We conclude with a number of open questions that would benefit from experiments and mathematical modelling.

2 Mechanisms of T cell sensitivity to antigen

There are a large number of diverse mechanisms that contribute to T cell antigen sensitivity. Using a coarse-grained view of signal transduction, we classify them into three categories (*Fig. 2*). We first discuss mechanisms that promote TCR/pMHC binding, which includes molecular processes that effectively increase the on-rate (k_{on}) and/or decrease the off-rate (k_{off}). Second, we discuss mechanisms that are able to quickly induce TCR signalling within the short timescale of a TCR/pMHC interaction (increasing k_{p}). Third, we discuss processes that amplify signalling from a small number of TCRs to allow for T cell activation (increasing k_{amp}).

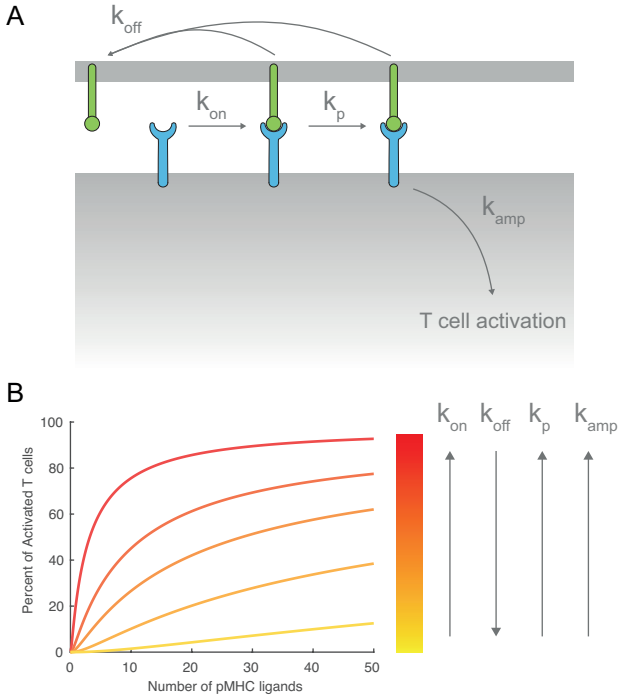


Figure 2: Mechanisms of T cell sensitivity to antigen can be broadly classified into three major categories. A) A simplified signalling schematic that classifies mechanisms of sensitivity into those that 1) promote TCR/pMHC binding by increasing the on-rate (k_{on}) and/or decreasing the off-rate (k_{off}), 2) induce rapid TCR signalling before pMHC unbinds (k_{p}), and 3) amplify TCR signalling allowing for T cell activation by a small number of bound TCRs (k_{amp}). This simplified panel omits feedbacks for clarity. B) A schematic dose-response curve showing that as k_{on}, k_{p}, and k_{amp} increase or as k_{off} decreases, the sensitivity of T cells to pMHC antigens is expected to increase. Arrow indicates direction of increasing kinetic rate.

2.1 Mechanisms that promote TCR/pMHC binding

2.1.1 Role of close-contacts in promoting TCR/pMHC binding

The TCR and pMHC are small molecules whose ectodomains measure ∼7 nm. Hence, a close contact between the T cell and APC membranes (spanning ∼14 nm) must be formed for TCR/pMHC interactions (17). However, the surface of both cells contain abundant, negatively charged glycoproteins, such as CD43 and CD45. These large glycoproteins are collectively referred to as long surface molecules (LSMs), and they normally prevent close membrane apposition (*Fig. 3A*). Based on its crystal structure, CD45, one of the most abundant cell surface proteins on T cells (18, 19), has recently been reported to extend ∼22 nm (6). Therefore, these LSMs reduce the effective on-rate for TCR/pMHC binding and must be segregated and/or compressed for TCR/pMHC binding.

How long would it take for CD45 to be passively (i.e. spontaneously) segregated from a small 100 nm membrane patch? This calculation was recently performed showing that at physiological densities of CD45, it would take an astronomical period of time (10^9 s) (20). A recent *in vitro* reconstitution of passive CD45 segregation showed that it would require ∼15 min to first observe short receptor/ligand interactions (21). The discrepancy between this experiment and the mathematical model may simply be down to the concentration of CD45, which the model predicts to have a highly nonlinear relationship to the segregation timescale (the model predicts segregation within 5 s with a 4-fold dilution of CD45). Nonetheless, these studies highlight that initial TCR/pMHC binding is unlikely to be driven by passive processes given that TCR signalling is observed within seconds (22).

Instead of waiting for passive close contact formation and hence TCR/pMHC binding, T cells actively produce close contacts. They use structures known as microvilli (23–25) or invadosome-like protrusions (ILPs) (26). These actin-rich 100-200 nm diameter protrusions enable T cells to push on nearby cells in order to achieve close membrane apposition compatible with TCR/pMHC interactions (24), which leads to CD45 segregation (25, 26) (*Fig. 3B*). It is noteworthy that these structures have short (∼5-50 s) lifetimes without antigen (24, 26) but upon antigen recognition they can be stabilied for long (∼10 min) timescales (26). This stabilisation may involve TCR signalling leading to sustained actin polymerisation, a phenomenon observed in these protrusions (24, 26).

2.1.2 Role of additional receptors in promoting TCR/pMHC binding

A number of additional receptors can modulate TCR/pMHC interactions. The adhesion receptors CD2 and LFA-1 have been shown to increase the sensitivity of T cells to antigens in functional studies (27, 28). Although detailed studies of LFA-1 and CD2 in the context of microvilli protrusions have yet to be reported, it is conceivable that the relatively large LFA-1/ICAM-1 interaction (∼40 nm length) (29) paves the way for the smaller CD2/CD58 association. CD2/CD58 are then capable of stabilising a close contact at an intermembrane distance compatible with TCR/pMHC interactions (30, 31) (*Fig. 3B*). Indeed, the CD2/CD58 pair spatially segregates from LFA-1/ICAM-1 complexes (32), which are found surrounding areas of TCR/pMHC interactions (33). Consistent with the role of CD2 in promoting close contact formation and hence TCR/pMHC interactions, it

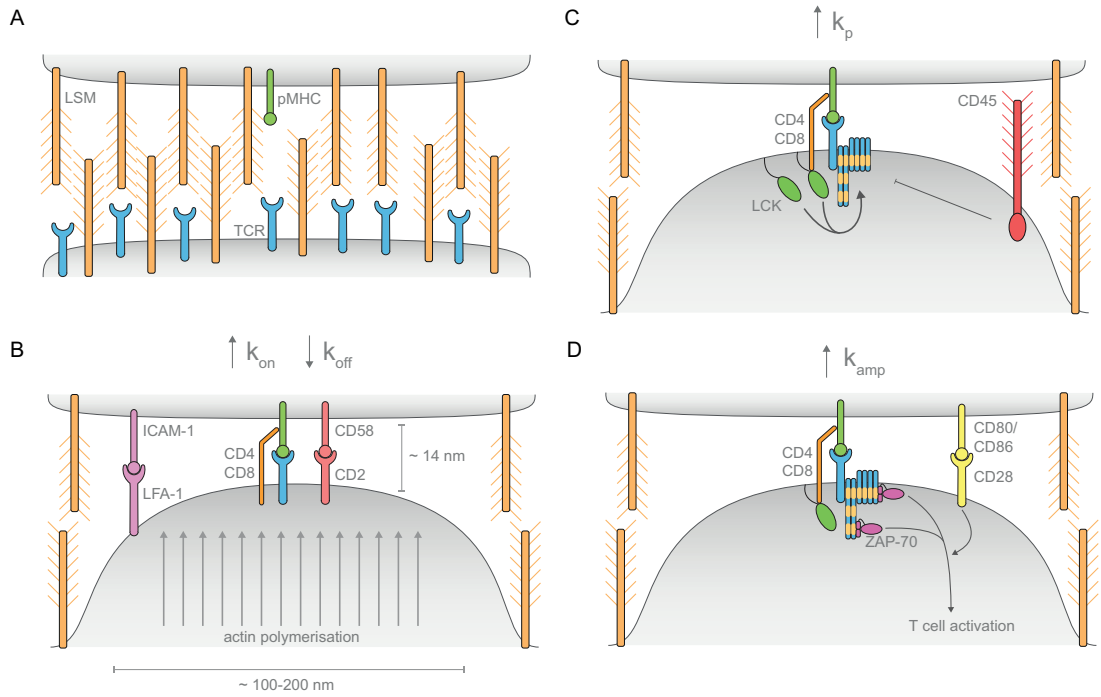


Figure 3: Molecular mechanisms of T cell sensitivity to antigen. A) The small size of TCR and pMHC molecules relative to LSMs means that their basal, effective on-rate is likely to be small. B) A close contact is actively produced by an actin-rich microvilli protrusion that results in the segregation of LSMs. The close contact may be stabilised peripherally by adhesion receptors such as LFA-1, and centrally by CD2. The stabilisation of the close contact allows repeated TCR/pMHC interactions and, potentially, reduced forces on the TCR/pMHC interaction. The CD4/CD8 coreceptors are able to interact with both pMHC and the TCR complex, further promoting TCR/pMHC association. C) The rate at which the TCR is converted into a state where it can signal downstream must be faster or on the same timescale as the TCR/pMHC lifetime for efficient signalling. The net rate of TCR phosphorylation is made large by the fact that the phosphatase that dephosphorylates the TCR (CD45) is an LSM that is segregated from the close contact. However, the kinase Lck is not segregated so the net phosphorylation of the TCR in a close contact is expected to be large. The net phosphorylation may be increased further because coreceptors are associated with Lck. D) Mechanisms that amplify the weak TCR signal include the fact that the TCR is able to potentially recruit multiple cytoplasmic ZAP-70 molecules in order to convert a single pMHC binding event into the activation of multiple enzymes. Costimulation by, for example, CD28 is able to amplify TCR signalling but does not modulate TCR/pMHC binding.

has been shown that human cytomegalovirus can specifically reduce CD58 expression leading to reduced recognition of infected cells by $CD8^+$ T cells (34). Additionally, knockout of CD58 in cancer cell lines can impair recognition and cytolysis by $CD8^+$ T cells (35).

The coreceptors CD4 and CD8 are well known to improve the sensitivity of T cells to pMHC, particularly when the pMHC has a weak affinity and is presented at low numbers (36–40) (*Fig.*

3B). These transmembrane receptors are able to bind to pMHC at a site that is independent of TCR binding (41, 42) and in addition, their cytoplasmic tails associate with the kinase Lck. In turn, Lck can interact with and phosphorylate the cytoplasmic tails of the TCR complex. It is thought that both the extracellular and intracellular interactions contribute to the ability of CD4/CD8 to improve sensitivity. A striking example of how CD8 can modulate TCR/pMHC association was observed by Zhu and colleagues using a micropipette adhesion assay (43). In that study, a steep increase in the probability of binding was observed, which critically relied on both CD8 binding to pMHC and the catalytic activity of Lck. Therefore, CD8 can be effectively thought of as a bivalent molecule able to bind both pMHC and TCR to increase their association rate. It should be noted that the CD4/MHC-II affinity is substantially lower than the CD8/MHC-I affinity (44) and therefore, modulation of TCR/pMHC binding may be less important for CD4 (45) (see below).

2.1.3 Role of serial binding and rebinding in promoting TCR/pMHC binding

Although the TCR/pMHC interaction is short lived, a stable close contact allows for various forms of repeated binding. First, pMHC can serially bind multiple localised TCRs. Mathematical analysis (*Box 1*) of a single pMHC interacting with localised (clustered) TCRs has shown that it can serially bind multiple TCRs before diffusing away (46). While it is well known that serial binding occurs, it is still unclear whether it is required for T cell activation (*Box 2*). Second, mathematical models explicitly accounting for slow membrane diffusion have predicted that upon unbinding, the pMHC is likely to rebind the same TCR multiple times before diffusing away (47). This rebinding hypothesis has been supported by a number of experiments (48–50). Third, the oligomerisation of the TCR has been observed biochemically and suggested to improve sensitivity (51–53). However, microscopy based techniques have failed to observed TCR oligomers instead suggesting that the TCR remains monomeric (54–56). Finally, nanometer-scale clustering of the TCR (57), as distinct from a physically associated oligomeric state, may effectively increase the on-rate for binding by increasing the local concentration of TCR (46, 47).

In summary, the formation and stabilisation of a close contact driven by an active microvilli protrusion combined with adhesion receptors and coreceptors generates an environment that effectively increases the on-rate between TCRs and pMHC. Stabilisation of close contacts is pMHC-dependent (24, 26) and likely involves TCR signalling, implying that feedback is operating to increase the effective TCR/pMHC on-rate. Consistent with such feedback, it has been observed that TCR binding becomes greater over time (58) and that increasing the number of pMHC molecules, and hence TCR signalling, can also increase the effective TCR/pMHC on-rate (59).

2.1.4 Role of molecular forces in modulating TCR/pMHC binding

There is now emerging data suggesting that the TCR/pMHC interaction is subjected to $\sim$10-20 pN tensile forces at the contact interface (9). An applied force is generally expected to reduce the interaction lifetime (increase the off-rate) (60), reducing the sensitivity of T cells to antigen (*Fig. 2B*). The source of these forces may include those actively generated by actin polymerisation and/or those passively generated by LSMs pushing on the membrane near TCR/pMHC interactions. A

mathematical model that coupled membrane mechanics to the compressional stiffness of LSMs highlights that, by pushing the membranes away, LSMs effectively generate a time-dependent tension on the TCR/pMHC complex that is predicted to dramatically increase the off-rate in some parameter regimes (61) (*Box 1*).

In order to increase antigen sensitivity, it would seem that T cells need to have mechanisms in place to reduce the force on the TCR/pMHC complex or limit the effect of force on the off-rate. A proposed mechanism is the suggestion that TCR/pMHC interactions do not form a slip bonds but rather catch bonds, whereby an applied force actually increases the lifetime (60). Catch bonds have been observed for the OT-1 TCR interacting with its agonist OVA pMHC (50). However, this phenomenon may not be universal because many activating pMHC variants for the 1G4 TCR displayed slip bond behaviours (62). An additional mechanism is that the applied force is simply shared by multiple receptor/ligand complexes. A mathematical modelling study predicts that forces can be shared provided complexes are within $\sim$80 nm (63), which is consistent with the spatial scale of a microvilli protrusion.

In summary, although forces are likely to be generated at the contact interface, mechanisms may be operating to reduce the tension on the TCR/pMHC interaction. Although beyond the scope of this review, it has been suggested that applied forces on the TCR may be required to induce TCR signalling (64), but there is also evidence that TCR signalling can take place without pMHC ligands and hence an applied force (6). The role of force in mechanically transducing signals is beyond the scope of this work and we refer the reader elsewhere (65).

2.2 Mechanisms that rapidly induce TCR signalling

The TCR/pMHC interaction is transient, with direct measurements reporting lifetimes of $\sim$0.1 s ($k_{\text{off}} \sim 10\ \text{s}^{-1}$) for pMHCs that can activate T cells (10, 11). This measurement implies that TCRs must be converted from their non-signalling state into their activated signalling-state on the order of this timescale. In the context of the simplified schematic (*Fig. 2*) this conversion rate is represented by k_{p}, which must be similar to k_{off} in order for the TCR to communicate the binding event to the cell.

A large value of k_{p} can be obtained if the net phosphorylation rate of the TCR is large upon pMHC binding. This is likely achieved because CD45, which is the primary phosphatase responsible for dephosphorylating the TCR, is a segregated LSM. In contrast, Lck, which is the primary kinase responsible for phosphorylating the TCR, is anchored to the inner leaflet of the plasma membrane and as a result it remains within close contacts (6). Moreover, Lck is constitutively active in T cells (66) and it has been shown to efficiently phosphorylate the TCR signalling chains with a rate of k_{cat} =6.2 s^{-1} (or average time of 0.16 s) (67), which is consistent with the short TCR/pMHC lifetime of 0.1 s.

To achieve this high catalytic rate, the TCR would need to experience a concentration of Lck that is larger than the K_{M} of 230 μm^{-2} reported for this reaction (67). The estimated concentration of Lck in T cells is $\sim$630 μm^{-2} (assuming 2x10^4 Lck molecules per T cell (68) with a radius of 5 μm), which is indeed larger than K_{M}. In addition, the association of Lck with coreceptors may

further increase its concentration at TCR/pMHC complexes. Recently, it has been shown that this association directly increases the intrinsic activity of Lck (69). In fact, mathematical modelling has suggested that the primary mechanism by which CD4 increases T cell sensitivity to antigen is to localise Lck at the TCR/pMHC complex (70).

We note that CD45 can directly dephosphorylate tyrosines on Lck that are inhibiting and activating (71, 72). In this way, segregation of CD45 from close contacts may reduce the activity of Lck. It has been observed that CD45 remains near close contacts (25) and this may facilitate the continued generation of active Lck required for TCR signalling. The complex biochemical regulation of Lck by CD45, combined with their dynamic spatial distributions means that mathematical modelling may be particularly useful in understanding how the net rate of TCR phosphorylation is affected by the formation of a close contact.

We note that the segregation of CD45 from TCR/pMHC interactions at close contacts has been proposed to be the mechanism by which TCR signalling is initiated upon pMHC binding, a process termed receptor triggering. This model of triggering is known as kinetic-segregation and it has been reviewed elsewhere, along with other proposed triggering models (65).

2.3 Mechanisms that amplify TCR signalling

In addition to promoting TCR/pMHC binding and to quickly inducing TCR signalling upon binding, antigen sensitivity requires the T cell signalling machinery to efficiently convert a small number of transiently signalling TCRs into a fully activated T cell. This amplification step is denoted by k_{amp} in our minimalistic model (*Fig. 2*).

The TCR complex uniquely contains 10 immunoreceptor tyrosine-based activation motif (ITAMs) distributed on 6 chains (73), which is the largest number of ITAMs found on any receptor (5). It is widely appreciated that multiple ITAMs contribute to signal amplification (73) with some evidence that they preferentially contribute to amplification at low antigen doses (74, 75). Mathematical models have previously suggested that multiple ITAMs may be important for generating switch-like responses by various mechanisms (76, 77) but experimental work has failed to observe this (67, 78).

A large number of ITAMs can amplify TCR signalling because each phosphorylated ITAM generates a docking site for the tyrosine kinase ZAP-70. When bound to the TCR, ZAP-70 can be activated to phosphorylate downstream targets that ultimately lead to T cell activation. Therefore, a single TCR/pMHC binding event can potentially be translated into the activation of multiple ZAP-70 molecules (79, 80). This signalling may also be sustained beyond pMHC binding because it has been suggested that, upon internalisation, TCRs may continue to signal within the T cell (81). As in other signal transduction cascades, phosphorylation by ZAP-70 of downsteam targets initiates signalling that involves cascades and feedbacks that can amplify a small number of activated molecules at the TCR into a large number that can lead to T cell activation (82, 83).

In addition to the adhesion receptors discussed above, there are costimulatory receptors that can amplify TCR signalling without directly promoting TCR/pMHC binding. The most heavily

studied costimulatory receptor is CD28 (84), which when ligated by its ligands CD80 or CD86 reduces the number of pMHC ligands required for T cell activation (85). The mechanism of this amplification involves the recruitment of multiple effectors, including Lck (86) and PI3K (87), to the cytoplasmic tail of CD28 that may contribute to amplifying feedbacks with TCR signalling (88). Importantly, unlike CD2 and LFA-1, CD28 amplifies TCR signalling without altering TCR/pMHC binding (27).

3 Relationship between antigen sensitivity and specificity

The primary task of T cells is to recognise APCs that express foreign pMHC ligands. Implicit in this task is to ignore APCs that do not express foreign pMHC even though they express large numbers of pMHCs derived from self proteins. This task is known as antigen discrimination (12, 13) and it is difficult to understand because, as a result of thymic positive selection, self pMHC ligands are also able to bind the TCR and generate signals required for T cell survival (89). Consistent with this discrimination, *in vitro* experiments have shown that a small $\sim$5-fold increase in the TCR/pMHC off-rate (e.g. by presenting T cells with altered pMHC ligands) can completely abolish the T cell response even if the altered pMHC is presented at large numbers (90–92). Collectively, these observations imply that T cells are not only highly sensitive to a pMHC ligand, but that they are also highly specific because altered pMHCs (e.g. self pMHC) with a marginally weaker affinity are unable to activate them.

Mathematical models have been instrumental to our understanding of antigen discrimination by T cells. The key mechanism underlying all models is kinetic proofreading, which relies on a delay between initial TCR binding and signalling (93). This delay is a result of a number of biochemical steps that must take place before the TCR is able to signal (e.g. phosphorylation of the TCR by Lck, binding and phosphoryaltion of ZAP-70 at the TCR, etc). This delay is effectively controlled by the rate of TCR conversion into an active signalling state (denoted by k_{p} in Fig. 2). The model shows that with a suitably long delay, there is a nonlinear relationship between the TCR/pMHC off-rate and the probability of TCR signalling. This means that a small increase in the off-rate can abolish the T cell response for a large variation in the pMHC dose. The models also show that, although this long delay preferentially reduces TCR signalling for larger off-rates, it reduces TCR signalling at all off-rates. This means that improving specificity comes at a cost to sensitivity (93, 94). A quantitative analysis suggested that there is no parameter regime where the standard kinetic proofreading model can explain the observed discrimination (92).

Given that T cells are both specific and sensitive, modifications of the basic kinetic proofreading model were required. Experimental data suggested that an intracellular negative feedback involving the phosphatase SHP-1 that can attenuate TCR proximal signalling can be overcome by a positive feedback involving ERK (95). Deterministic and stochastic models that modified kinetic proofreading to include these molecular feedbacks were able to explain antigen discrimination (92, 96). However, subsequent experimental work has questioned these feedbacks because positive feedback with ERK was not observed using an ERK inhibitior (97) and moreover, the key serine thought to be regulated by ERK to reduce SHP-1 activity did not impact antigen discrimi-

nation (98). A recent report has provided evidence for another TCR proximal negative feedback mediated by the negative regulation of ZAP-70 by a MAPK (99). In contrast to previously proposed feedbacks, this feedback would apply only after several proofreading steps and it would therefore be important to understand how this feedback impacts antigen discrimination.

In addition to intracellular feedbacks, a modification of kinetic proofreading to include induced rebinding has been shown to improve specificity whilst maintaining sensitivity (13). In this mechanism, a long delay in kinetic proofreading is used to produce specificity but sensitivity is maintained because the final signalling state is effectively sustained by a large probability of pMHC rebinding. The molecular mechanism(s) underlying this increase may include the signalling-dependent processes that stabilise the close contact to allow for TCR/pMHC interaction (see above).

4 Concluding remarks

T cells employ a diverse set of molecular mechanisms to achieve their high sensitivity to pMHC antigens. These mechanisms can be broadly classified into those that promote TCR/pMHC binding, induce rapid TCR signalling, and amplify TCR signalling (*Fig. 2A*). The requirement of T cells to discriminate antigens means that additional mechanisms, such as feedbacks, must be in place to ensure that their high sensitivity to foreign pMHC does not impact their specificity.

The sensitivity of T cells to antigens is also known to be regulated by the state of the T cell. For example, previously activated T cells are known to have higher antigen sensitivities (100) whereas T cells with a higher average affinity for self pMHC can exhibit reduced antigen sensitivities (101). It is also noteworthy that there is experimental evidence that different T cell responses may require a different number of pMHC ligands to be induced, with a general agreement that cytoxicity exhibits higher antigen sensitivities compared to cytokine production (102–105).

In addition to recognising virally infected cells, T cells are also known to recognise cancerous cells when they express, for example, neoantigens (i.e. altered self pMHC as a result of genetic mutations) or developmental antigens. Here, the number of pMHC antigens expressed on the cancer cell is also expected to be small (106). The additional challenge of recognising these few pMHC antigens on cancer cells is that the affinity of the TCR for cancer pMHCs is weaker than for viral pMHCs (107), which is likely a result of thymic selection.

As we have highlighted, mathematical models have been instrumental in our understanding of various aspects of T cell sensitivity and specificity. These models have largely been formulated based on a static contact interface but it is now appreciated that T cells locally probe APC surfaces using dynamic microvilli. To understand the impact of microvilli probing and close contact formation, it would be interesting to revisit previously published mechanical models that examined the passive spatial redistribution of the TCR based on size (108–111) to include forces generated by microvilli.

Although the sensitivity of T cells to pMHC ligands is well documented, it is unclear how this sensitivity compares to the ligand sensitivity of other receptors. In particular, the TCR belongs to

a large group of receptors known as non-catalytic tyrosine-phosphorylated receptors (NTRs) (5). Given that NTRs share many properties, it is interesting to speculate that other ITAM-containing NTRs also exhibit high ligand sensitivity. A detailed comparison of ligand sensitivities between NTRs may shed light on the mechanisms that specifically contribute to the high sensitivity of T cells.

The sensitivity of T cells to antigens is well documented but a number of open questions remain concerning the underlying molecular mechanisms (*Box 3*). An improved understanding of these mechanisms may be useful when designing therapies with, for example, chimeric antigen receptors to re-direct T cells to kill infected or cancerous cells (112).

Boxes

Box 1: Mathematical models

A variety of mathematical models have been used to study various aspects of T cell activation. Below we describe just two of the many approaches that have been previously used. We refer the reader to the primary sources referenced in the main text for details of other models.

Models for serial binding

First-passage time calculations were originally used to estimate the number of TCRs that a single pMHC can serially bind in the micrometer-scale contact between T cells and APCs (113). This calculation was subsequently adapted to the $\sim$100 nanometer-scale clusters of TCR (46)

These calculations proceed by directly solving for the mean first-passage time of the pMHC sojourn in the area of interest (e.g. cluster of TCR), subject to reversible binding with TCRs,

$$\begin{aligned} D_1\nabla^2 t_1 - k_{\text{on}}[\text{TCR}]t_1 + k_{\text{on}}[\text{TCR}]t_2 &= -1 \\ D_2\nabla^2 t_2 - k_{\text{off}}t_2 + k_{\text{off}}t_1 &= -1, \end{aligned}$$

where t_i is the mean first passage-time with $i = 1$ denoting the free pMHC state and $i = 2$ denoting the bound pMHC state. The first term of each equation represents the diffusion of pMHC in that state with the next two terms representing reversible binding. The form of these equations is not intutive (e.g. the fact that k_{on} appears twice in the first equation but not in the second) but they can be intuitively derived from an underlying discrete random walk (see Appendix A in (114)). Assuming adsorbing boundary conditions it is possible to obtain analytical solutions for specific geometries (46, 113). The number of TCR binding events is determined by dividing the mean passage-time by the cycle time for a single TCR binding event ($1/k_{\text{on}}[TCR] + 1/k_{\text{off}}$).

Stochastic spatial simulations of TCR/pMHC interactions based on the Gillespie algorithm revealed that in addition to serial binding of different TCRs, there can be substantial rebinding of the same TCR (47). Rebinding is not captured in standard determinstic models, such as the

first passage time calculations described above. However, rebinding can be explicitly accounted for using a simplified two-state ordinary-differential-equation model where binding (second state) requires the pMHC to arrive within proximity of the TCR (first state) (48). The rate of entering the first state is determined by the diffusion-limited on-rate on the membrane ($k_+ = 2\pi D/log(b/s)$, where b is the mean distance between TCR and s is the reaction radius). This two-state model has been used not only to study TCR/pMHC interactions (48, 49, 115) but also enzymatic reactions (76, 116).

Models for spatial segregation

Mechanical models were originally used to explain the micrometer-scale spatial segregation of surface molecules (108–111) and more recently, mechanical models have been used to study how nanometer-scale segregation modulates the tensile force on the TCR/pMHC interaction (61, 63).

As an example, we describe a mechanical model used to examine the nanometer-scale spatial redistribution of the LSM CD45 upon TCR/pMHC binding (61). The partial-differential-equation that tracked the spatial distribution of LSMs (P) included a diffusion term and an advection term,

$$\frac{\partial P}{\partial t} = D\nabla^2 P + \mu\nabla \cdot (P\nabla E_P),$$

where advection captures the tendency of LSMs to avoid being in membrane regions that compress/bend their large extracellular domain. The elasticity of LSMs is modelled as a Hookean spring with preferred height of z_p,

$$E_P = \frac{1}{2}k_p(z_p - z(r,t))^2.$$

To determine $z(r,t)$, the total mechanical energy of the membrane is minimized,

$$E = \iint \frac{1}{2}\kappa_M \left(\nabla^2 z\right)^2 + PE_P dA,$$

where the first term captures the membrane bending stiffness and the second term captures the deformation of the LSM. Therefore, the model couples membrane bending with LSM compression. It follows that by pushing the membranes apart, LSMs are able to generate a tensile force ($f(t)$) on the shorter TCR/pMHC interaction (located at $r = r_0$) and this key output of the model is calculated as follows,

$$f(t) = \partial E/\partial z(r,t)|_{r=r_0}.$$

Calculation of $f(t)$ revealed that although the TCR/pMHC interaction experiences a large ∼50 pN force initially upon binding, the spatial segregation of LSMs can reduce this force to below ∼20 pN within 1 s. It was proposed that a time-dependent force can contribute to antigen discrimination by preferentially accelerating the dissociation of short-lived TCR/pMHC interactions (61).

Recently, a stochastic version of this model was formulated to investigate the effects of membrane fluctuations on the TCR/pMHC interaction in the context of catch bonds (63). In both models, the applied force on the TCR/pMHC interaction is produced exclusively by membrane deformations resulting from size-based segregation. Future work is required to understand the contribution of actin polymerisation to molecular forces on the TCR/pMHC interaction.

Box 2: Serial binding in T cell sensitivity to antigen

A number of studies have invoked serial binding as a mechanism of T cell sensitivity to pMHC ligands. The concept is that a single pMHC can amplify its own signal by engaging multiple TCRs.

There is overwhelming evidence that a single pMHC can serially bind multiple TCRs. First, the TCR/pMHC lifetime is short ($\sim$0.1-10 s) as measured by recombinant proteins in solution (48, 117) and by direct measurements at contact interfaces (10, 11, 59, 79). This implies that a single pMHC is able to engage multiple TCRs, which is supported by mathematical modelling (46, 113). Second, quantitative analysis of TCR downregulation has shown that many more TCRs are downregulated than presented pMHCs suggesting that a single pMHC engages multiple TCRs (118).

Therefore, the key question is not whether serial binding takes place but whether it is necessary for T cell activation. In order for serial binding to be necessary, there must either be a penalty for TCR/pMHC interactions with long lifetimes or an advantage for short lifetimes (119). A penalty may arise if the TCR is only able to signal for a limited period of time even though pMHC remains bound. At a molecular level, this may happen if the TCR becomes ubiquitinated (120) and/or enters a membrane environment incompatible with signalling. An advantage may arise if the TCR is able to sustain signalling even without pMHC binding. In this case, a single pMHC can generate a large number of signalling TCRs. At a molecular level, this may happen if downregulated TCRs continue to signal (81).

A prediction of these limited signalling and sustained signalling models is that TCR/pMHC interactions with longer lifetimes (high affinities) would reduce signalling and therefore T cell activation. There is now abundant evidence that this is the case across different TCR/pMHC systems (121–124). However, T cell activation is generally only reduced with supra-physiological lifetimes. For example, we have systematically examined the T cell response to a 1-million fold variation in pMHC affinity (124). We found that reduced T cell responses at low pMHC doses can be observed but only when the lifetime exceed $\sim$60 s ($K_D \lesssim 0.01$ μM), which is larger than the lifetime for physiological TCR/pMHC interactions. We note that in addition to this optimal lifetime of $\sim$60 s at low pMHC doses, optimal lifetimes were also observed at high pMHC doses in the physiological range of $\sim$1 s.

In summary, there is substantial evidence for serial binding of multiple TCRs by a single pMHC. Although there is also evidence that serial binding is necessary for T cell activation, the current evidence suggests that this is only relevant when 1) the TCR/pMHC affinity is supra-physiological and 2) the number of pMHC presented is low. Therefore, available data suggests that serial binding may not be necessary for physiological interactions but may be important to consider when designing high affinity therapeutic receptors.

Box 3: Open questions in T cell sensitivity to antigen

• How unique is the sensitivity of the TCR compared to other NTRs (5)?

• Is serial binding of multiple TCRs by pMHC necessary for T cell activation? See Box 1.

• What is the applied force on the TCR/pMHC interaction at physiological close contact interfaces?

• How universal are catch bonds in TCR/pMHC interactions?

• What is the relative contribution to sensitivity of the intracellular and extracellular domains of coreceptors?

• What molecular feedbacks are responsible for producing T cell specificity and how do they impact sensitivity?

• What role do microvilli play in T cell sensitivity to antigen and how do they relate to microclusters? See Pettmann *et al.* (125) for a detailed discussion.

Acnowledgements

We thank P. Anton van der Merwe and Jesse Goyette for discussions and a critical reading of the manuscript. O.D. is supported by a Wellcome Trust Senior Research Fellowship (grant 207537/Z/17/Z). J.A.S.-F. acknowledges funding from the University of Oxford, the EPSRC & BBSRC Centre for Doctoral Training in Synthetic Biology (grant EP/L016494/1), the CONACyT-I^{2}T^2 consortium (grant 440334) and the Amelia Jackson Scholarship Fund.

Conflict of interest

The authors declare no conflict of interest.

References

1. Sykulev Y, Joo M, Vturina I, Tsomides TJ, Eisen HN (1996) Evidence that a Single Peptide–MHC Complex on a Target Cell Can Elicit a Cytolytic T Cell Response. *Immunity* 4:565–571.

2. Irvine DJ, Purbhoo MA, Krogsgaard M, Davis MM (2002) Direct observation of ligand recognition by T cells. *Nature* 419:845–849.

3. Huang J, Brameshuber M, Zeng X, et al (2013) A Single Peptide-Major Histocompatibility Complex Ligand Triggers Digital Cytokine Secretion in CD4+ T Cells. *Immunity* 39:846–857.

4. Purbhoo MA, Irvine DJ, Huppa JB, Davis MM (2004) T cell killing does not require the formation of a stable mature immunological synapse. *Nature Immunology* 5:524–530.

5. Dushek O, Goyette J, van der Merwe PA (2012) Non-catalytic tyrosine-phosphorylated receptors. *Immunological Reviews* 250:258–276.

6. Chang VT, Fernandes RA, Ganzinger KA, et al (2016) Initiation of T cell signaling by CD45 segregation at 'close contacts'. *Nature Immunology* 17:574–582.

7. Iezzi G, Karjalainen K, Lanzavecchia a (1998) The duration of antigenic stimulation determines the fate of naive and effector T cells. *Immunity* 8:89–95.

8. Huppa JB, Gleimer M, Sumen C, Davis MM (2003) Continuous T cell receptor signaling required for synapse maintenance and full effector potential. *Nature immunology* 4:749–55.

9. Liu Y, Blanchfield L, Ma VPy, et al (2016) DNA-based nanoparticle tension sensors reveal that T-cell receptors transmit defined pN forces to their antigens for enhanced fidelity. *Proceedings of the National Academy of Sciences* 113:5610–5615.

10. Huppa JB, Axmann M, Mörtelmaier Ma, et al (2010) TCR–peptide–MHC interactions in situ show accelerated kinetics and increased affinity. *Nature* 463:963–967.

11. Huang J, Zarnitsyna VI, Liu B, et al (2010) The kinetics of two-dimensional TCR and pMHC interactions determine T-cell responsiveness. *Nature* 464:932–6.

12. Feinerman O, Germain RN, Altan-Bonnet G (2008) Quantitative challenges in understanding ligand discrimination by alphabeta T cells. *Molecular immunology* 45:619–31.

13. Dushek O, van der Merwe PA (2014) An induced rebinding model of antigen discrimination. *Trends in Immunology* 35:153–158.

14. Yang H, Buisson S, Bossi G, et al (2016) Elimination of latently HIV-infected cells from antiretroviral therapy-suppressed subjects by engineered immune-mobilizing T-cell receptors. *Molecular Therapy* 24:1913–1925.

15. Dirk BS, Pawlak EN, Johnson AL, et al (2016) HIV-1 Nef sequesters MHC-I intracellularly by targeting early stages of endocytosis and recycling. *Scientific Reports* 6:1–13.

16. Lemmermann NAW, Gergely K, Böhm V, Deegen P, Däubner T, Reddehase MJ (2010) Immune evasion proteins of murine cytomegalovirus preferentially affect cell surface display of recently generated peptide presentation complexes. *Journal of virology* 84:1221–36.

17. Choudhuri K, Wiseman D, Brown MH, Gould K, van der Merwe PA (2005) T-cell receptor triggering is critically dependent on the dimensions of its peptide-MHC ligand. *Nature* 436:578–582.

18. Hermiston ML, Xu Z, Weiss A (2003) CD45: a critical regulator of signaling thresholds in immune cells. *Annual review of immunology* 21:107–37.

19. Evans EJ, Hene L, Sparks LM, et al (2003) The T cell surface–how well do we know it? *Immunity* 19:213–23.

20. Newby J, Allard J (2016) First-Passage Time to Clear the Way for Receptor-Ligand Binding in a Crowded Environment. *Physical Review Letters* 116:1–5.

21. Carbone CB, Kern N, Fernandes RA, et al (2017) In vitro reconstitution of T cell receptor-mediated segregation of the CD45 phosphatase. *Proceedings of the National Academy of Sciences* p 201710358.

22. Huse M, Klein LO, Girvin AT, et al (2007) Spatial and temporal dynamics of T cell receptor signaling with a photoactivatable agonist. *Immunity* 27:76–88.

23. Jung Y, Riven I, Feigelson SW, et al (2016) Three-dimensional localization of T-cell receptors in relation to microvilli using a combination of superresolution microscopies. *Proceedings of the National Academy of Sciences* p 201605399.

24. Cai E, Marchuk K, Beemiller P, et al (2017) Visualizing dynamic microvillar search and stabilization during ligand detection by T cells. *Science* 356:eaal3118.

25. Razvag Y, Neve-Oz Y, Sajman J, Reches M, Sherman E (2018) Nanoscale kinetic segregation of TCR and CD45 in engaged microvilli facilitates early T cell activation. *Nature Communications* 9:732.

26. Sage PT, Varghese LM, Martinelli R, et al (2012) Antigen recognition is facilitated by invadosome-like protrusions formed by memory/effector T cells. *Journal of immunology (Baltimore, Md. : 1950)* 188:3686–99.

27. Bachmann MF, McKall-Faienza K, Schmits R, et al (1997) Distinct Roles for LFA-1 and CD28 during Activation of Naive T Cells: Adhesion versus Costimulation. *Immunity* 7:549–557.

28. Bachmann MF, Barner M, Kopf M (1999) CD2 sets quantitative thresholds in T cell activation. *Journal of Experimental Medicine* 190:1383–1392.

29. Springer TA (1990) Adhesion receptors of the immune system. *Nature* 346:425–434.

30. Wild MK, Cambiaggi A, Brown MH, et al (1999) Dependence of T cell antigen recognition on the dimensions of an accessory receptor-ligand complex. *The Journal of experimental medicine* 190:31–41.

31. Dustin ML, Cooper JA (2000) The immunological synapse and the actin cytoskeleton: molecular hardware for T cell signaling. *Nature Immunology* 1:23–29.

32. Dustin ML, Olszowy MW, Holdorf AD, et al (1998) A novel adaptor protein orchestrates receptor patterning and cytoskeletal polarity in T-cell contacts. *Cell* 94:667–677.

33. Tane AH, Sakuma M, Ike H, et al (2016) Micro – adhesion rings surrounding TCR microclusters are essential for T cell activation. pp 1–17.

34. Wang ECY, Pjechova M, Nightingale K, et al (2018) Suppression of costimulation by human cytomegalovirus promotes evasion of cellular immune defenses. pp 1–6.

35. Patel SJ, Sanjana NE, Kishton RJ, et al (2017) Identification of essential genes for cancer immunotherapy. *Nature Publishing Group* 548.

36. Purbhoo MA, Boulter JM, Price DA, et al (2001) The Human CD8 Coreceptor Effects Cytotoxic T Cell Activation and Antigen Sensitivity Primarily by Mediating Complete Phosphorylation of the T Cell Receptor Chain. *Journal of Biological Chemistry* 276:32786–32792.

37. Holler PD, Kranz DM (2003) Quantitative analysis of the contribution of TCR/pepMHC affinity and CD8 to T cell activation. *Immunity* 18:255–64.

38. Hutchinson SL, Wooldridge L, Tafuro S, et al (2003) The CD8 T cell coreceptor exhibits disproportionate biological activity at extremely low binding affinities. *The Journal of biological chemistry* 278:24285–93.

39. Li QJ, Dinner AR, Qi S, et al (2004) CD4 enhances T cell sensitivity to antigen by coordinating Lck accumulation at the immunological synapse. *Nature immunology* 5:791–799.

40. Laugel B, Van Den Berg HA, Gostick E,et al (2007) Different T cell receptor affinity thresholds and CD8 coreceptor dependence govern cytotoxic T lymphocyte activation and tetramer binding properties. *Journal of Biological Chemistry* 282:23799–23810.

41. Wyer JR, Willcox BE, Gao GF, et al (1999) T Cell Receptor and Coreceptor CD8 Bind Peptide-MHC Independently and with Distinct Kinetics. *Immunity* 10:219–225.

42. Xiong Y, Kern P, Chang HC, Reinherz EL (2001) T Cell Receptor Binding to a pMHCII Ligand Is Kinetically Distinct from and Independent of CD4. *Journal of Biological Chemistry* 276:5659–5667.

43. Jiang N, Huang J, Edwards LJ, et al (2011) Two-stage cooperative T cell receptor-peptide major histocompatibility complex-CD8 trimolecular interactions amplify antigen discrimination. *Immunity* 34:13–23.

44. Jönsson P, Southcombe JH, Santos AM, et al (2016) Remarkably low affinity of CD4/peptide-major histocompatibility complex class II protein interactions. *Proceedings of the National Academy of Sciences* 113:5682–5687.

45. Hamad AR, O'Herrin SM, Lebowitz MS, et al (1998) Potent T cell activation with dimeric peptide-major histocompatibility complex class II ligand: the role of CD4 coreceptor. *The Journal of experimental medicine* 188:1633–40.

46. Dushek O, Coombs D (2008) Analysis of serial engagement and peptide-MHC transport in T cell receptor microclusters. *Biophysical journal* 94:3447–60.

47. Dushek O, Das R, Coombs D (2009) A role for rebinding in rapid and reliable T cell responses to antigen. *PLoS computational biology* 5:e1000578.

48. Aleksic M, Dushek O, Zhang H, et al (2010) Dependence of T cell antigen recognition on T cell receptor-peptide MHC confinement time. *Immunity* 32:163–74.

49. Govern CC, Paczosa MK, Chakraborty AK, Huseby ES (2010) Fast on-rates allow short dwell time ligands to activate T cells. *Proceedings of the National Academy of Sciences* 107:8724–9.

50. Liu B, Chen W, Evavold BD, Zhu C (2014) Accumulation of Dynamic Catch Bonds between TCR and Agonist Peptide-MHC Triggers T Cell Signaling. *Cell* 157:357–68.

51. Schamel WW, Arechaga I, Risueño RM, et al (2005) Coexistence of multivalent and monovalent TCRs explains high sensitivity and wide range of response. *The Journal of Experimental Medicine* 202:493–503.

52. Schamel WWa, Risueño RM, Minguet S, Ortíz AR, Alarcón B (2006) A conformation- and avidity-based proofreading mechanism for the TCR-CD3 complex. *Trends in immunology* 27:176–82.

53. Kumar R, Ferez M, Swamy M, et al (2011) Increased Sensitivity of Antigen-Experienced T Cells through the Enrichment of Oligomeric T Cell Receptor Complexes. *Immunity* 35:375–387.

54. James JR, White SS, Clarke RW, et al (2007) Single-molecule level analysis of the subunit composition of the T cell receptor on live T cells. *Proceedings of the National Academy of Sciences of the United States of America* 104:17662–7.

55. James JR, McColl J, Oliveira MI,et al (2011) The T cell receptor triggering apparatus is composed of monovalent or monomeric proteins. *Journal of Biological Chemistry* 286:31993–32001.

56. Brameshuber M, Kellner F, Rossboth BK, et al (2018) Monomeric TCRs drive T cell antigen recognition. *Nature Immunology* 19.

57. Pageon SV, Tabarin T, Yamamoto Y, et al (2016) Functional role of T-cell receptor nanoclusters in signal initiation and antigen discrimination. *Proceedings of the National Academy of Sciences* 113:E5454–E5463.

58. Zarnitsyna VI, Huang J, Zhang F, Chien YH, Leckband D, Zhu C (2007) Memory in receptor-ligand-mediated cell adhesion. *Proceedings of the National Academy of Sciences of the United States of America* 104:18037–42.

59. Pielak RM, O'Donoghue GP, Lin JJ, et al (2017) Early T cell receptor signals globally modulate ligand:receptor affinities during antigen discrimination. *Proceedings of the National Academy of Sciences* p 201613140.

60. Bell G (1978) Models for the specific adhesion of cells to cells. *Science* 200:618–627.

61. Allard JF, Dushek O, Coombs D, Anton van der Merwe P (2012) Mechanical Modulation of Receptor-Ligand Interactions at Cell-Cell Interfaces. *Biophysical Journal* 102:1265–1273.

62. Robert P, Aleksic M, Dushek O, Cerundolo V, Bongrand P, van der Merwe PA (2012) Kinetics and Mechanics of Two-Dimensional Interactions between T Cell Receptors and Different Activating Ligands. *Biophysical Journal* 102:248–257.

63. Pullen RH, Abel SM (2017) Catch Bonds at T Cell Interfaces: Impact of Surface Reorganization and Membrane Fluctuations. *Biophysical Journal* 113:120–131.

64. Feng Y, Brazin KN, Kobayashi E, Mallis RJ, Reinherz EL, Lang MJ (2017) Mechanosensing drives acuity of $\alpha\beta$ T-cell recognition. *Proceedings of the National Academy of Sciences of the United States of America* 114:E8204–E8213.

65. van der Merwe PA, Dushek O (2011) Mechanisms for T cell receptor triggering. *Nature Reviews Immunology* 11:47–55.

66. Nika K, Soldani C, Salek M, et al (2010) Constitutively active Lck kinase in T cells drives antigen receptor signal transduction. *Immunity* 32:766–77.

67. Hui E, Vale RD (2014) In vitro membrane reconstitution of the T-cell receptor proximal signaling network. *Nature Structural & Molecular Biology* pp 1–12.

68. Hukelmann JL, Anderson KE, Sinclair LV, et al (2015) The cytotoxic T cell proteome and its shaping by the kinase mTOR. *Nature Immunology* 17.

69. Liaunardy-Jopeace A, Murton BL, Mahesh M, Chin JW, James JR (2017) Encoding optical control in LCK kinase to quantitatively investigate its activity in live cells. *Nature structural & molecular biology* 24:1155–1163.

70. Artyomov MN, Lis M, Devadas S, Davis MM, Chakraborty AK (2010) CD4 and CD8 binding to MHC molecules primarily acts to enhance Lck delivery. *Proceedings of the National Academy of Sciences of the United States of America* 107:16916–21.

71. Acuto O, Di Bartolo V, Michel F (2008) Tailoring T-cell receptor signals by proximal negative feedback mechanisms. *Nature Reviews Immunology* 8:699–712.

72. McNeill L, Salmond RJ, Cooper JC, et al (2007) The differential regulation of Lck kinase phosphorylation sites by CD45 is critical for T cell receptor signaling responses. *Immunity* 27:425–37.

73. Love PE, Hayes SM (2010) ITAM-mediated signaling by the T-cell antigen receptor. *Cold Spring Harbor perspectives in biology* 2:a002485.

74. Holst J, Wang H, Eder KD, et al (2008) Scalable signaling mediated by T cell antigen receptor-CD3 ITAMs ensures effective negative selection and prevents autoimmunity. *Nature immunology* 9:658–66.

75. James JR (2018) Tuning ITAM multiplicity on T cell receptors can control potency and selectivity to ligand density. *Science Signaling* 11.

76. Dushek O, van der Merwe PA, Shahrezaei V (2011) Ultrasensitivity in multisite phosphorylation of membrane-anchored proteins. *Biophysical journal* 100:1189–97.

77. Mukhopadhyay H, Cordoba SP, Maini PK, van der Merwe PA, Dushek O (2013) Systems model of T cell receptor proximal signaling reveals emergent ultrasensitivity. *PLoS computational biology* 9:e1003004.

78. Mukhopadhyay H, Wet BD, Clemens L, et al (2016) Multisite phosphorylation of the T cell receptor z-chain modulates potency but not the switch-like response. *Biophys. J.* 110:1896–1906.

79. O'Donoghue GP, Pielak RM, Smoligovets AA, Lin JJ, Groves JT (2013) Direct single molecule measurement of TCR triggering by agonist pMHC in living primary T cells. *eLife* 2:e00778–e00778.

80. Katz ZB, Novotná L, Blount A, Lillemeier BF (2017) A cycle of Zap70 kinase activation and release from the TCR amplifies and disperses antigenic stimuli. *Nature Immunology* 18:86–95.

81. Willinger T, Staron M, Ferguson SM, De Camilli P, Flavell RA (2015) Dynamin 2-dependent endocytosis sustains T-cell receptor signaling and drives metabolic reprogramming in T lymphocytes. *Proceedings of the National Academy of Sciences of the United States of America* 112:4423–8.

82. Altan-Bonnet G, Germain RN (2005) Modeling T cell antigen discrimination based on feedback control of digital ERK responses. *PLoS Biology* 3:1925–1938.

83. Das J, Ho M, Zikherman J, et al (2009) Digital signaling and hysteresis characterize ras activation in lymphoid cells. *Cell* 136:337–51.

84. Esensten JH, Helou YA, Chopra G, Weiss A, Bluestone JA (2016) CD28 Costimulation: From Mechanism to Therapy.

85. Viola A, Lanzavecchia A (1996) T cell activation determined by T cell receptor number and tunable thresholds. *Science (New York, N.Y.)* 273:104–6.

86. Dobbins J, Gagnon E, Godec J,et al (2016) Binding of the cytoplasmic domain of CD28 to the plasma membrane inhibits Lck recruitment and signaling. *Science Signaling* 9:1–13.

87. Andreotti AH, Schwartzberg PL, Joseph RE, Berg LJ (2010) T-cell signaling regulated by the Tec family kinase, Itk. *Cold Spring Harbor perspectives in biology* 2:a002287.

88. Yang W, Pan W, Chen S, et al (2017) Dynamic regulation of CD28 conformation and signaling by charged lipids and ions. *Nature Structural and Molecular Biology* 24:1081–1092.

89. Surh CD, Sprent J (2008) Homeostasis of Naive and Memory T Cells. *Immunity* 29:848–862.

90. Matsui K, Boniface JJ, Steffner P, Reay PA, Davis MM (1994) Kinetics of T-cell receptor binding to peptide/I-Ek complexes: correlation of the dissociation rate with T-cell responsiveness. *Proc Natl Acad Sci U S A* 91:12862–12866.

91. Kersh GJ, Kersh EN, Fremont DH, Allen PM (1998) High- and low-potency ligands with similar affinities for the TCR: The importance of kinetic in TCR signaling. *Immunity* 9:817–826.

92. Altan-Bonnet G, Germain RN (2005) Modeling T cell antigen discrimination based on feedback control of digital ERK responses. *PLoS biology* 3:e356.

93. McKeithan TW (1995) Kinetic proofreading in T-cell receptor signal transduction. *Proceedings of the National Academy of Sciences of the United States of America* 92:5042–6.

94. Stark J, George A, Chan C (2003) T cell sensitivity and specificity - kinetic proofreading revisited.

95. Stefanová I, Hemmer B, Vergelli M, Martin R, Biddison WE, Germain RN (2003) TCR ligand discrimination is enforced by competing ERK positive and SHP-1 negative feedback pathways. *Nature immunology* 4:248–54.

96. Francois P, Voisinne G, Siggia ED, Altan-Bonnet G, Vergassola M (2013) Phenotypic model for early T-cell activation displaying sensitivity, specificity, and antagonism. *Proceedings of the National Academy of Sciences*.

97. Vogel R, Erez A, Altan-Bonnet G (2016) Dichotomy of cellular inhibition by small-molecule inhibitors revealed by single-cell analysis. *Nature communications* 7.

98. Paster W, Bruger AM, Katsch K, et al (2015) A THEMIS:SHP1 complex promotes T-cell survival. *The EMBO journal* 34:393–409.

99. Giardino Torchia ML, Dutta D, Mittelstadt PR, et al (2018) Intensity and duration of TCR signaling is limited by p38 phosphorylation of ZAP-70T293 and destabilization of the signalosome. *Proceedings of the National Academy of Sciences* p 201713301.

100. Fahmy TM, Bieler JG, Edidin M, Schneck JP (2001) Increased TCR avidity after T cell activation: a mechanism for sensing low-density antigen. *Immunity* 14:135–43.

101. Persaud SP, Parker CR, Lo WL, Weber KS, Allen PM (2014) Intrinsic CD4 + T cell sensitivity and response to a pathogen are set and sustained by avidity for thymic and peripheral complexes of self peptide and MHC. *Nature Immunology* 15:266–274.

102. Valitutti BS, Miiuer S, Dessing M, Lanzavecchia A (1996) Different Responses Are Elicited in Cytotoxic T Lymphocytes by Different Levels of T Cell Receptor Occupancy. 183:1917–1921.

103. Itoh, Y; Germain R (1997) Single cell analysis reveals regulated hierarchical T cell antigen receptor signaling thresholds and intraclonal heterogeneity. *The Journal of experimental medicine* 186.

104. Hemmer B, Stefanova I, Vergelli M, Germain RN, Martin R (1998) Relationships among TCR ligand potency, thresholds for effector function elicitation, and the quality of early signaling events in human T cells. *Journal of Immunology* 160:5807–5814.

105. van den Berg Ha, Ladell K, Miners K, et al (2013) Cellular-level versus receptor-level response threshold hierarchies in T-cell activation. *Frontiers in immunology* 4:250.

106. Purbhoo MA, Sutton DH, Brewer JE, et al (2006) Quantifying and Imaging NY-ESO-1/LAGE-1-Derived Epitopes on Tumor Cells Using High Affinity T Cell Receptors. *The Journal of Immunology* 176:7308–7316.

107. Aleksic M, Liddy N, Molloy PE, et al (2012) Different affinity windows for virus and cancer-specific T-cell receptors: Implications for therapeutic strategies. *European Journal of Immunology* 42:3174–3179.

108. Qi SY, Groves JT, Chakraborty AK (2001) Synaptic pattern formation during cellular recognition. *Proceedings of the National Academy of Sciences* 98:6548–6553.

109. Weikl TR, Groves JT, Lipowsky R (2002) Pattern formation during adhesion of multicomponent membranes. *Europhysics Letters* 59:916–922.

110. Burroughs NJ, Wülfing C (2002) Differential segregation in a cell-cell contact interface: The dynamics of the immunological synapse. *Biophysical Journal* 83:1784–1796.

111. Coombs D, Dembo M, Wofsy C, Goldstein B (2004) Equilibrium Thermodynamics of Cell-Cell Adhesion Mediated by Multiple Ligand-Receptor Pairs. *Biophysical Journal* 86:1408–1423.

112. Sadelain M, Rivière I, Riddell S (2017) Therapeutic T cell engineering. *Nature* 545:423–431.

113. Wofsy C, Coombs D, Goldstein B (2001) Calculations show substantial serial engagement of T cell receptors. *Biophysical journal* 80:606–12.

114. Goldstein B, Griego R, Wofsy C (1984) Diffusion-limited forward rate constants in two dimensions. Application to the trapping of cell surface receptors by coated pits. *Biophysical Journal* 46:573–586.

115. Jansson A (2010) A mathematical framework for analyzing T cell receptor scanning of peptides. *Biophysical Journal* 99:2717–2725.

116. Lawley SD, Keener JP (2016) Including Rebinding Reactions in Well-Mixed Models of Distributive Biochemical Reactions. *Biophysical Journal* 111:2317–2326.

117. Dushek O, Aleksic M, Wheeler R, et al (2011) Antigen potency and maximal efficacy reveal a mechanism of efficient T cell activation. *Science Signaling* 4:ra39.

118. Valitutti S, Müller S, Cella M, Padovan E, Lanzavecchia A (1995) Serial triggering of many T-cell receptors by a few peptide–MHC complexes. *Nature* 375:148–151.

119. Lever M, Maini PK, van der Merwe PA, Dushek O (2014) Phenotypic models of T cell activation. *Nature Reviews Immunology* 14:619–629.

120. Yang H, Gou X, Wang Y, Fahmy TM, Leung AYH, Lu J, Sun D (2015) A dynamic model of chemoattractant-induced cell migration. *Biophysical journal* 108:1645–51.

121. Kalergis AM, Boucheron N, Doucey MA, et al (2001) Efficient T cell activation requires an optimal dwell-time of interaction between the TCR and the pMHC complex. *Nature immunology* 2:229–34.

122. Thomas S, Xue SA, Bangham CRM, Jakobsen BK, Morris EC, Stauss HJ (2011) Human T cells expressing affinity-matured TCR display accelerated responses but fail to recognize low density of MHC-peptide antigen. *Blood* 118:319–29.

123. Irving M, Zoete V, Hebeisen M, et al (2012) Interplay between T cell receptor binding kinetics and the level of cognate peptide presented by major histocompatibility complexes governs CD8+ T cell responsiveness. *The Journal of biological chemistry* 287:23068–78.

124. Lever M, Lim HS, Kruger P, et al (2016) Architecture of a minimal signaling pathway explains the T-cell response to a 1 million-fold variation in antigen affinity and dose. *Proceedings of the National Academy of Sciences of the United States of America* 113:E6630–E6638.

125. Pettmann J, Santos AM, Dushek O, Davis SJ (2018) Membrane ultrastructure and T-cell activation. *Frontiers in Immunology* (Submitted).